



The Capillary Flow Experiments Aboard the International Space Station: Increments 9–15

August 2004 to December 2007

*Ryan M. Jenson, Mark M. Weislogel, Noel T. Tavan, Yongkang Chen, and Ben Semerjian
Portland State University, Portland, Oregon*

*Charles T. Bunnell
ZIN Technologies, Cleveland, Ohio*

*Steven H. Collicott
Purdue University, West Lafayette, Indiana*

*Jorg Klatte and Michael E. Dreyer
University of Bremen, Bremen, Germany*

NASA STI Program . . . in Profile

Since its founding, NASA has been dedicated to the advancement of aeronautics and space science. The NASA Scientific and Technical Information (STI) program plays a key part in helping NASA maintain this important role.

The NASA STI Program operates under the auspices of the Agency Chief Information Officer. It collects, organizes, provides for archiving, and disseminates NASA's STI. The NASA STI program provides access to the NASA Aeronautics and Space Database and its public interface, the NASA Technical Reports Server, thus providing one of the largest collections of aeronautical and space science STI in the world. Results are published in both non-NASA channels and by NASA in the NASA STI Report Series, which includes the following report types:

- **TECHNICAL PUBLICATION.** Reports of completed research or a major significant phase of research that present the results of NASA programs and include extensive data or theoretical analysis. Includes compilations of significant scientific and technical data and information deemed to be of continuing reference value. NASA counterpart of peer-reviewed formal professional papers but has less stringent limitations on manuscript length and extent of graphic presentations.
- **TECHNICAL MEMORANDUM.** Scientific and technical findings that are preliminary or of specialized interest, e.g., quick release reports, working papers, and bibliographies that contain minimal annotation. Does not contain extensive analysis.
- **CONTRACTOR REPORT.** Scientific and technical findings by NASA-sponsored contractors and grantees.

- **CONFERENCE PUBLICATION.** Collected papers from scientific and technical conferences, symposia, seminars, or other meetings sponsored or cosponsored by NASA.
- **SPECIAL PUBLICATION.** Scientific, technical, or historical information from NASA programs, projects, and missions, often concerned with subjects having substantial public interest.
- **TECHNICAL TRANSLATION.** English-language translations of foreign scientific and technical material pertinent to NASA's mission.

Specialized services also include creating custom thesauri, building customized databases, organizing and publishing research results.

For more information about the NASA STI program, see the following:

- Access the NASA STI program home page at <http://www.sti.nasa.gov>
- E-mail your question via the Internet to help@sti.nasa.gov
- Fax your question to the NASA STI Help Desk at 443-757-5803
- Telephone the NASA STI Help Desk at 443-757-5802
- Write to:
NASA Center for AeroSpace Information (CASI)
7115 Standard Drive
Hanover, MD 21076-1320



The Capillary Flow Experiments Aboard the International Space Station: Increments 9–15

August 2004 to December 2007

*Ryan M. Jenson, Mark M. Weislogel, Noel T. Tavan, Yongkang Chen, and Ben Semerjian
Portland State University, Portland, Oregon*

*Charles T. Bunnell
ZIN Technologies, Cleveland, Ohio*

*Steven H. Collicott
Purdue University, West Lafayette, Indiana*

*Jorg Klatte and Michael E. Dreyer
University of Bremen, Bremen, Germany*

Prepared under Cooperative Agreement NCC05–AA29A

National Aeronautics and
Space Administration

Glenn Research Center
Cleveland, Ohio 44135

Acknowledgments

This work is supported through NASA's Glenn Research Center; contract NNC05-AA29A monitored by A. Wilkinson and E. Rame. Authors J. Klatte and M. Dreyer of ZARM and the University of Bremen are in part supported by the Federal Ministry of Economy and Technology (BMWi) through the German Aerospace Center (DLR) under grant number 50 WM 0535. We are grateful for the project science and management support of R. Green and D. Bohman of NASA GRC, the engineering support of Debra Lyden of ZIN Technologies, and to all the NASA ISS cadre members at GRC, MSFC, and JSC. MMW would also like to thank Dr. Fred Kohl of NASA GRC who has enough vision for all of us, and Professors Paul Concus and Robert Finn for getting our attention so long ago. We happily acknowledge the terrestrial experimental support of Oregon high school summer students through the merit-based Apprenticeships in Science and Engineering Program (ASE) at Portland State University: D. Hahs, E. Garbacek, D. Masulis, B. Pederson, P. Bhide, K. Yamauchi, J. Green, A. Vasquez, S. Shin, C. Lee., R. Kimball, A. Nicolaysen, E. Kittlaus, W. Chan, and M. Justel. Finally, our unbounded thanks go to the astronauts who conducted the experiments on ISS on many occasions during their free time: Mike Fincke, William McArthur, Jeff Williams, Sunita Williams, Michael Lopez-Alegria, Clay Anderson, and Peggy Whitson.

Trade names and trademarks are used in this report for identification only. Their usage does not constitute an official endorsement, either expressed or implied, by the National Aeronautics and Space Administration.

Level of Review: This material has been technically reviewed by NASA technical management.

Available from

NASA Center for Aerospace Information
7115 Standard Drive
Hanover, MD 21076-1320

National Technical Information Service
5285 Port Royal Road
Springfield, VA 22161

Available electronically at <http://gltrs.grc.nasa.gov>

Contents

1	The Capillary Flow Experiments aboard ISS: Executive Summary	1
1.1	Introduction	1
1.2	Background and Motivation	2
1.2.1	Hardware and Setup	3
1.3	Contact Line (CL)	3
1.3.1	CL Hardware Description	4
1.3.2	CL Disturbance Types	6
1.3.3	CL Flight Operations Summary	7
1.3.4	CL Primary Science Summary	8
1.3.5	CL Numerical Comparison	8
1.3.6	CL Database Description	10
1.3.7	Extra Science	12
1.4	Vane Gap (VG)	15
1.4.1	Hardware Description	15
1.4.2	VG Flight Operations Summary	16
1.4.3	Static Wetting Configurations	18
1.5	Interior Corner Flow (ICF)	22
1.5.1	ICF Flight Operations Summary	23
1.5.2	ICF1 Results Summary	24
1.5.3	ICF2 Results Summary	26
1.6	Conclusion	28
2	CFE Contact Line Details	30
2.0.1	Hardware Review	30
2.1	Various CL Procedures	32
2.1.1	Setup Procedure	32
2.1.2	Interface Depinning and Recovery	33
2.1.3	Wetting Anomaly in CL1 Smooth Cylinder	34
2.2	Data Processing and Preparation	36
2.2.1	Scale Factor Details	36
2.2.2	Digitization Techniques	38
2.2.3	Tracking Method—Axial Mode	39
2.2.4	Tracking Method—Lateral Modes	39
2.3	Ray Trace Optical Correction	40

2.4	Data Analysis and Presentation	41
2.5	Representative Results	43
2.5.1	Liquid Depth Effect: Frequency	45
2.5.2	CL1 Depth Effect	46
2.5.3	CL2 Depth Effect	47
2.5.4	Linear Frequency Summary	52
2.6	Further Numerical Benchmark Comparisons	52
2.6.1	CL1 Numerical Comparison	53
2.6.2	CL2 Numerical Comparison	56
2.7	Extra Science	61
2.7.1	Axial Mode Droplet Ejection	61
2.7.2	Depinning Investigation	62
2.7.3	Volume Changes During the Experiments	64
2.7.4	Axial Mode Frequency and Contact Angle	64
2.8	Other Experimental Considerations	65
2.9	Directions	66
3	CFE Vane Gap Wetting Analysis	67
3.1	Introduction and Background	67
3.2	Analysis	72
3.2.1	Concus-Finn Method	72
3.2.2	C-singular Solution	75
3.2.3	Analysis: Perfectly Wetting Case (CFE VG-1)	75
3.2.4	Analysis: Partially Wetting Case (CFE VG-2)	82
3.3	Chapter Summary	84
4	CFE-ICF Model Background: Weakly 3-D Capillary Flows	86
4.1	Introduction	86
4.2	Model and Equation Formulation	87
4.2.1	Global Assumptions	88
4.2.2	Local Assumptions	89
4.2.3	Dimensional Equations	90
4.2.4	Scales and Nondimensional Equations	94
4.2.5	Limiting Cases	95
4.3	$O(1)$ Solution for Sections where $\beta = \beta_i \ll 1$	96
4.4	Discussion of Solution and Constraints	99
4.4.1	Impact of Geometry	100
4.4.2	Application	101
4.5	Supportive Drop Tower and CFE-ICF ISS Experiments	102
4.6	Chapter Summary	104
	References	105
5	Appendix: Abbreviated CFE Chronology and Accomplishments	108
5.1	Abbreviated Chronology	108
5.2	Abbreviated Scientific Accomplishments	110

6	Appendix: CFE-Related Dissemination Materials to Date (selection)	114
7	Appendix: Data Archive Conventions	117
7.1	Video Preparation Process	117
7.2	Naming Convention	118
8	Appendix: Contact Line Sample Data Sheets	120
8.1	Datasheet Descriptions	120
8.1.1	CL-1 Axial Mode Example Datasheet	122
8.1.2	CL-1 Push Mode Example Datasheet	130
8.1.3	CL-2 Axial Mode Example Datasheet	138
8.1.4	CL-2 Push Mode Example Datasheet	146
9	Appendix: Additional Vane Gap Images	155
10	Appendix: Complete CFE Design Drawings	158
11	Appendix: CFE Flight Crew Procedures	212

Chapter 1

The Capillary Flow Experiments aboard ISS: Executive Summary

Summary. This paper highlights the experimental, analytical, and numerical results of the Capillary Flow Experiment (CFE) performed aboard the International Space Station (ISS). The experiments were conducted in space beginning with Increment 9 through Increment 16, beginning August, 2004 and ending December, 2007. Both ‘primary’ and ‘extra science’ experiments were conducted during 19 operations performed by 7 astronauts including: M. Fincke, W. McArthur, J. Williams, S. Williams, M. Lopez-Alegria, C. Anderson, and P. Whitson. CFE consists of 6 approximately 1 to 2kg handheld experiment units designed to investigate a selection of capillary phenomena of fundamental and applied importance, such as large length scale contact line dynamics (CFE-Contact Line), critical wetting in discontinuous structures (CFE-Vane Gap), and capillary flows and passive phase separations in complex containers (CFE-Interior Corner Flow). Highly quantitative video from the simply performed flight experiments provide data helpful in benchmarking numerical methods, confirming theoretical models, and guiding new model development. A brief history of the experiment is provided before introducing the science investigated. A selection of experimental results and comparisons with both analytic and numerical predictions is given. Despite the simple nature of the experiments and procedures, many of the experimental results may be practically employed to enhance the design of spacecraft engineering systems involving capillary interface dynamics.

1.1 Introduction

Following the Space Shuttle Columbia accident, developments in NASA’s shuttle program allowed new opportunities for science experiments aboard ISS. Since the shuttle was temporarily unable to ferry planned science equipment to ISS, NASA sought substitute candidate experiments to take advantage of any possible available crew time. The design constraints for such experiments are stringent and include: safe operation, low mass $< 2.5\text{kg}$, low volume < 2 liters, minimal electrical interfacing, minimal power requirements, minimal to no crew training required, short hardware delivery schedule (i.e. months), and low cost. This list is not exhaustive, but is certainly restrictive, and stems from NASA’s desire to use in part the Russian Progress vehicle to deliver science experiment hardware to ISS—the available cargo weight and volume for science hardware aboard Progress being limited. Fortunately, a class of fluids experiments can be posed that fit this description, and the Capillary Flow Experiment (CFE) was proposed to NASA and competed on the basis of science and strategic research merit. The experiments address questions of both scientific and engineering importance and concern certain capillary phenomena as it relates to large

length scale fluid systems that commonly arise aboard spacecraft, but not in terrestrial laboratories.

CFE is composed of six vessels including three experiment pairs—Contact Line (CL), Vane Gap (VG), and Interior Corner Flow (ICF), performed essentially in this order. All vessels use similar fluid injection hardware, have similarly sized test chambers, and rely solely on video for quantitative data. The general engineering design characteristics common to the CFE vessels include: (1) mass < 2kg, (2) volume < 2.1L, (3) No electrical interfaces or power requirements, (4) experiment operation time < 3hr, (5) brief to no crew training needed, (6) low toxicity fluids (i.e. Silicone oils) and (7) double seals against fluid leak. The objective of the different CFE vessels are summarized as follows:

- The Contact Line (CL) experiments are highlighted in Section 1.3. These experiments required the most extensive data reduction effort in CFE and a database was established to categorize the greater than 350 tests performed. The primary objective of the CL experiments is to investigate the effect of contact line boundary conditions on dynamic interface response following a variety of perturbations. Both pinned- and smooth-wall conditions for both perfect and partial wetting conditions are studied in hopes of bracketing all possible responses between the two extremes of fixed and free contact line boundary conditions. Experimental and numerical results are presented along with extra science events depicting phenomena not part of the primary objectives.
- The Vane Gap (VG) experiments are reviewed in Section 1.4 and concern gap-wetting in a cylinder with elliptic cross-section. When rotated, an asymmetric vane oriented along the axis of the chamber achieves a variety of critical geometries leading to nearly discontinuous wetting and de-wetting of gaps formed between the vane and the container wall. The critical wetting conditions are compared to theoretical and numerical predictions and may be exploited for the purposes of controlling large quantities of liquids in reduced gravity environments. Both static and dynamic interfaces are studied.
- The Interior Corner Flow (ICF) experiments are outlined briefly in Section 1.5 and address passive capillary-driven corner flows in weakly 3-dimensional geometries. Experiments demonstrating passive phase separations are conducted. Comparisons of the heavily geometry-dependent flow with developing theoretical models are made.

1.2 Background and Motivation

As has been stated on numerous occasions by numerous investigators, capillary flows and phenomena are critical to myriad fluids management systems in low-g including: fuels/cryogen storage systems, thermal control systems (e.g. vapor/liquid separation), life support systems (e.g. water recycling), and materials processing in the liquid state. Under microgravity conditions, capillary forces can be exploited to control fluid orientation so that such mission-critical systems perform predictably. CFE is a simple fundamental scientific study that can yield quantitative results from a set of safe, handheld fluids experiments. The experiments aim to provide results of value to the capillary flow community that cannot

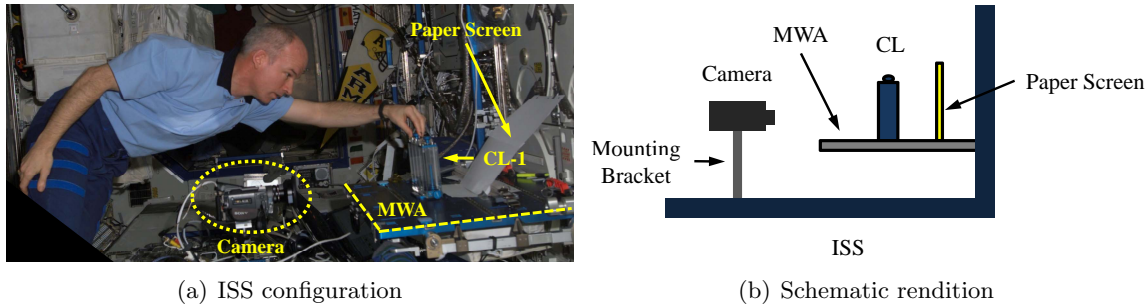


Figure 1.1: Astronaut J. Williams operating CL1 on ISS and schematic of a typical setup common to all CFE vessels.

be easily achieved in ground-based tests. Specific applications of the results tend to center on fluids challenges concerning propellant tanks. However, the knowledge gained may help spacecraft fluid systems designers in general by increasing confidence in current design tools to predict such large scale capillary phenomena.

1.2.1 Hardware and Setup

The handheld experiments are designed to be operated on the Maintenance Work Area (MWA), a portable workbench in the United States Laboratory of the ISS shown in Figure 1.1. Set up and operation are simple and intuitive, requiring minimal preparation. All of the experiments require use of an ISS video camera and a diffuse paper screen employed as a backlight. The camera is a standard rate Sony 720x480 CCD DVCam and is mounted to an ISS rail. Astronauts are allowed freedom in where and how the camera and experiment are configured with the primary requirement that the camera be perpendicular to the test vessel front face. The CFE vessels are rigidly mounted to the MWA by a setscrew.

1.3 Contact Line (CL)

The CFE Contact Line experiment consists of two vessels each containing two right circular cylinders, one smooth and the other with a machined groove serving as a pinning edge. Both cylinders are filled to identical levels and since the containers are closely and rigidly connected, any disturbance imparted to the vessel is felt by both fluid surfaces. Differences in fluid response is thus expected to be solely a result of differences in contact line boundary condition, which is readily observed in Figure 1.2. The simple operation of CL requires the astronaut to impart a variety of disturbances to the vessel allowing the interface oscillations to decay naturally in the field of view of the camera. Dynamic Bond numbers as low as 10^{-5} and greater than 20 are achieved spanning both visco- and inertial-capillary flow regimes. Video data is collected from which both the disturbance input and passive liquid response can be digitized. The brevity (5s–30s) of each experiment event (disturbance and damped fluid response) permitted a large number of tests to be conducted, the reduced data set of which comprises over 350 primary science events not counting numerous other tests referred to as ‘extra science’ tests.

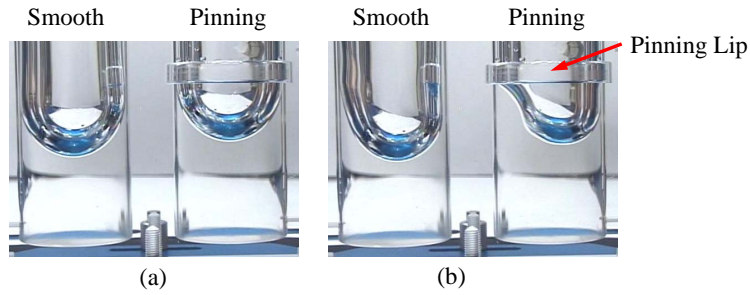


Figure 1.2: Image of CL2 interface: (a) equilibrium states, (b) arbitrary dynamic state.

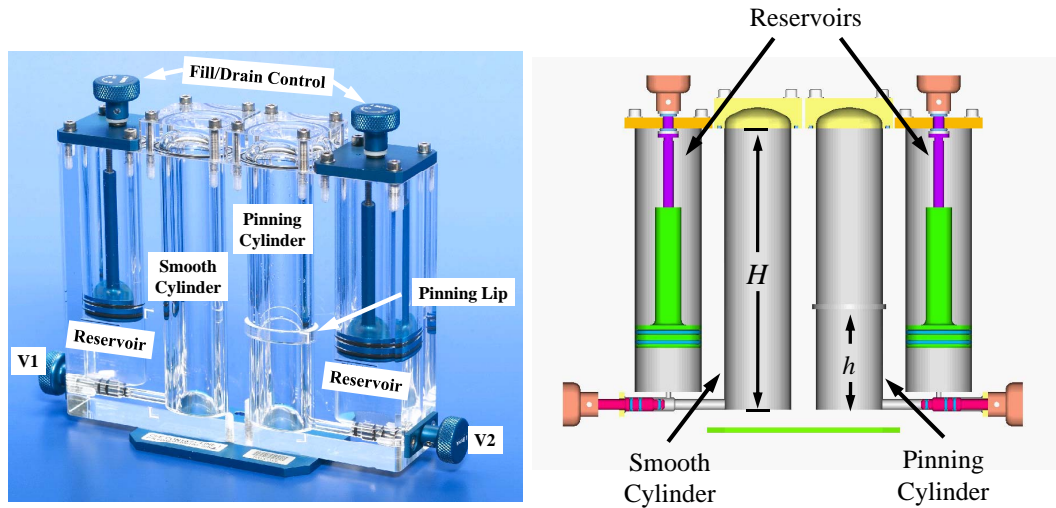


Figure 1.3: Photo of CFE CL1 on left and solid model at right showing Smooth and Pinning cylinder from camera view.

1.3.1 CL Hardware Description

A photograph of the CL2 flight unit is provided in Figure 2.2 along with a solid model of the design with key components noted. The two units are identical in all respects save wetting properties, fluid volume, and pinning lip location. The main body is machined from a single piece of cast acrylic and fitted with aluminum pistons and stainless steel piston drive screws. The right circular cylindrical test chambers have flat bases but elliptical acrylic lids. Each unit is secured to an aluminum base plate with a single slotted hole that is used for attachment to the ISS MWA via a captive fastener allowing for as much as 40mm lateral motion or adjustment. Turning a knob connected to a drive screw displaces the piston. The knob diameter and screw pitch are selected so that a slow and stable manual fill process is assured. The double O-ring sealed reservoirs, charged at atmospheric pressure ($\sim P_{atm}$), contain the silicone oil test liquid and employ pistons to dispense the liquid into the respective test sections. Thus, the blind test chambers are somewhat pressurized

Table 1.1: CL physical dimensions and properties.

Physical Dimensions	
Cylinder Diameter	$38.10 \pm 0.05\text{mm}$
Cylinder Height, H	$146.0 \pm 0.1\text{mm}$
Pinning Lip Height	$7.6 \pm 0.1\text{mm}$
Pinning Lip Diameter	$43.7 \pm 0.1\text{mm}$
Acrylic Refractive Index, N_D	1.491
CL1 Specifications	
Base to Pinning Lip, h	$36.9 \pm 0.1\text{mm}$
Maximum Fluid Volume	39.04mL
CL2 Specifications	
Base to Pinning Lip, h	$50.8 \pm 0.1\text{mm}$
Maximum Fluid Volume	43.44mL
Fluid Properties at 25°C	
Fluid Type	Silicone Oil
Kinematic Viscosity, ν	2cst $\pm 2\%$
Density, ρ	$872 \pm 5\text{kg/m}^3$
Surface Tension, σ	$0.0187\text{N/m} \pm 5\%$
Refractive Index, N_D	1.390
CL1 Specifications	
Receding Angle, θ_{rec}	$47.3^\circ \pm 2^\circ$
Equilibrium Angle, θ_{eq}	$48.7^\circ \pm 2^\circ$
Advancing Angle, θ_{adv}	$52.2^\circ \pm 2^\circ$

($\sim 1.3P_{atm}$) when the liquid is fully deployed. The design meets a single level of containment requirement for a ‘zero-hazard’ test liquid enabling the experiments to be performed by any crew member in the open ISS laboratories.

The CL1 unit tests a partially wetting liquid with a nominal contact angle of $\sim 50^\circ$ while the CL2 unit tests a perfectly wetting (spreading), zero contact angle liquid. The selection of a 38.1mm cylinder diameter is constrained by an ISS safety requirement for maximum fluid volume. The cylinder diameter is sized to be as large as possible within this constraint to access uniquely low-g inertial-capillary regimes without introducing overbearing depth effects. The liquid volume and height of the pinning lip are selected such that the liquid depth from the centerline of the low-g menisci to the cylinder base is the same for both CL1 and CL2 at 31.75mm (depth/radius = 1.67). These and other container specifics are summarized in Table 2.1.

Certain wetting barriers are applied to the containers to enhance control during the experiment operations. The surface coating conditions vary between CL1 and CL2. The entire interior surface of CL1 is rinse coated with FC-724, a transparent fluoro-polymer surface coating manufactured by the 3M Corporation. CL2 is intended to be a perfectly wetting experiment thus for the Pinning cylinder the interior surfaces above the pinning lip are coated, including the groove making up the pinning edge. The discontinuous wetting

boundary established across the pinning lip in CL2 creates a passive means of returning the fluid from above the pinning edge to below it via a favorable wetting discontinuity. The lid of the Smooth cylinder is also coated. All other surfaces of CL2 are uncoated and exhibit perfect wetting, $\theta = 0^\circ$. The equilibrium contact angle for the silicone oil on the FC-724 surface is determined by measuring advancing and receding contact angles using a tilted FC-724 coated glass capillary tube [1]. These values are listed in Table 1. The equilibrium angle is computed [2] to be $48.7 \pm 2^\circ$ but is frequently referred to as 50° in reference to CL1. Contact angle values identified during the flight experiments confirm these values despite the test unit being stored for approximately 2 years prior to testing.

1.3.2 CL Disturbance Types

A variety of disturbances were imparted by hand to the CL vessels by the astronauts and are briefly described here.

- **Tap:** This disturbance is a single tap imparted to the rigidly mounted container. The disturbance begins with small taps progressing to light knuckle raps. The fluid response is characterized by small amplitude high frequency oscillations which can only be marginally resolved.
- **Axial:** With the CL vessel rigidly mounted to the MWA, the axial mode disturbance is imparted by manually depressing and releasing the MWA in a similar manner as a diver on a diving board. The amplitude (acceleration) of the disturbance is controlled by the crew and a wide range is achievable from marginally discernable (0.21mm) to well beyond destabilization, and break-up of the interface ($> 13.60\text{mm}$).
- **Push:** The Push disturbance consists of a single lateral translation of the vessel. The set screw mounting the vessel to the MWA is loosened, allowing the astronaut to push the container left or right in the field of view creating an impulsive slosh-type disturbance. The translation distance begins small and increases to up to 33mm (spanning linear and nonlinear regimes until breakup of the interface).
- **Slide/Slosh:** This extension of the Push disturbance is called Slide or Slosh, and consists of a full period lateral oscillation. The input frequency is approximately that of the natural frequency of the interface as identified by the crew, and is held approximately constant while varying the amplitude.
- **Multi-Slide:** As the name suggests, the Multi-Slide disturbance is a sequence of Slide/Slosh disturbances imparted without pause and composed of more than one period. The frequency of oscillation is held approximately constant while the displacement amplitude is varied.
- **Swirl:** To impart the Swirl mode disturbances, the CL vessel is moved in a circular or elliptical pattern of approximately 30 to 40 millimeters in diameter in a motion consisting of 1–5 periods on the MWA surface. Large amplitude swirls create centrifugal force-dominated vortical flows. Such disturbances were only performed for CL2 and the data has not been reduced to date.

1.3.3 CL Flight Operations Summary

CFE-CL was performed 6 times aboard ISS by astronauts M. Fincke (2), W. McArthur (1), J. Williams (2), and P. Whitson (1) on Expeditions 9, 12, 13, and 16 between August 28th, 2004 and November 16th, 2007. The highlights of each operation are outlined below:

1. August 28th, 2004 (GMT 2004-241), CL2-1, M. Fincke, Nominal Science Run
 - Successfully completed all primary science objectives with the Pinning lip flooded in many cases
 - Introduced the method for imparting Axial mode disturbances.
 - Extra Science: Droplet ejection, ‘hourglass’ draining phenomena in Smooth cylinder, and droplet-wall impact and rebound dynamics.
2. September 19th, 2004 (GMT 2004-262), CL2-2, M. Fincke, Nominal (Extra Science) Run
 - Demonstrated a centrifugal spinning method used to clear the Pinning lip of liquid and reset the experiment. The method was only partially successful as the Pinning lip was not completely cleared of liquid
 - Repeat Push, Slide, and Axial mode disturbances
 - Supplemental Science: Depth effect on the Push disturbance type
3. December 20th, 2005 (GMT 2005-354), CL2-3, W. McArthur, Extra Science
 - Successfully cleared the Pinning lip of liquid using a refined version of Fincke’s centrifuge method, resulting in the ability to repeat the experiment indefinitely
 - Repeat Push, Slide, and Axial mode disturbances with the camera mounted to the MWA, which resulted in the inability to obtain certain Axial mode disturbances data due to the loss of a stationary reference point.
 - Extra Science: Additional droplet-wall impact and rebound dynamics and liquid jetting event due to large Axial disturbances
4. April 17th, 2006 (GMT 2006-107), CL2-4, J. Williams, Extra Science
 - Revision and perfection of McArthur’s centrifuge method used to clear the Pinning lip
 - Repeat Push, Slide, Multi-Slide and Axial mode disturbances with the camera correctly mounted to the ISS rail
 - Extra Science: Significant droplet/jet ejections, and droplet impact & rebound dynamics
5. August 30th, 2006 (GMT 2006-242), CL1-1, J. Williams, Nominal Science Run
 - Improvised method to address wetting anomaly
 - Successful completion of Axial and Push science objectives for Pinning and Smooth cases

- Supplemental Science: Depth effect on Push disturbance mode
6. November 16th, 2007 (GMT 2007-320), CL1-2, P. Whitson, Voluntary Science (Pinning cylinder, slide and depth effects)
- Large amplitude Axial disturbances with destabilization and droplet ejection
 - Due to increased stability of droplets residing in the Pinning lip (due to the larger contact angle), large accelerations were needed to clear the Pinning lip. Apparently, such high accelerations could not be easily generated by hand. During attempts to clear the Pinning lip, excessive force led to damage of the CL1 hardware resulting in premature termination of the experiment.

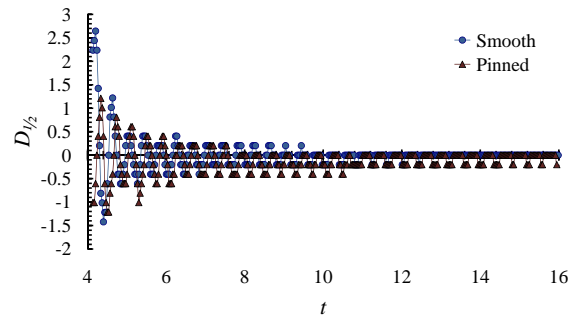
1.3.4 CL Primary Science Summary

Over 350 primary and extra science events have been reduced to date, where significant contributions include both experimental results and numerical comparisons. Only a small subset of the data is provided here. The complete database may be found at <http://cfe.pdx.edu>. To date, only damped interface oscillations (frequency and decay) as functions of fluid properties, wetting, contact line condition, disturbance type, and amplitude have been pursued. Representative results for Axial and lateral mode passive fluid response is shown in Figure 1.4 for CL1 (partial wetting) and CL2 (perfect wetting). In each figure Pinned and Smooth contact line boundary conditions are compared. There is a clear difference in damping rate, frequency, and qualitative waveform depending on the contact line condition.

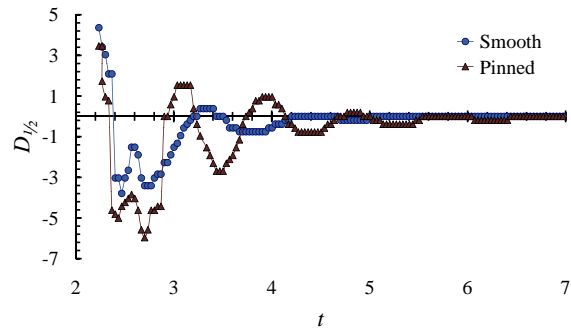
- The ‘stiffer’ pinning condition produces higher frequencies for all disturbance modes.
- Pinning interfaces generally exhibit lower damping rates than their Smooth cylinder counterparts.
- Larger contact angles produce higher frequencies and lower damping rates. This is immediately obvious by comparing CL1 and CL2 and gives rise to a CL1 natural frequency of approximately 2.5-fold that of CL2.
- The most prominent difference between Pinning and Smooth responses is found in the partially wetting CL1 lateral mode case in Figure 2.15. The first inertial peak of the Smooth response abruptly decays between 2 and 4 seconds while its pinned counterpart decays more gradually.
- The damped oscillation profiles diverge between Pinning and Smooth cylinders as disturbance amplitudes increase.
- For the current CL test conditions, fluid depth has only a slight effect on passive interface response—depth to radius ratios down to 0.26.

1.3.5 CL Numerical Comparison

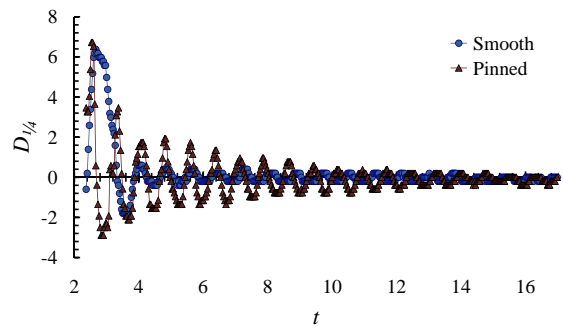
The CL database may be used to benchmark ‘large’ length scale CFD models. As part of such a demonstration, and in collaboration with J. Klatte and M. Dreyer (of ZARM and



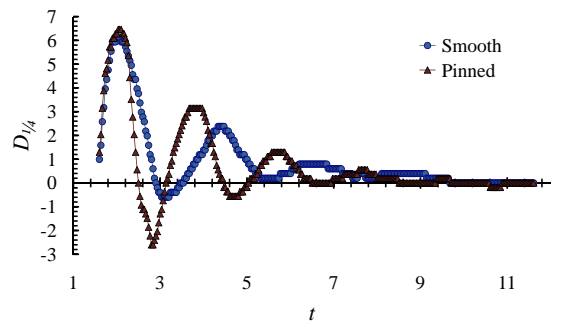
(a) CL1 Axial Mode



(b) CL2 Axial Mode



(c) CL1 Push Mode



(d) CL2 Push Mode

Figure 1.4: Comparisons of passive fluid response in Pinned and Smooth cylinders to Axial and Push disturbances for CL1 ($\theta = 48.7^\circ$) and CL2 ($\theta = 0^\circ$).

the University of Bremen, Germany), blind numerical predictions were made using the open source OpenFOAM CFD package in an effort to model the CL experiments. Details of the numerical configuration can be found elsewhere [3] with a brief overview and summary of results presented here.

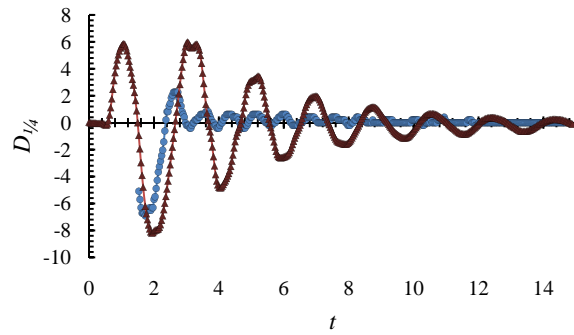
The numerical model was configured without knowledge of the experimental results; i.e. no hints were given as to run time, required mesh resolution, or any other numerical input parameters. Only physical dimensions, fluid properties, wetting conditions, and input accelerations were provided to the numerical analyst. [Note that the input disturbance acceleration was computed using the input disturbance position data, smoothed using a Loess method before central differences were computed. The smoothing methods were varied, but the CFD results were insensitive—coarse and highly smoothed data produced nearly identical results.] Optical distortions were accounted for in both numerical predictions and experimental data.

Comparisons were made for several Push and Axial mode disturbances possessing smooth and pinning boundary conditions. Example comparisons for Axial and Push modes are presented in Figure 1.5. In general, agreement is most favorable for the perfectly wetting condition of CL2, Figures 1.5(c) and 1.5(d). This is in part due to the highly damped nature of these flows, which naturally reduces the sensitivity of the flow on the particular boundary condition applied at the contact line—Smooth and Pinning cylinders respond similarly. Discrepancies arise most noticeably for the partial wetting case of CL1, where despite the poorer agreement the Pinning cylinder results (Figure 1.5(b)) fair better than those of the Smooth cylinder (Figure 1.5(a)). The increased inaccuracy is primarily due to the choice of contact line boundary condition, and is readily observed over the manifold weakly damped oscillations.

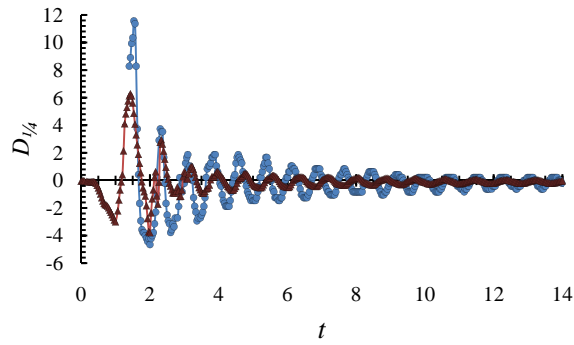
Several practical conclusions may be drawn for these oscillation comparisons: (1) The current OpenFoam model does surprisingly well to predict the large length scale capillary phenomena for highly wetting systems with a simple fixed contact angle boundary condition at the contact line. (2) The model may be successfully tuned via pre-calculations improving the likelihood of accurate and efficient ‘blind’ computations for design and analysis. (3) The greatest efforts to further improve the general numerical approach should focus on the boundary conditions necessary to specify partial wetting systems with contact angle hysteresis. Spacecraft fluid systems employing such fluids (i.e. water processing systems) will likely require parametric studies for the various conditions that can arise at the contact line represented in their extremes by perfect slip and perfectly pinned conditions.

1.3.6 CL Database Description

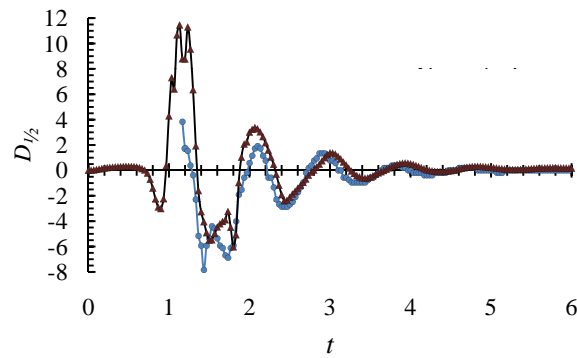
The CL database is publicly available at <http://cfe.pdx.edu> with digitized events categorized for subsequent data reduction and research. Each CL event is accompanied by an MPEG-1 video and corresponding datasheet describing physical parameters, tracking methods, raw data, and preliminary results. Datasheets are designed such that all information is presented in a manner such that one can repeat the data reduction exactly if desired. A summary page is also provided where information about each individual datasheet is presented in a single location along with video and datasheet links. The intent is to provide pertinent numerical information spanning all of the data in a single location allowing comparison of various



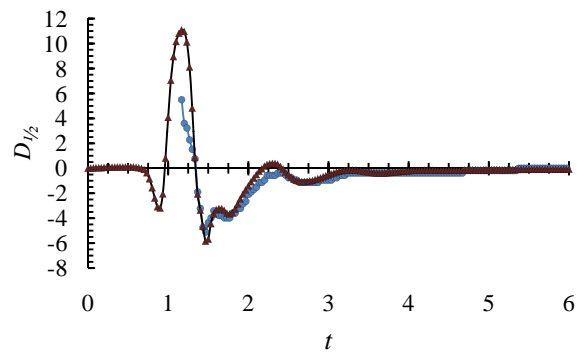
(a) CL1 Smooth Push



(b) CL1 Pinned Push



(c) CL2 Pinned Axial



(d) CL2 Smooth Axial

Figure 1.5: Representative numerical comparisons with sample CL experiments: triangles are numeric, circles are experiments.

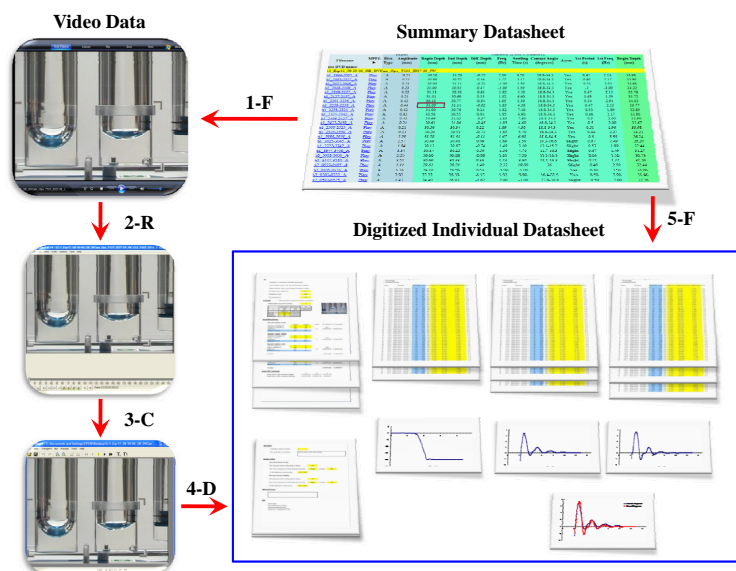


Figure 1.6: CFE CL database structure.

parameters. An overview of how the database can be used is shown in Figure 1.6. The primary components of the database are the summary page, MPEG-1 video, and the individual datasheets corresponding to each video or event. Each datasheet and corresponding video can be accessed through the summary page. In addition, the summary page contains select statistics and results obtained from the individual datasheets. The arrows 1-F and 5-F indicate this type of flow where ‘F’ indicates ‘File Open.’ In addition to simply reading the data, one can take the original video, prepare it, and digitize it on ones own terms. This is achieved by following the procedure between 2-Read, 3-Convert, and 4-Digitize. The original MPEG-1 video is read into the freeware program VirtualDub [4] and saved as an uncompressed AVI, which completes the conversion process. The converted video can then be digitized using the freeware program Spotlight-8 [5]. At this point the datasheets accompanying the video can be reconstructed by the user. The complete database along with video, updates, and current information can be found at <http://cfe.pdx.edu>. Custom versions of the data and video may be obtained on DVD by contacting the lead author (R.M.J.).

1.3.7 Extra Science

Numerous ‘extra science’ events were also captured on video and include liquid jetting, droplet impact and satellite rebound dynamics, air entrainment during Axial disturbances, annular ‘hourglass’ film draining, wetting gradient effects, contact line stability, and more. A selection of these extra events are briefly discussed here with the expressed purpose of demonstrating the range of phenomena that may be further mined from the CL experiments.

- **Jetting:** During CL operations the disturbance amplitudes were increased until surface breakup occurred. If an Axial mode disturbance is large enough, destabilization

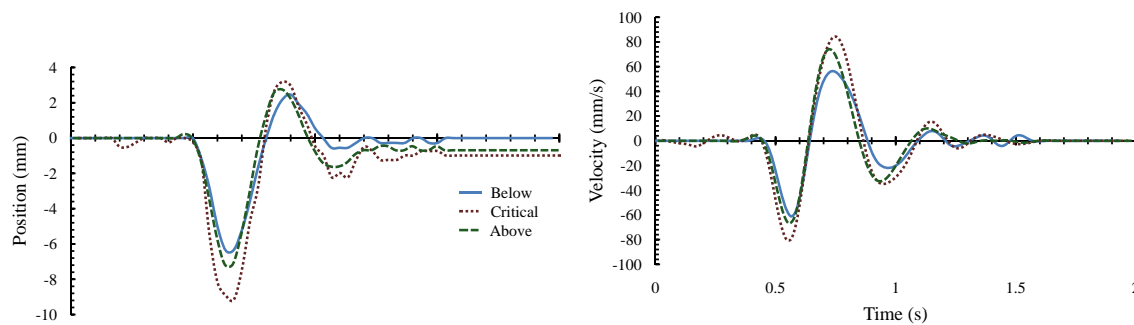


Figure 1.7: CL2 displacement and velocity plot depicting input disturbances that are below, at, and above the threshold that causes droplet ejection.



Figure 1.8: An example of a depinning event investigating contact line stability.

of the interface occurs resulting in droplet ejection. If the disturbance is further increased a liquid jet is formed which eventually breaks up into a stream of drops. Several parameters affect whether jetting occurs, including disturbance amplitude, frequency, and waveform. As amplitudes become large the possibility of ejection increases; however, it is found that it must be coupled with a sufficiently high frequency and appropriate waveform. This is evident in Figure 2.31 where the ‘below’ event produces no ejection, ‘critical’ produces a single stationary droplet, and the ‘above’ event results in jetting. The similarity between disturbances but very different fluid responses indicates that a narrow region in which drop ejection and jetting occurs. [Note that the critical frequency for CL2 is approximately 2.50Hz or 2.5-fold the natural frequency. Note also that the velocity waveform for the ‘critical’ case is nearly symmetric about the t -axis, while the ‘above’ (jetting) case has a net positive velocity, and the ‘below’ case has a net negative velocity.]

- **Contact Line Stability:** An analogous situation arises when lateral mode disturbances become large in the Pinning cylinder. In this case the contact line de-pins from the Pinning lip causing it to flood with liquid as shown in Figure 1.8. Such destabilization occurs repeatedly during the CL experiments providing opportunities to establish the critical acceleration environment that leads to depinning of the contact line.
- **Droplet Impact and Rebound Dynamics:** On numerous occasions following interface breakup, the astronauts would subject the vessel to very large axial mode



Figure 1.9: Sequence of images following large amplitude Axial Disturbance in CL2 at approximate times 0, 1, 6, and 11s. Coalescence in Smooth cylinder on left is retarded due to low efficiency impacts with liquid films on the cylinder walls. Partial wetting surfaces of Pinning cylinder result in high efficiency adhesion events with dry walls (100%), but eject satellite drops of decreasing size with each successive adhesion. Note: hourglass configuration observed in Smooth cylinder at left.



Figure 1.10: Various wetting condition in CL1 smooth cylinder as a function of fluid depth: 34° at far left, 4° at far right.

disturbances before resetting the experiment. The intent was to produce jetting and stream of droplets that would then bounce, slide, and roll about the chamber eventually adhering to dry walls or coalescing with liquid films or bulk interfaces. Several such images are displayed in Figure 1.9. It was found that if a droplet is greater than a certain size, when impacting and adhering to a dry wall of partial wettability a satellite droplet is ejected. The process repeats until the ejected droplet is small to the point viscous forces prevent further ejection. Several such events are provided in the CL database with only a handful being analyzed to date [3].

- Contact Angle Variation:** During the CL1 experiments anomalous wetting was observed in the Smooth cylinder. Various static interfaces are shown in Figure 1.10 as a function of fluid depth. The local essentially axial wetting variations, caused either by a poorly applied coating or by a locally crazed surface (observed in the flight hardware), led inadvertently to new science since an array of contact angles could be tested in a single cylinder by varying liquid depth. Contact angles were backsolved using the equilibrium surface curvature.
- Hourglass Formation and Draining:** During the first Slide tests of CL2, Astronaut M. Fincke quickly observed the gradual development of an ‘hourglass’ configura-

tion following repeated large amplitude disturbances in the perfectly wetting smooth cylinder only. An example may be observed in the first frame of Figure 1.9, Smooth cylinder. The configuration was a nuisance for the primary objectives and was frequently erased using the centrifuge methods, but data on the rate of its formation to a variety of input disturbances, its dimensions, its passive recovery to the desired equilibrium state, and its drainage under noticeable background accelerations was recorded and is available for further investigation. Such configurations are of practical interest because they readily form in highly wetting systems subject to various disturbances and time-dependent acceleration fields not uncommon to spacecraft fuel tanks. They are also of interest in that they contribute to axial pumping of the fluid in response to lateral excitations, a phenomena of which might be exploited or of concern to any number of applications. This non-equilibrium configuration is addressed in greater, but still superficial, detail elsewhere [3].

These extra science examples demonstrate the range of phenomena occurring during the CL operations as a byproduct of the primary science investigation. All cases of such ‘extra science’ events were not investigated exhaustively, but a number of the events are noted in the database and provide potential science opportunities for interested parties. Additional extra science data includes bubble entrainment due to Axial disturbances, entrained bubble coalescence, annular film draining, droplet-wall coalescence, droplet film rebound, swirl mode disturbances, and probably others. Original video can be found at <http://cfe.pdx.edu>.

1.4 Vane Gap (VG)

It is well known that careful selection of geometry has the potential to control large amounts of fluid in a reduced gravity environment. Containers with interior corners are one such choice as the corner tends to act as a capillary conduit driving spontaneous flows along its length. It is essential in such systems that the fluid ‘wets’ the corner which can be determined from the Concus-Finn critical corner wetting condition [6, 7]. Unfortunately, this condition is significantly complicated for interior corners that do not actually contact; such as in the gap formed by a vane and tank wall of a large propellant storage tank. Intended or unintended positional changes of such vanes can have a dramatic impact on the fluid configuration. Two CFE VG test vessels are devoted to investigate such phenomenon using a right cylinder with an elliptic cross-section and a single and rotatable central vane that does not contact the container walls as shown in Figure 1.11. Critical vane gap wetting, dewetting, and an asymmetric bulk fluid shift occur in such containers as a function of vane angle.

1.4.1 Hardware Description

The two VG vessels are identical in every aspect except wetting characteristics and vane dimensions. VG1 is perfectly wetting ($\theta = 0^\circ$), while VG2 is partially wetting ($\theta \simeq 48^\circ$). The major and minor diameters of the cylindrical ellipse are 5.08cm and 3.378cm, respectively. The internal height of the fluid chamber is 12.7cm measured from the base to the lid. A volume of 49.1cc of 10cs red-dyed Silicone oil is used in both vessels where the fluid depth is 3.81cm assuming a flat surface. The central vanes in both VG1 and VG2 are rectangular

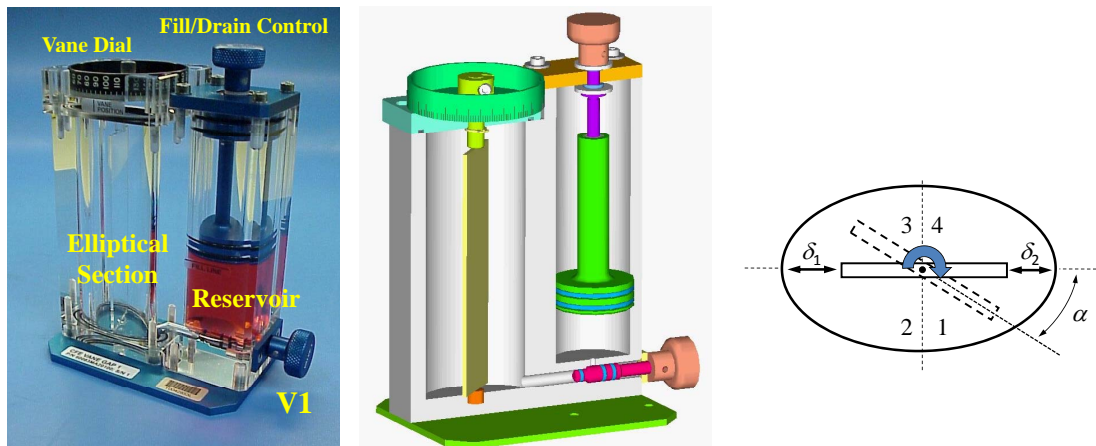


Figure 1.11: VG image, solid model, and a cross-sectional schematic indicating the quadrant number, gap distances, vane angle ϕ , and absolute acute interior angle α .

with dimensions 3.134cm by 11.43cm, and vane thicknesses 0.20cm and 0.50cm, respectively. The vane pivot axis is coaxial with the ellipse but gap dimensions are 0.0838cm and 0.167cm when the vane is aligned with the minor diameter as shown in Figure 1.11. These gap dimensions represent a 0.95 and 0.90 dimensionless gap using the minor axis radius for normalization. Thus two ‘gaps’ can be tested for each vane angle, δ_1 and δ_2 . The vane is able to rotate $\pm 360^\circ$ with $< \pm 1^\circ$ resolution. After the fluid is deployed, the crew rotates the vane at prescribed increments allowing significant time (up to 15 minutes) for the fluid to equilibrate between each rotation.

1.4.2 VG Flight Operations Summary

CFE-VG was performed aboard ISS during nine operations performed by astronauts J. Williams (1), S. Williams (6), C. Anderson (1), and P. Whitson (1) during Expeditions 13–16 between September 5th, 2006 and October 22nd, 2007. The highlights of each operation are highlighted below:

1. September 5th, 2006 (GMT 2006-248), VG1-1, J. Williams, Nominal Science Run
 - Successful completion of all science objectives for first half of crew procedures
 - Completed two complete CW vane rotations
 - Clearly identified critical wetting angles to better than anticipated precision
 - Data suggests third global critical wetting condition (later called bulk shift)
2. March 3rd, 2007 (GMT 2007-062), VG1-2, S. Williams, Nominal (revised) Science Run
 - Successful completion of revised science run to determine equilibrium configurations in Quadrant 1 (Q1)

- Positive identification of global asymmetric interface and associated critical vane angle
 - Identification of container asymmetry and impact on interface
3. March 26th, 2007 (GMT 2007-085), VG1-3, S. Williams, Nominal (revised) Science Run
- Successful completion of revised science run to determine equilibrium configurations in Q4
 - Positive identification of global asymmetric interface and associated critical vane angle
 - Identification of container asymmetry and impact on interface (global shift requires $> 15\text{min.}$)
 - Verification of critical global shift angle outside of gap wetting envelope
4. April 6th, 2007 (GMT 2007-096), VG2-1, S. Williams, Voluntary Science (360° CW dry and wet tests)
- Successful completion of nominal science run for CW vane rotations for dry and wet tests
 - Positive identification of critical wetting and dewetting angles and hysteresis
 - Global asymmetric wetting not observed
 - Preliminary symmetry of wetting conditions observed
5. April 23rd, 2007 (GMT 2007-113), VG2-2, S. Williams, Voluntary Science (360° , 360° CCW).
- Successful completion of all revised science run operation and objectives
 - Identified critical angles with high precision
 - Mapped critical de/wetting hysteresis
6. May 11th, 2007 (GMT 2007-131), VG2-3, S. Williams, Voluntary Science (180° CW and CCW, fine increment)
- De/wetting angles in Q1 and Q2 including hysteresis
 - Extra Science run relocating fluid to lid, identified new meta/stable interface configuration for all vane angles
 - Drain procedure reveals unstable film on ellipse walls following a rupture event initiated at the drain exit port
7. June 2nd, 2007 (GMT 2007-153), VG2-4, S. Williams, Voluntary Science (Alternate Interface Experiments)
- Demonstration of three new interface configurations: filament, asymmetric right (vane at 90°), asymmetric left (vane at 0°)

- Interface stability to a variety of input disturbances
8. July 14th, 2007 (GMT 2007-195), VG1-4, C. Anderson, Voluntary Science (Q2 test)
 - CCW 180° to 90°, CW 90° to 180°, and 180° to 90° quick turn
 - Accurate equilibrium data in Q2
 - Identification of critical vane wetting and bulk asymmetric wetting conditions
 9. October 22nd, 2007 (GMT 2007-295), VG1-5, P. Whitson, Voluntary Science (Q3 test)
 - CCW 180° to 270°, CW 270° to 180°, and 180° to 270° quick turn
 - Accurate equilibrium data in Q3
 - Identification of critical vane wetting and bulk asymmetric wetting conditions

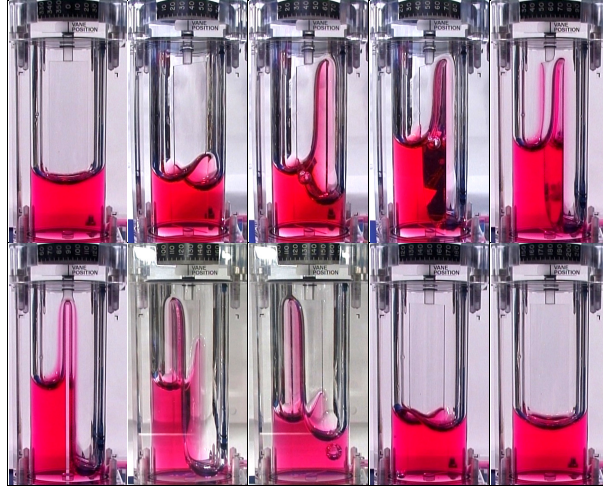
1.4.3 Static Wetting Configurations

The vane dial angle is converted to the absolute acute interior angle α between the vane and the major axis of the ellipse as shown in Figure 1.11. Thus, α in the various quadrants is determined from the vane angle ϕ : For $0 < \phi < 90^\circ$, $\alpha = \phi$, for $90^\circ < \phi < 180^\circ$, $\alpha = 180^\circ - \phi$, for $180^\circ < \phi < 270^\circ$, $\alpha = \phi - 180^\circ$, and for $270^\circ < \phi < 360^\circ$, $\alpha = 360^\circ - \phi$. The quadrant (Q1 through Q4) where the particular wetting occurs is also of concern and tabulated.

Each vane angle produces sub- and/or supercritical wetting conditions for the two vane gaps as shown in Figures 1.12 (VG1 and VG2). Supercritical conditions are characterized by spontaneous corner wetting. In addition to vane gap wetting and dewetting a third wetting regime is observed where the fluid shifts from one side of the vane to the other ($\phi = 53^\circ$, Figure 1.12(a)). A detailed theoretical analysis of this phenomenon has been completed and is presented elsewhere [8]. Experiment repeatability is high ($\pm 1^\circ$), but static interfaces are not always established at angles sufficiently close to the critical angles leading to a range within which the ‘critical angle’ is certainly crossed.

Figure 1.12(a) presents several key interfaces for a 0° to 180° sweep for VG1. The sequence begins with subcritical equilibrium surfaces at 0° and 36° . Small-gap wetting (SGW) is observed at 43° and a complete bulk shift (BS) at 53° where the fluid completely migrates to the left side of the vane. Notice that a bulk shift occurs before large-gap wetting (LGW) which takes place at 59.5° . Small-gap wetting (SGW) and large gap wetting (LGW) along with a complete bulk shift persist at 90° . Large gap dewetting (LGD) occurs at 127.5° followed by a reverse bulk shift (BSR) at 134.5° , and small gap dewetting (SGD) at 150.5° . The original but reflected configuration of 0° returns at 180° .

VG1 critical wetting and dewetting angles α are reported in Table 1.2 for the four quadrants. The data are arranged in order of occurrence: for increasing α ; small gap wetting, bulk shift, large gap wetting, and for decreasing α ; large gap dewetting, reverse bulk shift, and small gap dewetting. When considering all uncertainties these trends are common in all quadrants except in Quadrant 4 where the bulk shift clearly occurs before the small gap wetting. This result signals the certain presence of slight container asymmetries which have been quantified and will be published subsequently. This phenomena was uniquely



(a) Equilibrium interfaces for VG1 for vane dial angles: 0° , 36° , 43° , 53° , 59.5° , 90° , 127.5° , 134.5° , 150.5° , 180° (from top left to bottom right).



(b) Equilibrium interfaces for VG2 for vane dial angles: 0° , 45° , 50° , 58° , 72° , 76.5° , 90° , 120° , 135° , 180° (from top left to bottom right).

Figure 1.12: Equilibrium interfaces for VG1 and VG2 for vane angles between 0° and 180° .

Table 1.2: Critical wetting conditions for VG1: small gap wetting (SGW), bulk shift (BS), large gap wetting (LGW), large gap wetting (LGD), bulk shift reversal (BSR), small gap dewetting (SGD).

	Q1	Q2	Q3	Q4	Theory
SGW	$40.0^\circ \pm 3.0^\circ$	$43.3^\circ \pm 2.3^\circ$	$42.5^\circ \pm 2.0^\circ$	$47.3^\circ \pm 2.3^\circ$	42.94°
BS	$48.0^\circ \pm 5.0^\circ$	$46.3^\circ \pm 0.8^\circ$	$47.5^\circ \pm 2.5^\circ$	$42.5^\circ \pm 2.5^\circ$	-
LGW	$51.8^\circ \pm 0.8^\circ$	$47.3^\circ \pm 2.3^\circ$	$56.0^\circ \pm 3.0^\circ$	$50.8^\circ \pm 3.8^\circ$	51.29°
LGD	$52.8^\circ \pm 1.3^\circ$	$48.0^\circ \pm 2.0^\circ$	$58.3^\circ \pm 6.8^\circ$	$53.3^\circ \pm 4.3^\circ$	51.29°
BSR	$43.8^\circ \pm 7.8^\circ$	$47.0^\circ \pm 2.0^\circ$	$48.3^\circ \pm 1.8^\circ$	$42.3^\circ \pm 2.3^\circ$	-
SGD	$41.8^\circ \pm 5.8^\circ$	$41.0^\circ \pm 0.5^\circ$	$43.0^\circ \pm 2.0^\circ$	$45.8^\circ \pm 0.8^\circ$	42.94°

Table 1.3: Critical wetting conditions for VG2: small-gap wetting (SGW), large gap wetting (LGW), large gap dewetting (LGD), small gap dewetting (SGD).

	Q1	Q2	Q3	Q4	Theory
SGW	$57.8^\circ \pm 2.8^\circ$	$53.5^\circ \pm 3.5^\circ$	$57.0^\circ \pm 4.0^\circ$	$55.0^\circ \pm 3.0^\circ$	53.47°
LGW	$67.5^\circ \pm 5.5^\circ$	$67.5^\circ \pm 5.0^\circ$	$71.3^\circ \pm 5.3^\circ$	$68.3^\circ \pm 6.8^\circ$	62.29°
LGD	$53.8^\circ \pm 8.3^\circ$	$55.0^\circ \pm 8.0^\circ$	$58.3^\circ \pm 8.3^\circ$	$60.0^\circ \pm 10.0^\circ$	62.29°
SGD	$43.0^\circ \pm 5.0^\circ$	$45.8^\circ \pm 7.8^\circ$	$45.5^\circ \pm 5.5^\circ$	$43.8^\circ \pm 8.3^\circ$	53.47°

exploited providing a third dynamic wetting problem could be investigated for a potentially crucial critical wetting condition. Despite the presence of known vane alignment asymmetries, subsequent numerical computations confirm that the bulk shift can occur even for perfectly symmetric containers. These results are perhaps surprising and to be addressed in greater detail in a forthcoming article where both advantages and cautions for such strong dependence of fluid position on such slight changes or asymmetries in container geometry is addressed. Comparisons of experimental and theoretical interfaces are provided in Figure 1.13 for VG1. Theoretical critical angles are listed in Table 1.2. Only SGW and LGW are predicted for the ideally symmetric configurations analyzed.

Figure 1.12(b) provides several key interfaces for a 0° to 180° sweep for VG2. Static subcritical interfaces at 0° and 45° are shown before stick-slip small gap wetting is initiated at 50° and completed by 58° . Large gap wetting begins at 72° and is complete by 76.5° . No bulk shift is observed. Partial large-gap dewetting occurs at 120° and is complete by 135° , where small-gap dewetting begins. Small gap dewetting is complete by 180° . Table 1.3 lists the distilled critical wetting angles in the various quadrants for VG2. Tolerances and asymmetries in VG2 are similar to VG1 but symmetry and order in wetting and dewetting angles are consistent in all quadrants. The hysteresis in wetting behaviors is clear from the table entries. The experimental data is compared with numerical predictions in Figure 1.14 for VG2. Theoretically predicted [8] critical angles are listed in Table 1.3 where applicable.

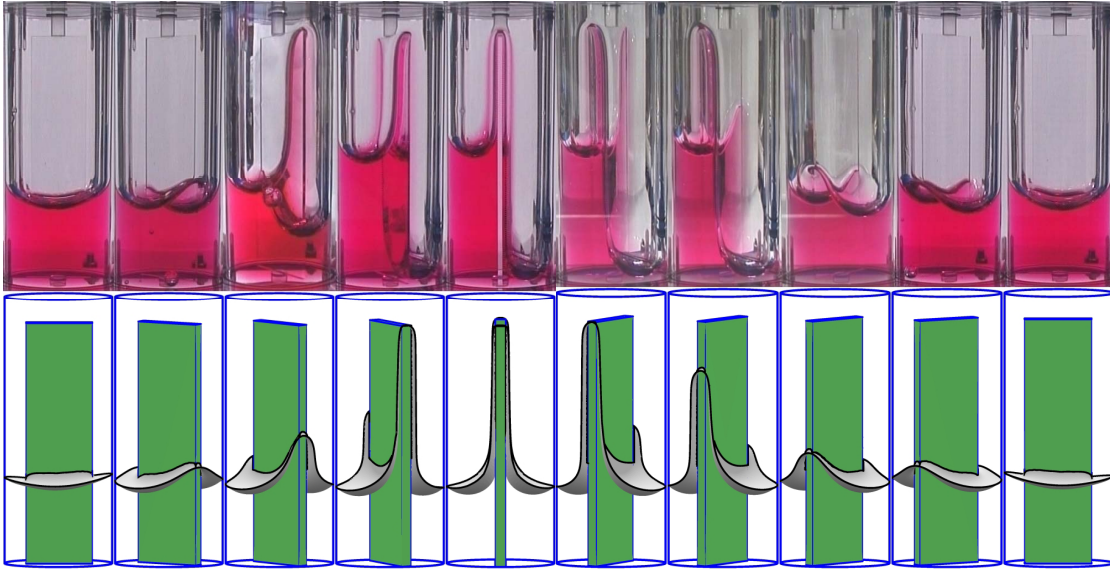


Figure 1.13: VG1 experiment and computations for vane angles: $0^\circ/0^\circ$, $30^\circ/30^\circ$, $43^\circ/45^\circ$, $59.5^\circ/60^\circ$, $90^\circ/90^\circ$, $125.5^\circ/125^\circ$, $131^\circ/130^\circ$, $139.5^\circ/140^\circ$, $150.5^\circ/150^\circ$, and $180^\circ/180^\circ$ (Experiment/*Surface Evolver*).

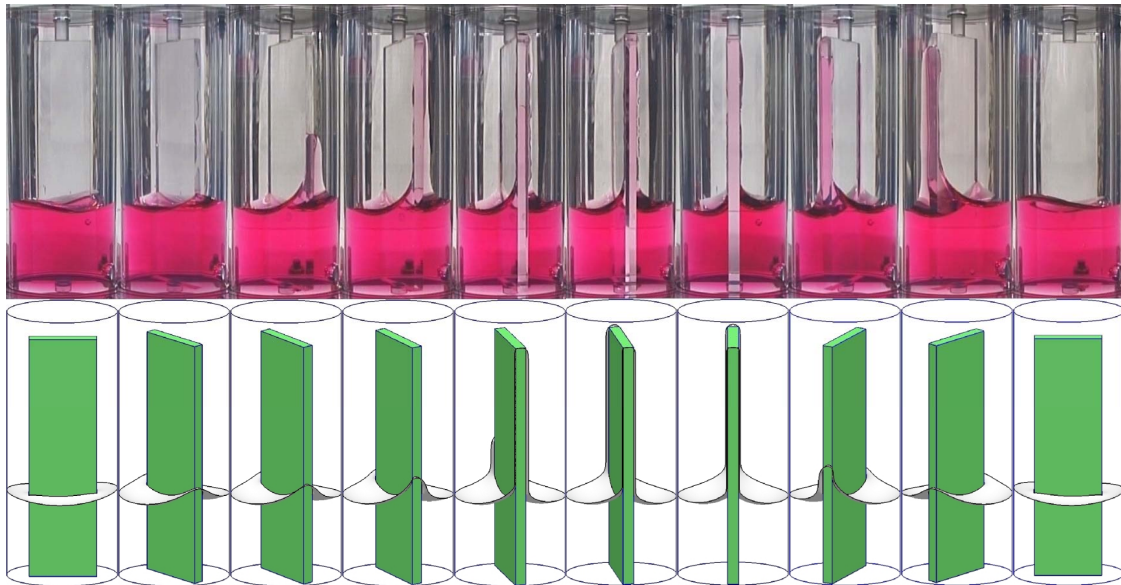


Figure 1.14: VG1 experiment and computations for vane angles: $0^\circ/0^\circ$, $45^\circ/45^\circ$, $50^\circ/51^\circ$, $58^\circ/57^\circ$, $72^\circ/72^\circ$, $76.5^\circ/78^\circ$, $90^\circ/90^\circ$, $120^\circ/120^\circ$, $135^\circ/135^\circ$, and $180^\circ/180^\circ$ (Experiment/*Surface Evolver*).

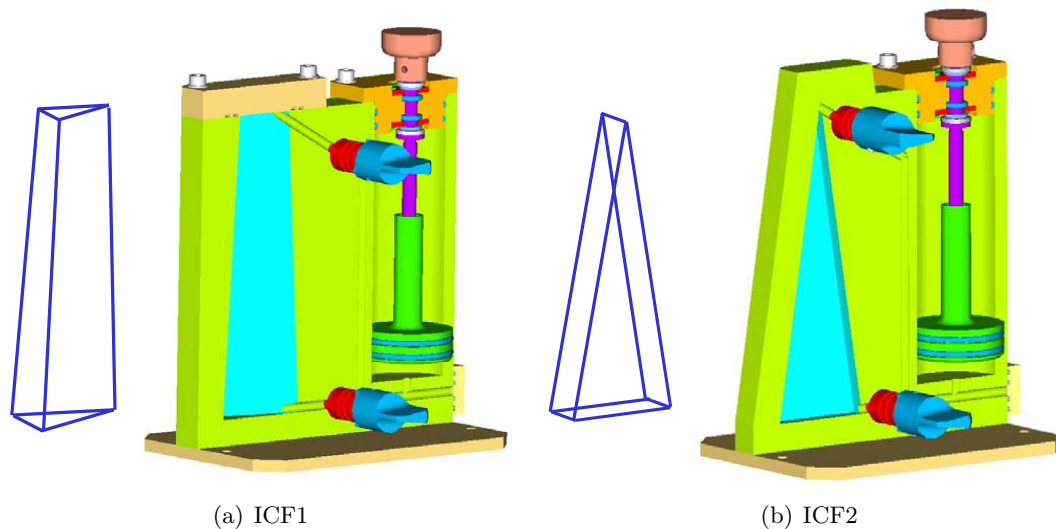


Figure 1.15: Solid model and wireframe representation of ICF1 and ICF2.

1.5 Interior Corner Flow (ICF)

The CFE Interior Corner Flow (ICF) experiments investigate bubble displacement as a result of secondary imbibition in tapered polygonal conduits. The ICF1 vessel has a geometric cross-section of a 30° - 75° - 75° isosceles triangle that tapers uniformly (geometrically similar triangles) as shown in Figure 1.15(a). The height of the triangular cross-section at the base is 40.0mm and at the top is 26.0mm over a height of 127.0mm—all faces tilt at 3.155° . The test fluid is 10ml of 5cs Silicone oil. ICF2 is a rectangular cross-section that tapers on two faces to a line as shown in Figure 1.15(b). The base rectangle measures 40.0mm wide by 10.0mm deep. The two faces tilt at 8.95° over a height of 127.0mm. The test fluid is 9.02ml of 2cs Silicone oil.

The basic operation of the experiment is as follows: the fluid is injected into the tapered test chamber from the reservoir. During injection, the fluid immediately wicks along the corners toward the vertex. A transition in the flow takes place once the liquid reaches the vertex. This secondary imbibition appears like a bubble migration where the ullage or ‘bubble’ migrates toward the base, an example of which is shown in Figure 1.16 for ICF2. The leading and trailing menisci are labeled in the figure as z_2 and z_1 , respectively. The bubble migration continues until the leading interface reaches the end of the conduit, the flow ceasing shortly thereafter. The experiment may be ‘reset’ to the initial state by manipulating the valves and reservoir piston or by using a centrifuge method to return the fluid to the base of the container. Either method permits the experiment to be re-run indefinitely. The four variations of the experiment are referred to as Dry, Wet, Open Loop, and Bubbly tests and defined below:

Dry: These tests are characterized by little to no liquid film on the interior surfaces during the flow. This situation occurs during the first run of the experiment since the interior surfaces are initially completely dry. However, during repeat tests, a thin prewetting

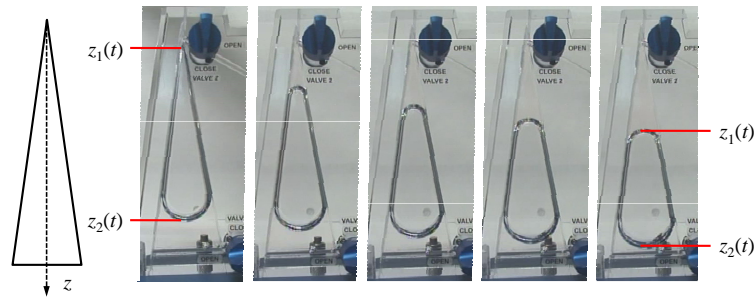


Figure 1.16: Image sequence of ICF2 bubble migration where each image is approximately 60 seconds apart.

film is present but the fluid behaves essentially identically to the initially dry test. Thus, all such tests are classified as ‘Dry’. These test conditions are achieved when using the valves and reservoir piston to reset the experiment.

Wet: When the fluid is manually returned to the base of the tapered section using a centrifuge method, significant liquid films remain on the interior walls that drain slowly. The presence of these thick films increases capillary flow rates. Such tests are classified as ‘Wet’.

Open Loop: For these tests the valves are opened permitting a parallel counter clockwise flow between the base and vertex through a bypass conduit. The ‘Open Loop’ tests are considered a subset of the Wet condition due to the moderately thick films established before each test.

Bubbly: The fourth event type is called ‘Bubbly’ flow which is a repeat of previous tests but with numerous bubbles in the fluid. A variety of bubble sizes are created by vigorously shaking the container, resetting the fluid to the base, and then allowing the flow to proceed passively. These tests are also a subset of the Wet condition due to the presence of thick films. The flow with entrained bubbles demonstrates the passive phase separation capability of such geometries and is used for theory development.

1.5.1 ICF Flight Operations Summary

CFE ICF was performed 4 times aboard ISS by astronauts M. Lopez-Alegria (1) and S. Williams (3) on Expeditions 14 and 15 between August 28th, 2004 and November 16th, 2007. The highlights of each operation are outlined below:

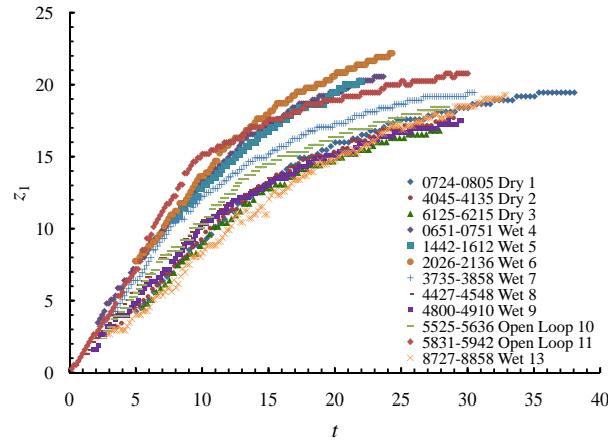
1. March 10th, 2007 (GMT 2007-069), ICF1-1, M. Lopez-Alegria, Nominal Science Run
 - Successful completion of all science objectives for first half of crew procedures
 - Completed dry fill and two wet fill tests
 - Low liquid volume limiting experiment duration observed

2. April 7th, 2007 (GMT 2007-097), ICF1-2, S. Williams, Voluntary Science (all nominal operations)
 - Successful completion of all revised science run operation and objectives
 - Demonstration of centrifugal method to rapidly redeploy liquid
 - Provision of critical data for global fluid reorientation
 - Demonstration of high Loop test flow rates
 - Demonstration of passive bubble separations
3. April 29th, 2007 (GMT 2007-119), ICF2-1, S. Williams, Voluntary Science (Complete nominal operations: Dry, Wet, Open Loop and Bubble tests)
 - Demonstration of centrifugal method to rapidly re-deploy liquid
 - Variety of large bubble migration/separation tests resulting from lateral excitations
 - Variety of small bubble migration/separation tests resulting from vigorous axial excitations
 - Demonstrated clear ability of corner flows to filter, separate, and coalesce bubbly two-phase systems passively
 - Coarsening was also observed for most cases involving multiple bubbles and long flow times
4. May 12th, 2007 (GMT 2007-132), ICF2-2, S. Williams, Voluntary Science
 - Additional Wet and Bubbly tests
 - Small numbers of large bubble interactions observed (smaller bubbles overtake and merge with larger bubbles)

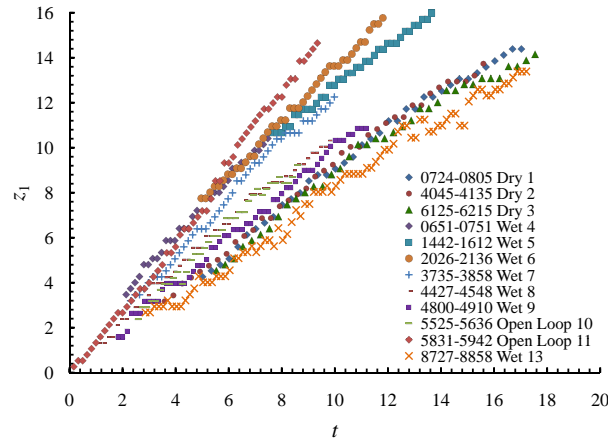
1.5.2 ICF1 Results Summary

A low volume of low viscosity fluid in the vessel permitted only limited duration data collection for the leading interface z_2 before it reached the base of the container. Even for the trailing meniscus z_1 , less than 20 seconds of ‘clean’ data could be obtained for the trailing interface before base effects became dominant. This trend is evident in Figure 1.17(a) which plots the full duration for the trailing interface z_1 . Figure 1.17(b) presents the first 20s where nearly linear trends are observed. The characteristic time scale computed from the theoretical model developed during the flight of the ICF experiments is ~ 680 assuming a virtual vertex [9], whereas the total experimental flow time is less than 40s. Thus, the data in effect represent only a snapshot of the intended idealized flow rather than a long-time characterization. However, for the ‘snapshot’ in Figure 1.17(b), the data is linear and can be thought of as a local derivative of the long-term behavior.

From Figure 1.17(b) it is immediately obvious that the results vary depending on the test type. In general, the Open Loop tests produce the highest flow rates followed by Wet and then Dry conditions. The flow rates are somewhat sporadic between event types; however, the Open Loop, Wet, and Dry cases produce average dimensional trailing meniscus velocities



(a) Full Duration



(b) Truncated Linear Regime

Figure 1.17: Complete data set for the ICF1 trailing interface.

of 1.37, 1.06, and 0.85mm/s, respectively. The linear trailing meniscus velocities for the various tests are non-dimensionalized (by way of an asymptotic theoretical analysis [9] to be published in greater detail elsewhere) and listed in Table 1.4. For the fluid properties and geometry of ICF1 the analytic dimensionless velocity is 1.52. The Open Loop, Wet, and Dry average dimensionless velocities are 2.33, 2.09, and 1.64, respectively. The most favorable agreement with the present theory is fortunately with the most applicable Dry tests yielding an average error of 7.3%. A complete set of comparisons can be found in Table 1.4 which includes dimensional and non-dimensional linear fit coefficients as well as statistical R^2 values and % error calculations with respect to the dimensionless analytic estimate.

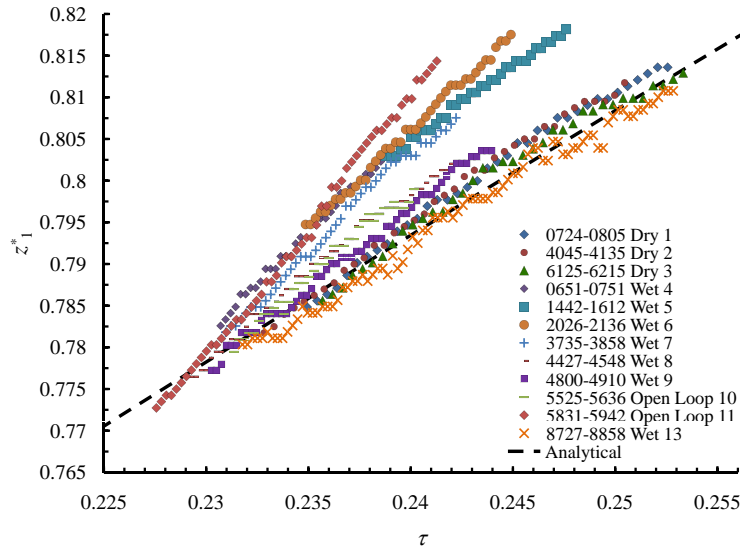


Figure 1.18: Comparison of dimensionless experimental results with theory.

1.5.3 ICF2 Results Summary

Unlike the underfilled ICF1 vessel, the ICF2 tests produced long-duration flow events lasting up to 7 minutes for trailing z_1 meniscus and nearly 4 minutes for leading z_2 meniscus. Figure 1.19 presents both z_1 and z_2 on a single plot with the conduit drawn at left to scale. As with ICF1, Dry, Wet, Open Loop, and Bubbly test are conducted. Approximately three distinct rates are obvious with Wet and Dry test behaving similarly, with Bubbly tests flowing faster and the Open Loop tests even faster. The Bubbly flows progress at a rate slightly greater than the Wet/Dry rate due to bubble coalescence which has been since addressed theoretically and will be addressed in a subsequent publication. An expanded scale of the leading and trailing interfaces can be found in Figure 1.20(a) for z_1 and Figure 1.20(b) for z_2 .

The initial Dry run produces a curve fit of $z_1 = 6.32t^{0.40}$ whereas Wet fits are $z_1 = 6.21t^{0.40}$ and $z_1 = 7.22t^{0.38}$. The rates are very similar, but if the two Wet rates are averaged they are slightly higher than the Dry rate, which is expected. The single Bubbly flow produces a curve fit of $z_1 = 5.18t^{0.44}$ and a rate which is always slightly higher than the Dry and Wet rates. During the bubble flows, bubbles are forced into the corner with only the smallest bubbles ($< 0.7\text{mm}$ diameter) passing without coalescing. The Open Loop power-law curve fits reveal higher rates, $z_1 = 13.91t^{0.30}$ and $z_1 = 16.00t^{0.27}$, than the other test types. The leading meniscus z_2 is shown in Figure 1.20(b) on an expanded scale. The curves are linear over the larger time scale, with R^2 values very near 1 when fit with linear regressions. Trends for z_2 are similar to those reported for z_1 , with the hierarchy of migration rates being the same.

In preliminary summary of the CFE ICF experiments, it appears that the geometric impact of ICF-like tapered polygonal sectioned containers can be reasonably and explicitly predicted [10]. This implies that systems can be designed to provide desired pumping

Table 1.4: Dimensional and dimensionless linear fit coefficient with R^2 statistics for ICF1 including % error with the theoretical dimensionless coefficient of 1.52.

Data Name	Dim'l Slope (mm/s)	Dim'less Slope	% Error	R^2
0724-0805 Dry 1	0.86	1.66	9.20%	0.9913
4045-4135 Dry 2	0.89	1.72	13.2%	0.9945
6125-5215 Dry 3	0.80	1.55	2.00%	0.9825
0651-0751 Wet 4	1.28	2.47	62.5%	0.9952
1442-1612 Wet 5	0.91	1.77	16.5%	0.9944
2026-2136 Wet 6	1.20	2.31	52.0%	0.9964
3735-3858 Wet 7	1.22	2.37	56.0%	0.9922
4427-4548 Wet 8	1.05	2.03	33.6%	0.9941
4800-4910 Wet 9	1.00	2.17	42.8%	0.9844
5525-5636 Open Loop 10	1.12	1.94	27.6%	0.9954
5831-5942 Open Loop 11	1.61	3.12	105%	0.9958
8727-8858 Wet 13	0.79	1.53	0.66%	0.9889

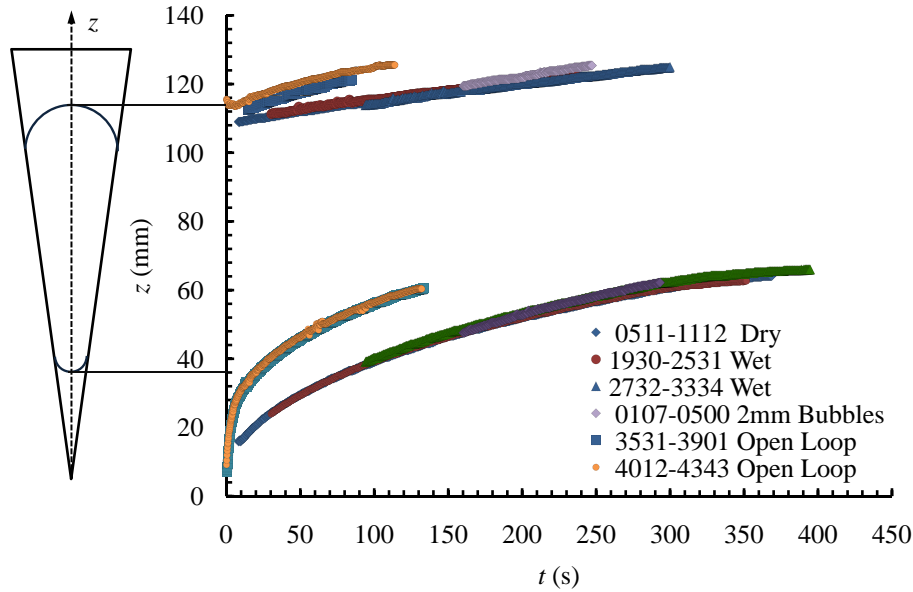
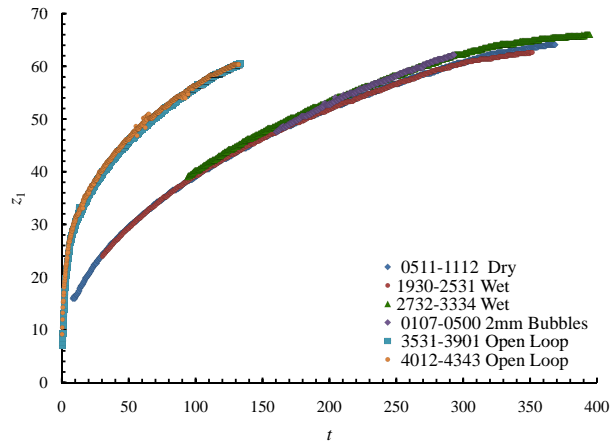
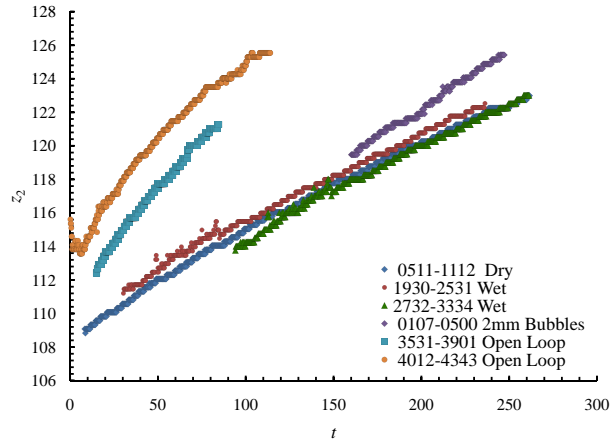


Figure 1.19: ICF2 data for z_1 and z_2 for Dry, Wet, Open Loop, and Bubbly flows with the conduit geometry drawn to scale at left.



(a) Trailing Interface z_1



(b) Leading Interface z_2

Figure 1.20: ICF-2 data representing the z_1 interface under various experimental conditions.

rates for a variety of applications including low speed bubbly flow separations. For such calculations the desired flow rate would be used as an input and the container geometry would be ‘derived’. Ground-based applications for such a method are also relevant to microfluidics phenomena.

1.6 Conclusion

The fact that such simple experiments can yield enough quantitative data to support fundamental and applied numerical and theoretical investigations argues well in support of continued efforts by space entities to pursue simple experiments benefitting from crew interest and interaction. Arguably more important, intricate, and automated experiments are of higher priority, but such small experiments can fit flexibly into time lines and even be conducted during the crew’s free time if desired (up to 50% of CFE was conducted in this manner). At least three journal articles are expected from the CFE work and several

of the tools developed to analyze the flows have been employed in advanced life support systems [11]. Several follow-on CFE-like experiments have been proposed to and are under development by NASA. The experiments are called CFE-2 and consist of refurbished CFE hardware as well as new builds. The experiments themselves focus on critical geometric wetting in systems with a wide disparity in capillary length scales using the CFE VG approach, and a family of weakly 3-D capillary conduits capable of passive phase separations relevant to liquid processing on spacecraft—akin to CFE ICF. The new hardware exploits design guides developed during this investigation.

Chapter 2

CFE Contact Line Details

Summary. The Contact Line (CL) Capillary Flow Experiments are part of the suite of low-g experiments flown onboard the International Space Station to observe the impacts of various conditions at the moving contact line for fluid interfaces in circular cylindrical containers. An ample CL review aboard ISS was presented in 1 and more may be found in [3], as well as in Appendix 7, but additional non-overlapping details are collected here that might prove of use to subsequent researchers interested in using either the raw or digitally reduced data. The chapter provides a minor review of the CL experiment hardware before discussing details of specific tests, data reduction methods, results, and more in depth comparisons of the experiments and the sample numerical benchmark investigation.

2.0.1 Hardware Review

CL-1 and CL-2 are identical in all respects except for surface coating, contact angle, Pinning lip location, and maximum fluid volume. A single container is composed of four chambers, with two serving as reservoirs and two as test chambers as shown in Figure 2.1. The reservoirs store the liquid when the experiment is not being operated. Figure 2.2 along with Table 2.1 identifies the critical dimensions.

The test chambers are composed of circular cylinders with ellipsoidal lids. The height of the cylinders from the base of the container to the top (excluding the lid) is 146.0mm. The

Table 2.1: CL physical dimensions, maximum fluid volumes, and refractive index.

Physical Dimensions	
Pinning Lip Width, w_{pl} (mm)	7.6 ± 0.1
Cylinder Height, H_c (mm)	146.0 ± 0.1
Cylinder Diameter, D_c (mm)	38.10 ± 0.05
Pinning Lip Diameter, D_{pl} (mm)	43.7 ± 0.1
Acrylic Refractive Index, N_{acr}	1.491
$\theta = 48.7^\circ$ (CL1)	
Base to Pinning Lip, h_{pl} (mm)	36.9 ± 0.1
Maximum Fluid Volume (mL)	39.04
$\theta = 0^\circ$ (CL2)	
Base to Pinning Lip, h_{pl} (mm)	50.8 ± 0.1
Maximum Fluid Volume (mL)	43.44

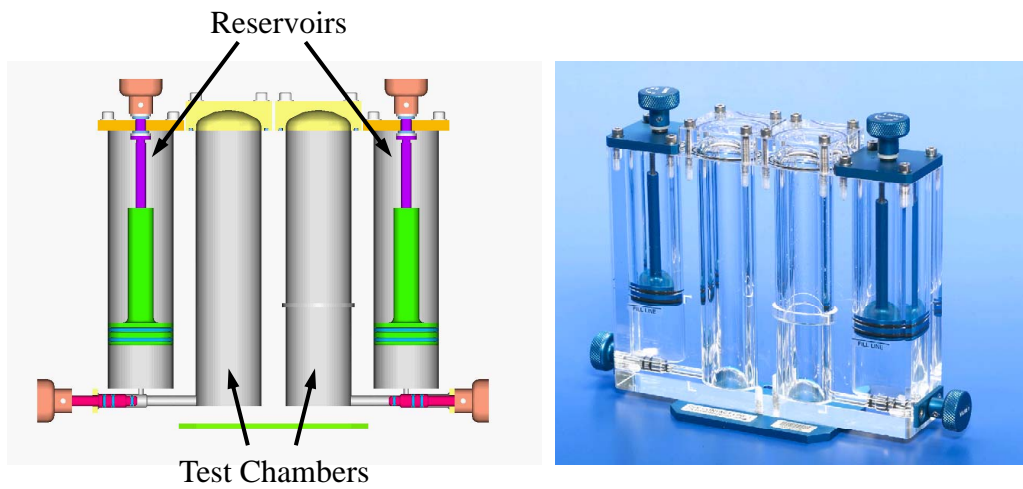


Figure 2.1: A solid model (left) and image (right) of the CL2 vessel.

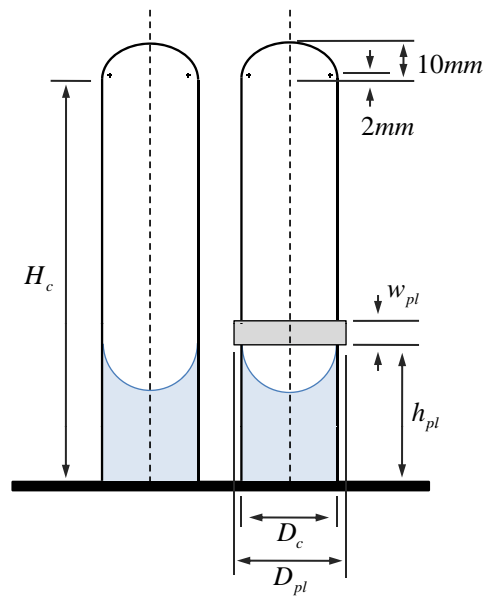


Figure 2.2: CL schematic indicating significant physical dimensions (drawn to scale for CL2).

diameter of both cylinders is 38.1mm with the Pinning lip diameter measuring 43.7mm. The location of the Pinning lip h_{pl} differs between CL1 and CL2 where the distances are 36.9 and 50.8mm, respectively. Maximum fluid volumes are 39.04mL for CL1 and 43.44mL for CL2.

Chemical coatings are applied to the test chambers in an effort to produce partial wetting in CL1 and enhance liquid control in CL2. The entire interior surface of CL1 is rinse coated with FC-724¹, a transparent fluoro-polymer surface coating manufactured by 3M Corporation. CL2 is intended to be perfectly wetting ($\theta = 0^\circ$) and only select surfaces are coated in an attempt to better control the liquid during operation. Coating is applied to CL2 above the Pinning lip, including the ellipsoidal cap and inside the groove of the Pinning edge itself. Its application above the Pinning lip promotes a passive return of the liquid as successfully demonstrated during the flight. Coating inside the Pinning lip deters liquid from flooding it. The coated surfaces are identified in Figure 2.3 for CL1 and CL2.

The equilibrium contact angle for Silicone oil on an FC-724 coated surface is determined by measuring the advancing and receding contact angles using a tilted FC-724 coated glass capillary tube [1]. Using the advancing and receding contact angles of $\theta_{rec} = 47.3^\circ \pm 2^\circ$ and $\theta_{adv} = 52.2^\circ \pm 2^\circ$ the equilibrium angle of $\theta_{eq} = 48.7^\circ \pm 2^\circ$ is calculated [2], which is similar to that of certain aqueous systems. All internal surfaces of CL1 are rinse coated, thus the expected equilibrium contact angle is 48.7° and is reported as such when referring to the experiment. Empirical measurements suggest that a lower contact angle is actually produced and is discussed in Section 2.5. Several key surfaces of CL2 are not coated and exhibit a perfectly wetting condition $\theta = 0^\circ$, which is similar to that of many liquid fuels and propellant for spacecraft. These contact angle values along with general fluid properties are listed in Table 2.1.

Contact angle measurements could also be made during the flight tests. For example, the contact angle is measured in each event using a simple method of measuring the meniscus diameter and distance between the contact line and lowest point of the meniscus (at the centerline). If D_c is the cylinder diameter and h_m is the meniscus height, then the contact angle is calculated from

$$\theta = \sin^{-1} \left(\frac{D_c - 2h_m}{D_c} \right). \quad (2.1)$$

Optical distortion does not affect the measurements due to the locations at which they are taken.

2.1 Various CL Procedures

As stated, the CL experiments are hand-operated, requiring disturbances to be imparted manually by the astronaut. Disturbances are applied to the containers followed by a quiet time where the fluid is allowed to passively settle.

2.1.1 Setup Procedure

Once the experiment is set up on the MWA (as shown in Figure 1.1), the fluid in the reservoirs must be dispensed into the test chambers. This is achieved by opening a valve

¹3M has replaced Fluorad coating FC-724 with NovecTM Electronic Coating EGC-1700.

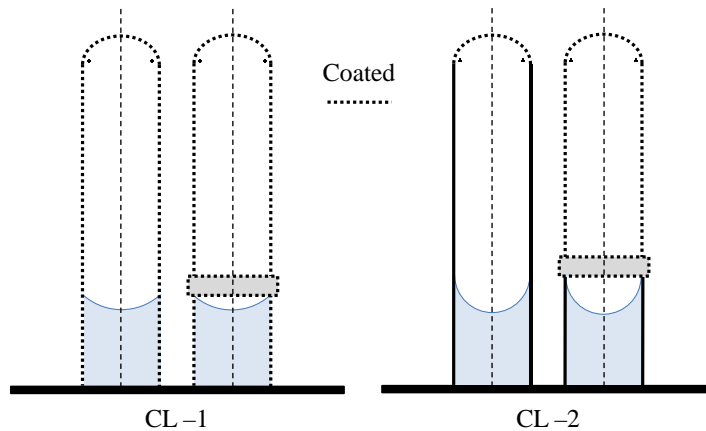


Figure 2.3: FC-724 coating conditions for CL1 and CL2, where dashed lines indicate surface coating.

and turning the fill knobs counter-clockwise, which displaces a piston, pushing the fluid into the test chambers (reference Figure 2.1). The fill knob can be turned clockwise, reversing the piston, returning the fluid back into the reservoirs. Not only is this the method of placing fluid into the test chambers, but also of adjusting the fill level. The fluid depth κ is the measure of fill level and is defined as the distance from the centerline of the interface to the bottom of the test cylinder (see Figure 2.2). Though the fill level can be modified by operating the fill knobs, it also changes passively as fluid is thrown up the cylinder walls after large disturbances. This is most pronounced in the Smooth cylinder of CL2 and is discussed in greater detail in Section 2.7.3. In general, all of the fluid in the reservoirs is pushed into the test chambers unless depth effects are being investigated. Fluid depth changes were also employed during CL1 tests and will be discussed on connection with a CL1 wetting anomaly in Section 2.1.3.

2.1.2 Interface Depinning and Recovery

As disturbance amplitudes increase, the Pinning surface may destabilize, the Pinning lip may ‘flood’, and the fluid fill the Pinning lip groove—effectively eliminating the ‘Pinned’ contact line boundary condition. The result is a condition very similar to the Smooth cylinder with the fluid behaving similarly in disturbance waveform, frequency, and damping rate. Flooding of the Pinning lip is loosely referred to as depinning. It is always the case for CL2 that depinning leads to the flooding condition. Figure 2.4 represents an image sequence of two Push disturbances where the Pinning lip is flooded after two events.

The experiment is designed to investigate the effects of Smooth and Pinning boundary conditions when subjected to an identical disturbance. With the Pinning lip flooded this is not possible, as both interfaces behave as if they were in Smooth cylinders; this creates twice as much data for investigating an effectively Smooth boundary condition, but detracts from the primary objective. For this reason, a procedure for clearing the liquid from the Pinning lip was developed by several astronauts on orbit (in order M. Fincke, W. McArthur,



Figure 2.4: A depinning event is depicted where the first Push disturbance causes the Pinning lip to partially flood (top sequence left to right) followed by a second disturbance causing a complete depinning (bottom sequence left to right).

J. Williams) and was perfected by astronaut Jeff Williams. The final procedure involves partially draining the Pinning Cylinder, removing the CL vessel from the MWA, and providing a combination of impulsive and centrifugal forces great enough to dislodge the liquid from the pinning edge and drive it to the base of the container. The centrifugal force is created by moving the vessel back and forth in a radial fashion. The impulsive force is created by hitting the container. Combined, the motion is much like the playing of a tamborine. Depinning events occurred many times for the CL2 vessel and only once during the last operation of CL1 by Peggy Whitson. Clearing the Pinning lip was significantly easier for CL2 due to the favorable wetting gradient and lower contact angle. It was found that CL1 required considerable centrifugal and lateral force to reset the experiment, so much in fact, that the force exerted by the astronaut resulted in physical damage to CL1 vessel. Interestingly, in both CL experiments the Pinning lip surface was coated ($\theta \sim 48.7^\circ$). For CL2 a discontinuous wetting gradient occurs between the Pinning lip and the surface below it where $\theta = 0^\circ$. The result is that the liquid desires to be below the Pinning lip where the contact angle is lower making it is easier to clear the liquid. For CL1 all internal surfaces are coated and no gradient exists in the Pinning cylinder, resulting in only partial success in clearing the Pinning lip, due to the large forces required.

2.1.3 Wetting Anomaly in CL1 Smooth Cylinder

Despite application of the coating in a clean room environment, the wetting characteristics of the CL1 Smooth cylinder exhibited unexpected behavior requiring changes to the in-flight procedures. CL1 is designed to be a partially wetting experiment with all internal surfaces coated with FC-724. However, the Smooth cylinder appeared to exhibit nonuniform wetting properties along the walls near the base of the container only (ref. Fig. 1.10).

With the maximum volume of liquid in the test chamber the interface assumed an

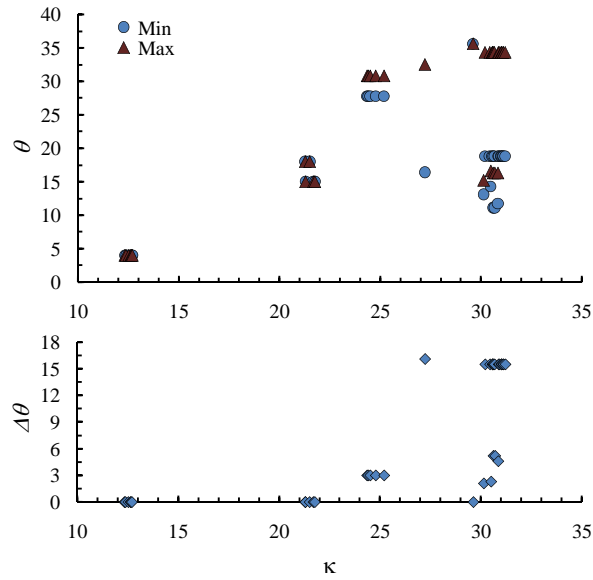


Figure 2.5: The upper plot represents the measured contact angle θ as a function of fluid depth κ , while the lower plot indicates the difference in measured contact angle $\Delta\theta$ in a single event due to asymmetry.

asymmetric configuration. After several perturbations of the cylinder, the interface settled to a nearly symmetric orientation where $\theta \approx 10^\circ$ – 16° . The fill level was then dropped slightly and a new symmetric contact angle of $\approx 36^\circ$ could be determined. Following two perturbations of the cylinder, the interface became asymmetric again taking on values that varied circumferentially between 16° and 33° . The liquid level was finally dropped to a point where $\theta = 4^\circ$, similar to a perfectly wetting (or uncoated) condition. Figure 2.5 indicates this trend where the fluid depth versus the measured contact angle is plotted. The ‘Min’ and ‘Max’ values account for the asymmetry that occurs during specific events, with the lower plot presenting the difference. Significant asymmetries occur near depths of 30.5mm and 27.2mm while symmetric interfaces occur at 29.6mm and below 22mm. The Smooth cylinder for CL1 was dropped to a fill level below 22mm for more than 72% of the events so that a consistent and symmetric interfaces were established. The cause of the wetting anomaly is not exactly known; however, a rough surface due to local crazing (observed pre- and post-flight), a poorly applied coating, or aging during the extended storage (~ 2 years) of the vessel may all be factors. The Pinning cylinder did not produce any wetting anomaly and was stored for the same length of time as the Smooth cylinder. In addition, the coating above the maximum fill level seemed to function properly. The most likely causes of the wetting anomaly seem to be either due to manufacture or improper application of the coating.

Discovery of the wetting anomaly during flight experiments required a special procedure to create both Pinning and Smooth boundary conditions at the prescribed contact angle. The Pinning cylinder was used to create both boundary conditions by changing the depth of the fluid. The Pinning condition is created as usual by filling the cylinder with

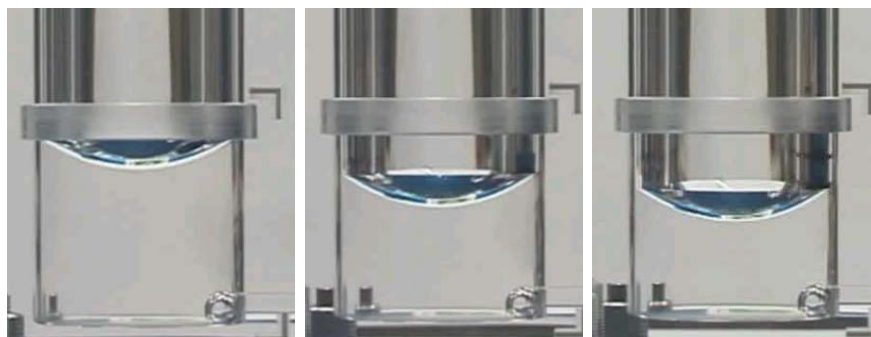


Figure 2.6: A Pinning and Smooth boundary condition were created with the right cylinder by modifying the fill level.

fluid to the Pinning lip, while a ‘Smooth condition’ is created in the Pinning cylinder by withdrawing liquid dropping the contact line below the Pinning lip as shown in Figure 2.6. Such conditions are referred to in the datasheets as ‘Pinned’ when filled and ‘Below Pin’ when the interface is dropped below the Pinning lip. There are at least two disadvantages caused by the procedure. The first is the introduction of a depth effect due to the change in interface height location. This was more pronounced in lateral/slosh disturbances (e.g. Push), but not of consequence for Axial disturbances as discussed in Section 2.5.1. The second disadvantage is that simultaneous responses to identical disturbances for Pinning and Smooth conditions could not be studied. Nonetheless, a large amount of data could be collected such that several similar disturbances were imparted that can be adequately compared, as is done in Section 2.5.

2.2 Data Processing and Preparation

The most generally useful data for follow-on investigations by independent researchers is the CFE CL video library available for download at <http://cfe.pdx.edu>. This data can be analysed in any manner desired by the user. However, for the data reduced in this effort a certain procedure was developed and followed. For example, the flight video for CL was cut, formatted, organized, optically corrected, and digitized for preliminary analysis. Formatting the video is the same process across all CFE tests and is detailed in Section 7.1. The basic process involves the conversion: MPEG-2 \rightarrow MPEG-1 \rightarrow 24-bit uncompressed AVI. Documenting, classifying, and organizing over 400 events requires a strict methodology that was outlined in Section 1.3.6 with further details provided here.

2.2.1 Scale Factor Details

CL requires the astronaut to visually align the vessel perpendicular to the camera. This is of course not always possible, especially during the manually imparted disturbances. For this reason a more dynamic scale factor is employed. To account for certain but small out-of-plane motion, three points are used and a ‘scale factor plane’ is created, both before and after the imparted disturbance. In general, the mathematical plane is derived by measuring

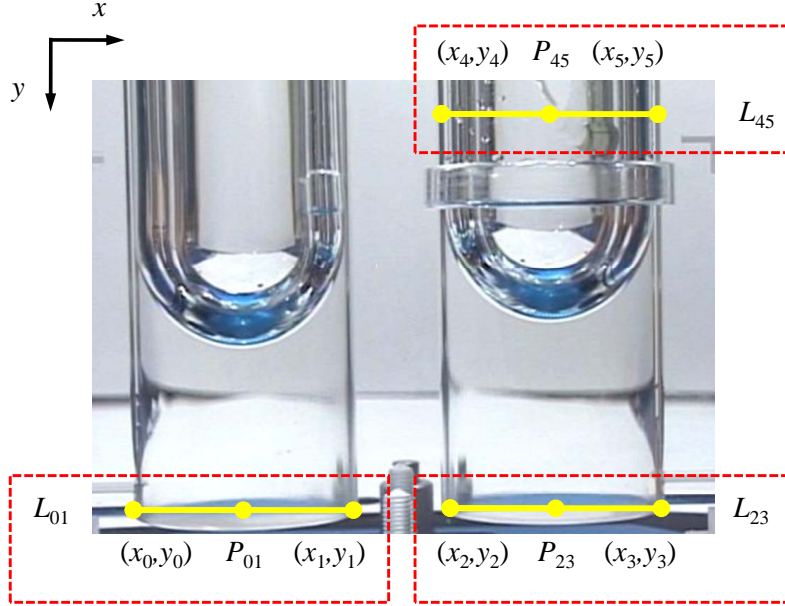


Figure 2.7: Typical measurement locations for determining the scale factor plane and notation.

the diameter of the cylinder in three different locations. In some cases the distance from the bottom of the Pinning cylinder to the bottom of the Pinning lip (distance h_{pl} , see Figure 2.2) is used if the Pinning cylinder is partially out of view and a measurement of the diameter cannot be obtained. Though rare, this generally occurs during lateral motion where the vessel is moved partially out of the camera field of view. Figure 2.7 depicts typical measurement locations and nomenclature. The endpoints of each line are recorded and the midpoint and length are calculated. The line length is used to calculate a local scale factor in the vicinity of the line. The line L_{01} endpoints are denoted as (x_0, y_0) and (x_1, y_1) with midpoint

$$P_{01} = \left(\frac{x_0 + x_1}{2}, \frac{y_0 + y_1}{2} \right) = (x_{01}, y_{01}), \quad (2.2)$$

and line length

$$L_{01} = \sqrt{(x_0 - x_1)^2 + (y_0 - y_1)^2}. \quad (2.3)$$

L_{01} is used to calculate the scale factor at point P_{01} , where

$$SF_{01} = \frac{\ell}{L_{01}}. \quad (2.4)$$

The parameter ℓ represents the true length of the object being measured (typically cylinder diameter). SF_{01} is determined in units of mm/pixel. Point (P_{01}, SF_{01}) is calculated with two additional points to construct a scale factor plane. Points (P_{23}, SF_{23}) and (P_{45}, SF_{45}) are calculated in the same manner as the '01' line. The scale factor plane is described by

$$SF = ax + by + c \quad (2.5)$$

where a , b , and c are found by solving the system

$$SF_{01} = a x_{01} + b y_{01} + c \quad (2.6)$$

$$SF_{23} = a x_{23} + b y_{23} + c \quad (2.7)$$

$$SF_{45} = a x_{45} + b y_{45} + c. \quad (2.8)$$

Simultaneous solution of the system yields coefficients

$$a = \frac{-SF_{23} y_{01} + SF_{45} y_{01} + SF_{01} y_{23} - SF_{45} y_{23} - SF_{01} y_{45} + SF_{23} y_{45}}{-x_{23} y_{01} + x_{45} y_{01} + x_{01} y_{23} - x_{45} y_{23} - x_{01} y_{45} + x_{23} y_{45}} \quad (2.9)$$

$$b = \frac{SF_{23} x_{01} - SF_{45} x_{01} - SF_{01} x_{23} + SF_{45} x_{23} + SF_{01} x_{45} - SF_{23} x_{45}}{-x_{23} y_{01} + x_{45} y_{01} + x_{01} y_{23} - x_{45} y_{23} - x_{01} y_{45} + x_{23} y_{45}} \quad (2.10)$$

$$c = \frac{SF_{01} (x_{23} y_{45} - x_{45} y_{23}) + SF_{23} (x_{45} y_{01} - x_{01} y_{45}) + SF_{45} (x_{01} y_{23} - x_{23} y_{01})}{-x_{23} y_{01} + x_{45} y_{01} + x_{01} y_{23} - x_{45} y_{23} - x_{01} y_{45} + x_{23} y_{45}}, \quad (2.11)$$

which are used in turn to determine the scale factor plane given by Equation (2.5). The plane is constructed twice per event: once before the input disturbance, and once after the input is complete. This corrects the scale factor after the input, which may have moved out of the original plane. Every data point recorded in pixels is scaled over the entire plane using Eq. 2.5. Scale factor values determined in this way range between 0.18mm/pixel and 0.25mm/pixel with an average value of 0.20mm/pixel for the wide variety of experiments performed. Tracking is accurate to ± 0.5 pixels, thus oscillations are tracked with between $90\mu\text{m}$ and $125\mu\text{m}$ resolution (standard deviation of $\pm 100\mu\text{m}$ resolution). Differences in scale factor are attributed to the field of view and zoom of the camera, which are variably established by the astronaut during set-up.

The scale factor plane is used to determine the out-of-plane motion. The plane can be thought of as being flush with the front face of the vessel. If multiple planes are constructed at different times, then rotation and translation of the vessel can be computed. Significant out of plane translation is not a significant factor in any of the events analyzed (except Swirl) as the vessel is constrained by a setscrew fastened in a slot. Rotation, however, is a possible factor and is computed by finding the angle between the two scale factor planes,

$$\vartheta = \cos^{-1} \left(\frac{\overrightarrow{SF_1} \cdot \overrightarrow{SF_2}}{\|\overrightarrow{SF_1}\| \|\overrightarrow{SF_2}\|} \right) \quad (2.12)$$

which is the angle of rotation between vectors $\overrightarrow{SF_1}$ and $\overrightarrow{SF_2}$ representing two scale factor planes calculated using Equation (2.6). Push, Slide/Slosh, Multi-Slide, and Swirl mode disturbances have the potential to rotate, while Axial mode rotation is not possible. Scale factor coefficients are reported twice for every event and can be used to compute the rotation angle before and after the input. Spot checks of the data have indicated that the rotation angle before and after the input is, in general, negligible.

2.2.2 Digitization Techniques

Before digitizing, the video is converted to a suitable format through a series of steps outlined in Section 7.1 including the NASA-developed Spotlight image analysis tool [5]. Spotlight

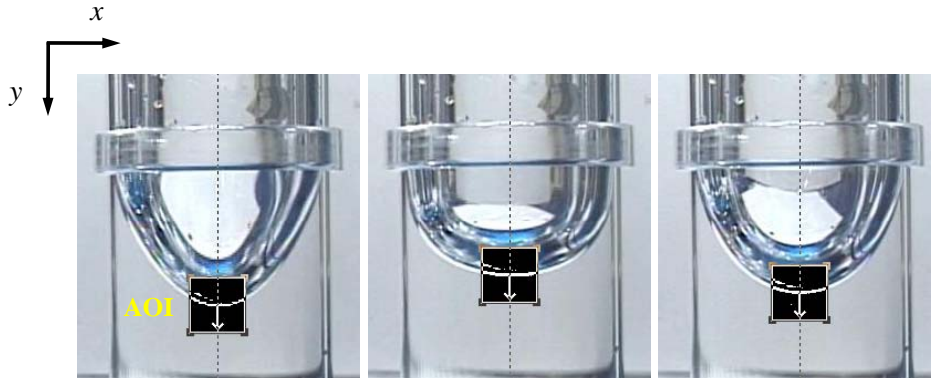


Figure 2.8: Axial response showing Threshold AOI tracking in Spotlight-8.

uses an Area of Interest (AOI) tracking method where image processing is performed on a specified area and a tracking technique is applied. In general, automated ‘Threshold’ tracking is preferred. When this method fails manual tracking is used.

For each event, an input disturbance, Smooth and Pinning cylinder dynamic interface response² are tracked with a small overlap (generally less than 10 frames or 0.3s) between the end of the input and beginning of the response. The video frame rate is 29.97fps resulting in a time step of ≈ 0.03 s.

2.2.3 Tracking Method—Axial Mode

Axial mode input and fluid response are the simplest to track. Rotation and translation of the vessel during input is not a concern as the container is rigidly mounted to the MWA. The input is tracked along a straight line on a feature that is fixed to the CL vessel with the choice of location often an issue of favorable lighting. Example tracking locations include: the bottom of cylinder, the setscrew, any of four white bracket stickers affixed to face of vessel, or other locations. All tracking locations and methods are documented in each event’s datasheet and can be recreated by the user.

The response for both Smooth and Pinning cylinders is tracked at the center of the cylinder/interface as represented by the x -locations of P_{01} and P_{23} in Figure 2.7. When tracking Axial events, the x -location is fixed along a line and the AOI is free to translate in the y -direction as shown in Figure 2.8. The location is denoted by $D_{1/2}$, a distance one-half the diameter from the cylinder wall. Because the image coordinate system is oriented with the origin in the upper left corner of the image and with the positive y -direction directed ‘downward’, the data collected is reflected about the x -axis.

2.2.4 Tracking Method—Lateral Modes

Push, Slide/Slosh, and Multi-Slide disturbances are composed of a lateral or side-to-side motion in the x -direction. Both disturbance input and fluid response are tracked in time

²The disturbance is commonly referred to as ‘input’ while the fluid passive oscillation is simply ‘response’ with terminology borrowed from signal processing.

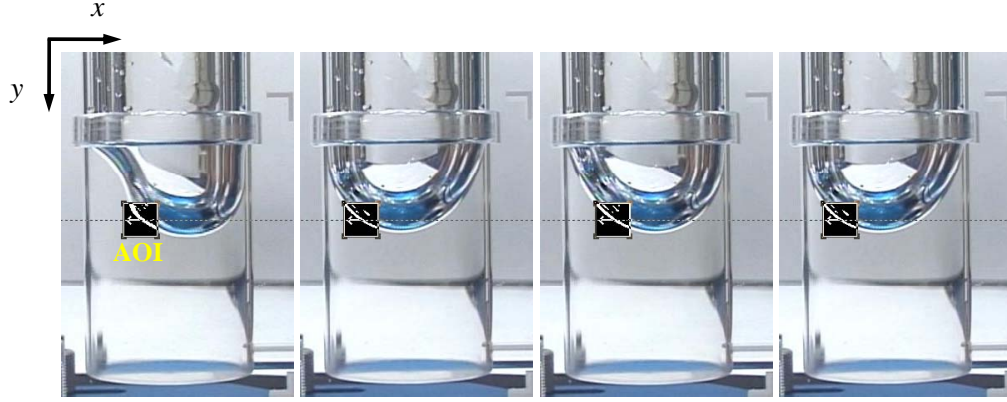


Figure 2.9: Multi-Slide response with Threshold AOI tracking.

using automatic threshold tracking methods if lighting conditions are satisfactory, or manual methods if automatic tracking fails. More complex tracking and processing techniques are possible, but generally not needed. Figure 2.9 depicts Threshold tracking of a Multi-Slide response in the Pinning cylinder. The tracking location for lateral modes is chosen as a fixed height $1/4$ diameter from either wall. This produces the best compromise between response amplitude and ease of tracking. The $1/4$ diameter *optical* location, denoted $D_{1/4}$, is chosen before the input disturbance by measuring $1/4$ the diameter from either wall and finding the y -position at which the interface is intersected. The interface may be tracked on either the left or right side of the interface, depending on lighting conditions, but must be consistent between the Pinning and Smooth cylinders per event. All of the data is obtained at ‘optical’ locations and not the ‘real’ locations. A ray trace analysis to correct optical distortions is discussed below. Tracking methods for all events are documented in each datasheet with sufficient information such that the reader can reconstruct the tracking methodology if desired.

2.3 Ray Trace Optical Correction

The data reduction for CL requires tracking a location on the interface, which can be distorted by mismatched refractive indices between the test fluid and acrylic container. Axial modes are unaffected by such distortion since they are tracked at the centerline where distortions are negligible. However lateral interface motions must be corrected. Figure 2.10 depicts the geometry under analysis where $(x/R)_d$ is the distorted location and $(x/R)_r$ is the real location. The light is assumed to be parallel to the observer but refracts at the Si oil/cylinder wall interface. The incident angle normal to the circular arc is

$$\theta_a = \sin^{-1} \left(\frac{x}{R} \right)_d, \quad (2.13)$$

which is also the normal angle θ_n . As the light hits the arc it is refracted by angle

$$\theta_b = \sin^{-1} \left[\frac{N_{acr}}{N_{sil}} \left(\frac{x}{R} \right)_d \right]. \quad (2.14)$$

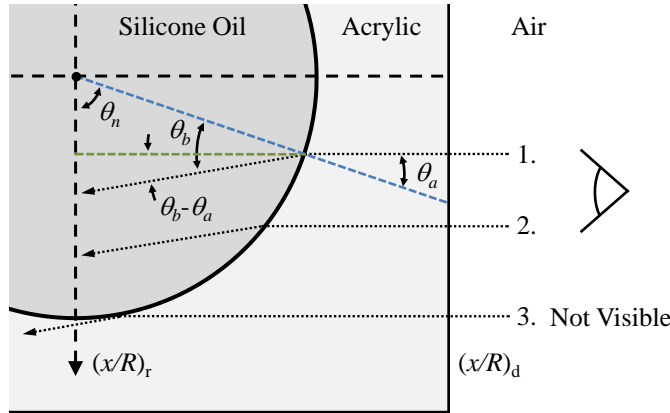


Figure 2.10: Ray trace schematic for optical correction of CL.

The refracted light is offset by distance δ depending on the distance the light travels and the angle θ_b ,

$$\delta = \left[1 - \left(\frac{x}{R} \right)_d \right]^{1/2} \tan(\theta_b - \theta_a), \quad (2.15)$$

which includes the distorted or apparent location $(x/R)_d$. The distance δ is essentially the correction to the distorted point,

$$\left(\frac{x}{R} \right)_r = \left(\frac{x}{R} \right)_d + \delta. \quad (2.16)$$

Using the optical properties for Si oil and acrylic (Table 2.1) where the distorted location is corrected by adding a distance δ . For lateral disturbances the percent correction is nearly constant ranging between 6.8% and 8.9%. The maximum error occurs when $(x/R)_d \approx 0.91$, which is mapped to the real point $(x/R)_r \approx 1$. Any values beyond $(x/R)_d \approx 0.91$ are erroneous as the ray of light is refracted out of view. The percent error correction is calculated from

$$\% \text{ Error} = \frac{(x/R)_d - (x/R)_r}{(x/R)_r} \times 100\%. \quad (2.17)$$

As the refraction angle increases, the transit length decreases, and the error is nearly constant until very near the walls as shown in Figure 2.11. All figures presented in this report are distortion-corrected, but the CL datasheets are always tracked at the apparent or distorted locations and must be corrected by the user.

2.4 Data Analysis and Presentation

Following digitization, the data can be analyzed for any number of characteristics. The most obvious quantities are the frequency and damping rate of the fluid response in the linear regime, defined as the regime where interface oscillation amplitudes are $< 0.1R$ ($\approx 2\text{mm}$). Frequency is calculated by first finding the average period in a specified time interval, and then inverting it to find the average frequency, $f = 1/P$. The average period is calculated

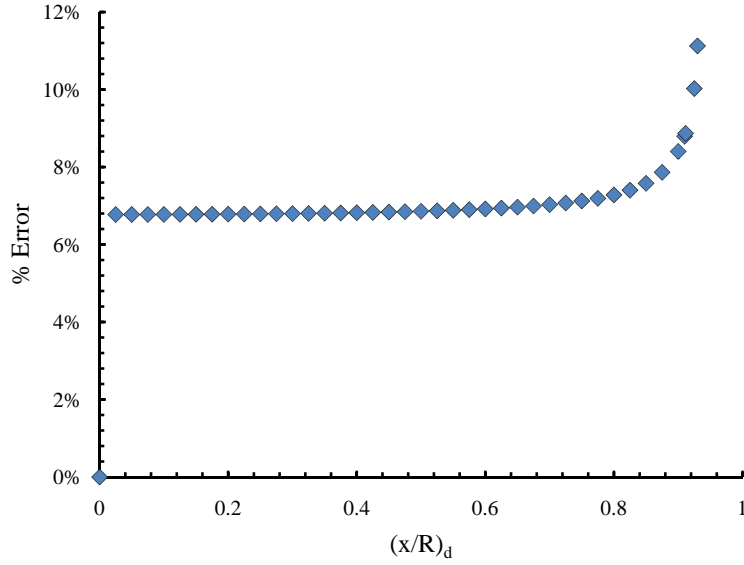


Figure 2.11: Percent error of $(x/R)_d$ and $(x/R)_r$ as a function of the distorted location $(x/R)_d$. (Note: the point at $x/R = 0$ is erroneous.)

by counting peaks in the linear regime and dividing by the time duration to obtain an average period. The method is increasingly accurate as the number of periods increase. CL1 average frequencies contain less scatter (> 15 peaks) whereas CL2 exhibits more (< 4 peaks).

The interface response data is always zeroed with the depth after the fluid has settled. In other words, the depth after the input disturbance and passive fluid response is used as the zero elevation. The idea is that after the disturbance has been imparted, the fluid should return to the original level. The fluid in the Pinning cylinder is not thrown onto the walls if the contact line is Pinned. However, if the Pinning lip is flooded it generally returns to the bulk due to the favorable wetting gradient (discussed in Section 2.7.3). This is less true for the CL2 Smooth cylinder, as residual wetting fluid films reside on the walls and can accumulate over time. In this way, large disturbances have the potential to change the fluid level in the Smooth cylinder. There is generally not a significant change in fluid depth before and after the input disturbance as documented in every datasheet.

The damping rate ξ is the coefficient in the exponential decay function $e^{-\xi t}$, which is the assumed peak-to-peak decay rate in the linear regime. Calculation of the damping rate is sensitive to the ‘zero’ location. The damping rate is calculated using absolute values and an exponential fit calculated from the peak data points. Two points are chosen for the calculation, with the first being near the beginning of the linear regime and the second being near the end of the response. If the two peak data points are represented as (x_1, y_1) and (x_2, y_2) then the damping rate is

$$\xi = \frac{\ln y_1/y_2}{x_1 - x_2}, \quad (2.18)$$

which is reported for several experiments in Section 2.6.1. The video processing protocol

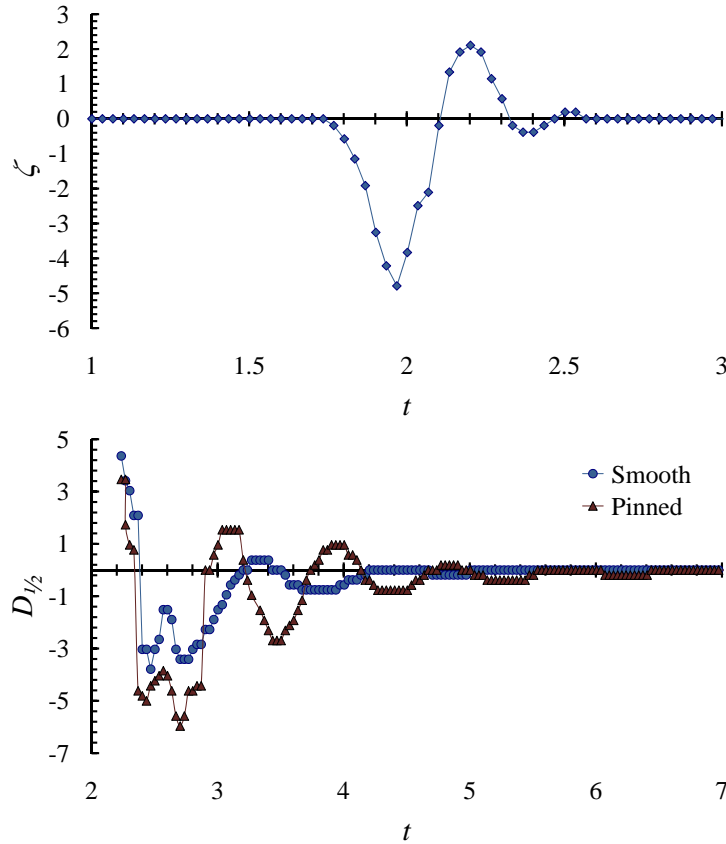


Figure 2.12: Axial mode input disturbance (top) and coupled passive fluid response for CL2 (bottom) where the coordinate system is corrected—up is positive and down is negative.

was reviewed in Section 1.3.6 with further details given in Section 7.1.

2.5 Representative Results

One objective of the experiments is to observe the difference in response due to the two extremes in boundary conditions. Representative results are presented for Smooth and Pinning boundary conditions for both CL1 and CL2 using differing modes and amplitudes. In addition, numerical results are calculated using the OpenFoam CFD software presented for comparisons. Four comparisons are presented for Axial and Push modes for CL1 and CL2. The Axial mode for CL2 is investigated first with a typical example shown in Figure 2.12. In this case the input disturbance consists of a little more than one full period, which is not always the case, but is generally observed for larger amplitude disturbances. For small amplitude disturbances the Pinning and Smooth fluid responses are similar. As the input amplitude increases, the discrepancy in the Pinning and Smooth responses becomes more pronounced. The lower plot in Figure 2.12 is typical, showing how the Smooth cylinder settles more quickly than the Pinning case due to increased damping in the contact line

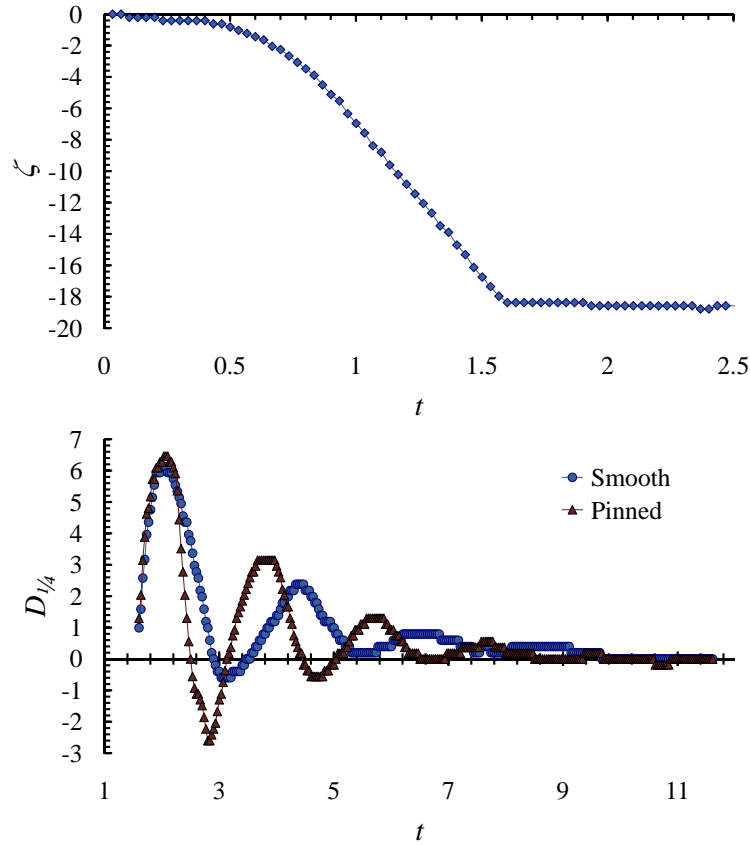


Figure 2.13: Push mode input disturbance (top) and coupled passive fluid response for CL2 (bottom).

region. This trend is common to all disturbance modes.

Figure 2.13 presents a Push mode disturbance with corresponding fluid response. It is clear that the damping rate of the disturbance is less than that of the Axial mode, which is true for all lateral mode disturbances including Slide and Multi-Slide. Another clear observation is that the response frequency is roughly half that of Axial modes.

As discussed above, the experimental procedure for CL1 is modified due to a wetting anomaly in the Smooth cylinder. For this reason a direct comparison between simultaneous Pinning and Smooth cylinders is not possible for a single disturbance. Instead, similar inputs are sought for disturbances to the Pinning cylinder when the liquid is at the Pinning lip (the pinned condition) and when the liquid is below the Pinning lip (the smooth contact line boundary condition, but in the Pinning cylinder), refer to Figure 2.6. The liquid depth changes in such tests reveal a negligible effect on Axial modes and only a slight effect for Push modes.

Figure 2.14 compares Pinning and Smooth boundary conditions for CL1 Axial modes. The input disturbances are of a similar form and amplitude. The frequency for both CL1 Smooth and Pinning is much higher than CL2 and the damping rate is much lower for CL1.

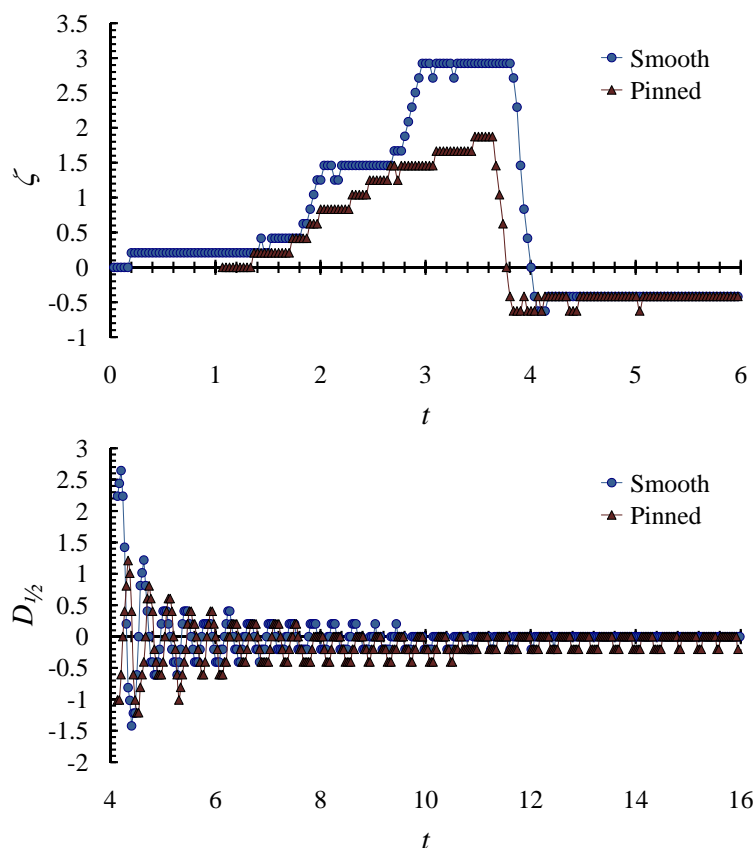


Figure 2.14: CL1 Axial mode input disturbance (top) and passive fluid response (bottom).

Both trends are due solely to differences in contact angle. Figure 2.15 depicts Push mode results for CL1 with input disturbances that are nearly identical. The differences in Pinning and Smooth responses are obvious. In the Smooth case the contact line moves along the wall maintaining a large contact angle. This motion apparently dissipates significant energy as can be seen in the plot where the difference between the first and second peak is over 600%. The Pinning response shows a different profile and slightly higher frequency, but the linear damping rate is nearly identical.

2.5.1 Liquid Depth Effect: Frequency

In certain tests the liquid depth is manually varied by changing the volume of liquid in the test chambers. In other instances liquid accumulates in an annular film on the cylinder wall above the bulk meniscus essentially removing liquid from the bulk and lowering the overall interface height. This occurs almost exclusively in the CL2 Smooth cylinder where the uncoated perfectly wetting surfaces allow the liquid to ‘migrate up’ the walls following large disturbances. The CL2 Pinning cylinder is coated above the Pinning lip and liquid rarely moves above it; if it does, it passively returns to the bulk. A slight decrease in liquid depth is still possible when the Pinning lip is flooded, as it removes some liquid from the

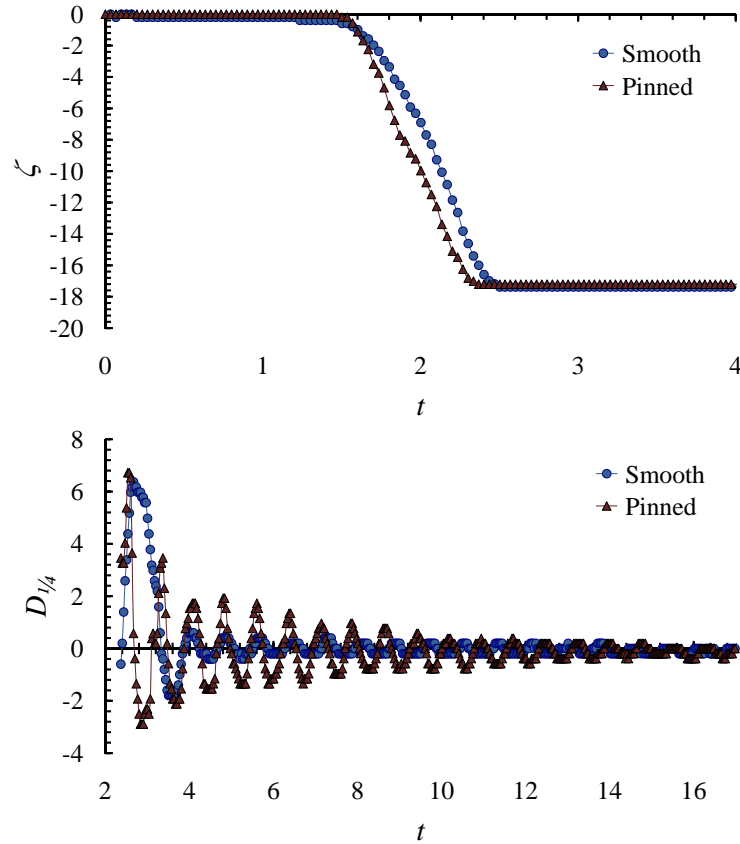


Figure 2.15: CL1 Push mode input disturbance (top) and passive fluid response (bottom).

bulk. Depth is varied systematically for CL1 data by adjusting the fill level.

Sample depth effects will be shown for linear perturbations defined as having peaks less than $0.1R \sim 2\text{mm}$. For the measurement to follow, frequency and fluid depth are determined with uncertainties $f \pm 0.01\text{s}$ and $\kappa \pm 0.05\text{mm}$, respectively.

2.5.2 CL1 Depth Effect

Depth effects for CL1 are reported here for Push and Axial input disturbances. Significant depth effect data was not collected for other disturbance modes (Slide, Multi-Slide, Swirl). Table 2.2 and Figure 2.16 provide CL1 Push mode data and reveal the change in frequency as a function of depth. The figure and table include Pinning and Smooth conditions with the assumption that in the linear regime they behave similarly. A linear curve yields $f = 0.0071 \kappa + 1.10$ with R^2 value of 0.996. A 15% change in linear frequency is observed between maximum and minimum fill levels. At the shallow end, the exact range of applicability can not be determined from the experiments for CL1, but, as will be seen, the linear fit persists for CL2 to depths of less than 5mm ($R_{cyl} = 19.05\text{mm}$). It is clear the linear relationship will not apply at either deep or shallow depth limits. Axial mode disturbances are less sensitive to liquid depth as Table 2.3 and Figure 2.17 indicate.

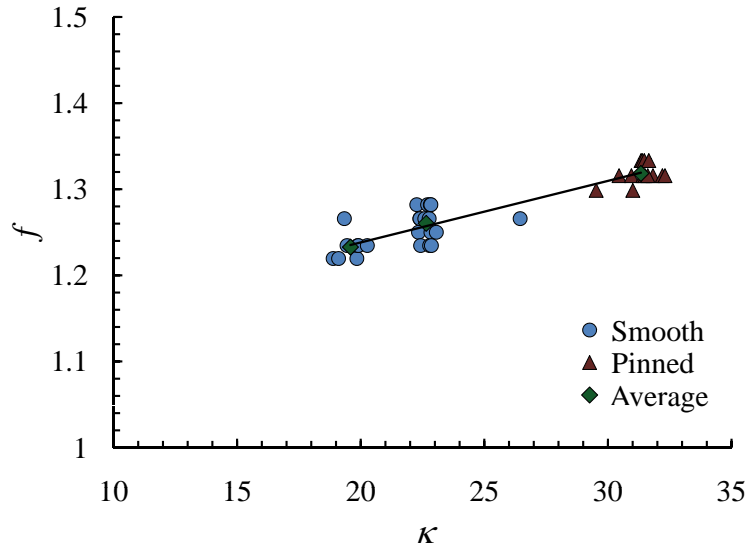


Figure 2.16: CL1 Push mode, frequency f vs. fluid depth κ .

Table 2.2: CL1 Push mode depth effect statistics for Figure 2.16.

κ_{avg} (mm)	σ_{κ} (mm)	f_{avg} (Hz)	σ_f (Hz)	$N =$	$\kappa_1 - \kappa_2$ (mm)
19.60	0.50	1.23	0.02	8	18.80–20.30
22.70	0.20	1.26	0.02	13	22.20–23.10
31.30	0.70	1.32	0.01	14	29.60–32.40

2.5.3 CL2 Depth Effect

Depth effects for CL2 are reported here for all disturbance modes with significant depth ranges for Slide and Multi-Slide disturbances. In addition, coupled disturbances across all lateral/slosh modes are presented. In this context the term ‘coupled’ means that the reported Pinned and Smooth frequencies are determined simultaneously from the same disturbance events. ‘Decoupling’ disturbances are reported when the Pinning lip is flooded and the Pinned and Smooth response are not directly compared in a single event. (It was found that events where the Pinning lip is flooded could be treated as having a Smooth boundary condition, a result which is telling of conditions at the contact line for low contact

Table 2.3: CL1 Axial mode depth effect statistics for Figure 2.17.

κ_{avg} (mm)	σ_{κ} (mm)	f_{avg} (Hz)	σ_f (Hz)	$N =$	$\kappa_1 - \kappa_2$ (mm)
31.80	0.50	2.53	0.03	22	30.70–32.80
26.20	0.00	2.53	0.05	2	26.20–26.20
22.30	0.40	2.50	0.02	15	21.80–23.00

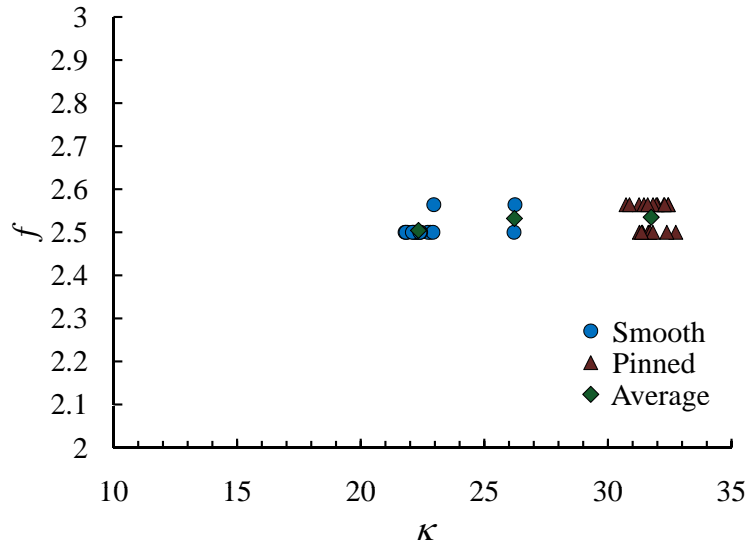


Figure 2.17: CL1 Axial mode, f vs. κ .

angle. Again, thin viscous film damping for low contact angle fluids masks the specific damping contribution tied to the moving contact line.)

The first comparisons shown here are for lateral/slosh mode disturbances including: Push, Slide, and Multi-Slide for coupled Pinning and Smooth response frequencies. By comparing the coupled disturbances one can determine the difference in the linear frequency as a result of the boundary condition. Figure 2.18 presents all coupled modes, while Figure 2.19 presents a sub-selected range of the data. A quick observation of Figure 2.18 reveals the roughly linear relationship between frequency and depth for the Smooth Multi-Slide case. Slide mode frequency also varies with depth, while Push mode depths do not span a large enough depth range to draw significant conclusions. Figure 2.19 reveals a difference in linear frequency between Pinning and Smooth boundary conditions. Recall that the data represented in the figure is coupled, further strengthening the argument that there is a difference in linear frequency for the two boundary conditions. The difference increases with disturbance type, for Push 4%, Slide 8%, and Multi-Slide 18%, all calculated for depths greater than 30mm and similar to the depth of the Pinning cylinder. Similar to Figure 2.17, Figure 2.20 indicates a 10% difference between Pinning and Smooth boundary condition frequencies. Push modes suffer from insufficient data to deduce a trend as shown in Figure 2.21. Larger depth range data are collected for both Slide and Multi-Slide tests where power and linear trends are reported. Figure 2.22 portrays a roughly linear trend between 31mm and 10mm before becoming nonlinear below 10mm. A 3-parameter power-law regression is applied with a best fit equation of $f = 0.072 + 0.24\kappa^{0.13}$. Multi-Slide responses exhibit a linear behavior between 5mm and 33mm and are fit by $f = 0.002\kappa + 0.36$. The data and trendline are presented in Figure 2.23.

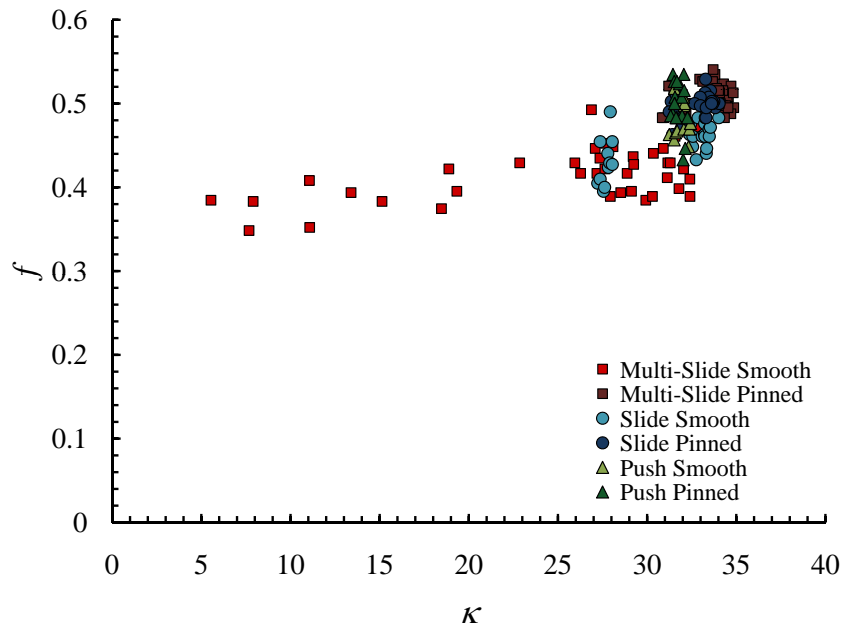


Figure 2.18: CL2 coupled lateral modes, f vs. κ .

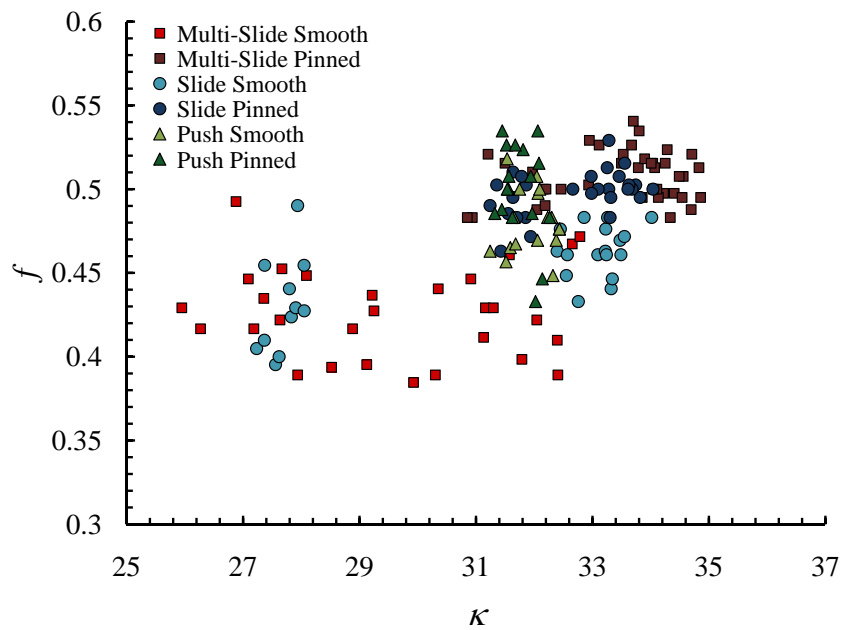


Figure 2.19: CL2 coupled lateral/slosh modes (magnified region of Fig. 2.18), f vs. κ .

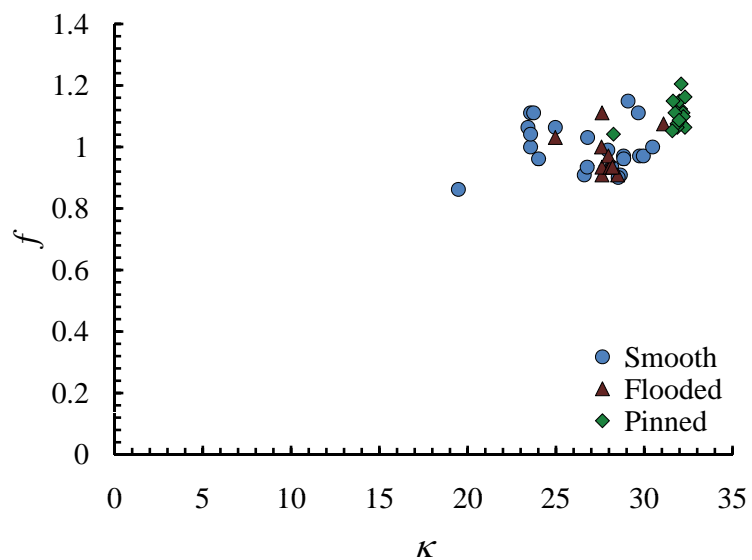


Figure 2.20: CL2 Axial mode, f vs. κ .

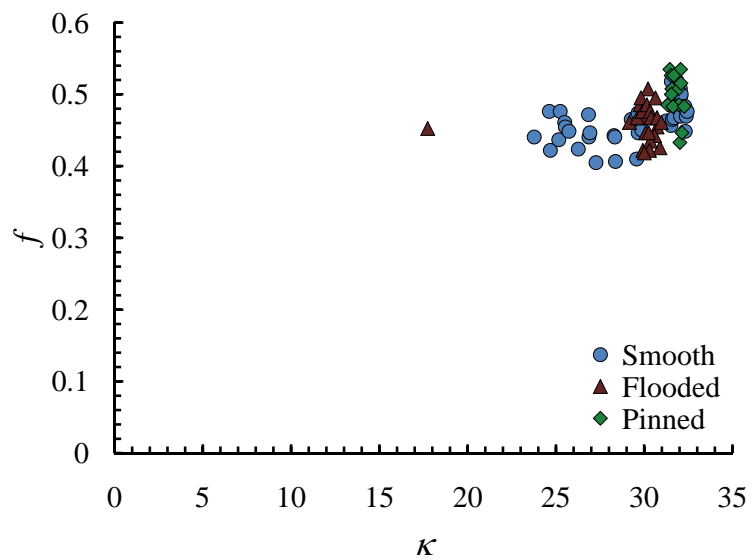


Figure 2.21: CL2 Push mode, f vs. κ .

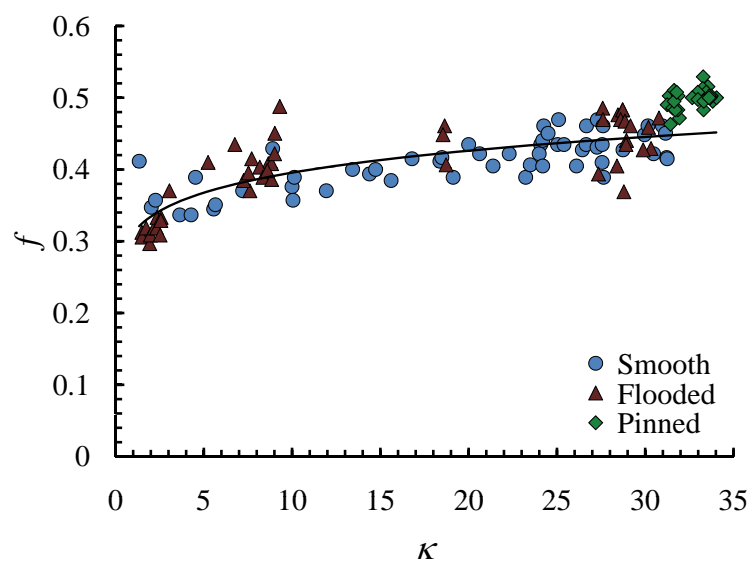


Figure 2.22: CL2 Slide mode, f vs. κ .

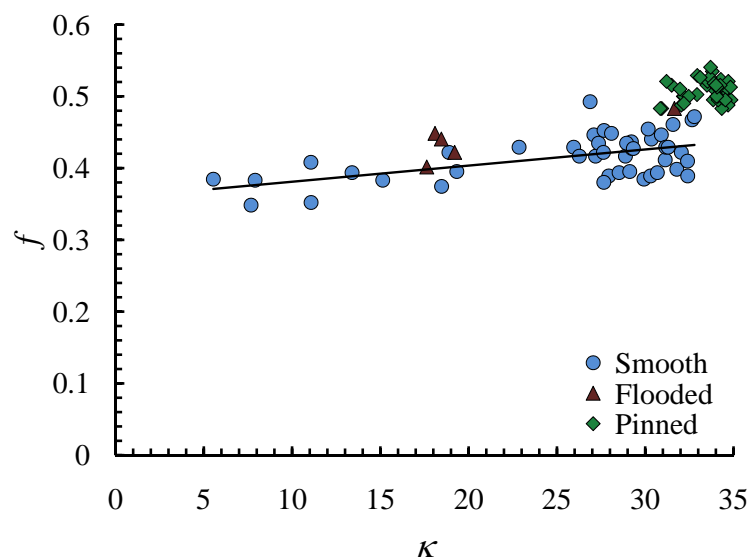


Figure 2.23: CL2 Multi-Slide mode, f vs. κ .

Table 2.4: CL1 statistics for the linear frequency in the Pinning cylinder.

Input Mode	B.C.	θ	f_{avg} (Hz)	St.dev. (Hz)	N	$\kappa_1-\kappa_2$ (mm)
Axial	Pinned	51°	2.75	0.04	14	32.90–34.70
Axial	Smooth	41°	2.51	0.02	17	21.80–26.20
Axial	Pinned	44°	2.53	0.03	22	30.70–32.80
Push	Smooth	41°	1.25	0.02	23	18.90–26.50
Push	Pinned	44°	1.32	0.01	14	29.50–32.30
Multi-Slide	Smooth	41°	1.24	0.02	14	18.90–20.30

Table 2.5: CL1 statistics for the linear frequency in the Smooth cylinder exhibiting the wetting anomaly.

Input Mode	BC	θ	Avg. (Hz)	Stdev (Hz)	$N =$	$\kappa_1-\kappa_2$ (mm)
Axial	Smooth	29°	1.97	0.02	5	24.35–25.20
Axial	Smooth	16°	1.58	0.01	5	21.30–21.80
Axial	Smooth	4°	1.04	0.03	19	12.15–12.70
Push	Smooth	4°	0.46	0.01	35	11.70–13.70
Multi-Slide	Smooth	4°	0.46	0.02	13	12.50–13.40

2.5.4 Linear Frequency Summary

Depth effect statistical data is presented in Table 2.4 for the CL1 Pinning cylinder, Table 2.5 for the CL1 Smooth cylinder, and Table 2.6 for CL2 containing both Smooth and Pinning results. The Smooth cylinder of CL1 which suffered the wetting anomaly discussed in Section 2.1.3 provided results for several effective contact angles as shown in Table 2.5. Most of the disturbances are Axial and reflect change in frequency with contact angle, and, to a lesser degree, depth. Recall that the Axial mode frequency was not particularly sensitive to depth as shown in Figure 2.17. The depth affects measured are rarely significant ($\lesssim 10\%$) unless a depth of less than 5mm, in which cases differences of up to 25% are reported. Multi-Slide mode trends (5mm–30mm) are very similar.

2.6 Further Numerical Benchmark Comparisons

As introduced in Chapter 1, blind numerical predictions were made with the OpenFoam CFD package in an effort to demonstrate the use of the CFE CL database for code benchmarking where the specific numerical implementation of the moving contact line boundary condition is central to the computational flow phenomena. Details of our numerical approach can be found in [3] with the highlights presented below. It is important to note that the benchmark process was not ‘closed’ in that the requisite second round of computations using improved boundary conditions was not carried out in keeping with the ‘blind’ demonstration. It is certain that a second effort would produce results of increased accuracy.

For the comparisons to follow, all optical distortions are corrected in both numerical predictions and experimental data with numerical values taken at the apparent tracking

Table 2.6: CL2 statistics for the linear frequency where a * indicates significant depth ranges.

Input Mode	BC	Avg. (Hz)	Stdev (Hz)	$N =$	$\kappa_1 - \kappa_2$ (mm)
Axial	Smooth	0.99	0.07	32	19.50–30.50*
Axial	Pinned	1.10	0.05	16	28.30–32.30
Push	Smooth	0.46	0.03	72	17.70–33.20*
Push	Pinned	0.50	0.03	22	31.30–34.40
Slide	Smooth	0.41	0.05	103	1.40–31.20**
Slide	Pinned	0.50	0.02	29	31.20–34.00
Multi-Slide	Smooth	0.42	0.03	48	5.50–32.80**
Multi-Slide	Pinned	0.51	0.01	40	30.90–34.90

location. The ray trace used to correct the optics is detailed in Section 2.3. Similar numerical modeling and experimentation for perfectly wetting Axial mode disturbances have been investigated [12]. Numerical results and experimental comparisons are presented here for Axial and Push mode disturbances with Smooth and Pinning boundary conditions. Numerical computations are carried out for CL1 with $\theta = 50^\circ$, despite the theoretically determined value of $\theta = 48.7 \pm 2^\circ$ [2] and experimental measurements between 41° and 44° ($\pm 3^\circ$).

In the comparisons certain numerical data points are represented by triangles while experimental points are circles. Several key parameters are chosen for comparison including linear damping rate ξ , frequency f , number of peaks N used to calculate frequency, amplitude ratio λ , maximum experimental peak-to-peak amplitude A_{exp} , and dynamic Bond number Bo ; all of which are documented for CL1 in Table 2.7. The damping rate ξ is the coefficient in the exponential decay $e^{-\xi t}$. The amplitude ratio λ is the maximum experimental versus numerical peak amplitude ratio in the linear (subscript l) and nonlinear (subscript nl) regions. Recall that the linear region is defined as an amplitude of $\sim 0.1R$ ($\sim 2\text{mm}$). The maximum peak-to-peak amplitude A_{exp} is the maximum peak from which the next minimum peak is subtracted and used to provide an measure of dynamic interface deflection. Figure 2.24 depicts the parameters under investigation for a generic decaying sinusoid.

2.6.1 CL1 Numerical Comparison

CL1 is compared first for the Pinned Axial mode case shown in Figure 2.25. It is apparent by inspection that the initial amplitude and damping rate of the numerical results are less than the experiment; however, frequency is correctly predicted. The Smooth Axial mode comparison is shown in Figure 2.26. In this case the contact line is able to translate, adding a degree of freedom which the numerical calculations that employ fixed contact angle boundary conditions at the contact line are unable to recreate. However, the damping rate is modeled correctly in the linear region. Push modes for both Pinning and Smooth boundary conditions are presented in Figures 2.27 and 2.28, respectively. The Pinning solution captures both damping rate and frequency well, while the Smooth solution misses frequency, damping rate, and amplitude ratios.

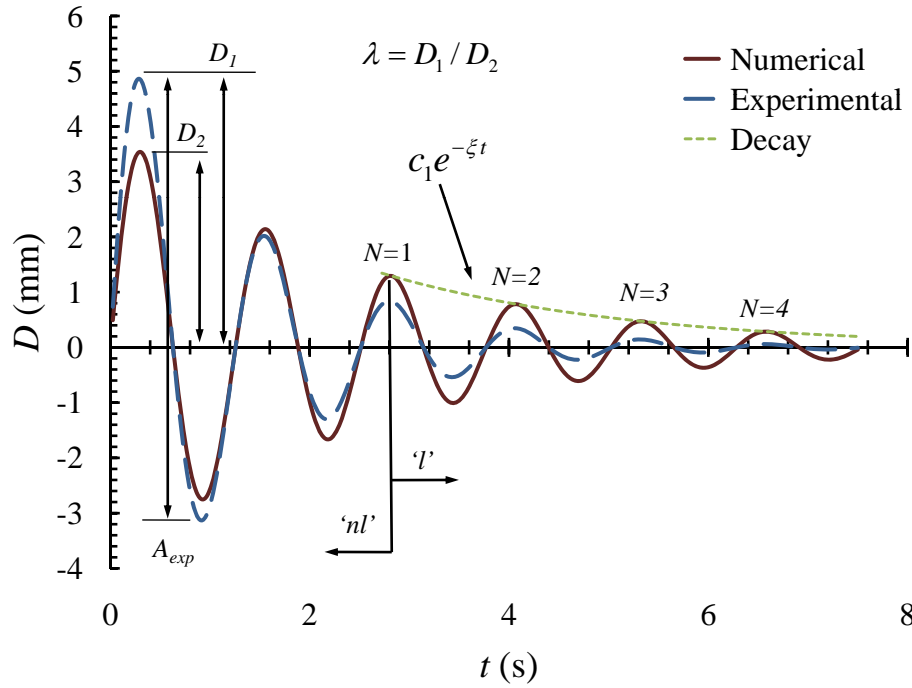


Figure 2.24: Example plot describing nomenclature used in the numerical (solid) and experimental (dashed) comparisons.

The comparisons for CL1 are summarized in Table 2.7 and discussed in detail below.

- Numerical predictions of the frequency are within 2% for the Pinned Axial response (Figure 2.25), which is the best agreement for any of the CL1 cases. However, damping is under-predicted by 55%. Amplitudes are poorly predicted, especially in the nonlinear region where the experimental amplitude is over 5 times greater than the numerical prediction.
- Smooth Axial (Figure 2.26) predictions do not fare as well in terms of frequency where a 33% under-prediction is reported. Damping rate is within 4% of the experiment and the linear amplitude ratio is at best 0.65 for CL1.
- Pinned Push mode (Figure 2.27) calculations are in good agreement with only an 11% error in frequency and are similar for damping rates. Amplitude ratios vary between 1.85 to 2.68, but overall characteristics and shape are well-predicted.
- Smooth Push mode (Figure 2.28) computations produced the widest discrepancies $> 50\%$ for frequency and damping rate. Frequency was significantly under-predicted while damping rate was over-predicted. Surprisingly, the nonlinear amplitude ratio was well predicted, which happened to be the best of all CL1 cases. Overall the combination of high contact angle and free slip boundary condition proved difficult for the numerical solution, indicating the already obvious need for a refined moving

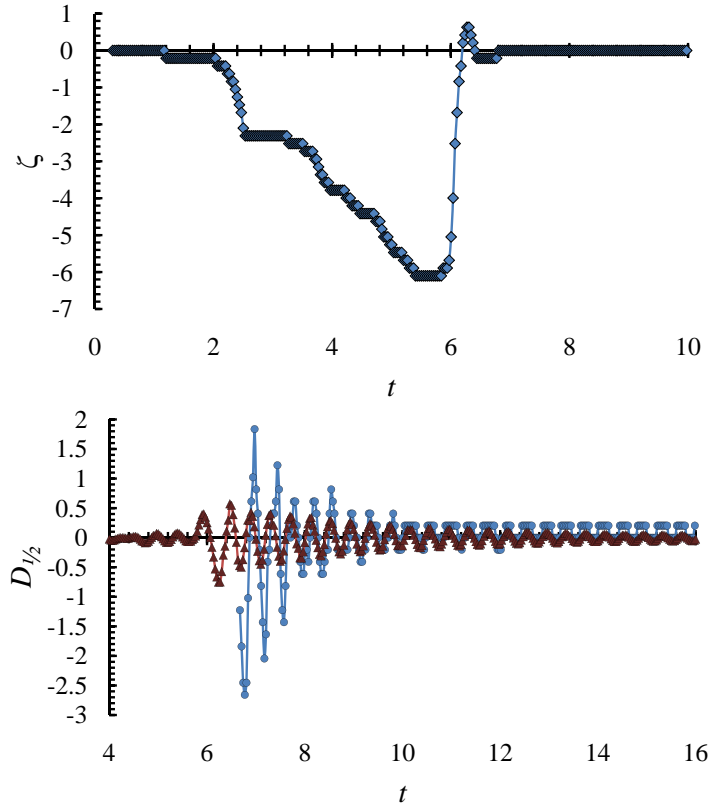


Figure 2.25: CL1 Axial mode input (top) and experimental (●) Pinned response with numerical (▲) comparison (event 4124).

Table 2.7: Summary of CL1 numerical and experimental comparison.

	Axial		Push		
	Pinned	Smooth	Pinned	Smooth	Error
f_{exp}	2.55	2.50	1.31	1.24	$\pm 1\%$ Hz
f_{num}	2.50	1.66	1.17	0.54	$\pm 1\%$ Hz
ξ_{exp}	0.67 (10)	0.52 (10)	0.15 (10)	0.17 (10)	$\pm (\% \text{ err.})$
ξ_{num}	0.30 (5)	0.50 (5)	0.15 (5)	0.27 (5)	$\pm (\% \text{ err.})$
N_{exp}	20	20	16	10	-
N_{num}	20	15	14	5	-
λ_l	3.58	0.65	2.68	0.79	-
λ_{nl}	5.65	-	1.85	0.08	-
A_{exp}	4.50	3.10	16.20	8.50	$\pm 0.05\text{mm}$
Bo_{max}	1.9	3.2	3.1	3.0	-

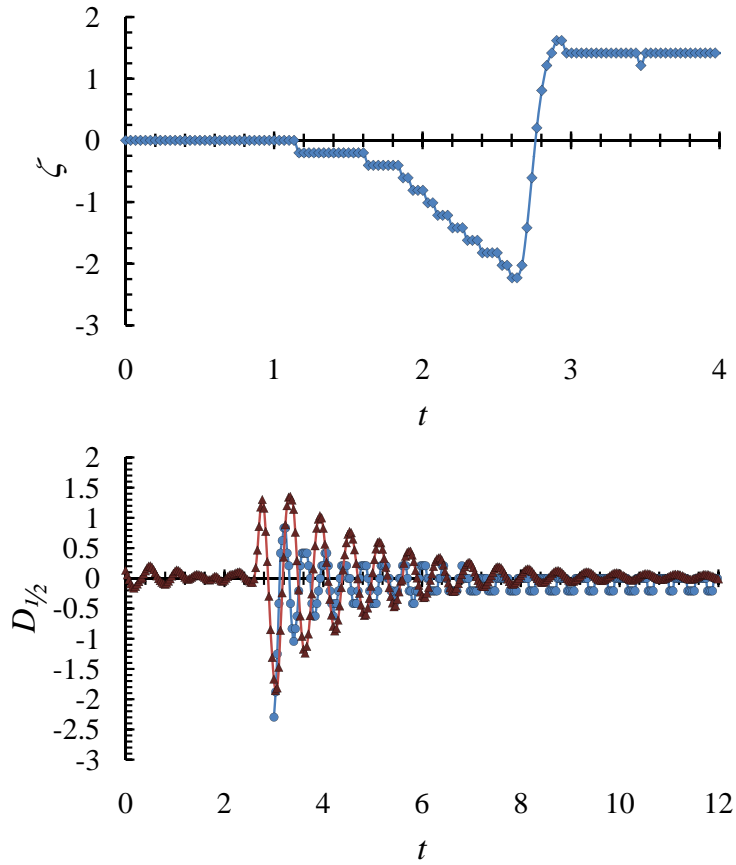


Figure 2.26: CL1 Axial mode input (top) and experimental (●) Smooth response with numerical (▲) comparison (event 7879).

contact line boundary condition. This challenge was certainly appreciated a priori. A next logical step would be to repeat the computations with a more physically inspired boundary condition tuned to reproduce the data.

2.6.2 CL2 Numerical Comparison

CL2 ($\theta = 0^\circ$) is calculated for coupled cases, meaning the Smooth and Pinned responses are simultaneous, the result of a single input disturbance. CL2 results are summarized in Table 2.8 with some details listed below.

- The Pinning Axial mode (Figure 2.29) fluid response is predicted well where frequency is within 2% of the experiment and damping rate is within 6%. Amplitude ratios indicate small under predictions in the nonlinear region and over-predictions in the linear region.
- The Smooth Axial case (Figure 2.29) is also well predicted in all respects including frequency (2%), damping rate (4%), and amplitude ratio (0.84). These results are

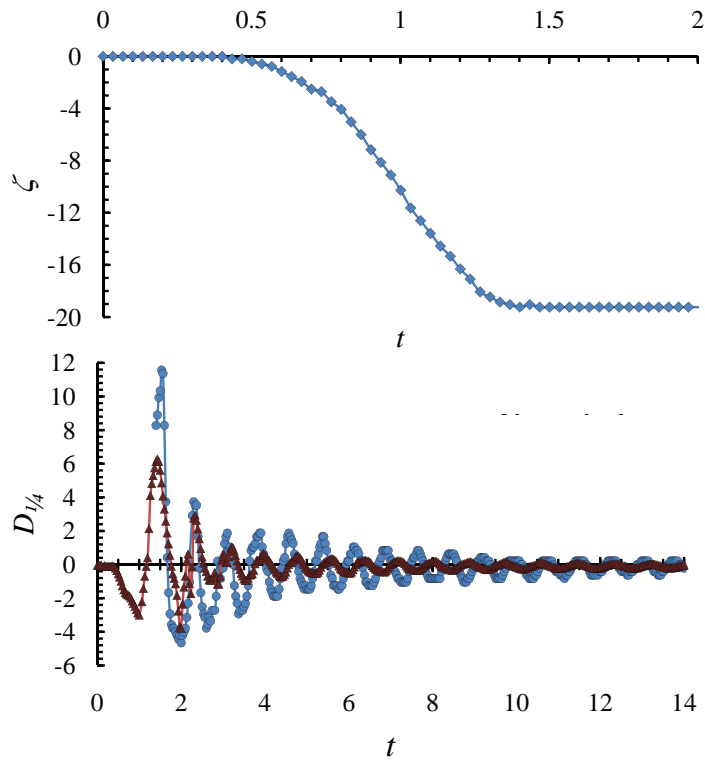


Figure 2.27: CL1 Push mode input (top) and experimental (●) Pinned response with numerical (▲) comparison (event 5665).

Table 2.8: Summary of CL2 numerical and experimental comparisons.

	Axial		Push		
	Pinned	Smooth	Pinned	Smooth	Error
f_{exp}	1.13	1.05	0.48	0.48	$\pm 1\%$ Hz
f_{num}	1.11	1.07	0.45	0.48	$\pm 1\%$ Hz
ξ_{exp}	1.11 (4)	1.00 (-)	0.62 (4)	0.70 (8)	\pm (% err.)
ξ_{num}	1.04 (3)	1.04 (-)	0.30 (3)	0.73 (2)	\pm (% err.)
N_{exp}	3	2	4	3	-
N_{num}	5	2	5	3	-
λ_l	0.60	-	0.65	4.10	-
λ_{nl}	1.45	0.84	0.85	1.60	-
A_{exp}	9.80	5.50	10.00	7.4	± 0.05 mm
Bo_{max}	13.4	13.4	2.0	2.0	-

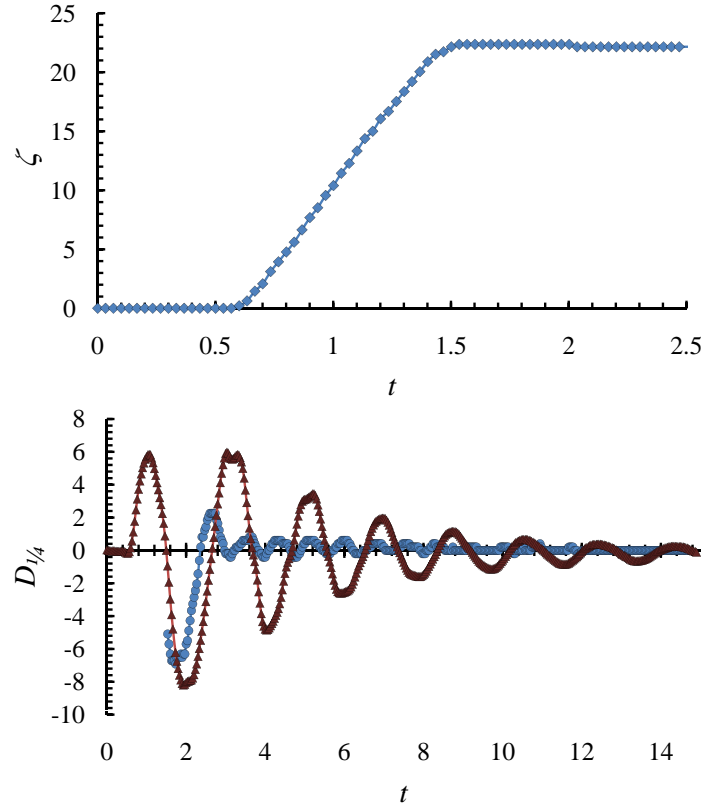


Figure 2.28: CL1 Push mode input (top) and experimental (•) Smooth response with numerical (▲) comparison (event 11020).

excellent because these are commonly occurring conditions.

- Pinned Push response (Figure 2.30) frequency is predicted within 6% of the experiment, but the damping rate is $> 50\%$ below the experimental result with numerical oscillations lasting much longer than expected. Amplitudes are calculated lower than the experiment at values in the nonlinear region and become over-predicting in the linear region.
- The Smooth Push response (Figure 2.30) predicts frequency perfectly and damping rate is within 2%. Amplitudes in the nonlinear region are well predicted while the linear region is off by a factor of 4.

Several important observations from the comparisons are provided below:

- Overall, the perfectly wetting case (CL2) is modeled most accurately for both the Pinning and Smooth boundary conditions.
- Axial and Push modes for perfectly wetting (CL2) are modeled well with similar accuracy.

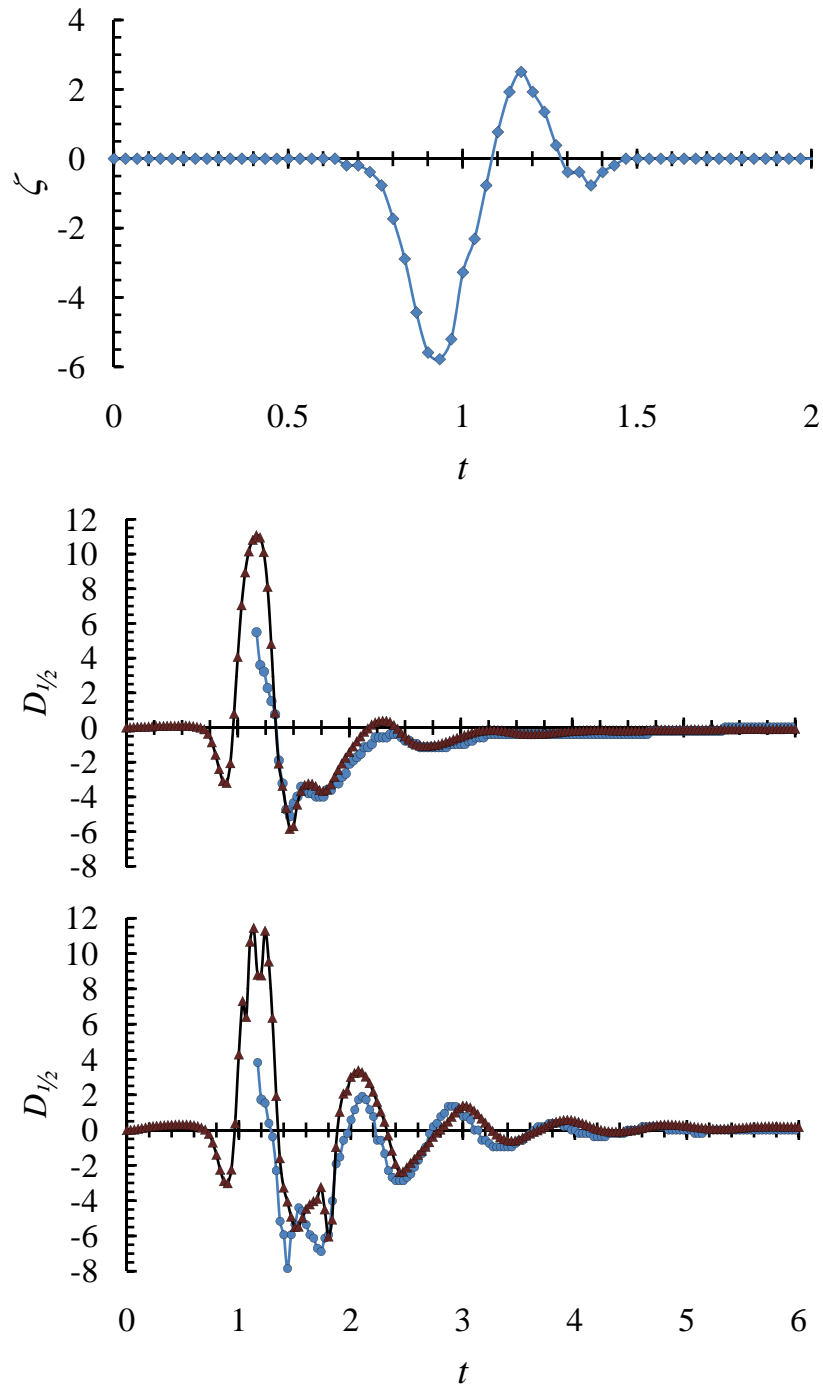


Figure 2.29: CL2 Axial mode input (top) with experimental (\bullet) Smooth (middle) and Pinned response numerical (\blacktriangle) comparisons (event 878).

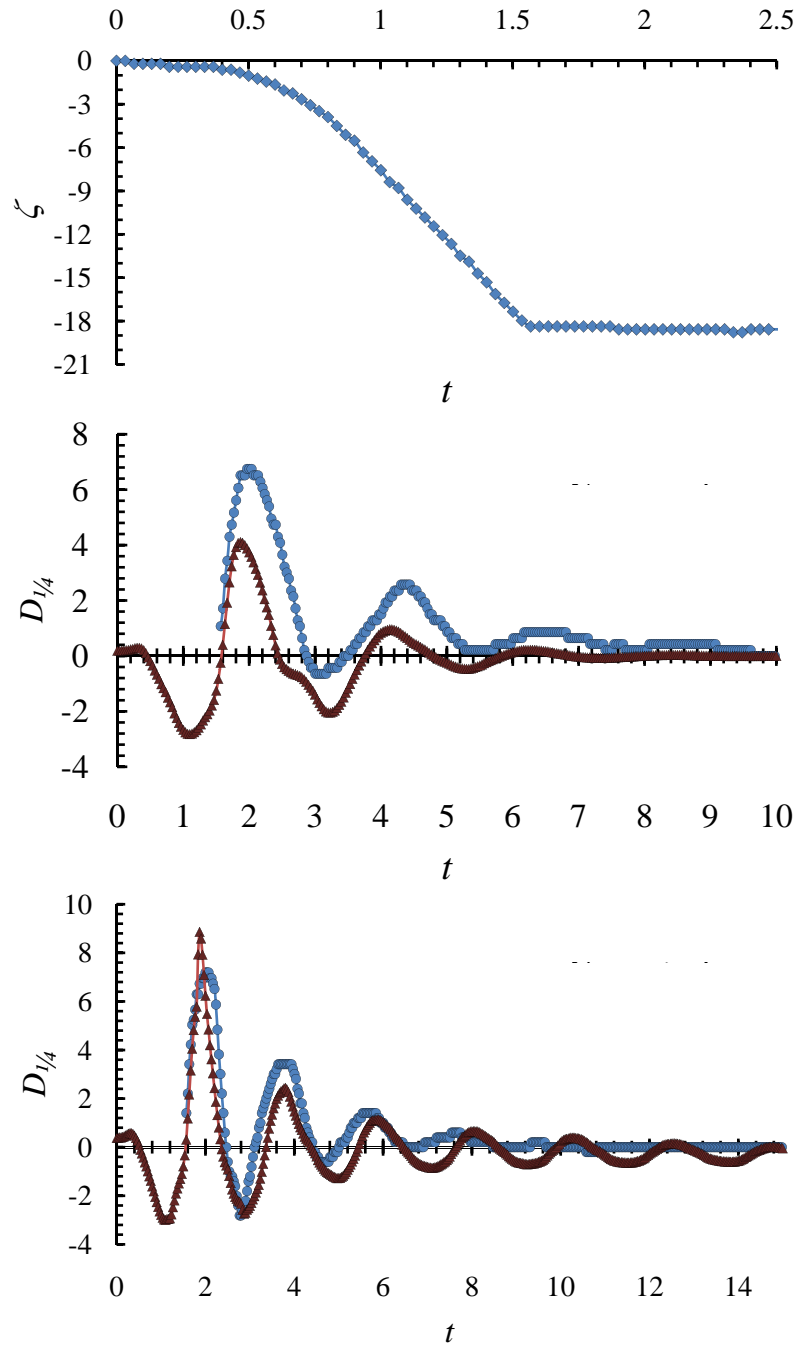


Figure 2.30: CL2 Push mode input (top) with experimental (\bullet) Smooth (middle) and Pinned response numerical (\blacktriangle) comparisons (event 2814).

- High contact angle (CL1) Push mode with free slip ('Smooth') boundary conditions is the worst predicted of all the comparisons. The model is not able to capture the contact line correctly, resulting in large errors for high contact angle (CL1) Smooth boundary conditions.
- In general, Pinned boundary conditions are more accurately predicted as the boundary condition is most suited to the modeling boundary condition of a fixed contact line.

2.7 Extra Science

As mentioned in 1, extra science refers to experimental data that was obtained in addition to the primary science objectives. Numerous extra science events/experiments were conducted and recorded on video including: liquid jetting, droplet impact and satellite rebound dynamics, air entrainment caused by Axial disturbances, 'hourglass' interface formation and draining, Pinning due to a wetting gradient, Pinned interface stability, and more. In this section a few extra science topics are discussed with the purpose of demonstrating the wide range of phenomena that may be examined from the simple CL experiments. Any or all may be studied to greater depth by the reader using the CFE video database (<http://cfe.pdx.edu>).

2.7.1 Axial Mode Droplet Ejection

If the Axial disturbance amplitude is large, destabilization of the interface may occur resulting in droplet ejection or liquid jetting. Several parameters affect whether ejections occur, including disturbance amplitude, frequency, and waveform. Figure 2.31 represents the displacement and velocity for Axial mode disturbances that are subcritical, critical, and supercritical. The event labeled 'Below' does not cause a droplet to eject. The 'Critical' event ejects a droplet with nearly no inertia—the ejected drop hovers over the bulk meniscus. The event labeled 'Above' produces jetting with significant ejected droplet momentum and is characterized as being above the critical condition (supercritical). All of the events are for Smooth contact line boundary conditions. Ejection or near ejection occurs at approximately 0.95s. The disturbance motion is characterized by a single depression of the MWA followed by its release and rebound.

The displacement frequency for all of the disturbances is $\sim 2.50\text{Hz}$ which is 2.5 times the fundamental Axial frequency. The velocity plot gives an idea of how waveform plays a role. The primary peaks are -80mm/s and 84mm/s for the critical event, -62mm/s and 56mm/s for the subcritical event, and -67mm/s and 74mm/s for the supercritical event. The symmetry of the signal seems to be important, where net momentum in the upward direction promotes ejection and net downward momentum inhibits ejection. Adequate velocity or Bond number is not sufficient to cause ejection as Figure 2.32 indicates. The critical event produces a larger Bond number than the supercritical event, indicating that a lesser Bond number produces droplets if the waveform has a significant upward component. The data represented in this section provides a glimpse of Axial ejection dynamics, with the full database providing additional data.

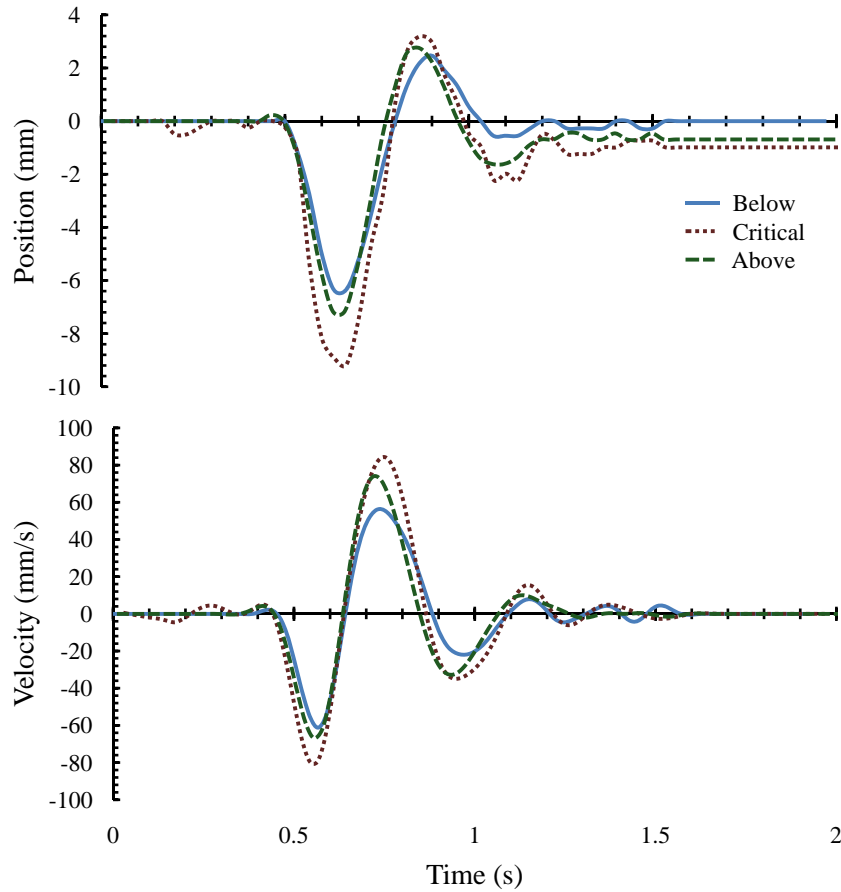


Figure 2.31: CL2 displacement and velocity plot depicting input disturbances that are below, at, and above the threshold that causes droplet ejection. (Drop ejection occurs at $t = 0.95\text{s}$.)

2.7.2 Depinning Investigation

Large Axial mode disturbances produce jetting dynamics while large lateral mode disturbances generally cause depinning. A depinning event occurs in the Pinning cylinder when the input acceleration is sufficiently large to cause the contact line to break free of the Pinning lip. An example of a depinning event was shown in Figure 2.4 while an input acceleration plot is shown in Figure 2.33 for a Multi-Slide disturbance. The interface moves in the opposite direction of the container when accelerating, thus depinning occurs on the right hand side of the Pinning lip in the figure as the disturbance velocity changes direction. Complete depinning occurs at 4.56s due to an acceleration of -99.45mm/s^2 ($\text{Bo}_d \sim 1.7$), while critical depinning occurs at 3.39s and -130.08mm/s^2 ($\text{Bo}_d \sim 2.2$). Greater accelerations are reported at 1.79s and 4.13s , yet depinning does not occur, indicating acceleration alone is not sufficient to explain dynamic depinning. Frequencies for depinning are approximately twice the passive response frequency ($f \gtrsim 1\text{Hz}$ for Multi-Slide events). Additional

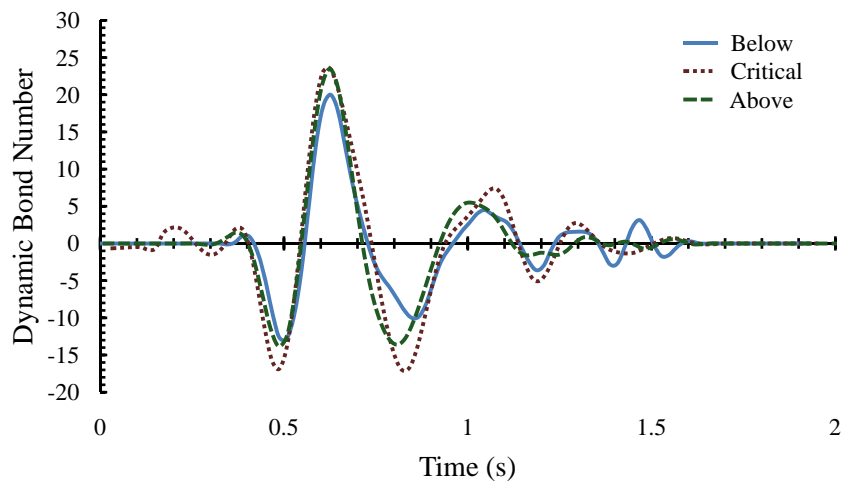


Figure 2.32: CL2 dynamic Bond number as a function of time for Axial events comparing droplet ejection dynamics.

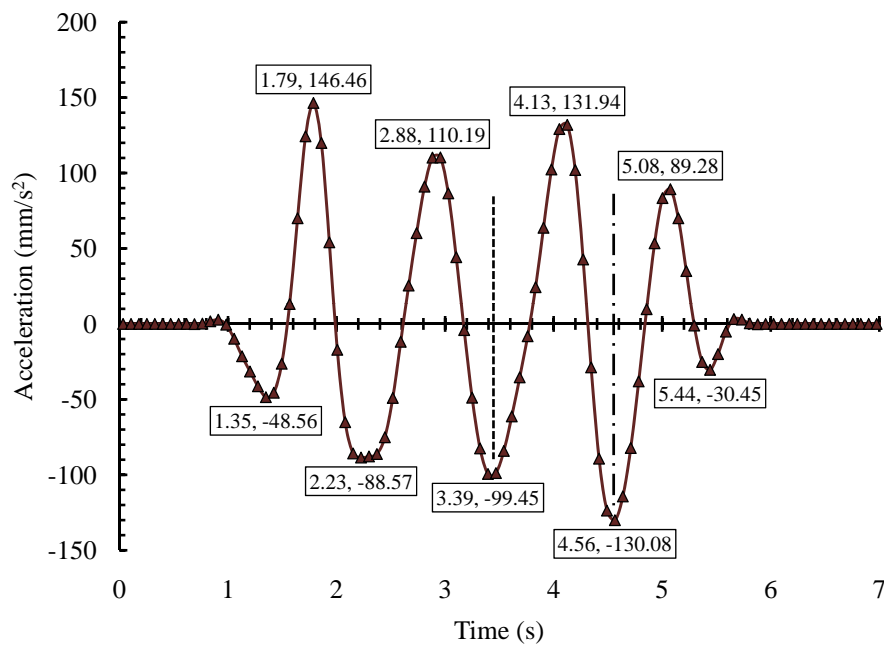


Figure 2.33: CL2 Multi-Slide input acceleration causing depinning, where the dashed line indicates partial depinning and the dash-dotted line represents full depinning (cf 2.4.

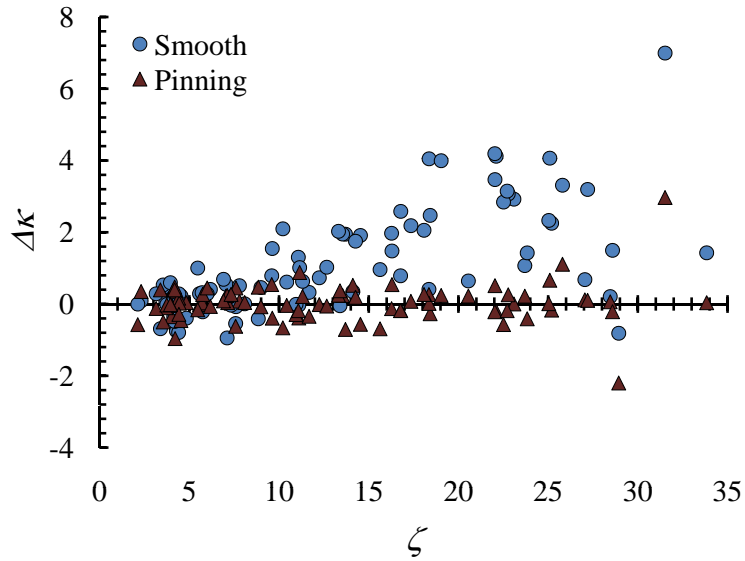


Figure 2.34: Demonstration of passive liquid return for CL2 Slide events as a function of the depth difference and disturbance amplitude, $\Delta\kappa$ vs. ζ (mm).

depinning phenomena could be studied for CL. More controlled investigations have been conducted ([13] and others), but the CL dataset adds large capillary length as a parameter in addition to low-g equilibrium initial conditions.

2.7.3 Volume Changes During the Experiments

As discussed previously, the Smooth cylinder is not coated while the Pinning cylinder is coated above the Pinning lip (see Section 2.0.1). Figure 2.34 presents the difference in fluid depth before and after the input disturbance $\Delta\kappa$ versus the input displacement amplitude ξ for Slide events. The Pinning data includes dry events where the Pinning lip is intact, and wet events where the Pinning lip is flooded. It is clear that as the disturbances become large, the liquid depth changes significantly for the Smooth cylinder while the Pinning cylinder is largely unchanged. The coating above the Pinning lip discourages fluid from accumulating on the walls and promotes a return to the bulk even for the flooded cases. The Smooth cylinder is not coated and thus fluid films ‘thrown up’ onto the walls remain there for a much longer time. This can also be thought of as a local axial wall pumping phenomenon resulting from lateral oscillations. Over time the films drain back into the bulk liquid lowering $\Delta\kappa$ further than what is indicated in Figure 2.34.

2.7.4 Axial Mode Frequency and Contact Angle

The wetting anomaly tests in the CL1 Smooth cylinder, the depth change tests in the CL1 Pinning cylinder, and the CL2 tests provide dynamics for a variety of contact angles for Axial mode disturbances. Data is gathered from Tables 2.4, 2.5, and 2.6, along with other data obtained from the CL database [14] and presented in Figure 2.35. Surprisingly, the axial

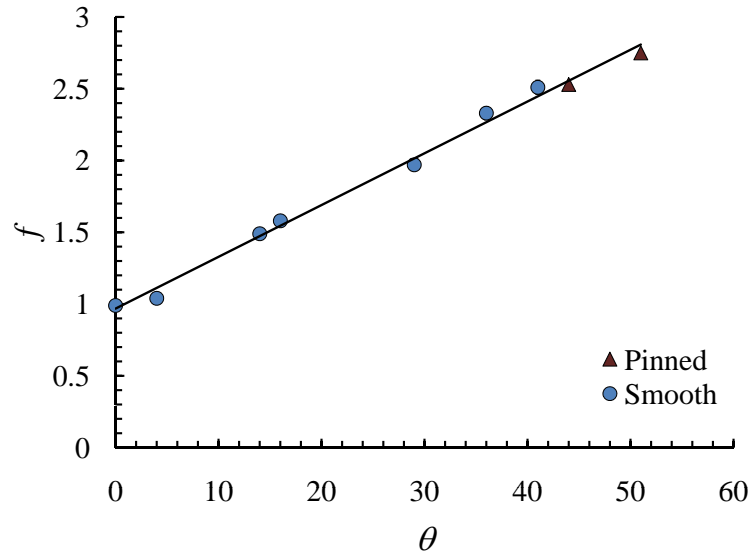


Figure 2.35: CL Axial mode frequencies at varying contact angles, f (Hz) vs. θ (degrees).

mode frequency appears linear with a fit $f = 0.036\theta + 0.968$ with $R^2 = 0.994$ and over a 50° range in θ .

2.8 Other Experimental Considerations

Each disturbance event is considered a miniature experiment where unique low-g phenomena can be studied. It is clear there is little repeatability in such manually imparted disturbances. However, it is also clear that each input can be quantified to a high degree, that each individual disturbance is imparted simultaneously and essentially identically to a given Smooth and Pinning Cylinder pair, and that with numerous disturbances a broad data set of a variety of fluid responses can be observed. In part due to the lack of total control of these experiments, an assortment of experiment anomalies occurred of which the reader should be aware if further analyses are carried out. This is not an exhaustive representation of all peculiarities witnessed in the experiments, and many more are sure to be discovered by anyone interested in analyzing the data.

One such example pertains to the Pinning cylinder in CL2 and CL1 where the contact angle varies with fill level. When bubbles are entrained in the bulk they displace liquid; thus, when the cylinder is fully filled and bubbles are present, the interface is displaced higher than designed for creating a ‘larger’ than intended contact angle. The fill level is adjusted in a manner that creates ‘effective’ contact angles. Nonetheless, fill level (fluid depth) has the ability to modify the contact angle in the Pinning cylinder (this is especially true for CL1). For this reason the effective contact angle in the Pinning cylinder must be measured for each event (refer Section 2.1.3).

As described previously, the Pinning lip may become flooded following large amplitude disturbance. During the first two operations of CL2, the effects of a flooded Pinning lip

were not entirely known and many of the disturbance events were conducted in the flooded condition. As reported, this condition behaves nearly identically to the Smooth cylinder data and is easily identifiable in the CFE database movies.

2.9 Directions

Independent study by other researchers is strongly encouraged. An attempt is made here to inspire future work. Such studies might use the statistical data already digitized, but entirely independent studies can be conducted using only the video database. The simple Contact Line experiments produced a wealth of information with only a portion presented here. Primary investigations focused on frequency across several axial and lateral disturbance modes, depth effects on frequency, and numerical comparisons. Sample extra science is reported to give the reader an idea of additional phenomena that may be investigated using the database. The complete database, updates, and additional information can be found at <http://cfe.pdx.edu>.

Chapter 3

CFE Vane Gap Wetting Analysis

Summary. The Vane Gap Capillary Flow Experiments are part of a suite of low-g experiments flown onboard the International Space Station to observe critical wetting phenomena in ‘large length scale’ capillary systems. The Vane Gap geometry consists of a right cylinder with elliptic cross-section and a single central vane that does not contact the container walls. The vane is slightly asymmetric so that two gaps between the vane and container wall are not of the same size. In this study, we identify the critical wetting conditions of this geometry using the Concus-Finn method for both perfectly and partially wetting fluids as a function of container asymmetry. In a cylindrical container in zero-g, single-valued finite height equilibrium capillary surfaces fail to exist if a critical wetting condition is satisfied. This nonexistence results in significant redistribution of the fluids in the container. It will be shown that there could be three critical geometric wetting conditions that include one in each gap region and one for a global shift of bulk fluid which, among the three, is the most significant.

3.1 Introduction and Background

Experiments aboard the International Space Station (ISS) provide a clear picture of the extent to which liquid behavior aboard spacecraft can be controlled by wetting and container geometry. The experiments are referred to as the ‘Vane-Gap’ (VG) experiments and are part of a more general set of simple handheld Capillary Flow Experiments[15](CFE) designed and developed at the NASA’s Glenn Research Center for conduct on ISS. The CFE-VG experiments clearly illustrate the sensitivity of a capillary fluid surface to container shape and how small changes to said shape may result in global shifts of the fluids within the container. Understanding such behaviors is key to the passive management of liquids aboard spacecraft and in certain cases permits us the ability to move large quantities (potentially tons!) of liquid by a simple choice of container shape. In other words, in the absence of significant gravity the container geometry can act as a pump to position the fluid in a desirable location within the container (i.e. liquid fuel over the fuel exit port).

The CFE-VG experiments are the latest of a line of experiments performed in low-g environments and sponsored in part by NASA to observe critical corner wetting phenomena in ‘large length scale’ capillary systems[16, 17, 18]. Mathematicians Concus and Finn[19] were perhaps first to construct the mathematical foundations of the critical interior corner wetting condition that, if satisfied, spontaneously draws the liquid into and along the corner to an impressive extent, and at known rates[20]. Such critical wetting conditions dictate the design of systems seeking to exploit the passive pumping capacity of the interior corner

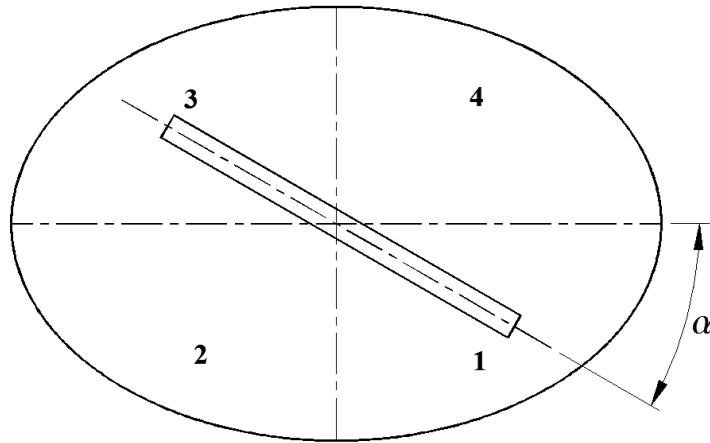


Figure 3.1: Test cell VG1. Definition of the vane angle α and depiction of four quadrants.

geometry. Critical wetting conditions also dictate how to design system in which the goal is to maintain liquid in one location.

Adding geometric complexity introduces significant complexity to the critical geometric wetting criteria. For example, an intricate geometric wetting condition arises for interior corners that do not actually contact. Such conditions arise in certain large propellant tanks where a gap is formed between a vane and the tank wall, as studied by Chen and Collicott[21]. The CFE-Vane Gap experiments are devised to investigate such phenomena and provide a benchmark to both confirm and guide methods of design for systems of increased complexity.

An image of a Vane Gap test unit is shown in Figure 3.2 with a schematic view shown in Figure 3.3. The test unit employs a right cylinder with elliptic cross-section and a single central vane that does not contact the container walls. The vane pivots 360° clockwise (CW) and counter-clockwise (CCW) varying the angle between the vane and the wall and consequently the size of the vane-wall gaps. The vane is also slightly asymmetric so that two gaps can be tested for each container. Two wetting conditions are studied between two Vane Gap containers (VG-1 with $\gamma = 0^\circ$ and VG-2 with $\gamma = 55^\circ$).

Example images of CFE VG-1 from the ISS operations are presented in Figure 3.4 along with *Surface Evolver* [22] computations for the same vane angles. The images show a selection of several equilibrium interface configurations following prescribed clockwise vane movements in quadrant 1 which is depicted in the figure. The vane angle α is defined as the acute angle between the vane and the major axis of the ellipse. At a critical vane angle the fluid wicks up along the small gap and corners forming a slender column over the entire extent of the vane. The fluid also wicks up the large gap corner with a further increase of the vane angle. Note that in between the small and large gap wetting there is another critical wetting condition resulting in a bulk shift of fluid from right to left side of the vane as shown in the 4th and 5th image in the top row of Figure 3.4. This bulk shift is significant because of the amount of fluid involved. It is observed that the bulk shift takes place between the



Figure 3.2: VG1 test vessel.

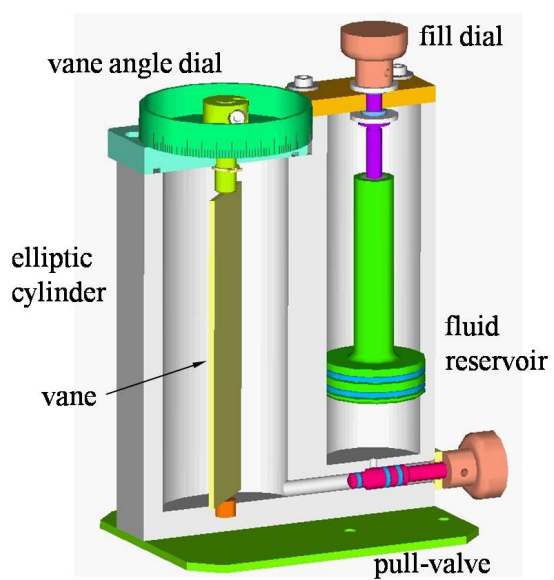


Figure 3.3: VG1 3D schematic view.

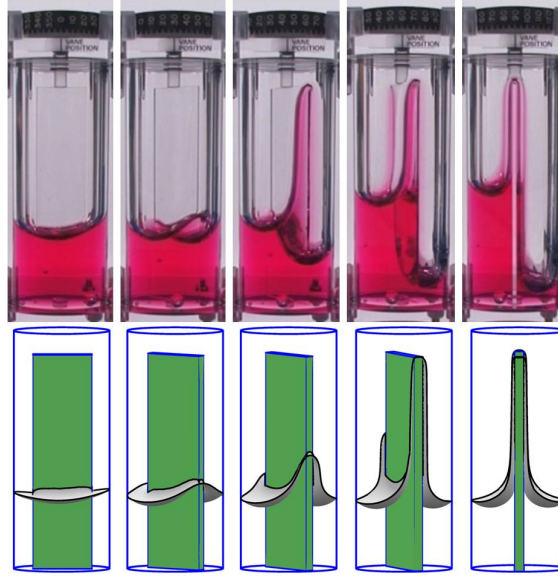


Figure 3.4: Equilibrium configurations in CFE-VG-1 for various critical vane wetting angles during 90° clockwise vane rotation. From top left to right vane angles are 0, 30, 44, 60, and 90°, respectively. *Surface Evolver* computations of the same vane angles are shown in the bottom row.

Table 3.1: Experimentally determined critical wetting conditions(α) for CFE VG-1. SGW: small gap wicking; SGD: small gap dewetting; LGW: large gap wicking; LGD: large gap dewetting; BS: bulk shift; BSR: bulk shift reversal. All values in degrees.

Quad.	SGW	SGD	LGW	LGD	BS	BSR
1	41.5 ± 1.5	40.0 ± 0.5	56.0 ± 1.0	54.0 ± 2.0	47.5 ± 2.5	39.0 ± 1.0
2	44.5 ± 1.0	41.0 ± 1.5	53.5 ± 1.5	51.5 ± 1.5	46.25 ± 0.7	44.0 ± 1.0
3	42.0 ± 2.0	40.0 ± 0.5	51.0 ± 1.0	49.0 ± 0.5	47.5 ± 2.5	45.5 ± 0.5
4	46.5 ± 1.5	44.7 ± 0.5	48.5 ± 0.5	48.7 ± 1.2	42.5 ± 2.5	40.5 ± 0.5

small and large gap wicking when the small gap is in quadrant 1-3. However, for the small gap in quadrant 4 it is found that the bulk shift takes place before the wicking in the two gaps takes place, as shown in Figure 3.5, in which it can be seen that the fluid shifts from left to right. The critical vane angles for the small gap in different quadrants are listed in Table 3.1. The data shows that there is asymmetry present in the geometry.

It is interesting to note that the bulk shift is not observed in the preliminary *Surface Evolver* computations as shown in the bottom row of Figure 3.4. The computations assume perfect geometry which is apparently not true with the experiment vessels where finite tolerance of fabrication, however small, is present. This suggests that tiny asymmetries in fabrication result in significant differences in the behavior of the fluid interfaces.

Critical vane angles for CFE VG-2 are listed in Table 3.2. For the VG-2 only small



Figure 3.5: Equilibrium configurations in CFE-VG-1 for various vane angles in quadrant 4. Left: vane angle 45° , bulk shift only; right: vane angle 50° , bulk shift and wicking in the gaps.

and large gap wickings are observed throughout the entire range of the vane angle. Note that a vane angle range is provided in each quadrant for wetting and de-wetting cases. The range is substantially larger as compared to that of CFE VG-1. It is believed that this is caused by contact angle hysteresis. In the experiments, it is observed that the movement of the meniscus tip in the gap is relatively slow and ‘stick-slip’. It often resumes advancing when the vane angle is increased. In addition, due to the contact angle difference, the cross-sectional area of the wetting liquid column in the gap region is smaller than that of CFE VG-1. A sample image is shown in Figure 3.6.

The critical vane angles for both the wetting and de-wetting are provided in Table 3.1 and 3.2. De-wetting takes place when the vane is rotated from the position aligning with the short axis towards that aligning with the long axis of the ellipse. The critical vane angle for the de-wetting is lower than that for the wetting. It is believed that this is caused by the contact angle hysteresis due to the pinning edges of the vane.

In the remainder of this paper, the various critical wetting conditions are identified theoretically following the established Concus-Finn method of analysis[23]. Each condition results in a significant redistribution of the fluid in the container, either covering the base, or along a particular wall leaving a portion of the base uncovered. In addition to the vane angle and fluid wetting properties (for ideal sharp corners) the critical geometric wetting conditions for the Vane Gap vessels depend on the specific vane gap, vane thickness, ellipse size and shape as shown by analysis. The results are then compared to experiments. Exploiting such phenomena, fluids may be positioned as desired by simply and slightly changing the geometry of container. Conversely, knowledge of such critical geometric wetting behavior might avoid mishaps. For example, a slight but uncontrolled container asymmetry might lead to a highly unfavorable shift in fluid preventing or limiting system function. As a result, the ISS CFE-Vane Gap experiments help provide a means for specifying container tolerance.



Figure 3.6: Equilibrium configuration with fluids wicking up in the small gap in quadrant 1 in CFE VG-2, $\alpha = 62^\circ$.

Table 3.2: Experimentally determined critical wetting conditions (α) for CFE VG-2.

Quad.	SGW	SGD	LGW	LGD
1	$53^\circ - 62^\circ$	$44^\circ - 37.5^\circ$	$69^\circ - 79^\circ$	$60^\circ - 50^\circ$
2	$52^\circ - 59.5^\circ$	$48^\circ - 38^\circ$	$70^\circ - 75^\circ$	$60^\circ - 52^\circ$
3	$56^\circ - 61^\circ$	$48^\circ - 41^\circ$	$66^\circ - 75^\circ$	$54^\circ - 46^\circ$
4	$47^\circ - 58^\circ$	$50^\circ - 37^\circ$	$66^\circ - 73^\circ$	$58^\circ - 48^\circ$

3.2 Analysis

3.2.1 Concus-Finn Method

The analytic method described below identifies the existence of equilibrium surfaces in any cylindrical container. To avoid confusion, the equilibrium surface refers to a finite-height single-valued fluid surface that covers the base of the container, see Figure 3.7. Note that there is only one simply connected contact line on each simply connected solid wall boundary for such equilibrium fluid configurations. This type of equilibrium surface is called a simple surface. In a generic cylindrical container as shown in Figure 3.7, such equilibrium simple surfaces in general exist in terrestrial conditions where gravity overwhelms capillary forces. In zero gravity, however, the existence of such a surface can not always be guaranteed. Nevertheless, a surface ‘non-existence’ is desirable in many applications as it provides a passive means to transport and/or locate fluids. The non-existence of a simple surface means that there is always a curvature gradient along the free surface such that part of the interface rises to infinity while the bulk surface remains one of constant mean curvature given that there is enough liquid to cover the base of the container. Such a situation is not likely to take place in practice. In reality, what happens is that the fluid wicks along part of the container wall with relatively high curvature until it either reaches the top of the container or part of the base of the container is exposed. Of course, the fluid surface will ultimately possess some equilibrium shape in a container of finite size. Such equilibrium surfaces are

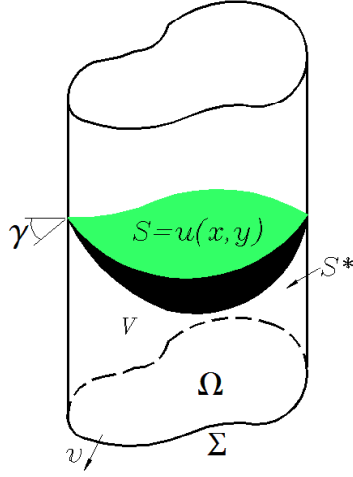


Figure 3.7: A generic cylindrical container and a simple equilibrium surface.

different from simple surfaces and are called complex surfaces. In general, complex surfaces may either have multiple disconnected contact lines on every simply connected solid wall or have portions of contact lines pinned along edges of the boundary walls. Essentially, the Concus-Finn method predicts the transition from a simple surface to a complex one in a cylindrical container of finite extent.

In zero gravity, simple equilibrium capillary surfaces in a cylindrical container are described by the Young-Laplace-Gauss equation

$$\nabla \cdot \mathbf{T}u = 2H \equiv \frac{\Sigma}{\Omega} \cos \gamma , \quad (3.1)$$

where

$$\mathbf{T}u = \frac{\nabla u}{\sqrt{1 + |\nabla u|^2}} , \quad (3.2)$$

and with contact angle boundary condition

$$\nu \cdot \mathbf{T}u = \cos \gamma \quad (3.3)$$

on the container walls where ν is the exterior normal vector of the wall. Note that the mean curvature of equilibrium surfaces is determined by the area Ω and perimeter Σ of the container cross-section along with the contact angle γ , as shown in Eq.(3.1).

A necessary condition for the existence of a simple surface in a cylindrical container is established by Concus and Finn. The derivation of the condition is only outlined here. A complete presentation can be found in Finn[24] and references contained therein. For a general cross section shown in Figure 3.8, Ω represents both the entire domain and its area and Σ represents the entire boundary of Ω and its length. In the domain Ω one can draw arcs Γ of radius

$$R_\gamma = \Omega / (\Sigma \cos \gamma) \quad (3.4)$$

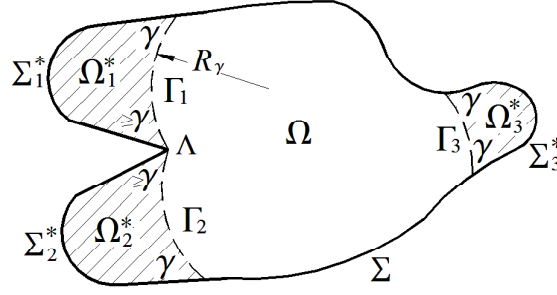


Figure 3.8: General Ω domain and $\{\Gamma; \gamma\}$ configurations.

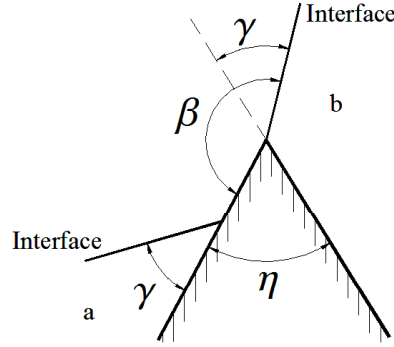


Figure 3.9: Demonstration of Gibbs's inequality, γ is the equilibrium contact angle and η the corner angle at the solid edge. Here is shown one extreme location at which $\beta = \pi - \eta + \gamma$ for the interface meeting the solid edge.

that meet the boundary Σ at contact angle γ . Note that the angle that Γ meets at a corner Λ can be greater than or equal to γ . The angle of the corner Λ measured inside of Ω is greater than 180° and is called a reentrant corner. The angle at which Γ meets Λ is dictated by Gibbs's inequality

$$\gamma \leq \beta \leq \pi - \eta + \gamma, \quad (3.5)$$

where γ is the equilibrium contact angle, β is the angle at which the free surface meets the edge of the corner measured within fluid 'a', and η is the angle of the corner at the edge (measured in the solid) as depicted in Figure 3.9. A rigorous description of Gibbs's inequality can also be found in Finn[24].

Single or multiple arcs Γ and part of boundary $\Sigma^* \subset \Sigma$ bound a subdomain $\Omega^* \subset \Omega$. A necessary condition for the existence of a simple equilibrium capillary surface on Ω is

$$\Phi(\Gamma) = \Gamma - (\cos \gamma) \Sigma^* + \left(\frac{\Sigma \cos \gamma}{\Omega} \right) \Omega^* > 0 \quad (3.6)$$

for every Ω^* configuration as shown in Figure 3.8. In general, there are a finite number of

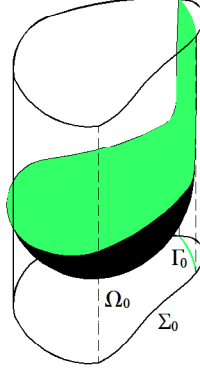


Figure 3.10: Demonstration of a C-singular solution in a cylindrical container.

admissible $\{\Gamma; \gamma\}$ configurations for a given domain such that it is possible to evaluate the value of Φ on every Ω^* .

3.2.2 C-singular Solution

A natural question following the non-existence of the simple equilibrium surface is what will happen to the fluid surface. Finn and Neel[25] point out that there is a solution surface in a singular sense, called a Cylindrically singular solution, referred to as C-singular solution. Typically, there is a subdomain Ω_0 as shown in Figure 3.10 over which the free surface has constant mean curvature; the surface meets the solid wall at contact angle γ , while it becomes asymptotically a vertical cylindrical surface when approaching an arc Γ_0 with radius of curvature R_0 . In other words, the surface rises to infinity for any approach to Γ_0 from within Ω_0 . Over the subdomain $\Omega - \Omega_0$, the interface rises to infinity. Arc Γ_0 serves as a barrier between the subdomain Ω_0 over which the simple surface exists and the subdomain $\Omega - \Omega_0$ over which the simple surface fails to exist. Note that when $\Phi = 0$, the radius of curvature $R_0 = R_\gamma$. However, for cases where $\Phi < 0$ the radius of curvature $R_0 > R_\gamma$ and R_0 is determined by integrating the Young-Laplace-Gauss equation

$$\nabla \cdot \mathbf{T}u = 2H_0 \quad (3.7)$$

over Ω_0 and applying divergence theorem to obtain

$$\Gamma_0 + (\cos \gamma)\Sigma_0 - 2H_0\Omega_0 = 0. \quad (3.8)$$

Solving Eq.(3.8) gives rise to R_0 .

3.2.3 Analysis: Perfectly Wetting Case (CFE VG-1)

For the perfectly wetting case where the contact angle is zero, it can be shown that there are at least five Ω^* configurations as shown in Figure 3.11. For each configuration two or more arcs Γ are necessary with various portions of the solid boundary to enclose subdomains Ω^* and evaluate Φ . Note that the four corners of the vane are all reentrant as sketched in

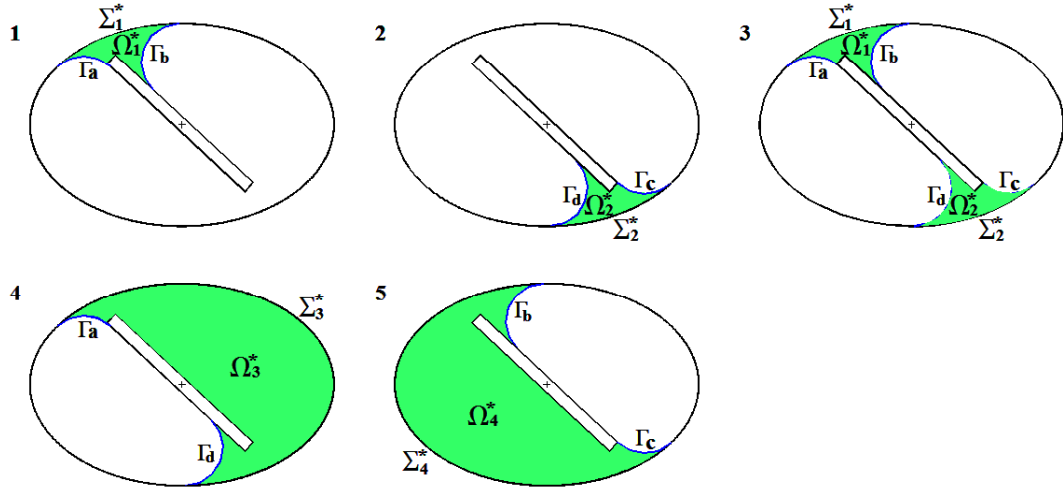


Figure 3.11: Demonstration of Γ configurations. 1. Small gap region; 2. Large gap region; 3. Combined gap regions; 4. Right bulk region; 5. Left bulk region.

Figure 3.8. Based on the vane angle, arc Γ either meets the vane surface at contact angle γ , or it can meet the vane corner at any angle within the range specified by Eq.(3.5). Arc Γ in the former case is called regular while the latter is called irregular. With the vane centerline aligned with the center of the ellipse and when all arcs Γ are regular, Γ_a and Γ_c , and Γ_b and Γ_d are antisymmetric about the axes of the ellipse. Otherwise, for certain vane angles, Γ_a and Γ_c are not antisymmetric (i.e. not the same) and must be determined independently; Γ_b is regular for the entire range of the vane angle so Γ_d does not need to be identified independently. Furthermore, when both Γ_a and Γ_c are regular, it can be shown that Φ has the same value for cases 4 and 5.

Φ values as a function of the vane angle α are computed and plotted in Figure 3.12. In general, Φ decreases with increasing α ; Φ for the small gap is lower than that of all the other cases crossing through zero first. The Φ values for case 4 and 5 are slightly different from each other (indistinguishable on plot) over certain vane angles when either one or both of Γ_a and Γ_c are irregular. It is found that $\Phi_1 = 0$ at $\alpha = 42.94^\circ$. Once $\Phi_1 = 0$ in the small gap region a simple equilibrium surface fails to exist in the container and fluid wicks up the small gap. This is in agreement with the experiment where the critical vane angle $41.5^\circ \leq \alpha_{cr} \leq 46.5^\circ$, see SGW, Table 3.1.

$\Phi_1 < 0$ for further increases of the vane angle α and C-singular solutions for the free surface persist. As mentioned above, arcs Γ_0 can be identified that separate the small gap region from the rest of the domain in the sense that the surface rises to infinity over the small gap region while remaining a simple surface of constant mean curvature in the rest of the domain. With further increases of the vane angle α , the question remains whether there is always a simple solution over the rest of the problem domain. Since Γ_0 serves as a barrier between the small gap region and the rest of the domain it is necessary to subtract the small gap region Ω_1 from the entire domain Ω in order to analyze the rest of the domain.

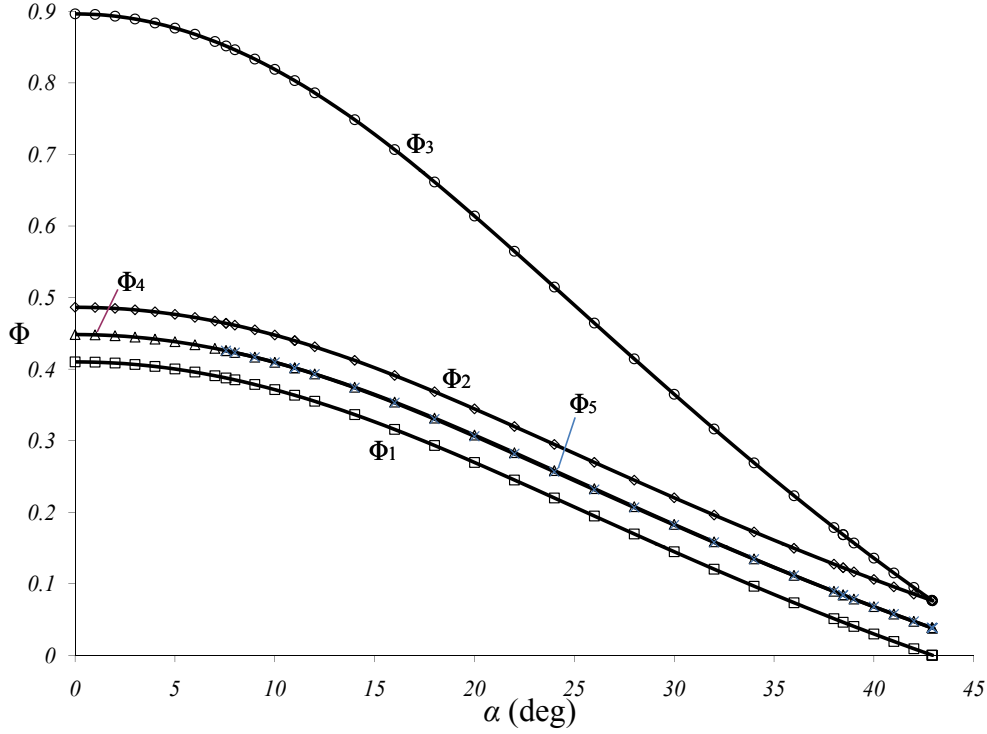


Figure 3.12: Φ for various Γ configurations as a function of vane angle α for VG-1; Φ_1 - Φ_5 are the values of Φ for cases 1-5 in figure 3.11 respectively.

The approach employed here is as follows. For *each* vane angle α one needs to first locate Γ_0 whose radius R_0 satisfies Eq.(3.8) as shown in Figure 3.13a. Subsequently, the small gap region included on the convex side of the arcs Γ_{0a} and Γ_{0b} is subtracted giving rise to a new modified domain shown in Figure 3.13b. In the new domain, one draws arc Γ wherever possible. Note that for Γ the radius $R_\gamma = R_0$. Accordingly, there are at least three Ω^* configurations as shown in Figure 3.13c-e.

Φ values for each configuration are computed and shown in Figure 3.14. Note that $\Phi_d = \Phi_e$ and that both are smaller than Φ_c . Φ in all configurations passes through zero at the same vane angle $\alpha = 51.29^\circ$. $\Phi = 0$ for all configurations which we prove as follows. Using the notation in Figure 3.15, when $\Phi_c = 0$, one has

$$\Phi_c = \Gamma_c + \Gamma_d - \Sigma_2^* + \frac{\Omega_2^*}{R_0} = 0. \quad (3.9)$$

The two C-singular solutions Γ_{0a} and Γ_{0b} satisfy Eq.(3.8) which can be written as

$$\Gamma_{0a} + \Gamma_{0b} + (\Sigma_2^* + \Sigma_3 + \Sigma_4) - \frac{\Omega_2^* + \Omega_3 + \Omega_4}{R_0} = 0, \quad (3.10)$$

which, with $\Gamma_{0a} = \Gamma_c$, $\Gamma_{0b} = \Gamma_d$, $\Sigma_3 = \Sigma_4$, $\Omega_3 = \Omega_4$, and subtracting Eq.(3.9) from Eq.(3.10)

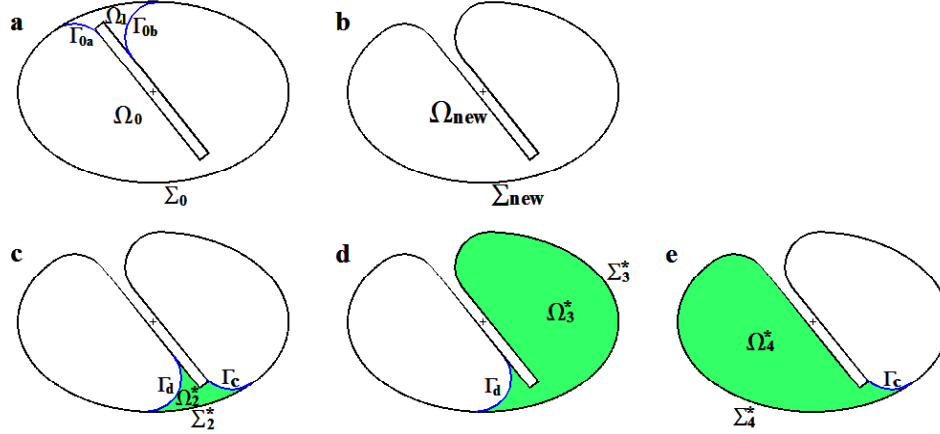


Figure 3.13: Arcs Γ configurations in the modified problem domain. a. C-singular solutions Γ_{0a} and Γ_{0b} ; b. Modified domain with small gap region subtracted; c. Large gap region; d. Modified right bulk region; e. Modified left bulk region.

yields

$$(\Sigma_2^* + \Sigma_3) - \frac{\Omega_2^* + \Omega_3}{R_0} = 0, \quad (3.11)$$

and since $\Gamma_{0b} = \Gamma_d$,

$$\Gamma_d - (\Gamma_{0b} + \Sigma_2^* + \Sigma_3) + \frac{\Omega_2^* + \Omega_3}{R_0} = \Phi_d = \Phi_e = 0. \quad (3.12)$$

Note that this is only possible when $\Phi_d = \Phi_e$, which is true when both Γ_{0a} and Γ_c are regular. This shows that multiple C-singular solutions co-exist at the present vane angle. It is not definite which solution takes place in such a situation. However, it shows that the bulk shift can not take place any sooner than wicking in the large gap region. Interestingly, experiments show that the bulk shift takes place at vane angles below 50° , which is several degrees lower than the critical vane angle $\alpha_{cr} = 51.29^\circ$ identified in Figure 3.14. It will be shown that the most possible cause for this is container asymmetries.

To compare the analytical and experimental results critical vane angles in different quadrants for the small gap, large gap, and bulk shift are listed in Table 3.1. A comparison of theoretical predictions and the experimental results is shown in Figure 3.16, which reveals that the critical vane angle differs from quadrant to quadrant. The bulk shift takes place between the small gap and large gap wetting when the small gap is in quadrant 1, 2, and 3, while it takes place before either gap wetting when the small gap is in quadrant 4. The difference is apparently caused by the asymmetry in the geometry currently presumed within the specified tolerance of fabrication. The asymmetry could mean that the gap size is not exact or the vane is somehow misaligned such that the vane center-line does not exactly pass through the center of the ellipse. The experiment also shows that the bulk shift always takes place at the same side of the vane for both clockwise and counter-clockwise operation

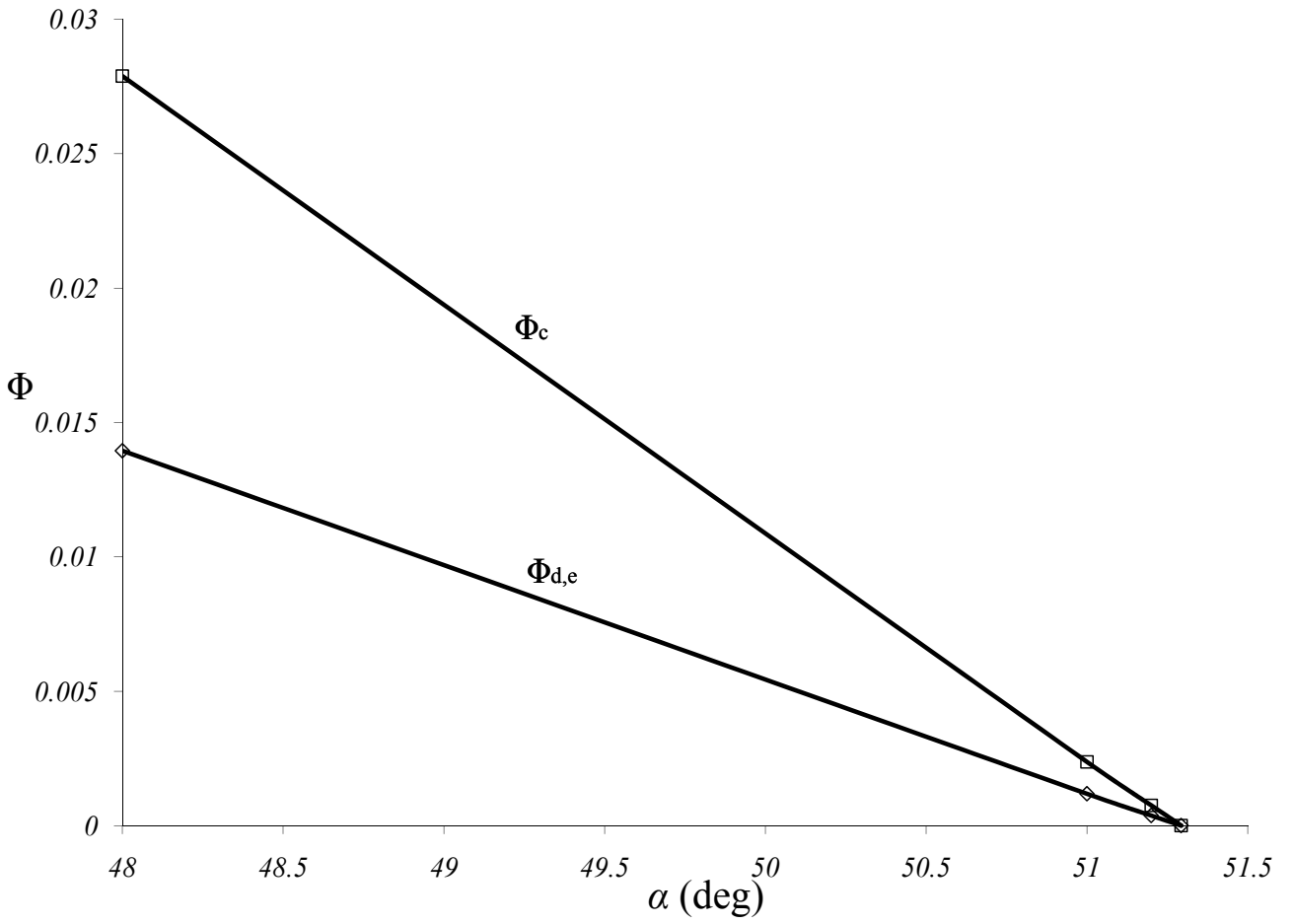


Figure 3.14: Φ for the three Γ configurations in the modified domain in VG-1.

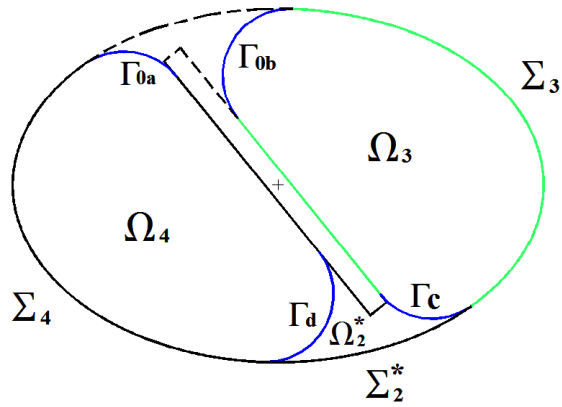


Figure 3.15: Problem domain with C-singular solutions in the small gap region.

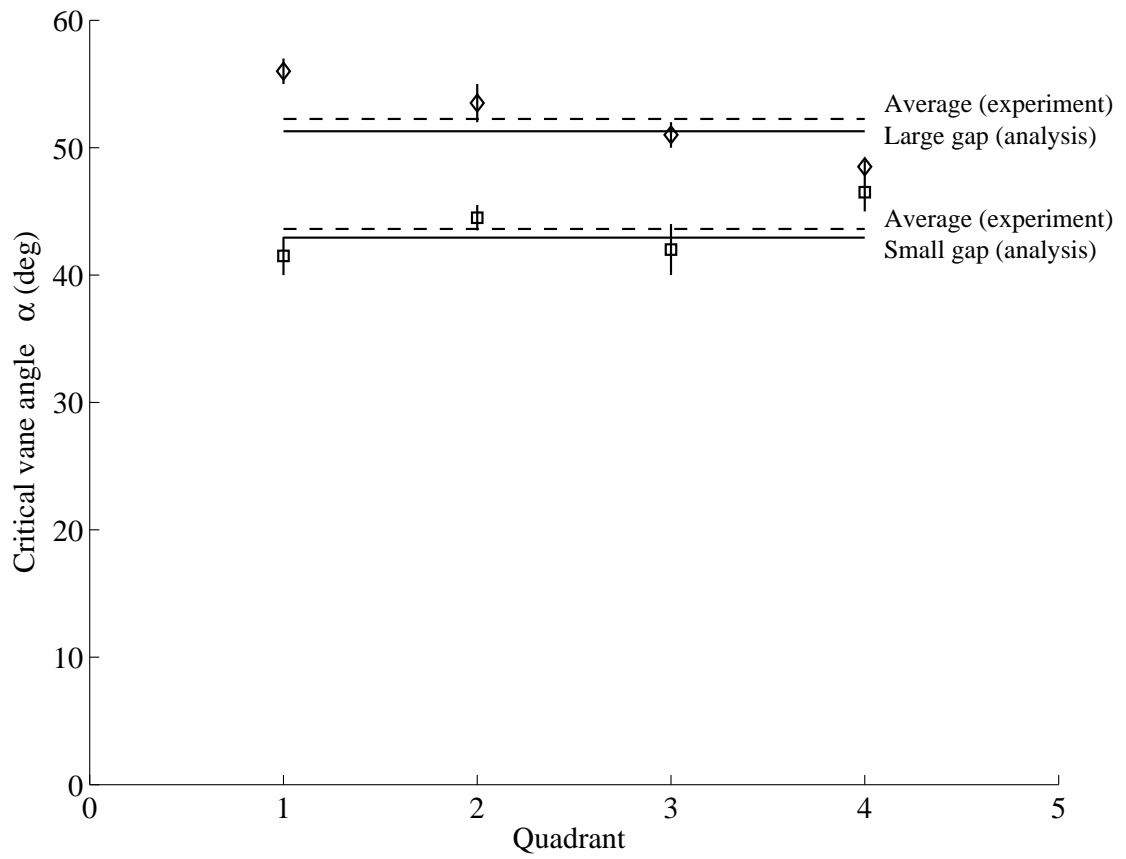


Figure 3.16: Comparison between analytic predictions and experiment results for CFE VG-1. □, Small gap; ◇, Large gap.

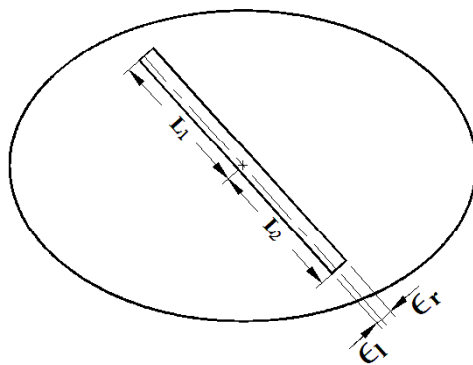


Figure 3.17: A definition of vane thickness and length about the center of the ellipse.

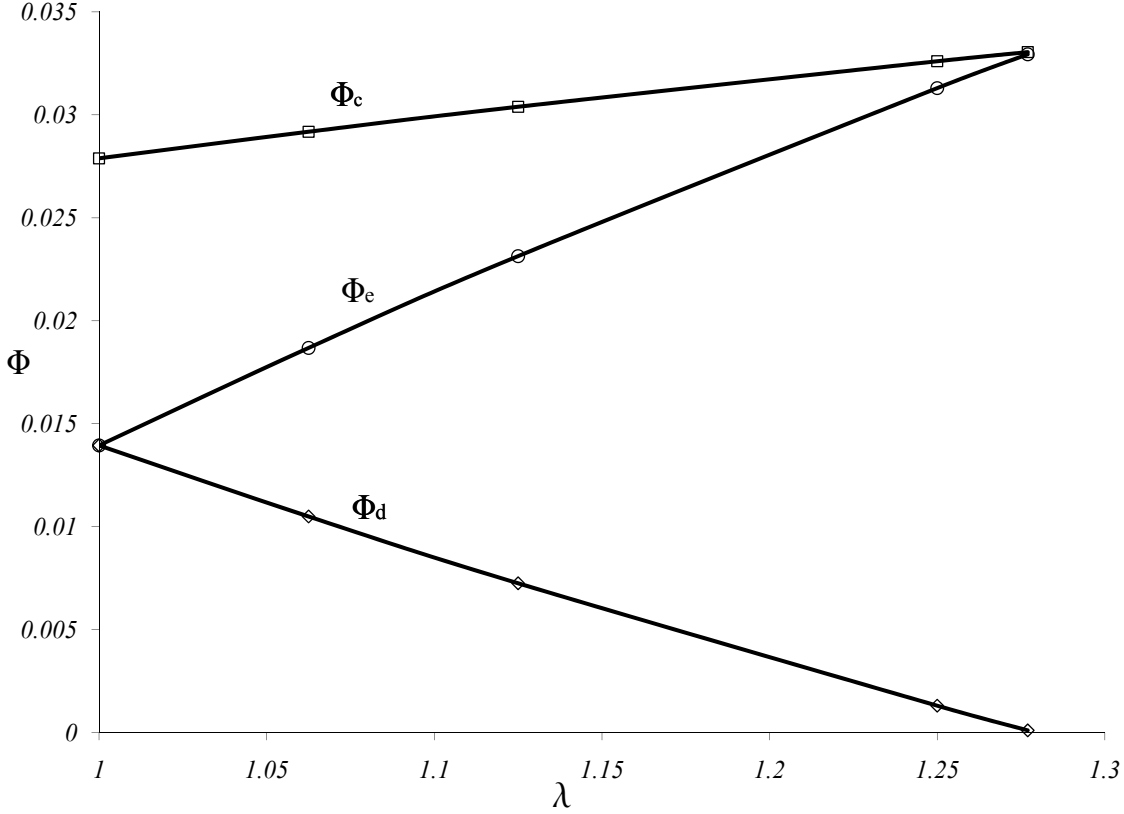


Figure 3.18: Φ of three configurations in modified domain at different λ for $\alpha = 48^\circ$.

of the vane, which further suggests that there are geometric asymmetries. It is also remotely possible that asymmetry of the ellipse contributes to the difference observed. A detailed inspection of the test cell is not possible at present. However, a preliminary investigation of the gap size and misalignment of the vane is carried out analytically below.

It can be shown that if there is any misalignment of the vane then $\Phi_d \neq \Phi_e$ such that Φ of the three configurations in Figure 3.13 will not pass through zero simultaneously. For example, the experiment data shows that in quadrant 1 the bulk shift takes place at $\alpha = 47.5^\circ$ with 2.5° uncertainty. Quantities $\lambda \equiv \epsilon_r/\epsilon_1$ and $\Pi \equiv L_2/L_1$ are defined from ϵ_r , ϵ_1 , L_1 , and L_2 shown in Figure 3.17. Note that L_1 is the length of the vane on the small gap side. Given by design that $L_1 = 16.091$ mm and $L_2 = 15.253$ mm, $\Pi = 0.948$. It can be shown that at $\alpha = 48^\circ$ in quadrant 1 in order for the bulk shift to take place one should have $\lambda = 1.277$ if Π is held constant as shown in Figure 3.18.

It is necessary to point out that what happens in quadrant 4 is very interesting because the bulk shift takes place first at $\alpha = 42.5^\circ$. A detailed analysis shows that in order for this to happen, it is necessary to have $\lambda = 0.541$ while Π is held constant. The effect of Π is found to be negligible. Once there is a bulk shift, corresponding C-singular solutions exist. Note that even though there are C-singular solutions and the fluid on one side of the vane

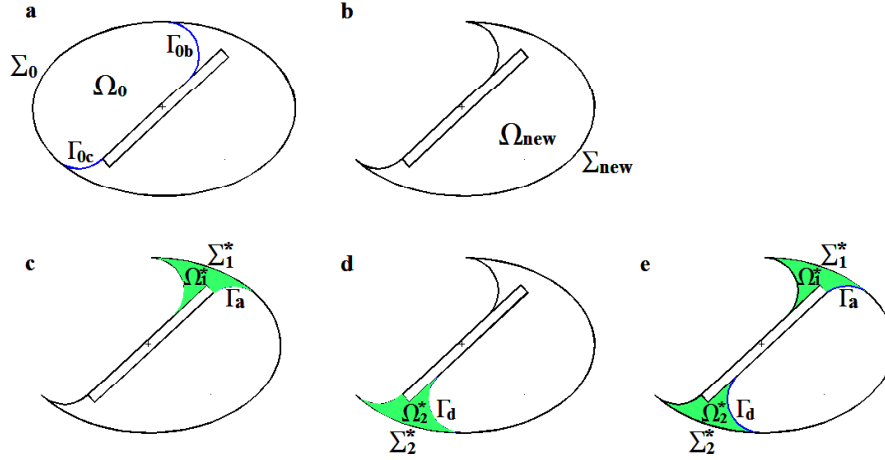


Figure 3.19: Modified domain for the vane in the quadrant 4 where the bulk shift takes place first

would rise to infinity, the free surface on this side of the vane still has certain constant mean curvature. This means that it is still possible to analyze this part of the free surface for the critical wetting condition. The modified domain is shown in Figure 3.19b. In a sense, this is the opposite of what happens when the small gap wetting first takes place as previously discussed, see Figure 3.13. The critical wetting in the gap regions can be analyzed in the modified domain as shown in Figure 3.19c and d. By keeping $\lambda = 0.541$, it is found that $\Pi = 0.971$ in order for the wetting to take place in the small gap region at $\alpha = 46.5^\circ$. This gives the offset of the vane rotation center relative to the ellipse center. Based on this offset, for the other quadrants, the critical vane angles are computed and compared in Figure 3.20. Agreement in quadrant 2 and 3 is not as good as that in quadrant 1 and 4. Obviously the determination of the vane rotation center is not the only explanation. Further analysis and/or test cell measurements are necessary to fully identify the cause.

Note that once there is wicking in both the small and large gaps, the C-singular solutions in the two regions have the same radius of curvature. The free surface between the two C-singular solutions has constant mean curvature which is actually greater than the curvature of the free surface on the other side of the vane. As a result, the bulk shift co-exists with the wicking in the two gap regions. This also implies that the arcs Γ on the two sides of each gap actually have different radii of curvature. This is different from cases where there is no misalignment of the vane for which the radii of curvature should always be same.

3.2.4 Analysis: Partially Wetting Case (CFE VG-2)

CFE VG-2 test cell examines a partially wetting case. The interior surface is coated such that the effective contact angle of the test fluid is around 55° . Except for the thickness of the vane which is twice that of the vane in the CFE VG-1 test cell, all other dimensions are the same for VG-1 and VG-2.

The critical wetting conditions are found in the same manner as that for the perfectly

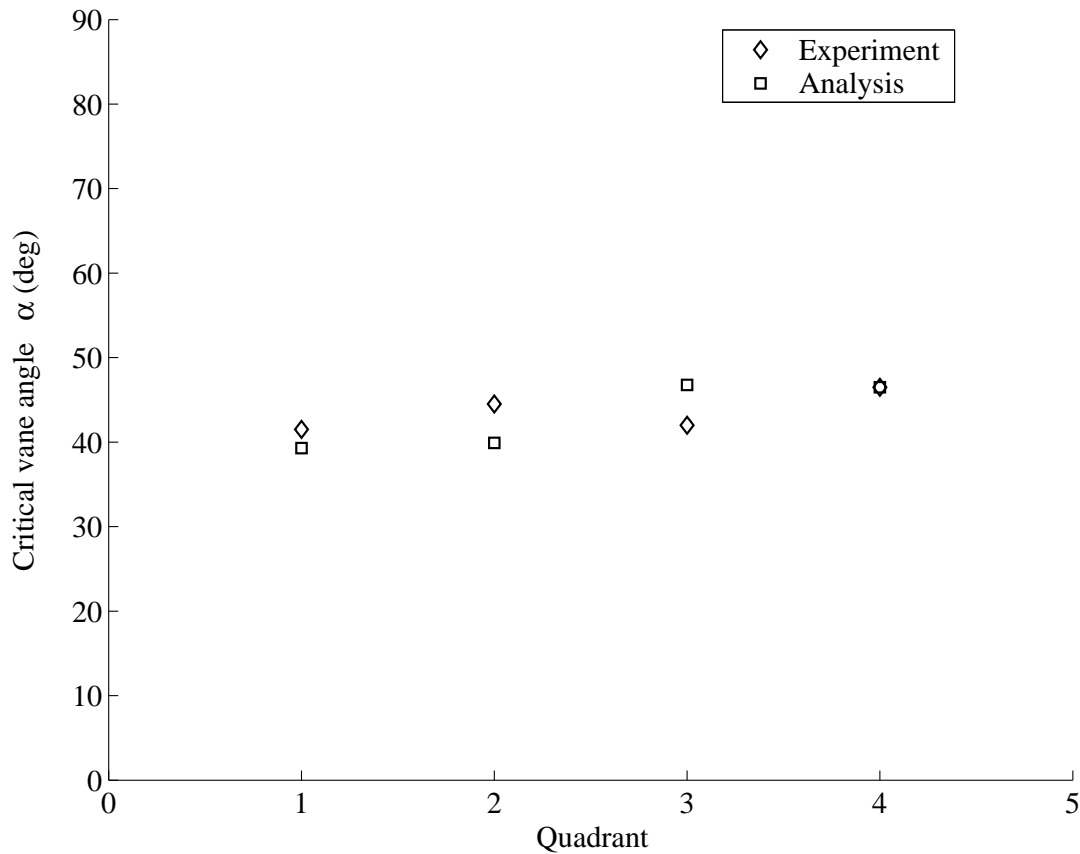


Figure 3.20: A comparison between the analytical prediction and the experimental results for small gap critical wetting condition based on the offset of the vane rotation center determined in quadrant 4.

wetting case. It can be shown that for any given vane angle arcs Γ of both regular and irregular types exist. However, only the irregular type yields critical wetting conditions where the functional Φ vanishes at certain vane angles α . It is found that the small gap wetting takes place at $\alpha = 53.47^\circ$ whereas the large gap wetting takes place at $\alpha = 62.29^\circ$, which compares suitably with the experimentally determined angles $47^\circ \leq \alpha_{\text{cr}} \leq 62^\circ$ and $66^\circ \leq \alpha_{\text{cr}} \leq 79^\circ$, respectively. The experimental results are listed in Table 3.2. A comparison between the analysis and the experiment is shown in Figure 3.21. The difference between the average experimental value and the prediction is 4.8% for the small gap wetting while it is 14.2% for the large gap wetting. It is speculated that both geometric asymmetry and contact angle hysteresis could play a role causing the difference and this shall be clarified once detailed measurements of the test cells is available. A bulk shift is not observed in the experiment which can be shown to be possible only when there is substantial misalignment of the vane.

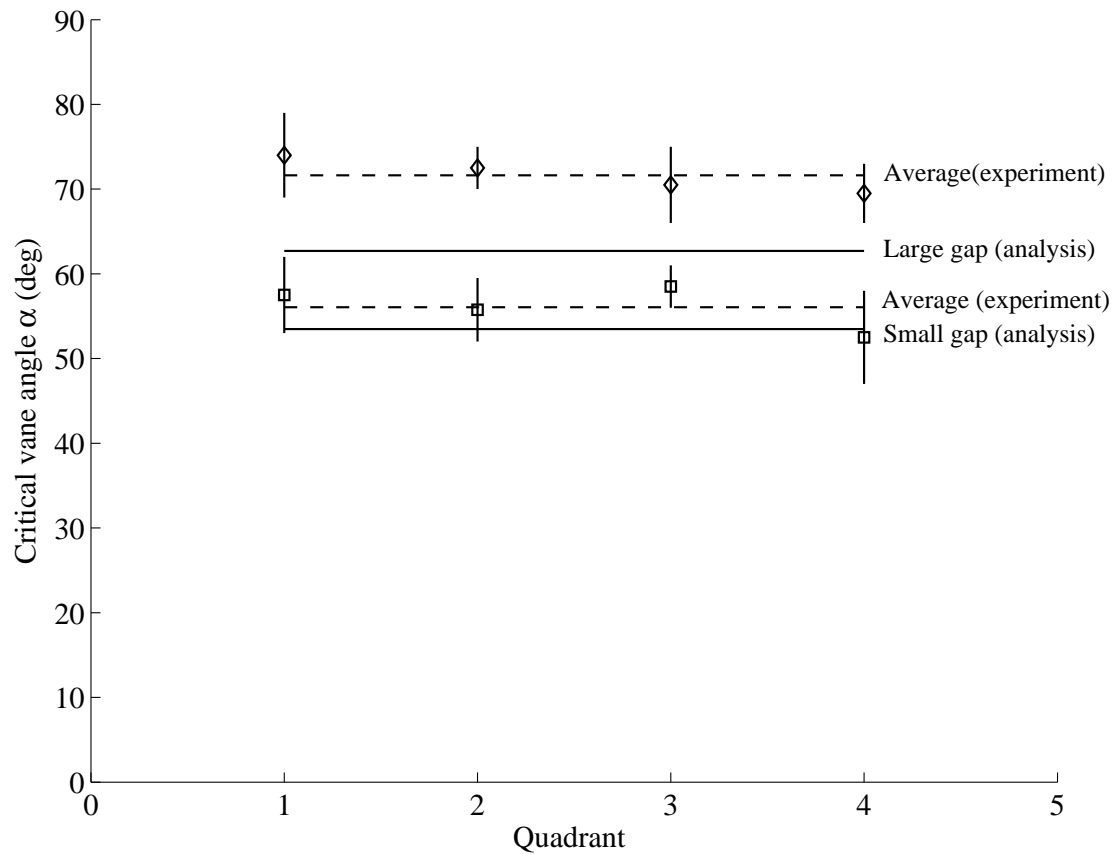


Figure 3.21: A comparison between the predictions and the experiment results for partial wetting case. \square , Small Gap; \diamond , Large gap.

3.3 Chapter Summary

Critical capillary wetting phenomena can be observed in many situations. It has important applications in fuel systems, fluids handling, and material processing in the liquid state on spacecraft. To fully understand it provides important and useful means to perform operations more efficiently. In this work a Vane Gap geometry is studied as part of the Capillary Flow Experiments conducted onboard the International Space Station. This geometric configuration features typical critical wetting phenomena that can be analyzed using the Concus-Finn method. The geometry is relatively simple while the phenomena observed through experiments and its analysis is rich.

In general, it is observed that there are three wetting configurations for the perfectly wetting fluid in CFE VG-1 test cell. Those are the small gap wetting, the large gap wetting, and the bulk shift. Among the three the bulk shift is most significant because of the amount of the liquid involved. Analysis shows that the bulk shift is not likely to happen if there is perfect symmetry. It also shows that fractions of a millimeter of misalignment of the vane can cause the bulk shift to take place revealing the geometric sensitivity of the critical

wetting. In contrast, only the small gap wetting and large gap wetting are observed for the partially wetting fluid in CFE VG-2 test cell. Bulk shift is unlikely unless there is substantial vane misalignment or the contact angle is small enough with relatively small misalignment.

Chapter 4

CFE-ICF Model Background: Weakly 3-D Capillary Flows

Summary. Spontaneous capillary flows in containers of increasing complexity are currently under investigation to determine important transients for low-g propellant management. Significant progress has been made for complex containers that are cylindrical, but many practical systems involve geometries that are tapered. For example, the taper of an irregular polygonal cross section provides particular design advantages by preferentially locating the liquid where desired and by providing a passive means for fluid phase separation. Passive capillary flow in such containers is termed imbibition and cannot be studied easily on the ground for large, significantly 3-D geometries. For certain flows the governing equations are known but have not been solved analytically to date due to a lack of experimental data identifying the appropriate boundary conditions for the flow. The experimental results of the CFE-ICF test vessels as well as drop tower tests support the analysis of imbibition in tapered polygonal sections, and, in particular, a variety of regular n -gonal pyramids. The theory can be used to aid in the design and analysis of capillary devices such as 3-D vane networks for bubble-free collection and positioning of fuels for satellites, an important problem concerning propellant and/or cryogenic liquid management aboard spacecraft.

4.1 Introduction

Capillary-driven flows along the interior corners of containers have been studied in detail and a selection of geometries and flow scenarios were recently reviewed [26]. Many such flows are applicable to fluids management aboard spacecraft. For example, a typical flow is shown in Figure 1 where a right cylinder of polygonal section is partially filled with a wetting fluid and released in a drop tower. The fluid is drawn along the corners by capillary forces in the low-g environment and advances at a rate proportional to $t^{1/2}$. The fluid rapidly establishes a constant height (a.k.a. constant pressure) at a specific location in the container as denoted by H in the figure. This fixed height serves as an essential boundary condition for the analysis of the flow and leads to the predicted $t^{1/2}$ behavior. H may be determined a priori for a large family of cylindrical vessels [27][28].

In general, for slender fluid columns, the lubrication approximation may be applied to quantify the nonlinear diffusive flows that occur in corners under favorable wetting conditions. In conditions where a certain container possesses a slight taper the flows are observed to transition between various regimes. For example, in Figure 2 the edges of a polygonal sectioned container taper uniformly at an angle characterized by ψ . For such ‘pyramidal’ containers whose edges meet at a vertex or virtual vertex, the cross-sectional area is pro-

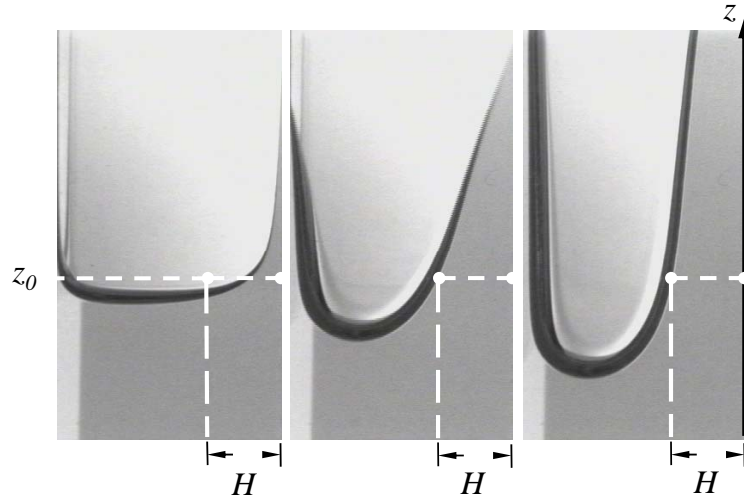


Figure 4.1: Spontaneous capillary rise (imbibition) in an equilateral triangular container during a drop tower experiment. Vertex on right observed in profile. The constant height (pressure) location rapidly achieved by fluid is identified by H .

portional to $z^2 \tan^2 \psi$ as identified in Figure 2a. Provided wetting conditions are favorable and fluid content is ample, a visco-capillary dominated fluid introduced to the base of the container will wick to the vertex of the container at a rate $t^{1/2}$ (Figure 2b-c). However, once the fluid arrives there, new boundary conditions arise that change the transient response of the fluid which continues to wick at an altered rate toward the vertex. The flow of liquid toward the vertex effectively displaces the ‘ullage’ away from the vertex and toward the ‘base’ of the container as shown in Figures 2d-e. The pressure gradient for the global flow is maintained by the varying curvature of the bulk meniscus as sketched in Figures 2d-e and to be discussed in further detail in context with Figure 3a. The individual capillary driven corner flows represent local flows that contribute to the migration of the bulk menisci that define the ullage.

The relevance of such flows is obvious for fuels and fluids handling and the quantitative dependence on specific container geometry adds significant design capability to engineers optimizing flow channels for a variety of passive fluids positioning and phase separation tasks in spacecraft fluids systems. In this work, a zeroth order solution is reported for what we define here as ‘weakly 3-D’ capillary driven flow—the flow process that characterizes the migration of the ullage depicted in Figure 2c-e. Higher order solutions will be reported in a subsequent publication.

4.2 Model and Equation Formulation

A simplified analysis of the flow is possible by employing a number of modeling assumptions at local and global levels. These are first listed below before they are applied in the mathematical development. Similar approaches have been employed to analyze capillary

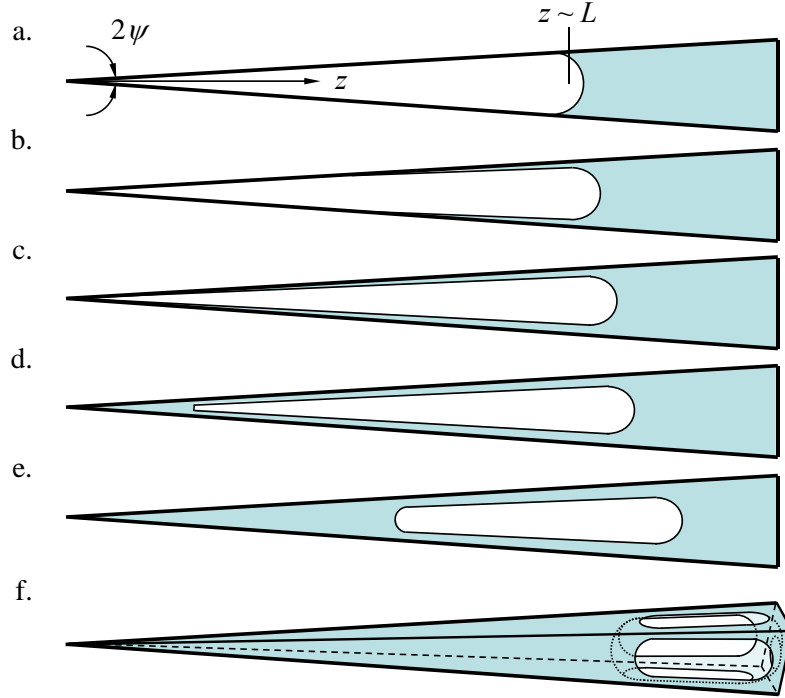


Figure 4.2: Capillary flow in a slightly tapered pyramidal container, conduit, or pore. Liquid introduced into the base of the cell a) imbibes towards the vertex at a rate characterized by $t^{1/2}$, b) and c). Once the vertex is reached d), new boundary conditions apply and continued capillary driven corner flows displace the ullage towards the base of container, e) and f). The container described is that of a right square pyramid shown in perspective in f).

flows in contracting square pores related to transport in porous media [29][30][31].

4.2.1 Global Assumptions

1. An ullage in a tapered container is represented schematically in Figure 3a. For small taper angles the container axis coordinate z may be approximated by corner axis coordinate z' such that $z' = z + O(\psi)$. This assumption requires $\psi \ll 1$.
2. Referring to Figure 3a, provided the volume of the ullage is large compared to the volume of the ullage contained solely within the regions of bulk meniscus curvature (R_1 and R_2), the ullage may be modeled as one with flat ends as shown in Figure 3b. It can be shown that this assumption is valid for the most part provided the taper angle is small, $\psi \ll 1$. Further support for this assumption will be provided herein. The leading and trailing bulk menisci are identified at positions 2 and 1 as shown on Figure 3a and represented by z_2 and z_1 in Figure 3b, respectively.

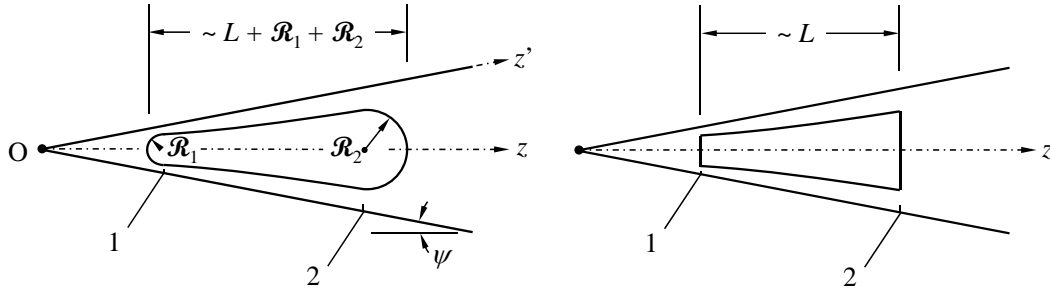


Figure 4.3: Schematic of capillary flow in a tapered conduit: a) Ullage shown with effective radii of curvature at leading (2) and trailing (1) bulk menisci, b) simplified ullage illustrated as modeled herein.

3. The local radius of curvature and thus the pressure in the liquid at the leading and trailing bulk menisci may be determined by the method of de Lazzer et al. [27][28][32]. This assumption permits the clean and closed-form calculation of the constant height boundary condition $h_1(z_1)$ and $h_2(z_2)$ required for solution of the local problem and allows the bulk meniscus leading and trailing locations to be modeled by $z_2(t)$ and $z_1(t)$. Fortunately, this assumption also requires the same constraint as assumption #1, $\psi \ll 1$. Experimental support for this assumption applied to tapered geometries is provided by way of simple drop tower tests to be highlighted in summary.
4. Not necessarily in general, but for the purposes of the present analysis a further restriction is made to tapered section types where, at any section along the ullage, the total cross flow area A of the spreading fluid is small compared to the container cross-section area A_s . Thus, $A/A_s \ll 1$ and represents a low liquid saturation at any section across the ullage. As will be discussed in context with Figure 4, $A/A_s \equiv \beta \ll 1$ is maintained for a large number of polygonal container types such as n -side regular polygonal sections, rectangular sections, and general sections where α_i interior corner half angles are typically larger than 30° . Sections with highly acute interior angles do not necessarily meet this criterion and require a higher order analysis.

The local flow problem concerns the capillary driven interior corner flow from the leading bulk meniscus region of the ullage at z_2 to the trailing region at z_1 , Figures 3 and 4. The local flow is represented schematically in Figure 5 and might be effectively modeled provided several conditions are satisfied.

4.2.2 Local Assumptions

5. The liquid columns that flow along the corners are assumed slender. This assumption requires that $\epsilon^2 \ll 1$, where $\epsilon = h_2/(z_2 - z_1)$ is the slenderness ratio. This assumption allows the lubrication approximation to describe the corner flow.

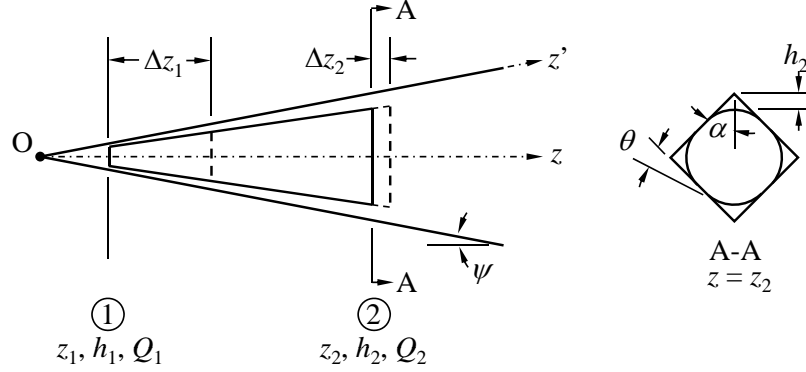


Figure 4.4: a) Schematic of ullage with notation identified as employed in the analysis for n -sided polygonal containers, conduits, or pores. A right, square pyramid is sketched here, where section A-A in b) identifies fluid cross flow area identified in a) at $z = z_2$.

6. For slender columns, streamwise curvature of the interface in the z -direction can be ignored provided $\epsilon^2 f \ll 1$ where f is a cross-stream geometric curvature function to be defined ($R = f_i H_i$). This assumption is frequently satisfied by the previous assumption $\epsilon^2 \ll 1$ and, with the lubrication approximation, reduces the Navier-Stokes and mass conservation equations to a single transient 1-D nonlinear diffusion equation for the interface height $h(z, t)$ along the corner. (Note that $h_{i1} = h_i(z_1, t)$ and $h_{i2} = h_i(z_2, t)$.)
7. Inertia in the corner flows is assumed negligible. This assumption is frequently satisfied by the slender column assumption $\epsilon^2 \ll 1$ as well.
8. The influence of gravity on the flow is presently neglected.

4.2.3 Dimensional Equations

A. Local Mass Balance and Flow Profile. The dimensional equation for the local flow along the i th of m wetted corners in a container of n interior corners derives from the Navier-Stokes equation and a local mass balance for each corner; namely,

$$\frac{\partial A_i}{\partial t} = -\frac{\partial \dot{Q}_i}{\partial z}, \quad (4.1)$$

where $\dot{Q}_i = A_i \langle w_i \rangle$ is the i th corner volumetric flow rate and $\langle w_i \rangle$ is the average corner flow velocity through flow area A_i . As shown elsewhere [33][34], Eq. (4.1) may be expressed dimensionally in terms of local fluid height h_i ,

$$\frac{\partial h_i^2}{\partial t} = \frac{\sigma}{\mu} \frac{F_{ii} \sin^2 \alpha_i}{f_i} \frac{\partial}{\partial z} \left(h_i^2 \frac{\partial h_i}{\partial z} \right), \quad (4.2)$$

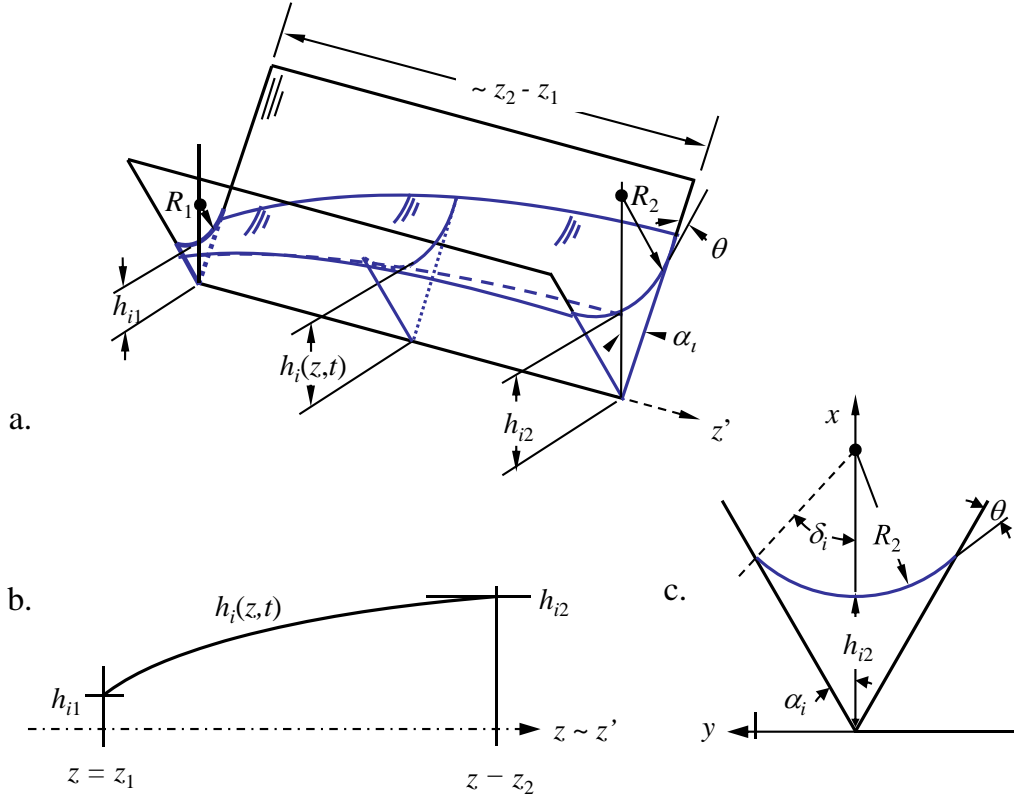


Figure 4.5: Schematic of the local flow along the i th wetted corner: a) notation employed to describe the flow between the bulk meniscus regions 1 and 2, Figures 3 and 4, b) fluid interface profile along corner bisector, and c) cross flow section at $z = z_2$.

subject at least to boundary conditions at the trailing and leading bulk menisci locations $h_i(z_1) = h_{i1}$ and $h_i(z_2) = h_{i2}$. In Eq. (4.2), σ is the fluid surface tension, μ is the dynamic viscosity, and F_{ii} is a numerical dimensionless resistance coefficient which can in many practical circumstances be treated as a constant $1/8 \leq F_{ii}(\alpha, \theta) \leq 1/6$ (see refs. [34] and [35]). In Eq. (4.2) the geometric surface curvature function f_i is given by

$$f_i = \frac{\sin \alpha_i}{\cos \theta - \sin \alpha_i}, \quad (4.3)$$

where θ is the contact angle and α_i is the particular corner half angle. Again, subscript i denotes the i th of m wetted corners in a container with n interior corners.

When possible, solutions to Eq. (4.2) and associated boundary and initial conditions may be used in turn to compute the total flow rate at bulk menisci locations 1 and 2 using

$$\dot{Q}_1 = \sum_{i=1}^m A_i \langle w_i \rangle = \sum_{i=1}^m F_{Ai} h_{i1}^2 \frac{\sigma F_{ii} \sin^2 \alpha_i}{\mu f_i} \frac{\partial h_{i1}}{\partial z}, \quad (4.4)$$

and

$$\dot{Q}_2 = \sum_{i=1}^m A_i \langle w_i \rangle = \sum_{i=1}^m F_{Ai} h_{i2}^2 \frac{\sigma}{\mu} \frac{F_{ii} \sin^2 \alpha_i}{f_i} \frac{\partial h_{i2}}{\partial z}, \quad (4.5)$$

where F_{Ai} is a dimensionless i th wetted corner geometric flow area function defined such that $A_i = F_{Ai} h_i^2$ with

$$F_{Ai} = f_i^2 \left(\frac{\cos \theta \sin \delta_i}{\sin \alpha_i} - \delta_i \right), \quad (4.6)$$

where $\delta_i = \pi/2 - \alpha_i$ is the surface curvature angle (refer to Figure 5c). The total local volumetric flow rates determined from eqs. (4.4) and (4.5) may be substituted into a global mass balance and solved for the transient position of the ullage identified by $z_1(t)$ and $z_2(t)$ which are further defined below.

B. Global Mass Balance. Under the global assumptions #1, #2, and #3, dimensional global mass balance equations may be written at both bulk meniscus locations 1 and 2 (ref. Figure 4a), such that

$$\dot{Q}_1 = \frac{d}{dt} (V_s - V) \Big|_{z_1} = (A_s - A) \frac{dz}{dt} \Big|_{z_1} \quad (4.7)$$

and

$$\dot{Q}_2 = \frac{d}{dt} (V_s - V) \Big|_{z_2} = (A_s - A) \frac{dz}{dt} \Big|_{z_2}, \quad (4.8)$$

where, in general,

$$V_s = \int_{z_1}^{z_2} A_s d\hat{z} \quad \text{and} \quad V = \int_{z_1}^{z_2} A d\hat{z}. \quad (4.9)$$

Areas $A_s = A_s(z)$ and $A = A(z(t))$ are the respective local cross-sectional areas of the container and liquid as sketched in Figure 4b. For pyramidal containers, conduits, and pores whose edges converge to a single vertex or virtual vertex,

$$A_s = F_{As} z^2, \quad (4.10)$$

where F_{As} is a dimensionless geometric function for the section inclusive of characteristic taper angle ψ . Concerning the total area of liquid in the section at time t ,

$$A = A(z, t) = \sum_{i=1}^m A_i = \sum_{i=1}^m F_{Ai} h_i^2. \quad (4.11)$$

The height of the fluid along the i th corner is described by $h_i(z, t)$ as depicted in Figure 5. In general, $A(z, t)$ is unknown because h_i for each wetted corner is unknown. However, at bulk menisci locations 1 and 2, h_i may be evaluated via global assumption #3 where the bulk radius of curvature is known by

$$R = \frac{P_s \cos \theta}{2\Sigma} \left[1 - \left(1 - \frac{4\Sigma A_s}{P_s^2 \cos^2 \theta} \right)^{1/2} \right], \quad (4.12)$$

where P_s is the section perimeter and Σ is the normalized flow area at fixed z defined by

$$\Sigma \equiv \frac{A}{R^2} = \sum_{i=1}^m \frac{A_i}{R^2} = \sum_{i=1}^m \frac{F_{Ai}}{f_i^2}. \quad (4.13)$$

For pyramidal containers the section perimeter is proportional to z , or $P_s \equiv F_{P_s} z$. Thus, noting $A_s = F_{As} z^2$ from Eq. (4.10), Eq. (4.12) becomes

$$R = \frac{F_{P_s} z \cos \theta}{2\Sigma} \left[1 - \left(1 - \frac{4\Sigma F_{As}}{F_{P_s}^2 \cos^2 \theta} \right)^{1/2} \right] \equiv F_R z \quad (4.14)$$

The bulk radius R is related to h in the bulk region by

$$R_1 \equiv f_i h_{i1} \quad \text{and} \quad R_2 \equiv f_i h_{i2} \quad (4.15)$$

from which

$$h_{i1} = \frac{F_R}{f_i} z_1 \quad \text{and} \quad h_{i2} = \frac{F_R}{f_i} z_2 \quad (4.16)$$

Thus, at menisci locations z_1 and z_2 , A from Eq. (4.11) may be determined by combining eqs. (4.14) and (4.16) such that

$$A(z_1) = \sum_{i=1}^m F_{Ai} \left(\frac{F_R}{f_i} \right)^2 z_1^2 \equiv z_1^2 \sum_{i=1}^m F_{Afi} \quad (4.17)$$

and

$$A(z_2) = \sum_{i=1}^m F_{Ai} \left(\frac{F_R}{f_i} \right)^2 z_2^2 \equiv z_2^2 \sum_{i=1}^m F_{Afi}. \quad (4.18)$$

Substitution of eqs. (4.10), (4.17), and (4.18) into (4.7) and (4.8) yields

$$\dot{Q}_1 = \left(F_{As} - \sum_{i=1}^m F_{Afi} \right) z_1^2 \frac{dz_1}{dt} \quad (4.19)$$

and

$$\dot{Q}_2 = \left(F_{As} - \sum_{i=1}^m F_{Afi} \right) z_2^2 \frac{dz_2}{dt}, \quad (4.20)$$

subject to initial conditions $z_1(t=0) = 0$ and $z_2(t=0) = z_{2ini}$.

C. Volume Constraint. Lastly, under global assumption #2, for a fixed ullage volume V_u , z_1 and z_2 are related by the dimensional volume constraint

$$V_u = \int_{z_1}^{z_2} (A_s - A) dz = \int_{z_1}^{z_2} F_{As} z^2 dz - \sum_{i=1}^m F_{Ai} \int_{z_1}^{z_2} h_i^2 dz, \quad (4.21)$$

the first term on the right hand side of which may be integrated to give

$$V_u = \frac{F_{As}}{3} (z_2^3 - z_1^3) - \sum_{i=1}^m F_{Ai} \int_{z_1}^{z_2} h_i^2 dz. \quad (4.22)$$

4.2.4 Scales and Nondimensional Equations

The governing system of equations represented dimensionally by eqs. (4.2), (4.19), (4.20), and (4.22) is nondimensionalized by the following scales:

$$z \sim L \quad (4.23)$$

$$h_i \sim \frac{F_R}{f_i} L, \quad (4.24)$$

$$\dot{Q} \sim \sum_{i=1}^m W_i A_i \sim L^2 \sum_{i=1}^m W_i F_{Afi}, \quad (4.25)$$

$$W_i = \frac{h_{iL}}{L} \frac{\sigma}{\mu} \frac{F_{ii} \sin^2 \alpha_i}{f_i} = \frac{F_R}{f_i} \frac{\sigma}{\mu} \frac{F_{ii} \sin^2 \alpha_i}{f_i}, \quad (4.26)$$

and

$$L \equiv \left(\frac{3V_u}{F_{As}} \right)^{1/3}. \quad (4.27)$$

The characteristic initial ullage length L is the initial z -coordinate dimension of the ullage in the absence of any fluid in the corners as depicted in Figure 2a. Scales for characteristic heights h_i , flow areas A_i , and the global volumetric flow rate \dot{Q} are evaluated at $z \sim L$. W_i is the i th corner velocity scale also evaluated at $z \sim L$. The global mass balance Eq. (4.8) at $z = z_2$ is used to compute the global flow time scale

$$t_s \sim \frac{A_{sL} L}{\dot{Q}} \sim \frac{A_{sL} L}{\sum_{i=1}^m W_i A_{iL}} = \frac{F_{As} L}{\sum_{i=1}^m W_i F_{Afi}}, \quad (4.28)$$

where $A_{sL} \equiv A_s(z = L)$. Employing these scales the resulting nondimensional system is the following:

A. The i th corner flow local mass balance (Eq. 2):

$$\beta_i \frac{\partial h_i^{*2}}{\partial t^*} = \frac{\partial}{\partial z^*} \left(h_i^{*2} \frac{\partial h_i^*}{\partial z^*} \right) \quad (4.29)$$

subject to $h_i^*(z_1^*) = z_1^*$ and $h_i^*(z_2^*) = z_2^*$, from which evaluated at z_1^* (eqs. 4 and 5)

$$\dot{Q}_1^*(z_1^*) = \frac{\sum_{i=1}^m W_i F_{Afi} h_i^{*2} \partial h_i^* / \partial z^*}{\sum_{i=1}^m W_i F_{Afi}} \quad (4.30)$$

and evaluated at z_2^*

$$\dot{Q}_2^*(z_2^*) = \frac{\sum_{i=1}^m W_i F_{Afi} h_i^{*2} \partial h_i^* / \partial z^*}{\sum_{i=1}^m W_i F_{Afi}}. \quad (4.31)$$

B. The global bulk meniscus mass balance (eqs. 19 and 20):

$$\dot{Q}_1^* = (1 - \beta) z_1^{*2} \frac{dz_1^*}{dt^*} \quad (4.32)$$

subject to $z_1^*(0) = 0$ and

$$\dot{Q}_2^* = (1 - \beta) z_2^{*2} \frac{dz_2^*}{dt^*} \quad (4.33)$$

subject to $z_2^*(0) = z_{2ini}^*$. Parameters β and β_i are closely related and defined by

$$\beta \equiv \frac{\sum_{i=1}^m F_{Afi}}{F_{As}} \quad (4.34)$$

and

$$\beta_i \equiv \frac{\sum_{i=1}^m W_i F_{Afi}}{W_i F_{As}}. \quad (4.35)$$

C. The volume constraint (Eq. 22):

$$1 = z_2^{*3} - z_1^{*3} - 3 \sum_{i=1}^m \left(\frac{F_{Afi}}{F_{As}} \int_{z_1^*}^{z_2^*} h_i^{*2} dz^* \right). \quad (4.36)$$

With $h_i^*(z^*, 0)$, $z_1^*(0)$, and $z_{2ini}^*(0)$ known, eqs. (4.29)-(4.33), and the volume constraint Eq. (4.36) represent a coupled integro-differential system of $m + 5$ nonlinear equations for m local dependent variables $h_i^*(z^*, t^*)$ and the four global dependent variables: $\dot{Q}_1^*(z_1^*)$, $\dot{Q}_2^*(z_2^*)$, $z_1^*(t^*)$, $z_2^*(t^*)$. Numerical solution to the system is possible and will be pursued at a later date. At present however, it is sufficient to observe that β and β_i appear as parameters, which under certain limiting values allow approximate analytical solutions to the system.¹

4.2.5 Limiting Cases

Below are listed 4 limiting cases addressed here for an arbitrary i th corner (note that β_i can be less than or greater than β):

1. $\beta \sim \beta_i \sim O(1)$: This scenario implies that the global and local time scales are of similar order and the system of equations is strongly coupled requiring a fully numerical approach.
2. $\beta_i \gg 1$, $\beta \ll 1$: In this case, Eq. (4.29) becomes singular at $O(1)$ (cannot satisfy all boundary conditions) and reveals that h_i^* is either a constant or not a function of t . Either way the result is no i th corner flow at $O(1)$ and thus no contribution of the i th corner to the ullage migration. This scenario is met for corners where the Concus-Finn wetting condition $\theta \leq \pi/2 - \alpha_i$ is only marginally satisfied and characteristic velocities approach 0, Eq. (4.26), while other wetting corners contribute significantly to the global flow.
3. $\beta \ll 1$ and $\beta_i \ll 1$: As viewed in Eq. (4.34), this is the condition of small liquid flow area compared to container section area. The implication is that the average corner

¹Alternate scalings are possible for the m local flow equations, Eq. 4.29. For example, an average or maximum velocity scale may be used to normalize both sides of the m local flow equations along with the global time scale. Such a scaling is preferred because it renders all m local corner flows $O(1)$ or less. Nonetheless, the β_i scaling is employed below only to be removed during subsequent developments.

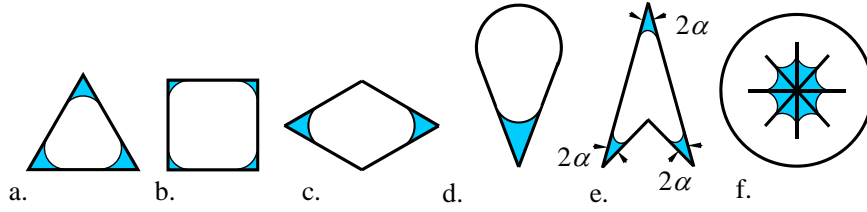


Figure 4.6: Selection of 'equi- W_i ' container section types and corner wetting scenarios, several of which have been analyzed in detail as non-tapering right cylindrical sections⁷: a) and b) regular n -gons, c) wetted acute edges of rhombic section, d) 'ice cream cone', e) equi-angle section ($\alpha < \pi/6$), and f) sample symmetric vaned section.

flow time scale $\sim O(\beta)$ as well as all individual corner flow time scales $\sim O(\beta_i)$ are much shorter than the global flow time scale $\sim O(1)$, and that the local corner flows Eq. (4.29) may be treated as quasi-steady and solved with time dependent boundary conditions. The system of equations is thus significantly decoupled at zeroth order under this constraint.

4. $\beta = \beta_i \ll 1$: A subset of case 3 above, this significantly simplifying condition requires a container section such that $W_i = \text{constant}$ for all m wetted corners. A sketch of several container section-types that meet this 'equi- W_i ' criterion is provided in Figure 6. For brevity in this presentation, it is this condition that will be pursued analytically.

4.3 $O(1)$ Solution for Sections where $\beta = \beta_i \ll 1$

For 'equi- W_i ' sections the velocity scale $W_i = W$ is identical for all wetted corners and $\beta = \beta_i$. Furthermore, when $\beta \ll 1$, the expansions

$$h^* = h_0^* + \beta h_1^* + O(\beta^2), \quad (4.37)$$

$$z_1^* = z_{10}^* + \beta z_{11}^* + O(\beta^2), \quad (4.38)$$

and

$$z_2^* = z_{20}^* + \beta z_{21}^* + O(\beta^2) \quad (4.39)$$

serve as naive approximations of the dependent variables of the problem. Employing eqs. (4.37)-(4.39), the $O(4.1)$ system reduces to the i th corner flow local evolution equation

$$0 = \frac{\partial}{\partial z^*} \left(h_{i0}^{*2} \frac{\partial h_{i0}^*}{\partial z^*} \right) \quad (4.40)$$

subject to $h_{i0}^*(z_{10}^*) = z_{10}^*$ and $h_{i0}^*(z_{20}^*) = z_{20}^*$, from which the global flow rates may be computed using

$$\dot{Q}_{10}^* = h_{i0}^{*2} \left. \frac{\partial h_{i0}^*}{\partial z^*} \right|_{z_{10}^*} \quad \text{and} \quad \dot{Q}_{20}^* = h_{i0}^{*2} \left. \frac{\partial h_{i0}^*}{\partial z^*} \right|_{z_{20}^*}. \quad (4.41)$$

For the time being, the volume constraint remains Eq. (4.36), while the global bulk meniscus mass balance eqs. (4.32) and (4.33) reduce to

$$\dot{Q}_{10}^* = z_{10}^{*2} \frac{dz_{10}^*}{dt^*} \quad (4.42)$$

subject to $z_1^*(0) = 0$ and

$$\dot{Q}_{20}^* = z_{20}^{*2} \frac{dz_{20}^*}{dt^*} \quad (4.43)$$

subject to $z_{20}^*(0) = 1$.

Solving Eq. (4.40) yields

$$h_{i0}^* = \left[z_{20}^{*3} + \left(\frac{z_{20}^{*3} - z_{10}^{*3}}{z_{20}^* - z_{10}^*} \right) (z^* - z_{20}^*) \right]^{1/3}. \quad (4.44)$$

Substituting Eq. (4.44) into the volume constraint Eq. (4.36) reveals that the summation-integral term on the right hand side is $\sim O(\beta)$ and may be ignored at $O(1)$. Thus, Eq. (4.36) reduces conveniently to

$$1 = z_{20}^{*3} - z_{10}^{*3} \quad (4.45)$$

allowing z_{20}^* to be determined explicitly in terms of z_{10}^* . This simplification is indeed fortunate, unique to pyramidally tapered sections (or sections where $A \sim z^2$ and $P_s \sim z$, and reduces Eq. (4.44) further to

$$h_{i0}^* = \left[z_{20}^{*3} + \left(\frac{z^* - z_{20}^*}{z_{20}^* - z_{10}^*} \right) \right]^{1/3}. \quad (4.46)$$

From this solution the flow rate eqs. (4.41) are found to be redundant,

$$\dot{Q}_0^* = \dot{Q}_{10}^* = \dot{Q}_{20}^* = \frac{1}{3(z_{20}^* - z_{10}^*)}. \quad (4.47)$$

Now employing eqs. (4.47) and (4.45), the global meniscus mass balance Eq. (4.42) may be solved for z_{10}^* yielding the first order ordinary differential equation

$$\frac{1}{3((1 + z_{10}^{*3})^{1/3} - z_{10}^*)} = z_{10}^{*2} \frac{dz_{10}^*}{dt^*} \quad (4.48)$$

subject to initial condition $z_{10}^*(0) = 0$. When integrated, Eq. (4.48) yields

$$t^* = \frac{3}{4} \left[(1 + z_{10}^{*3})^{4/3} - z_{10}^{*4} - 1 \right], \quad (4.49)$$

and from Eq. (4.44)

$$t^* = \frac{3}{4} \left[z_{20}^* - (z_{20}^{*3} - 1)^{3/4} - 1 \right], \quad (4.50)$$

The implicit solutions for $t^*(z_{10}^*)$ and $t^*(z_{20}^*)$ are inverted and plotted in Figure 7. The asymptotic forms of the solutions are provided below and noted on the figure where applicable: At short times $t^* \ll 1$, eqs. (4.49), (4.45), and (4.47) may be represented by expansions

$$z_{10}^* \approx t^{*1/3} + \frac{1}{4}t^{*2/3} + \frac{3}{16}t^* + \frac{35}{192}t^{*4/3} + O(t^{*5/3}), \quad (4.51)$$

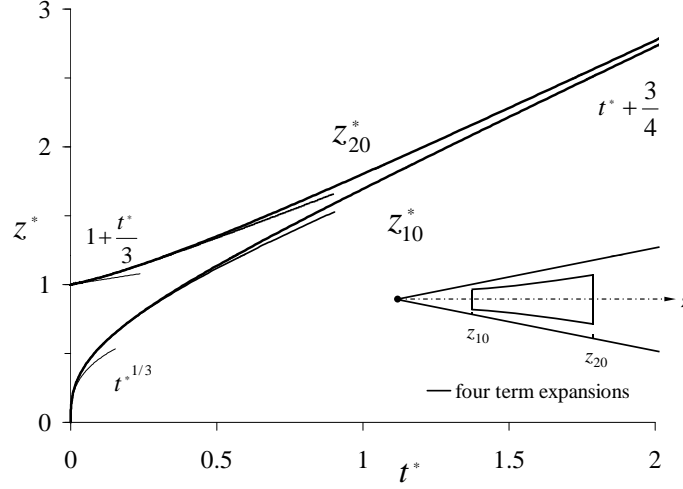


Figure 4.7: Ullage positions and from eqs. (49) and (53) for transient imbibition in ‘equi- W_i ’ tapered pyramidal sections. One- and 4-term expansions to the $O(1)$ solution for z_{10}^* from Eq. (50) are shown for comparison.

$$z_{20}^* \approx 1 + \frac{1}{3}t^* + \frac{1}{4}t^{*4/3} + O(t^{*5/3}), \quad (4.52)$$

and

$$\dot{Q}_0^* \approx \frac{1}{3} + \frac{1}{3}t^{*1/3} + \frac{5}{12}t^{*2/3} + \frac{65}{144}t^* + \frac{31}{64}t^{*4/3} + O(t^{*5/3}). \quad (4.53)$$

The expansions represent a reasonable description of the flow to $\sim O(t^{*5/3})$. However, significantly less error in the predicted values for z_{20}^* and \dot{Q}_0^* are obtained using exact expressions

$$z_{20}^* = (1 + z_{10}^{*3})^{1/3} \quad (4.54)$$

from Eq. (4.45), \dot{Q}_0^* from Eq. (4.47), and the four-term expansion for z_{10}^* , Eq. (4.51). As shown in Figures 7 and 8, expansion errors from terms computed in this manner remain small $\approx 5\%$, even for $t^* \approx 1.0$. At long times $t^* \gg 1$

$$z_{10}^* = z_{20}^* = t^* + \frac{3}{4} + O(t^{*-2}). \quad (4.55)$$

The bulk meniscus and therefore ullage velocities are determined from

$$\begin{aligned} \frac{dz_{10}^*}{dt^*} &= \frac{1}{3 z_{10}^{*2} ((1 + z_{10}^{*3})^{1/3} - z_{10}^*)} \\ &\approx \frac{1}{3} t^{*-2/3} + \frac{1}{6} t^{*-1/3} + \frac{3}{16} + O(t^{*1/3}) \end{aligned} \quad (4.56)$$

and

$$\frac{dz_{20}^*}{dt^*} = \frac{1}{3 z_{20}^{*2} (z_{20}^* - (z_{20}^{*3} - 1)^{1/3})} \quad (4.57)$$

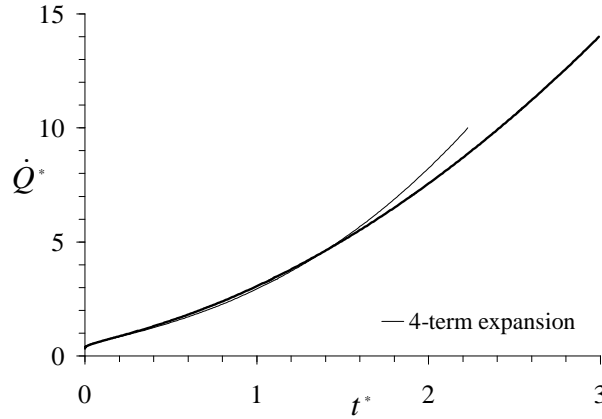


Figure 4.8: Dimensionless flow rate, \dot{Q}_{10}^* from Eq. (47). Solution is compared to the four-term expanded solution for z_{10}^* , Eq. (50), substituted into (53) and (47).

$$\approx \frac{1}{3} + \frac{1}{3}t^{*1/3} + \frac{5}{12}t^{*2/3} + O(t^*)$$

and are plotted on Figure 9. The expanded forms below eqs. 4.56 and 4.56 include 3-term expansions for $t^* \ll 1$ which are also noted on Figure 9. Keeping more than 3 terms in the expansions does not improve the agreement. Note that the 4-term expanded solution for z_1^* from Eq. (4.51) and Eq. (4.54) for z_2^* , when substituted into the exact expressions for these velocities, produce values that coincide (typically with errors $< 1\%$) with the exact solution over the full domain of t^* . As observed in Figure 9, both velocities approach 1 as $t^* \rightarrow \infty$.

4.4 Discussion of Solution and Constraints

From the expanded eqs. (4.51) and (4.55) it is apparent that the trailing meniscus first progresses as $\sim t^{*1/3}$ and then later as $\sim t^*$, while the leading meniscus moves as $\sim t^*$ for the majority of the flow, eqs. (4.52) and (4.55). As observed from Eq. (4.47) and Figure 8, the flow rate across the ullage increases in inverse proportion to the ullage length. At $t^* \approx 1$, a ten-fold reduction in ullage length results in a ten-fold increase in flow rate across the ullage.

For $t^* \rightarrow \infty$, from Figure 7 the ullage appears to lose its slender nature in violation of the model and significant 3-D curvature effects are expected to dominate the flow which will eventually produce a stationary spherical bubble if the container is long enough. At the other end of the spectrum, for $t^* \rightarrow 0$, from Figure 9 the unbounded trailing meniscus velocity dz_1^*/dt^* is unphysical and speaks to the fact that at such short times the global trailing meniscus time scale is of similar order to the local corner flow time scale also in violation of the model which assumes $\beta \ll 1$.

The solution of eqs. (4.49), (4.54), and (4.46) may be used in turn to provide more quantitative time regimes under which the modeling assumptions are valid. For example,

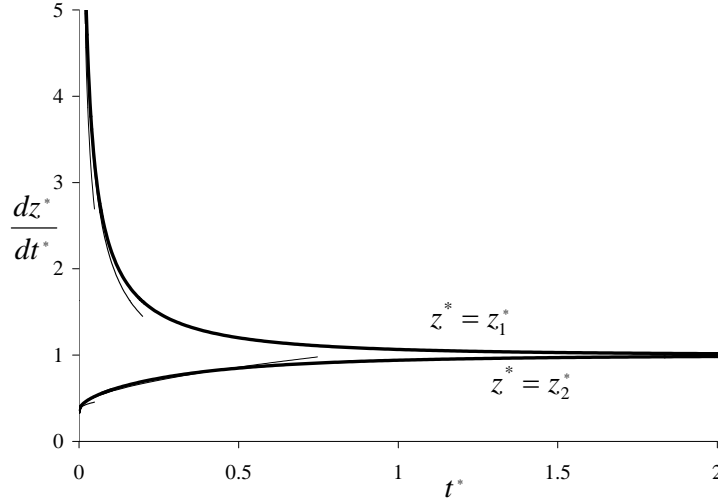


Figure 4.9: Leading and trailing bulk meniscus velocities. Exact solutions from eqs. (55) and (56) are presented (heavy solid lines) as well as 1- and 3-term approximations for small times for z_1^* , and 2- and 3-term approximations for z_2^* . Note that the 4-term approximation for z_1^* , Eq. (50), at small times is indistinguishable from the exact solution on this plot.

for pyramidal vessels it can be shown that the most pivotal global assumption #2 is satisfied provided

$$16\pi \frac{F_R^3}{F_{As}} z_2^{*3} \ll 1, \quad (4.58)$$

which for fixed geometry obviously becomes increasingly difficult to satisfy as z_2^* increases in time. However, it may also be shown that $F_R^3/F_{As} \sim \tan \psi$, and that this constraint is readily satisfied for $z_2^* \sim O(4.1)$ provided ψ is small enough (global assumption #1).

The most pivotal local modeling assumption is the slender column assumption #5. Again, for pyramidal vessels, it can be shown that this constraint requires

$$\epsilon^2 \sim \left(\frac{F_R}{f_i} \right)^2 \left(\frac{z_2^*}{z_2^* - z_1^*} \right)^2 \ll 1, \quad (4.59)$$

which for fixed geometry again becomes increasingly difficult to satisfy both as z_2^* increases in time and as $z_2^* - z_1^*$ decreases in time. Nonetheless, it can be shown that $F_R^2/f_i^2 \sim \tan^2 \psi$ which readily maintains the constraint of Eq. (4.59) for $z_2^* \sim O(4.1)$ for many practical problems provided ψ is small enough.

4.4.1 Impact of Geometry

The intricate dependence of the flow on container geometry can be interrogated by the present analysis. For example, redimensionalizing the flow rate for $t^* \ll 1$ for the equi- W_i pyramidal sections described above yield

$$\dot{Q} = K_{geo} \frac{1}{3} (1 + t^{*1/3}) \quad (4.60)$$

where

$$K_{geo} \equiv \underbrace{\sum_{i=1}^m F_{Ai} \left(\frac{F_R L}{f_i} \right)^2}_{\text{cross flow area}} \underbrace{\left(\frac{F_R \sigma}{f_i \mu} \frac{F_{ii} \sin^2 \alpha_i}{f_i} \right)}_{\text{velocity scale}} \equiv F_{geo} \left(\frac{L^2 \sigma}{\mu} \right). \quad (4.61)$$

K_{geo} is a dimensional flow rate coefficient separated into cross flow area and velocity scale components in Eq. (4.61). The length scale L appears in the cross flow area term only and stems from $h \sim h_2(z_2 = L) \propto L$. The velocity scale term may be broken down further into the slenderness ratio F_R/f_i , the capillary velocity σ/μ , and the geometric ratio component of the capillary to viscous force, $F_{ii} \sin^2 \alpha_i/f_i$. Viscous effects are contained only within the velocity scale term in Eq. (4.61), where no length dimensions appear because the viscous length, also characterized by L , is cancelled by the same capillary driving force length scale $\sim L$. Thus, K_{geo} serves as the measure of the flow intensity at small times and provides a clear path for comparisons of like geometries or for optimizations given certain container, conduit, or pore dimensions. F_{geo} is a dimensionless geometric function that collects purely geometric quantities.

4.4.2 Application

To demonstrate the value and ease with which container, conduit, or pore geometries are compared, a brief analysis of equi-length, equi-volume, n -regular pyramidal containers is provided here. By fixing L , ψ can be varied such that all such containers possess the same volume and can be compared on this basis. Such a comparison is effectively one of comparing iso-porosity structures in which pore geometry is the sole distinguishing characteristic. A sketch of three n -sided regular pyramidal containers is provided in Figure 10. F_{geo} from Eq. (4.61) is

$$F_{geo} \equiv \frac{n F_A F_i F_R^3 \sin^2 \alpha}{f^4}, \quad (4.62)$$

where

$$\alpha = \frac{\pi(n-2)}{2n}. \quad (4.63)$$

An overview of the terms appearing in Eq. (4.62) would include the fact that $F_A \sim \tan \alpha$, $F_i \approx 1/7$, and that for this container type,

$$F_{As} = n \tan^2 \psi \sin^2 \alpha \tan(\pi/n) \quad (4.64)$$

and

$$F_{Ps} = 2n \tan \psi \sin \alpha \tan(\pi/2) \quad (4.65)$$

from which F_R may be computed via Eq. (4.14). $F_{geo}(10^5/F_i)$ is plotted against $1/n$ in Figure 11. For cases where $n \gg 1$, it can be shown that $F_A \sim 4n/3\pi$, $F_R \sim (1/2) \tan \psi$, $\sin \alpha \sim 1$, and $f \sim 2n^2/\pi^2$. Thus, in this limit, with all assumptions for the analysis satisfied (i.e. $\psi \ll 1$), it is found that $F_{geo} n^{-6}$ and in turn, $\dot{Q} \sim n^{-6}$. In the limit $n \rightarrow \infty$, $F_{geo} \rightarrow \pi^7 \tan^3 \psi / 96n^6$. This power law dependence is reflected in the straight line fit on Figure 11. It is from such results that transport rates are readily observed to be strong functions of geometry. In this case for instance a change from a square ($n = 4$) conduit to an

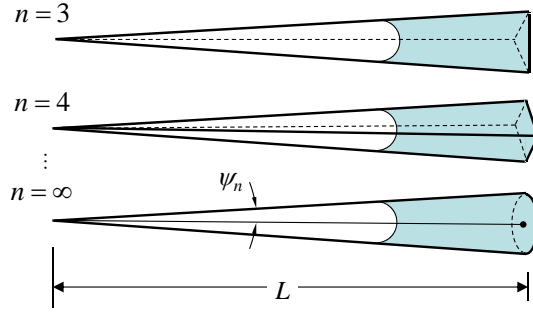


Figure 4.10: Sketch of three constant volume, constant length, n -regular pyramidal containers. ψ_n is varied to maintain volume constant between vessels.

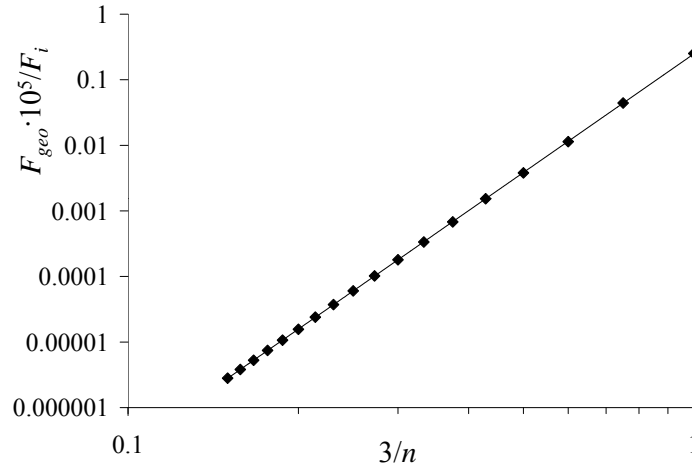


Figure 4.11: For containers of Figure 11, F_{geo} from Eq. (69) multiplied by constant $10^5/F_i$ and plotted against $3/n$, for $n = 3, 4, 5, \dots, 20$. The slope identified using the straight line shows $1/n^6$ dependence.

equilateral triangular one ($n = 3$) of identical volume and length produces a corresponding 5.6-fold increase in flow rate across the cell, $(4/3)^6$. A similar change from a hexagon to a triangle yields a 64-fold increase $(6/3)^6$.

4.5 Supportive Drop Tower and CFE-ICF ISS Experiments

Evidence supporting the flat bulk meniscus modeling assumption #3 applied to right cylindrical vessels is provided in earlier works on the subject [28][32][34]. Support for application of this assumption to the tapered containers investigated herein is provided in Figure 12 where 2.2s drop tower tests at NASA's Glenn Research Center are conducted for the sudden

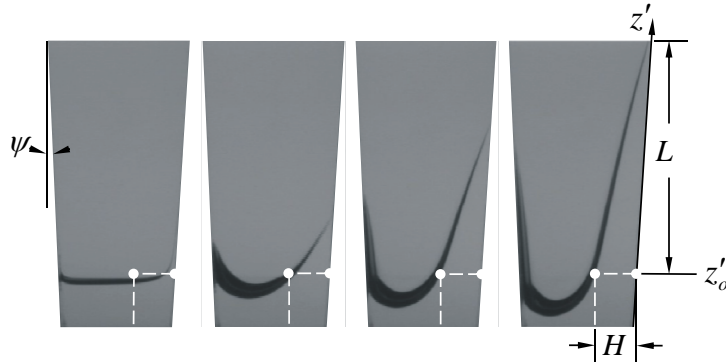


Figure 4.12: Select images from 2.2s drop tower test of a perfectly wetting 2cs Si Oil ($\sigma = 0.0187\text{N/m}$, $\mu = 0.00174\text{kg/ms}$, $\theta = 0^\circ$) in an inverted $\psi = 8^\circ$ tapered $75^\circ\text{-}30^\circ\text{-}75^\circ$ right isosceles pyramid at times 0, 0.23, 1, and 2s. The 30° corner ($\alpha_i = 15^\circ$) is viewed in profile on the right hand side of the container (compare with Figure 1).

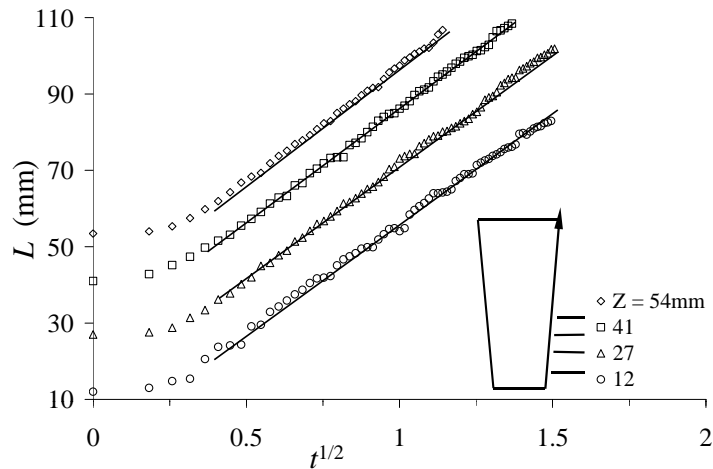


Figure 4.13: Advancing tip histories for drop tests performed at various initial fill levels Z for the test cell of Figure 12 (the inset is approximately to scale). Linear predictions $\pm 5\%$ shown as continuous lines on plot lend further support for the application of the flat bulk meniscus assumption and the use of the de Lazzer et al.^{2,3} method to compute bulk meniscus curvature as function of its axial location.

imbibition problem in a uniformly tapered right isosceles pyramid (compare with Figure 1). As shown in Figure 13 tests performed at several initial fill levels to determine the meniscus advance location are well predicted by current theory $t^{1/2}$ which assumes that the method of de Lazzer et al. [27][32] may be applied to compute the surface height boundary condition (bulk meniscus curvature) at the coordinate origin for the flow. Unfortunately, for these tests ψ is sufficiently small such that the predicted and measured slopes in Figure 14 do not vary significantly between tests. As a result, the experiments only provide ‘support’ for the use of the de Lazzer method to compute the constant height $H(z)$ location for the flow. Proof of this claim awaits further experiments over a broader range of geometric parameters.

CFE-ICF data from ISS experiments outlined in Chapter 1 clearly confirm these trends and in some cases provide further evidence of quantitative agreement with experiments. However, test cell ICF2, which provides excellent data during the flight is not a pyramidal taper and does not lend itself to closed form solution (at present).

4.6 Chapter Summary

An analytic approach predicting liquid flow rates and/or ullage migration rates in partially filled containers, conduits, or pores that are slightly tapered is presented. Closed form solutions are offered for the special case of symmetric pyramidally-tapered sections where $A_s \sim z^2$. Solutions are also in hand for the special case of symmetric, tapered sections of high aspect ratio where $A_s \sim z$ as well as other geometries and boundary conditions which will be reported elsewhere. The $O(1)$ analytic solutions permit relatively easy comparisons and optimizations for various container shapes as demonstrated herein for pyramids of n -sided regular polygonal section. The method can be used as a tool to design specific capillary fluid elements for large length scale systems such as spacecraft fuel tanks, as well as to design microfluidic systems for terrestrial applications such as high performance porous wicks.

References

- [1] M.M. Weislogel. Steady spontaneous capillary flow in partially coated tubes. *AIChE Journal*, 43(3):645 – 654, 1997.
- [2] R. Tadmor. Line energy and the relation between advancing, receding, and Young contact angles. *Langmuir*, 20(18):7659 – 7664, 2004.
- [3] M.M. Weislogel, R.M. Jenson, J. Klatte, and M.E. Dreyer. Interim results from the capillary flow experiment aboard ISS: The moving contact line boundary condition. volume 13, pages 9252 – 9259, Reno, NV, United States, 2007.
- [4] A. Lee. VirtualDub 1.8.1. <http://www.virtualdub.org/>, 1998-2008.
- [5] R. Klimek and T. Wright. Spotlight-8: Image analysis and object tracking software. <http://exploration.grc.nasa.gov/spotlight/>, 2005.
- [6] P. Concus and R. Finn. On the behavior of a capillary surface in a wedge. *Proceedings of the National Academy of Sciences of the United States of America*, 63(2):292–299, 1969.
- [7] Y. Chen and S.H. Collicott. Investigation of the symmetric wetting of vane-wall gaps in propellant tanks. *AIAA Journal*, 42(2):305 – 314, 2004.
- [8] Y. Chen, R. Jenson, M. Weislogel, and S. Collicott. Capillary wetting analysis of the CFE-Vane Gap geometry. Reno, NV, United States, 2008.
- [9] R.M. Jenson. Capillary-driven corner flow in weakly 3-dimensional conduits and contact line interface dynamics in reduced gravity environments. Master’s thesis, Portland State University, 2008.
- [10] M.M. Weislogel, R.M. Jenson, and D.A. Bolleddula. Capillary driven flows in weakly 3-dimensional polygonal containers. volume 13, pages 9260 – 9272, Reno, NV, United States, 2007.
- [11] M.M. Weislogel, E.A. Thomas, and J.C. Graf. A novel device addressing design challenges for passive fluid phase separations aboard spacecraft. *J. Microgravity Sci. Technol.*, page 12, 2008.
- [12] M.E. Dreyer. *Free Surface Flows Under Compensated Gravity Conditions*. Springer, Berlin, first edition, 2006.

- [13] M. Weislogel. Stability of capillary surfaces. Portland, OR, June 1991. Paper No. FED-Vol. 111, Forum on Microgravity Flows, Book No. G00599-1991.
- [14] M.M. Weislogel and R.M. Jenson. The Capillary Flow Experiments (CFE). <http://cfe.pdx.edu>, 2008.
- [15] M.M. Weislogel, S. H. Collicott, D. J. Gotti, C. T. Bunnell, C. E. Kurta, and E. Golliher. The capillary flow experiments: Handheld fluids experiments for the international space station. January 2004. AIAA-2004-1148.
- [16] P. Concus and R. Finn. Capillary surfaces in microgravity. In *Low-gravity fluid dynamics and transport phenomena*, volume 130 of *Progress in astronautics and aeronautics*, pages 183–205. American institute of aeronautics and astronautics, USA, 1990.
- [17] F. Concus, R. Finn, and M. Weislogel. Measurement of critical contact angle in a microgravity space experiment. *Experiments in fluids*, 28(3):197–205, 2000.
- [18] D. Langbein. *Capillary Surfaces: Shape-Stability-Dynamics, in Particular Under Weightlessness*. Number 178 in Springer Tracts in Modern Physics. Springer, 2001.
- [19] P. Concus and R. Finn. On the behavior of a capillary surface in a wedge. *Proceeding of National Academy of Science of U.S.A., Applied Mathematical Sciences*, 63(2):292–299, 1969.
- [20] M.M. Weislogel and S. Lichter. Capillary flow in an interior corner. *Journal of Fluid Mechanics*, 373:349–378, 1998.
- [21] Y. Chen and S.H. Collicott. Study of wetting in an asymmetrical vane-wall gap in propellant tanks. *AIAA Journal*, 44(4):859–867, April 2006.
- [22] K.A. Brakke. The Surface Evolver. *Experimental Mathematics*, 1(2).
- [23] R. Finn. A subsidiary variational problem and existence criteria for capillary surfaces. *J. Reine Angew. Math.*, 353:196–214, 1984.
- [24] R. Finn. *Equilibrium capillary surfaces*, volume 284 of *A series of comprehensive studies in mathematics*. Springer-Verlag, New York, 1986. Chapter 6.
- [25] R. Finn and R.W. Neel. C-singular solutions of the capillary problem. *Journal fur die und angewandte Mathematik*, 512:1–25, 1999.
- [26] M.M. Weislogel. Some analytical tools for fluids management in space: Isothermal capillary flows along interior corners. *Advances in Space Research*, 32(2):163 – 170, 2003.
- [27] A. de Lazzer, D. Langbein, M.E. Dreyer, and H.J. Rath. Mean curvature of liquid surfaces in cylindrical containers of arbitrary cross-section. *Microgravity Science and Technology*, 9(3):208 – 219, 1996.
- [28] M. M. Weislogel. Capillary flow in containers of polygonal section. *AIAA J.*, 39(12):2320–2326, 2001.

- [29] B. Legait. Laminar flow of two phases through a capillary tube with variable square cross-section. *J. Colloid and Int. Sci.*, 96(1), 1983.
- [30] T.C. Ransohoff, P.A. Gauglitz, and C.J. Radke. Snap-off of gas bubbles in smoothly constricted noncircular capillaries. *AIChE J.*, 33(5):753–765, 1987.
- [31] A.R. Kavscek and C.J. Radke. Gas bubble snap-off under pressure driven flow in constricted noncircular capillaries. *Colloids and Surfaces A*, 117:56–76, 1996.
- [32] M.M. Weislogel and S.H. Collicott. Capillary re-wetting of vaned containers: Spacecraft tank rewetting following thrust resettling. *AIAA J.*, 42(12):2551–2607, 2004.
- [33] T.C. Ransohoff and C.J. Radke. Laminar flow of a wetting liquid along corners of a predominantly gas-occupied noncircular pore. *J. Colloid and Int. Sci.*, 121(2):392, 1988.
- [34] M.M. Weislogel and S. Lichter. Capillary flow in an interior corner. *Journal of Fluid Mechanics*, 373:349 – 378, 1998.
- [35] M.M. Weislogel and C.L. Nardin. Capillary driven flow along interior corners formed by planar walls of varying wettability. *Micro-gravity Sci. Technol.*, XVII(3):45–55, 2005.

Chapter 5

Appendix: Abbreviated CFE Chronology and Accomplishments

5.1 Abbreviated Chronology

An abbreviated chronology of the CFE experiments development and performance is as follows:

- March, 2003: Authority to proceed with design and fabrication
- September, 2003: CL-2 Pre-Ship and Phase III Safety Reviews, Hardware Turnover (JSC)
- November, 2003: CL-2 Shipped to Russia
- January 29, 2004: CL-2 launched to ISS on Progress mission, 13P
- February 2, 2004: 1.5hr Crew Training, M. Fincke (JSC)
- August 28, 2004: 1st Performance of CL-2 experiment by M. Fincke, Expedition-9, Saturday Science, Nominal Science Operations
- September 18, 2004: 2nd Performance of CL-2 experiment by M. Fincke, Expedition-9, Saturday Science: Extra Science
- February 1, 2005: 1.5hr Crew Training, B. McArthur (JSC)
- February 2, 2005: 1.5hr Crew Training, J. Williams (JSC)
- February 9, 2005: CL-1/CL-2 Preship and Phase III Safety Reviews, Hardware Turnover (JSC)
- July 10, 2005: CFE-CL-1 (with CFE-VG and -ICF vessels, 2ea) launched to ISS aboard Shuttle STS-114
- December 20, 2005: 3rd performance of CL-2 by B. McArthur, Expedition-12, Hard Schedule, Extra Science
- April 18, 2006: 4th performance of CL-2 by J. Williams, Expedition-13, Hard Schedule, Extra Science
- August 30, 2006: 1st performance of CL-1 by J. Williams, Expedition-13, Nominal Science Operations

- September 5, 2006: 1st performance of CFE-VG-1 by J. Williams, Expedition-13, 1/2 of Nominal Operations
- September 21, 2006: Flight data tapes for CFE operation on ISS to date returned to Earth (including data for CFE-VG-1) aboard Shuttle flight STS-115 (received by PI team 12/2006)
- March 3, 2007: second performance of CFE-VG1-2, S. Williams, Increment 14, Saturday Science (Quadrant I tests, symmetry test)
- March 10, 2007: first performance of CFE-ICF1-1, M. Lopez-Alegria, Increment 14, Saturday Science (dry and 2 wet tests)
- March 26, 2007: third performance of CFE-VG1-3, S. Williams, Increment 14, Hard Schedule (Quadrant IV tests, symmetry test)
- April 6, 2007: first performance of CFE-VG2-1, S. Williams, Increment 14, Saturday Science (360° CW dry and wet tests)
- April 7, 2007: second performance of CFE-ICF1-2, S. Williams, Increment 14, Saturday Science (all operations including loop tests and bubble tests)
- April 23, 2007?: CFE-VG2-2, S. Williams, Increment 14, Saturday Science (360° CW for critical angles, the 360deg CCW for hysteresis)
- April 29, 2007: CFE-ICF2-1 S. Williams, Increment 14, Saturday Science (Complete nominal operations: dry, wet, loop and bubble tests)
- May 11, 2007: CFE-VG2-3, S. Williams, Increment 14, Saturday Science (180° CW and CCW, critical angle and hysteresis with fine increments)
- May 12, 2007: CFE-ICF2-2 S. Williams, Increment 14, Saturday Science (extra science Wet and Bubbly, reservoir and test chamber axial and lateral shakes to generate bubbles)
- June 2, 2007: CFE-VG2-4, S. Williams, Increment 14, Saturday Science (alternate interface experiments)
- July 14, 2007: CFE-VG1-4, C. Anderson, Increment 15, Saturday Science (Quadrant II test)
- Oct. 22, 2007: CFE-VG1-4, P. Whitson, Increment 16, Voluntary Science (Quadrant III test)
- Nov 16, 2007: CFE-CL1-2, P. Whitson, Increment 16, Voluntary Science, (pinned cylinder, slide depth effects)

5.2 Abbreviated Scientific Accomplishments

A More detailed list of scientific accomplishments during the various CFE operations on ISS is provided below. The progress points out some of the piecemeal development of certain methods and capabilities by the astronauts, e.g. centrifugal methods and the axial disturbance methods for CFE-CL, Quadrant tests for CFE-VG, etc.

1. CFE-CL-2-1 (Fincke): Nominal Science Run
 - (a) Successful completion of all science objectives
 - (b) Demonstration of centrifugal technique to reset experiment for certain repeat runs
 - (c) Identified controlled method to impart axial mode disturbance using MWA
 - (d) Noteworthy additional science: droplet ejection, drop-wall impacts and rebound, hourglass formation
2. CFE-CL-2-2 (Fincke): Extra Science
 - (a) Repeat Push, Slide, and new data using Axial mode
 - (b) Noteworthy additional science: Depth effects to Push disturbance
3. CFE-CL-2-3 (McArthur): Extra Science
 - (a) Demonstrate augmented version of Fincke centrifuge method to fully clear pinning lip of liquid allowing for the indefinite repetition of the experiments
 - (b) Repeat Push, Slide, and Axial mode (camera mounted to MWA)
 - (c) Noteworthy additional science: more droplet/jet ejections, drop-wall impacts, and rebound
4. CFE-CL-2-4 (J. Williams): Extra Science
 - (a) Perfection of McArthur's augmented centrifuge method
 - (b) Repeat Push, Slide, and Axial mode (camera mounted ISS rail)
 - (c) Noteworthy additional science: significant droplet/jet ejections and manifold droplet-wall and free surface impacts and rebound events
5. CFE-CL-1-1 (J. Williams): Nominal Science Run
 - (a) Successful completion of all science objectives
 - (b) Noteworthy additional science: some depth effects
6. CFE-VG-1-1 (J. Williams): Nominal Science Run
 - (a) Successful completion of all science objectives for first half of crew procedures
 - (b) completed two complete CW vane rotations
 - (c) Clearly identified critical wetting angles to better than anticipated precision (1)

- (d) Data suggests third global critical wetting condition
- 7. CFE-VG-1-2 (S. Williams): Nominal (revised) Science Run
 - (a) Successful completion of revised science run to determine equilibrium configurations in Quadrant I
 - (b) Positive identification of global asymmetric interface and associated critical vane angle
 - (c) Identification of container asymmetry and impact on interface
- 8. CFE-ICF-1-1 (M. Lopez-Alegria): Nominal Science Run of first half of procedures
 - (a) Successful completion of all science objectives for first half of crew procedures
 - (b) completed dry fill and two wet fill tests
 - (c) Data clearly identified wetting regimes depending on container geometry
- 9. CFE-VG-1-3 (S. Williams): Nominal (revised) Science Run
 - (a) Successful completion of revised science run to determine equilibrium configurations in Quadrant IV
 - (b) Positive identification of global asymmetric interface and associated critical vane angle
 - (c) Identification of container asymmetry and impact on interface (global shift requires ≈ 15 min.)
 - (d) Verification of critical global shift angle outside of gap wetting envelope
 - (e) Completion of all science for VG1 vessel
- 10. CFE-VG-2-1, S. Williams, Increment 14, Saturday Science (360° CW dry and wet tests)
 - (a) Successful completion of nominal science run for CW vane rotations for dry and wet tests
 - (b) Positive identification of critical wetting and dewetting angles and hysteresis
 - (c) Global asymmetric wetting not observed
 - (d) Preliminary symmetry of wetting conditions observed
- 11. CFE-ICF-1-2, S. Williams, Increment 14, Saturday Science (all nominal operations)
 - (a) Successful completion of all revised science run operation and objectives
 - (b) Demonstration of centrifugal method to rapidly redeploy liquid
 - (c) Provision of critical data for global fluid reorientation
 - (d) Demonstration of high loop test flow rates
 - (e) Demonstration of passive bubble separations

12. CFE-VG2-2, S. Williams, Increment 14, Saturday Science (360° CW for critical angles, 360° CCW)
 - (a) Successful completion of all revised science run operation and objectives
 - (b) Identified critical angles with high precision
 - (c) Mapped critical de/wetting hysteresis
13. CFE-ICF2-1, S. Williams, Increment 14, Saturday Science (Complete nominal operations: dry, wet, loop and bubble tests)
 - (a) Successful completion of all revised nominal operations for dry test, wet test (2ea), loop tests (3ea), and bubble tests (6ea)
 - (b) Demonstration of centrifugal method to rapidly redeploy liquid
 - (c) Provided variety of large bubble migration/separation test resulting from lateral excitations
 - (d) Provided variety of small bubble migration/separation tests resulting from vigorous axial excitations
 - (e) Demonstrated clear ability of corner flows to filter, separate, and coalesce bubbly two-phase systems passively
14. CFE-VG2-3, S. Williams, Increment 14, Saturday Science (180° CW and CCW, fine increment)
 - (a) De/wetting angles in Quadrants I and II including hysteresis
 - (b) Extra Science run relocating fluid to lid, identified new meta/stable interface configuration for all vane angles. Drain procedure reveals unstable film on ellipse walls following a rupture event initiated at the drain exit port.
15. CFE-ICF2-2, S. Williams, Increment 14, Saturday Science (extra science)
 - (a) Additional Wet and Bubbly tests
 - (b) Small numbers of large bubbles interactions observed (small bubbles 'overtake' and merge with larger bubbles)
 - (c) Bubbles production in reservoir fails, bubble production in test vessel succeeds (later and axial shaking)
16. CFE-VG2-4, S. Williams, Increment 14, Saturday Science (Alternate Interface Experiments)
 - (a) Demonstration of three new interface configurations: filament, asymmetric right (vane at 90°), asymmetric left (vane at 0°).
 - (b) Interface stability to a variety of input disturbances.
17. CFE-VG1-4, C. Anderson, Increment 15, Saturday Science (Quadrant II test)
 - (a) CCW 180° to 90°, CW 90° to 180°, and 180° to 90° quick turn.

- (b) Accurate equilibrium data in Quadrant II
 - (c) Certain identification of critical vane wetting and bulk asymmetric wetting conditions.
18. CFE-VG1-5, P. Whitson, Increment 16, Voluntary Science (Quadrant III test)
- (a) CCW 180° to 270°, CW 270° to 180°, and 180° to 270° quick turn.
 - (b) Accurate equilibrium data in Quadrant III
 - (c) Certain identification of critical vane wetting and bulk asymmetric wetting conditions.
19. CFE-CL1-2, P. Whitson, Expedition 16, Voluntary Science (pinning cylinder, slide and depth effects)
- (a) Bubbles on fill, couldn't remove, went ahead, first large axial disturbance broke pinning lip, 15 minute recovery. Subsequent disturbances de-pinned readily and subsequent de-pinning efforts ultimately lead to a break of the container (hit on ISS hand rail). (It was difficult to clear the pinning edge, apparently requiring a large acceleration level not possible to impart by hand.)
 - (b) Nonetheless, a significant number of large amplitude pinned oscillations and destabilizations were recorded and will prove invaluable to the finalization of our CFE-CL database.

Chapter 6

Appendix: CFE-Related Dissemination Materials to Date (selection)

Journal Publications

1. M.M. Weislogel, R. Jenson, Y. Chen, S.H. Collicott, J. Klatte, and M. Dreyer, The Capillary Flow Experiments Aboard the International Space Station: Status, *Acta Astronautica*, April 10, 2009. DOI: 10.1016/j.actaastro.2009.03.008, online at: <http://dx.doi.org/10.1016/j.actaastro.2009.03.008>
2. Jenson, R.M., Weislogel, M.M., Klatte, J., Dreyer, M.E., Dynamic Interface and Contact Line Experiments aboard ISS: a Database for Spacecraft Numerical Benchmarks, *AIAA J.* (in Preparation)
3. Baker, J.A., Jenson, R.M., Weislogel, M.M., Weakly Three-dimensional capillary driven flow in containers with interior corners, *Phys. Fluids* (in preparation)
4. Weislogel, M.M., Tavan, N.T., Williams, S.L., Chen, Y., Collicott, S.H., Semerjian, B., Critical Wetting in Complex Geometries: Macro-Capillary Experiments in Space, *J. Fluid Mech.* (in preparation)
5. M.M. Weislogel, E.A. Thomas, J.C. Graf, A Novel Device Addressing Design Challenges for Passive Fluid Phase Separations Aboard Spacecraft, *J. Microgravity Sci. Technol.*, ISSN 0938-0108 (Print) 1875-0494 (Online), DOI 10.1007/s12217-008-9091-7, August 06, 2008. (12 pages)
6. M.M. Weislogel, Y. Chen, D. Bolleddula, A Better Non-Dimensionalization Scheme for Slender Flows: The Laplacian Operator Scaling Method, *Phys. Fluids*, Vol. 20, Issue 9, 093602 (2008); DOI:10.1063/1.2973900, September.
(<http://link.aip.org/link/?PHF/20/093602>)

Published Presentations

1. Jenson, R.M., Weislogel, M.M., Tavan, N.T., Bunnell, C.T., "The Capillary Flow Experiments aboard ISS," AIAA-2009-0614, 47th AIAA Aerospace Sciences Meeting, Orlando, January 5-8, 2009.
2. Weislogel, M.M., Chen, Y., Collicott, S.H., Bunnell, C.T., Green, R.D., Bohman, D.Y., "More Handheld Fluid Interface Experiments for the International Space Station (CFE-2)," AIAA-2009-0615, 47th AIAA Aerospace Sciences Meeting, Orlando, January 5-8, 2009. (10 pages)

3. M.M. Weislogel, R.M. Jenson, Y. Chen, S. Collicott, C.T. Bunnell, J. Klatte, M.E. Dreyer, Postflight summary of the Capillary Flow Experiments aboard the International Space Station, No. IAC-08-A2.6.A8, 59th International Astronautical Congress-2008, Glasgow, Scotland, September 29-Oct. 3, 2008.
4. M.M. Weislogel, R.M. Jenson, The Capillary Flow Experiments aboard ISS: weakly 3-D interior corner flows, No. 11523, XXII ICTAM, August 25-29, Adelaide, Australia, 2008. (ISBN 978-0-9805142-0-9)
5. M.M. Weislogel, R.M. Jenson, J. Klatte M.E. Dreyer, The Capillary Flow Experiments aboard ISS: Moving Contact Line Experiments and Numerical Analysis, AIAA-2008-0816, 46th AIAA Aerospace Sci. Meeting and Exhibit, Reno, Nevada, January 7-10, 2008.
6. Y. Chen, R. Jenson, M. Weislogel, S. Collicott, Capillary Wetting Analysis of the CFE-Vane Gap Geometry, AIAA-2008-0817, 46th AIAA Aerospace Sci. Meeting and Exhibit, Reno, Nevada, January 7-10, 2008.
7. M.M. Weislogel, R.M. Jenson, Y. Chen, S.H. Collicott, and S. Williams, Geometry Pumping on Spacecraft: The CFE-Vane Gap Experiments on ISS, 3rd International Symposium on Physical Sciences in Space (ISPS) 2007, Abstracts A11-2, pp. 443-444, Nara Japan, October 22-26. (J. Jpn. Soc. of Microgravity Appl., Vol. 25, No. 3, 2008)
8. M.M. Weislogel, R. Jenson, Y. Chen, S.H. Collicott, J. Klatte, and M. Dreyer, The Capillary Flow Experiments Aboard the International Space Station: Status, paper IAC-07-A2.6.02, 58th International Astronautical Congress-2007, Hyderabad, India, September 24-28.
9. Ma, Y., Thomas, C., Jiang, H., Manolache, S., Weislogel, M., Results of Plasma-Generated Hydrophilic and Antimicrobial Surfaces for Fluid Management Applications, 2007-01-3139, ICES 2007. (SAE Transactions, J. of Aerospace, Section 1, Vol. 116, pp 225-234, 2007)
10. M. Weislogel, R. Jenson, J. Klatte, M. Dreyer, Interim Results from the Capillary Flow Experiment Aboard ISS: The Moving Contact Line Boundary Condition. AIAA-2007-747, 45th AIAA Aerospace Sci. Meeting and Exhibit, Reno, Nevada, January 8-11, 2007.
11. M. Weislogel, R. Jenson, D. Bolleddula, Capillary Driven Flows in Weakly 3-Dimensional Polygonal Containers, AIAA-2007-748, 45th AIAA Aerospace Sci. Meeting and Exhibit, Reno, Nevada, January 8-11, 2007.
12. M.M. Weislogel, C.T. Bunnell, C.E. Kurta, E.L. Golliher, R.D. Green, J.M. Hickman, "Preliminary Results from the Capillary Flow Experiment on ISS: the Moving Contact Line Boundary Condition," Paper No. AIAA-2005-1439, 43rd AIAA Aerospace Sci. Meeting and Exhibit, Reno, Nevada 10-13, January 2005.

Other Publications and presentations; Reports, Brochures, etc. (selection)

1. Jenson, R.M., Weislogel, M.M., Chen, Y., Tavan, N.T., Bunnell, C.T., The Capillary Flow Experiments aboard the International Space Station: Increments 9-15, 8/2004-12/2007, NASA/CR-2009-215586, March 2009 (in press).
2. Robinson, J.A., Rhatigan, J.L., Baumann, D.K., Tate, J., Thumm, T., International Space Station Research Summary Through Expedition 10, NASA/TP-2006-213146, September, 2006. (M. Weislogel Capillary Flow Experiment pp. 85-86)
3. M. Weislogel, Y. Chen, D. Bolleddula, A better nondimensionalization scheme for slender laminar flows: The Laplacian scaling method, 2008 APS Division of Fluid Dynamics, 61st Annual Meeting, November 2008, San Antonio.
4. M.M. Weislogel, Microgravity fluids management challenges aboard spacecraft and the contributions of handheld space experiments, Association of Space Explorers (ASE) XXI Planetary Congress, Seattle, 14-20 September 2008.
5. Y. Chen, R. Jenson, M.M. Weislogel, S H Collicott, A study of critical wetting conditions of the CFE-Vane Gap Geometry, APS Division of Fluid Dynamics 60th Annual Meeting, November 2007, Salt Lake City, Utah, 2007.
6. R. Jenson, Y. Chen, M.M. Weislogel, Capillary Flow in Weakly 3-Dimensional Conduits, 2007 APS Division of Fluid Dynamics 60th Annual Meeting, November 2007, Salt Lake City, Utah, 2007.
7. M.M. Weislogel, R. Jenson, S.H. Collicott, Y. Chen, J. Klatte, M. Dreyer, Capillary Flows Experiments aboard ISS, International Space Development Conference, Dallas, TX, May 24-28, 2007.
8. M.M. Weislogel, CFE Flight Operations Update, NASA GRC Microgravity Fluid Physics Seminar, Cleveland OH, March 9, 2007.
9. S. Collicott, M. Weislogel, 'Current Space Station Experiments', Kentland Rotary, Kentland IN, October 16, 2006.
10. R. Jenson, Y. Chen, M. Weislogel, Capillary flow in weakly 3-dimensional conduits, 59th Ann. Mtg. of the APS Div. of Fluid Dynamics, Nov. 19-21, 2006, Tampa Bay, Florida, 2006.
11. M. Weislogel, The Capillary Flow Experiment, Joint NASA/ESA Increment 13 Science Symposium, NASA Johnson Space Center, March 22, 2006.
12. Weislogel, M.M., Weir, T., M. Dreyer, Capillary Solutions: Passive Containment and Transport for Low-g Fluids Systems, Habitation 2006, Int. Journal for Human Support Research, Vol. 10, No. 3/4, p. 244, February, 2006.

Chapter 7

Appendix: Data Archive Conventions

7.1 Video Preparation Process

All of the experiments presented are captured on video and must be converted to a numerical representation in space and time. Such a process requires the original video to be conditioned and converted so that it is in a suitable format for analysis. Once in a compatible format, events must be digitized, which requires a technique unique to the experiment. The process of formatting the video is documented below and is applicable to all of the experiments presented.

CFE is conducted aboard ISS with video being captured on a 720x480 Sony DVCam. This video is of the highest quality and is termed ‘onboard’ or ‘flight’ video. Flight video is only accessible in its native form when the DV media makes it to earth, which can take several months from the date the experiment is performed. On orbit the video is also recorded to the Video Tape Recorder (VTR), which is located aboard ISS. Immediately following the experiment, video stored upon the VTR is sent to earth, digitally recorded, and copied to DVDs. In addition, ‘realtime’ video is sent to earth during the experiment, which is recorded while in orbit, and is available immediately after completion of the experiment. Down-linked realtime and VTR video are available shortly following the experiment; however, such video is of significantly lower quality than flight video. Media obtained from NASA is on DVD in MPEG-2 format, which must be converted to comply with the image analysis software. The freeware program Spotlight-8 [?] is used to track events contained on video and can read uncompressed 24-bit AVI or Quicktime video. The objective of the video formatting is to render the video in a compatible 24-bit AVI format. This is achieved by the following conversion process: MPEG-2 \rightarrow MPEG-1 \rightarrow 24-bit AVI. Sony Vegas Video 6.0 with DVD Architect 3.0 is used to open the DVD VOB files (MPEG-2) contained on each DVD. Experimental events are selected from the DVD and rendered as high quality MPEG-1 videos. The MPEG-1 video is then imported into VirtualDub [?] where it is converted to a uncompressed 24-bit AVI video, being a suitable format for Spotlight-8. When converting from a compressed MPEG-1 to an uncompressed AVI, the file size increases significantly, often becoming $\sim 120\times$ greater, and requiring large amounts of disk space. To reduce disk space and increase portability, video is stored in MPEG-1 format until digitization is required. In addition, MPEG-1 video is portable, compact, useful for presentation, and easily converted to other formats. With the MPEG-1 video, one only needs VirtualDub to convert the MPEG-1 to a suitable AVI format and subsequently read into Spotlight-8 for digitizing. When converting between formats there is always a risk of quality loss; however, there is very little degradation in quality and no effect on digitization as a result of the

video formatting.

7.2 Naming Convention

The video files and resulting datasheets are named in a very specific manner with the objective of identifying the experiment, expedition, astronaut, DVD, and time.

Identification of Experiment Operation

1. Experiment (CL1, CL2, ICF1, ICF2)
2. Expedition (Exp##)
3. Date of Operation (##-##-##)

Identification of Video and Media

4. Video Origin (**OB**-Onboard, **RT**-Realtime, **VTR**-Video Tape Recorder)
5. Recording Media (DVCam, Hi8mm)
6. Content (**Ops**-Operations, Setup)

Identification of DVD

7. GMT Time of Experiment (##m##s-##m##s, if available)
8. Tape Number (T#, single digit, if available)
9. Tape ID (ID##-##, two digits, if available)
10. Astronaut Initials (MF, BM, JW, SW, CA, LA)

Event Location on DVD

11. DVD Chapter (Ch#, single digit if more than one chapter, otherwise excluded)
12. Time of Event (##m##s-##m##s)
13. Disturbance Type (CL only, A-Axial, P-Push, S-Slide, MS-Multi-Slide)

Examples are given for two experiments using the naming convention outlined above.

CL1_Exp13_08-30-06_OB_DVCam_Ops_T123_ID27-29_JW_Ch2_1108-1138_A

The name references the **Contact Line-1** experiment performed by the **Expedition 13** crew on **August 30th, 2006**. The video is from a physical **onboard** media captured with a Sony **DVCam**. The DVD is of experimental **operations** including **tapes 1, 2, and 3** with **ID numbers 27, 28, and 29**. The operations were performed by astronaut **Jeff Williams**. Video from the DVD was cut from **chapter 2** between the times **11:08 and 11:38** (mm:ss). The disturbance type is **Axial**.

ICF1_Exp15_04-07-07_OB_DVCam_Ops_0511-0733_SW_0651-0751

The name references the **Interior Corner Flow-1** experiment performed by the **Expedition 15** crew on **April 7th, 2007**. The video is from a physical **onboard** media captured with a Sony **DVCam**. The DVD is of experimental **operations** with markings on the DVD identifying GMT times between **05:11–07:33**. Note that ID and tape numbers were not found on this particular DVD. The operations were performed by astronaut **Sunita Williams**. Video from the DVD was cut between the times **06:51 and 07:51** (mm:ss).

Chapter 8

Appendix: Contact Line Sample Data Sheets

8.1 Datasheet Descriptions

Representative datasheets are presented with explanations of major features¹. The right and bottom of all page images (except data pages) are numbered columns and rows. These are used for referencing only and are not part of the datasheets outside the Thesis. Each Excel datasheet contains several ‘tabs’ which are:

1. Notes & Dim (Notes and Dimensions)
2. Input & Response Notes
3. Input Data
4. Smooth Response Data
5. Pinned Response Data
6. Below Pin Response Data (CL-1 only, replaces 5.)
7. Input Plot
8. Smooth Response Plot
9. Pinned Response Plot
10. Below Pin Response Plot (CL-1 only, replaces 9.)
11. Comparison Plot

Datasheets are formatted and notated in a descriptive manner where most features are self-explanatory. The ‘Notes & Dim’ tab contains three pages of information separated into five different categories that are described below.

1. **Notes:** General notes are provided and may differ between CL-1 and CL-2. All of the information is heavily notated and self explanatory.
2. **Fluid Depth:** Measurements are taken before and after the input disturbance at the centerline of the interface. Depths are measured in pixels and converted to millimeters using the scale factors calculated at the representative points.

¹A feature is anything in a datasheet—though generally a phrase, number, character, object, or image.

3. **Physical Dimensions:** Measurements are taken before and after the input disturbance and used to calculate the scale factor plane described in Section 2.2.1. Three different locations are measured and related to known distances to obtain the local scale factors, which, when coupled with the midpoints, can be used to calculate the scale factor constants.
4. **Input/Response SF Constants:** Scale factor constants based on Equations 2.9–2.11 are reported before and after the input disturbance.
5. **Approximate Results:** A subset of results are calculated per event for the Pinning and Smooth cylinders. Result categories are subject to change and may include additional or different results in the future (e.g. damping rate). A value of ‘–1’ indicates the quantity cannot be measured accurately and is not reported.

Features highlighted in yellow (■) are generally input by the user between events while blue (■) indicates calculated results. In the tabs with rows of data the opposite is true, where blue indicates raw data used to calculate the results in yellow. Red (■) indicates a feature that causes significant changes to the experiment.

The second tab, labeled ‘Input & Response Notes’, is separated into four sections documenting how the input and response are tracked. The page is heavily notated with most features being self-explanatory. In some cases a ‘Labels’ section is present, and is used only to notate the plots in the datasheet. Finally, the first page of the input disturbance, Smooth and Pinning response data is presented for all of the example datasheets. The method of tracking is documented along with the filename and other output from Spotlight-8. The scale factor in the right-most column is calculated using the scale factor plane equation (see Equation 2.5)—utilizing the x and y coordinates. It should be noted that optical correction is not applied in any of the datasheets and must be post-processed by the user. Updated datasheets and additional information can be found at <http://cfe.pdx.edu>.

8.1.1 CL-1 Axial Mode Example Datasheet

General Notes/Physical Measurements

C

Notes

720x480 DV Converted to 640x480 square pixels.

"Left Cylinder" refers to the cylinder with the 'Smooth' boundary condition

"Right Cylinder" refers to the cylinder with the 'Pinning' boundary condition

The frame rate is (frames/s): 29.97 Left Contact Angle (deg) 15

Disturbance Type: Axial Left Interface Asymmetry No

The pinning lip is: Dry Right Contact Angle (deg) 44

Fluid Depth

(Measured from meniscus to bottom of cylinder)

Fluid depths measured at frame: 0

	Rep. Point 1	Rep. Point 2	SF
<i>x</i>	202.5	472.5	0.202798541
<i>y</i>	345.5	319.5	0.200156642
	Depth (px)	Depth (mm)	
Smooth	105	21.2938468	
Pinning	159	31.8249062	
Difference	54	10.5310594	



Physical Dimensions:

Smooth Cylinder (Left)

	<i>x</i> -pixel	<i>y</i> -pixel	Actual	SF (in/pixel)	SF (mm/pixel)
Bottom of Cylinder <i>P1</i>	109	398			
Bottom of Cylinder <i>P2</i>	296	398		SF0	
Difference	187	0	1.5	0.00802139	0.203743316
Midpoint (<i>X0,Y0</i>)	202.5	398			

Pinning Cylinder (Right)

Bottom of Cylinder <i>P1</i>	567	399			
Bottom of Cylinder <i>P2</i>	378	399		SF1	
Difference	189	0	1.5	0.00793651	0.201587302
Midpoint (<i>X1,Y1</i>)	472.5	399			

Smooth Cylinder (Left)

Top of Cylinder <i>P1</i>	296	160			
Top of Cylinder <i>P2</i>	105	160		SF2	
Difference	191	0	1.5	0.0078534	0.19947644
Midpoint (<i>X2,Y2</i>)	200.5	160			

Average 0.0079371 0.201602352

1	2	3	4	5	6	7	8	9
---	---	---	---	---	---	---	---	---

Input SF Constants

	a	b	c
Scale Factor (SF) constants (in/px):	-3.17003E-07	7.08493E-07	0.0078036
Scale Factor (SF) constants (mm/px):	-8.05189E-06	1.79957E-05	0.19821153

The following information is taken after the response settles at frame:

924

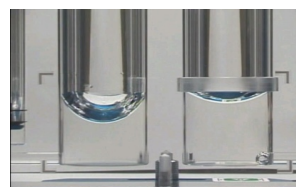
Fluid Depth

(Measured from meniscus to bottom of cylinder)

Fluid depths measured at frame:

924

	Rep. Point 1	Rep. Point 2	SF
x	201.5	473	0.202673027
y	352	327	0.201093782
	Depth (px)	Depth (mm)	
Smooth	108	21.8886869	
Pinning	158	31.7728175	
Difference	50	9.88413062	



Physical Dimensions:

Smooth Cylinder (Left)

	x-pixel	y-pixel	Actual	SF (in/pixel)	SF (mm/pixel)
Bottom of Cylinder P1	295	406			
Bottom of Cylinder P2	108	406		SF0	
Difference	187	0	1.5	0.00802139	0.203743316
Midpoint (X0,Y0)	201.5	406			

Pinning Cylinder (Right)

Bottom of Cylinder P1	379	406			
Bottom of Cylinder P2	567	406		SF1	
Difference	188	0	1.5	0.00797872	0.202659574
Midpoint (X1,Y1)	473	406			

Smooth Cylinder (Left)

Top of Cylinder P1	104	138			
Top of Cylinder P2	296	138		SF2	
Difference	192	0	1.5	0.0078125	0.1984375
Midpoint (X2,Y2)	200	138			

Average				0.00793754	0.201613463
---------	--	--	--	------------	-------------

Response SF Constants

	a	b	c
Scale Factor (SF) constants (in/px):	-1.57153E-07	7.80321E-07	0.00773625
Scale Factor (SF) constants (mm/px):	-3.99168E-06	1.98202E-05	0.19650065

1	2	3	4	5	6	7	8	9
---	---	---	---	---	---	---	---	---

Approximate Results

Input Amplitude (mm) 3.13

Smooth Cylinder (Left)

1st Period (s) 0.50

Period of Smooth Response (s): 0.64

Frequency of Smooth Response (1/s): 1.56

Settling Time of Smooth Response (s): 7.10

Pinning Cylinder (Right) **Dry** **Pinned**

1st Period (s) 0.46

Period of Pinned Response (s): 0.39

Frequency of Pinned Response (1/s): 2.56

Settling Time of Pinned Response (s): 11.70

Additional Notes

Enter Text....

1	2	3	4	5	6	7	8	9	
---	---	---	---	---	---	---	---	---	--

101
102
103
104
105
106
107
108
109
110
111
112
113
114
115
116
117
118
119
120
121
122
123
124
125
126
127
128
129
130
131
132
133
134
135
136
137
138
139
140
141
142
143
144
145
146
147
148
149
150

Input & Response Notes

Input Notes

Tracking is started at frame:

0

The input data was tracked:

at the bottom of the right cylinder.

Response Notes

Smooth Cylinder (Left)

The response with overlap starts at frame:

322

The center of the cylinder is at x -pixel location:

215

at frame

322

The meniscus was threshold tracked:

Upward

Pinning Cylinder (Right)

The response with overlap starts at frame:

322

The center of the cylinder is at x -pixel location:

395

at frame

322

The meniscus was threshold tracked:

Downward

Additional Notes

Enter Text....

Labels

Axial Input

Smooth Response-Axial (CA ~ 15 deg, Left)

Pinned Response-Axial (CA = 44 deg, Right)

Response Comparison-Axial

Smooth (CA ~ 15 deg, Left)

Pinned (CA = 44 deg, Right)

1	2	3	4	5	6	7	8	9	
---	---	---	---	---	---	---	---	---	--

CL1_Exp13_08-30-06_OB_DVCam_Ops_T123_ID27-29_JW_Ch2_1108-1138_A_VDUB.avi

Scale Factor - user units: 1.00000 image units: 1.00000

Aoi 1: WholeImage

Aoi 2: ThresholdTracking

Abs Frame	Filename	Rel Frame	x -px	y -px	Time (s)	y -Scaled (mm)	0'd y -Scaled (mm)	SF in/px
1	CL1.....1108-1138...VDUB ->	1	493	390	0.033	78.492	0.000	0.201
2	CL1.....1108-1138...VDUB ->	2	493	390	0.067	78.492	0.000	0.201
3	CL1.....1108-1138...VDUB ->	3	493	390	0.100	78.492	0.000	0.201
4	CL1.....1108-1138...VDUB ->	4	493	390	0.133	78.492	0.000	0.201
5	CL1.....1108-1138...VDUB ->	5	493	390	0.167	78.492	0.000	0.201
6	CL1.....1108-1138...VDUB ->	6	493	390	0.200	78.492	0.000	0.201
7	CL1.....1108-1138...VDUB ->	7	493	390	0.234	78.492	0.000	0.201
8	CL1.....1108-1138...VDUB ->	8	493	390	0.267	78.492	0.000	0.201
9	CL1.....1108-1138...VDUB ->	9	493	390	0.300	78.492	0.000	0.201
10	CL1.....1108-1138...VDUB ->	10	493	390	0.334	78.492	0.000	0.201
11	CL1.....1108-1138...VDUB ->	11	493	390	0.367	78.492	0.000	0.201
12	CL1.....1108-1138...VDUB ->	12	493	390	0.400	78.492	0.000	0.201
13	CL1.....1108-1138...VDUB ->	13	493	390	0.434	78.492	0.000	0.201
14	CL1.....1108-1138...VDUB ->	14	493	390	0.467	78.492	0.000	0.201
15	CL1.....1108-1138...VDUB ->	15	493	390	0.501	78.492	0.000	0.201
16	CL1.....1108-1138...VDUB ->	16	493	390	0.534	78.492	0.000	0.201
17	CL1.....1108-1138...VDUB ->	17	493	390	0.567	78.492	0.000	0.201
18	CL1.....1108-1138...VDUB ->	18	493	390	0.601	78.492	0.000	0.201
19	CL1.....1108-1138...VDUB ->	19	493	390	0.634	78.492	0.000	0.201
20	CL1.....1108-1138...VDUB ->	20	493	390	0.667	78.492	0.000	0.201
21	CL1.....1108-1138...VDUB ->	21	493	390	0.701	78.492	0.000	0.201
22	CL1.....1108-1138...VDUB ->	22	493	390	0.734	78.492	0.000	0.201
23	CL1.....1108-1138...VDUB ->	23	493	390	0.767	78.492	0.000	0.201
24	CL1.....1108-1138...VDUB ->	24	493	390	0.801	78.492	0.000	0.201
25	CL1.....1108-1138...VDUB ->	25	493	390	0.834	78.492	0.000	0.201
26	CL1.....1108-1138...VDUB ->	26	493	390	0.868	78.492	0.000	0.201
27	CL1.....1108-1138...VDUB ->	27	493	390	0.901	78.492	0.000	0.201
28	CL1.....1108-1138...VDUB ->	28	493	390	0.934	78.492	0.000	0.201
29	CL1.....1108-1138...VDUB ->	29	493	390	0.968	78.492	0.000	0.201
30	CL1.....1108-1138...VDUB ->	30	493	390	1.001	78.492	0.000	0.201
31	CL1.....1108-1138...VDUB ->	31	493	390	1.034	78.492	0.000	0.201
32	CL1.....1108-1138...VDUB ->	32	493	390	1.068	78.492	0.000	0.201
33	CL1.....1108-1138...VDUB ->	33	493	390	1.101	78.492	0.000	0.201
34	CL1.....1108-1138...VDUB ->	34	493	390	1.134	78.492	0.000	0.201
35	CL1.....1108-1138...VDUB ->	35	493	390	1.168	78.492	0.000	0.201
36	CL1.....1108-1138...VDUB ->	36	493	390	1.201	78.492	0.000	0.201
37	CL1.....1108-1138...VDUB ->	37	493	390	1.235	78.492	0.000	0.201
38	CL1.....1108-1138...VDUB ->	38	493	390	1.268	78.492	0.000	0.201
39	CL1.....1108-1138...VDUB ->	39	493	390	1.301	78.492	0.000	0.201
40	CL1.....1108-1138...VDUB ->	40	493	390	1.335	78.492	0.000	0.201
41	CL1.....1108-1138...VDUB ->	41	493	390	1.368	78.492	0.000	0.201
42	CL1.....1108-1138...VDUB ->	42	493	390	1.401	78.492	0.000	0.201
43	CL1.....1108-1138...VDUB ->	43	493	390	1.435	78.492	0.000	0.201

CL1_Exp13_08-30-06_OB_DVCam_Ops_T123_ID27-29_JW_Ch2_1108-1138_A_VDUB.avi

Scale Factor - user units: 1.00000 image units: 1.00000

Aoi 1: WholeImage

Aoi 2: ThresholdTracking

Abs Frame	Filename	Rel Frame	x -px	y -px	Time (s)	y -Scaled (mm)	0'd y -Scaled (mm)	SF in/px
1	CL1....1108-1138...VDUB ->	323	202	297	10.777	59.870	-0.415	0.202
2	CL1....1108-1138...VDUB ->	324	202	294	10.811	59.247	-1.037	0.202
3	CL1....1108-1138...VDUB ->	325	202	292	10.844	58.833	-1.452	0.201
4	CL1....1108-1138...VDUB ->	326	202	293	10.878	59.040	-1.245	0.202
5	CL1....1108-1138...VDUB ->	327	202	297	10.911	59.870	-0.415	0.202
6	CL1....1108-1138...VDUB ->	328	202	300	10.944	60.492	0.208	0.202
7	CL1....1108-1138...VDUB ->	329	202	304	10.978	61.323	1.038	0.202
8	CL1....1108-1138...VDUB ->	330	202	306	11.011	61.738	1.454	0.202
9	CL1....1108-1138...VDUB ->	331	202	307	11.044	61.946	1.662	0.202
10	CL1....1108-1138...VDUB ->	332	202	307	11.078	61.946	1.662	0.202
11	CL1....1108-1138...VDUB ->	333	202	306	11.111	61.738	1.454	0.202
12	CL1....1108-1138...VDUB ->	334	202	304	11.144	61.323	1.038	0.202
13	CL1....1108-1138...VDUB ->	335	202	303	11.178	61.115	0.831	0.202
14	CL1....1108-1138...VDUB ->	336	202	301	11.211	60.700	0.415	0.202
15	CL1....1108-1138...VDUB ->	337	202	300	11.245	60.492	0.208	0.202
16	CL1....1108-1138...VDUB ->	338	202	298	11.278	60.077	-0.208	0.202
17	CL1....1108-1138...VDUB ->	339	202	296	11.311	59.662	-0.622	0.202
18	CL1....1108-1138...VDUB ->	340	202	294	11.345	59.247	-1.037	0.202
19	CL1....1108-1138...VDUB ->	341	202	294	11.378	59.247	-1.037	0.202
20	CL1....1108-1138...VDUB ->	342	202	294	11.411	59.247	-1.037	0.202
21	CL1....1108-1138...VDUB ->	343	202	294	11.445	59.247	-1.037	0.202
22	CL1....1108-1138...VDUB ->	344	202	295	11.478	59.455	-0.830	0.202
23	CL1....1108-1138...VDUB ->	345	202	296	11.512	59.662	-0.622	0.202
24	CL1....1108-1138...VDUB ->	346	202	298	11.545	60.077	-0.208	0.202
25	CL1....1108-1138...VDUB ->	347	202	299	11.578	60.285	0.000	0.202
26	CL1....1108-1138...VDUB ->	348	202	301	11.612	60.700	0.415	0.202
27	CL1....1108-1138...VDUB ->	349	202	302	11.645	60.907	0.623	0.202
28	CL1....1108-1138...VDUB ->	350	202	303	11.678	61.115	0.831	0.202
29	CL1....1108-1138...VDUB ->	351	202	304	11.712	61.323	1.038	0.202
30	CL1....1108-1138...VDUB ->	352	202	304	11.745	61.323	1.038	0.202
31	CL1....1108-1138...VDUB ->	353	202	303	11.778	61.115	0.831	0.202
32	CL1....1108-1138...VDUB ->	354	202	302	11.812	60.907	0.623	0.202
33	CL1....1108-1138...VDUB ->	355	202	301	11.845	60.700	0.415	0.202
34	CL1....1108-1138...VDUB ->	356	202	299	11.879	60.285	0.000	0.202
35	CL1....1108-1138...VDUB ->	357	202	298	11.912	60.077	-0.208	0.202
36	CL1....1108-1138...VDUB ->	358	202	297	11.945	59.870	-0.415	0.202
37	CL1....1108-1138...VDUB ->	359	202	296	11.979	59.662	-0.622	0.202
38	CL1....1108-1138...VDUB ->	360	202	296	12.012	59.662	-0.622	0.202
39	CL1....1108-1138...VDUB ->	361	202	296	12.045	59.662	-0.622	0.202
40	CL1....1108-1138...VDUB ->	362	202	296	12.079	59.662	-0.622	0.202
41	CL1....1108-1138...VDUB ->	363	202	297	12.112	59.870	-0.415	0.202
42	CL1....1108-1138...VDUB ->	364	202	298	12.145	60.077	-0.208	0.202
43	CL1....1108-1138...VDUB ->	365	202	298	12.179	60.077	-0.208	0.202

CL1_Exp13_08-30-06_OB_DVCam_Ops_T123_ID27-29_JW_Ch2_1108-1138_A_VDUB.avi

Scale Factor - user units: 1.00000 image units: 1.00000

Aoi 1: WholeImage

Aoi 2: ThresholdTracking

Abs Frame	Filename	Rel Frame	x-px	y-px	Time (s)	y-Scaled (mm)	0'd y-Scaled (mm)	SF in/px
1	CL1.....1108-1138...VDUB ->	323	471	246	10.777	49.076	-0.204	0.199
2	CL1.....1108-1138...VDUB ->	324	471	244	10.811	48.667	-0.613	0.199
3	CL1.....1108-1138...VDUB ->	325	471	243	10.844	48.463	-0.817	0.199
4	CL1.....1108-1138...VDUB ->	326	471	247	10.878	49.280	0.000	0.200
5	CL1.....1108-1138...VDUB ->	327	471	251	10.911	50.098	0.818	0.200
6	CL1.....1108-1138...VDUB ->	328	471	253	10.944	50.508	1.227	0.200
7	CL1.....1108-1138...VDUB ->	329	471	254	10.978	50.712	1.432	0.200
8	CL1.....1108-1138...VDUB ->	330	471	251	11.011	50.098	0.818	0.200
9	CL1.....1108-1138...VDUB ->	331	471	248	11.044	49.485	0.204	0.200
10	CL1.....1108-1138...VDUB ->	332	471	244	11.078	48.667	-0.613	0.199
11	CL1.....1108-1138...VDUB ->	333	471	242	11.111	48.259	-1.022	0.199
12	CL1.....1108-1138...VDUB ->	334	471	241	11.144	48.055	-1.226	0.199
13	CL1.....1108-1138...VDUB ->	335	471	242	11.178	48.259	-1.022	0.199
14	CL1.....1108-1138...VDUB ->	336	471	245	11.211	48.872	-0.409	0.199
15	CL1.....1108-1138...VDUB ->	337	471	247	11.245	49.280	0.000	0.200
16	CL1.....1108-1138...VDUB ->	338	471	249	11.278	49.689	0.409	0.200
17	CL1.....1108-1138...VDUB ->	339	471	252	11.311	50.303	1.023	0.200
18	CL1.....1108-1138...VDUB ->	340	471	253	11.345	50.508	1.227	0.200
19	CL1.....1108-1138...VDUB ->	341	471	252	11.378	50.303	1.023	0.200
20	CL1.....1108-1138...VDUB ->	342	471	248	11.411	49.485	0.204	0.200
21	CL1.....1108-1138...VDUB ->	343	471	246	11.445	49.076	-0.204	0.199
22	CL1.....1108-1138...VDUB ->	344	471	244	11.478	48.667	-0.613	0.199
23	CL1.....1108-1138...VDUB ->	345	471	243	11.512	48.463	-0.817	0.199
24	CL1.....1108-1138...VDUB ->	346	471	242	11.545	48.259	-1.022	0.199
25	CL1.....1108-1138...VDUB ->	347	471	243	11.578	48.463	-0.817	0.199
26	CL1.....1108-1138...VDUB ->	348	471	244	11.612	48.667	-0.613	0.199
27	CL1.....1108-1138...VDUB ->	349	471	246	11.645	49.076	-0.204	0.199
28	CL1.....1108-1138...VDUB ->	350	471	249	11.678	49.689	0.409	0.200
29	CL1.....1108-1138...VDUB ->	351	471	251	11.712	50.098	0.818	0.200
30	CL1.....1108-1138...VDUB ->	352	471	252	11.745	50.303	1.023	0.200
31	CL1.....1108-1138...VDUB ->	353	471	251	11.778	50.098	0.818	0.200
32	CL1.....1108-1138...VDUB ->	354	471	248	11.812	49.485	0.204	0.200
33	CL1.....1108-1138...VDUB ->	355	471	246	11.845	49.076	-0.204	0.199
34	CL1.....1108-1138...VDUB ->	356	471	245	11.879	48.872	-0.409	0.199
35	CL1.....1108-1138...VDUB ->	357	471	244	11.912	48.667	-0.613	0.199
36	CL1.....1108-1138...VDUB ->	358	471	243	11.945	48.463	-0.817	0.199
37	CL1.....1108-1138...VDUB ->	359	471	244	11.979	48.667	-0.613	0.199
38	CL1.....1108-1138...VDUB ->	360	471	245	12.012	48.872	-0.409	0.199
39	CL1.....1108-1138...VDUB ->	361	471	247	12.045	49.280	0.000	0.200
40	CL1.....1108-1138...VDUB ->	362	471	250	12.079	49.894	0.613	0.200
41	CL1.....1108-1138...VDUB ->	363	471	251	12.112	50.098	0.818	0.200
42	CL1.....1108-1138...VDUB ->	364	471	251	12.145	50.098	0.818	0.200
43	CL1.....1108-1138...VDUB ->	365	471	250	12.179	49.894	0.613	0.200

8.1.2 CL-1 Push Mode Example Datasheet

General Notes/Physical Measurements

C

Notes

720x480 DV Converted to 640x480 square pixels.

"Left Cylinder" refers to the cylinder with the 'Smooth' boundary condition

"Right Cylinder" refers to the cylinder with the 'Pinning' boundary condition

The frame rate is (frames/s): 29.97 Left Contact Angle (deg) 4

Disturbance Type: Push Left Interface Asymmetry No

The pinning lip is: Dry Right Contact Angle (deg) 41

Fluid Depth

(Measured from meniscus to bottom of cylinder)

Fluid depths measured at frame: 0

	Rep. Point 1	Rep. Point 2	SF
x	221	491.5	0.200124416
y	395.5	378	0.198817588
	Depth (px)	Depth (mm)	
Smooth	61	12.2075894	
Pinning	100	19.8817588	
Difference	39	7.67416941	



Physical Dimensions:

Smooth Cylinder (Left)

	x-pixel	y-pixel	Actual	SF (in/pixel)	SF (mm/pixel)
Bottom of Cylinder P1	126	426			
Bottom of Cylinder P2	316	426		SF0	
Difference	190	0	1.5	0.00789474	0.200526316
Midpoint (X0,Y0)	221	426			

Pinning Cylinder (Right)

Bottom of Cylinder P1	587	428			
Bottom of Cylinder P2	396	428		SF1	
Difference	191	0	1.5	0.0078534	0.19947644
Midpoint (X1,Y1)	491.5	428			

Smooth Cylinder (Left)

Top of Cylinder P1	123	189			
Top of Cylinder P2	316	189		SF2	
Difference	193	0	1.5	0.00777202	0.197409326
Midpoint (X2,Y2)	219.5	189			

Average 0.00784005 0.199137361

1	2	3	4	5	6	7	8	9
---	---	---	---	---	---	---	---	---

Input SF Constants

	a	b	c
Scale Factor (SF) constants (in/px):	-1.56641E-07	5.18781E-07	0.00770835
Scale Factor (SF) constants (mm/px):	-3.97867E-06	1.3177E-05	0.19579218

The following information is taken after the response settles at frame:

543

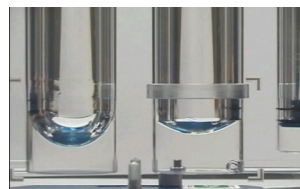
Fluid Depth

(Measured from meniscus to bottom of cylinder)

Fluid depths measured at frame:

543

	Rep. Point 1	Rep. Point 2	SF
x	133.5	404.5	0.20092448
y	395	378	0.200539616
	Depth (px)	Depth (mm)	
Smooth	62	12.4573177	
Pinning	98	19.6528823	
Difference	36	7.19556458	



Physical Dimensions:

Smooth Cylinder (Left)

	x-pixel	y-pixel	Actual	SF (in/pixel)	SF (mm/pixel)
Bottom of Cylinder P1	228	426			
Bottom of Cylinder P2	39	426		SF0	
Difference	189	0	1.5	0.00793651	0.201587302
Midpoint (X0,Y0)	133.5	426			

Pinning Cylinder (Right)

Bottom of Cylinder P1	310	427			
Bottom of Cylinder P2	499	427		SF1	
Difference	189	0	1.5	0.00793651	0.201587302
Midpoint (X1,Y1)	404.5	427			

Smooth Cylinder (Left)

Top of Cylinder P1	229	183			
Top of Cylinder P2	35	183		SF2	
Difference	194	0	1.5	0.00773196	0.196391753
Midpoint (X2,Y2)	132	183			

Average

0.00786832 0.199855452

Response SF Constants

	a	b	c
Scale Factor (SF) constants (in/px):	-3.10622E-09	8.41785E-07	0.00757832
Scale Factor (SF) constants (mm/px):	-7.8898E-08	2.13813E-05	0.19248938

1	2	3	4	5	6	7	8	9	
---	---	---	---	---	---	---	---	---	--

Approximate Results

Input Amplitude (mm) 17.38072045

Smooth Cylinder (Left)

1st Period (s) 2
Period of Smooth Response (s): 2.26
Frequency of Smooth Response (1/s): 0.442477876
Settling Time of Smooth Response (s): 9.3

Pinning Cylinder (Right) **Dry** **Below Pin**

1st Period (s) 1.3
Period of Pinned Response (s): 0.81
Frequency of Pinned Response (1/s): 1.234567901
Settling Time of Pinned Response (s): 13.7

Additional Notes

Enter Text....

1	2	3	4	5	6	7	8	9	
---	---	---	---	---	---	---	---	---	--

101
102
103
104
105
106
107
108
109
110
111
112
113
114
115
116
117
118
119
120
121
122
123
124
125
126
127
128
129
130
131
132
133
134
135
136
137
138
139
140
141
142
143
144
145
146
147
148
149
150

Input & Response Notes

Input Notes

Tracking is started at frame:

0

The input data was tracked:

at the left side of the pinning cylinder.

Response Notes

Smooth Cylinder (Left)

The response with overlap starts at frame:

70

The AOI is tracked at 1/4 the diameter from the:

Left

at frame

70

1/4 the diameter is at the point:

(70, 349)

Pinning Cylinder (Right)

The response with overlap starts at frame:

70

The AOI is tracked at 1/4 the diameter from the:

Left

at frame

70

1/4 the diameter is at the point:

(342, 316)

Additional Notes

Labels

Push Input

Smooth Response-Push (CA ~ 4 deg, Left)

Smooth (CA ~ 4 deg, Left)

Below Pin Response-Push (CA = 41 deg, Right)

Below Pin (CA = 41 deg, Right)

Response Comparison-Push

1	2	3	4	5	6	7	8	9	
---	---	---	---	---	---	---	---	---	--

CL1_Exp13_08-30-06_OB_DVCam_Ops_T123_ID27-29_JW_Ch2_5445_5503_P_VDUB.avi

Scale Factor - user units: 1.00000 image units: 1.00000

Aoi 1: WholeImage

Aoi 2: ThresholdTracking

Abs Frame	Filename	Rel Frame	x-px	y-px	Time (s)	x-Scaled (mm)	O'd x-Scaled (mm)	SF in/px
1	CL1.....5445-5503...VDUB ->	1	398	344	0.033	79.099	0.000	0.199
2	CL1.....5445-5503...VDUB ->	2	397	344	0.067	78.902	-0.197	0.199
3	CL1.....5445-5503...VDUB ->	3	398	344	0.100	79.099	0.000	0.199
4	CL1.....5445-5503...VDUB ->	4	398	344	0.133	79.099	0.000	0.199
5	CL1.....5445-5503...VDUB ->	5	398	344	0.167	79.099	0.000	0.199
6	CL1.....5445-5503...VDUB ->	6	397	344	0.200	78.902	-0.197	0.199
7	CL1.....5445-5503...VDUB ->	7	397	344	0.234	78.902	-0.197	0.199
8	CL1.....5445-5503...VDUB ->	8	397	344	0.267	78.902	-0.197	0.199
9	CL1.....5445-5503...VDUB ->	9	397	344	0.300	78.902	-0.197	0.199
10	CL1.....5445-5503...VDUB ->	10	397	344	0.334	78.902	-0.197	0.199
11	CL1.....5445-5503...VDUB ->	11	397	344	0.367	78.902	-0.197	0.199
12	CL1.....5445-5503...VDUB ->	12	397	344	0.400	78.902	-0.197	0.199
13	CL1.....5445-5503...VDUB ->	13	397	344	0.434	78.902	-0.197	0.199
14	CL1.....5445-5503...VDUB ->	14	397	344	0.467	78.902	-0.197	0.199
15	CL1.....5445-5503...VDUB ->	15	397	344	0.501	78.902	-0.197	0.199
16	CL1.....5445-5503...VDUB ->	16	397	344	0.534	78.902	-0.197	0.199
17	CL1.....5445-5503...VDUB ->	17	397	344	0.567	78.902	-0.197	0.199
18	CL1.....5445-5503...VDUB ->	18	397	344	0.601	78.902	-0.197	0.199
19	CL1.....5445-5503...VDUB ->	19	397	344	0.634	78.902	-0.197	0.199
20	CL1.....5445-5503...VDUB ->	20	397	344	0.667	78.902	-0.197	0.199
21	CL1.....5445-5503...VDUB ->	21	397	344	0.701	78.902	-0.197	0.199
22	CL1.....5445-5503...VDUB ->	22	397	344	0.734	78.902	-0.197	0.199
23	CL1.....5445-5503...VDUB ->	23	397	344	0.767	78.902	-0.197	0.199
24	CL1.....5445-5503...VDUB ->	24	397	344	0.801	78.902	-0.197	0.199
25	CL1.....5445-5503...VDUB ->	25	397	344	0.834	78.902	-0.197	0.199
26	CL1.....5445-5503...VDUB ->	26	397	344	0.868	78.902	-0.197	0.199
27	CL1.....5445-5503...VDUB ->	27	397	344	0.901	78.902	-0.197	0.199
28	CL1.....5445-5503...VDUB ->	28	397	344	0.934	78.902	-0.197	0.199
29	CL1.....5445-5503...VDUB ->	29	397	344	0.968	78.902	-0.197	0.199
30	CL1.....5445-5503...VDUB ->	30	397	344	1.001	78.902	-0.197	0.199
31	CL1.....5445-5503...VDUB ->	31	397	344	1.034	78.902	-0.197	0.199
32	CL1.....5445-5503...VDUB ->	32	397	344	1.068	78.902	-0.197	0.199
33	CL1.....5445-5503...VDUB ->	33	397	344	1.101	78.902	-0.197	0.199
34	CL1.....5445-5503...VDUB ->	34	397	344	1.134	78.902	-0.197	0.199
35	CL1.....5445-5503...VDUB ->	35	397	344	1.168	78.902	-0.197	0.199
36	CL1.....5445-5503...VDUB ->	36	397	344	1.201	78.902	-0.197	0.199
37	CL1.....5445-5503...VDUB ->	37	396	344	1.235	78.705	-0.394	0.199
38	CL1.....5445-5503...VDUB ->	38	396	344	1.268	78.705	-0.394	0.199
39	CL1.....5445-5503...VDUB ->	39	396	344	1.301	78.705	-0.394	0.199
40	CL1.....5445-5503...VDUB ->	40	396	344	1.335	78.705	-0.394	0.199
41	CL1.....5445-5503...VDUB ->	41	396	344	1.368	78.705	-0.394	0.199
42	CL1.....5445-5503...VDUB ->	42	396	344	1.401	78.705	-0.394	0.199
43	CL1.....5445-5503...VDUB ->	43	396	344	1.435	78.705	-0.394	0.199
44	CL1.....5445-5503...VDUB ->	44	396	344	1.468	78.705	-0.394	0.199

CL1_Exp13_08-30-06_OB_DVCam_Ops_T123_ID27-29_JW_Ch2_5445_5503_P_VDUB.avi

Scale Factor - user units: 1.00000 image units: 1.00000

Aoi 1: WholeImage

Aoi 2: ThresholdTracking

Abs Frame	Filename	Rel Frame	x -px	y -px	Time (s)	x-Scaled (mm)	0'd x-Scaled (mm)	SF in/px
1	CL1.....5445-5503...VDUB ->	71	70	349	2.369	13.996	-3.199	0.200
2	CL1.....5445-5503...VDUB ->	72	70	349	2.402	13.996	-3.199	0.200
3	CL1.....5445-5503...VDUB ->	73	72	349	2.436	14.396	-2.799	0.200
4	CL1.....5445-5503...VDUB ->	74	73	349	2.469	14.596	-2.599	0.200
5	CL1.....5445-5503...VDUB ->	75	78	349	2.503	15.596	-1.600	0.200
6	CL1.....5445-5503...VDUB ->	76	82	349	2.536	16.395	-0.800	0.200
1	CL1.....5445-5503...VDUB ->	77	90	349	2.569	17.995	0.800	0.200
2	CL1.....5445-5503...VDUB ->	78	95	349	2.603	18.995	1.799	0.200
3	CL1.....5445-5503...VDUB ->	79	94	349	2.636	18.795	1.599	0.200
4	CL1.....5445-5503...VDUB ->	80	98	349	2.669	19.594	2.399	0.200
5	CL1.....5445-5503...VDUB ->	81	98	349	2.703	19.594	2.399	0.200
6	CL1.....5445-5503...VDUB ->	82	100	349	2.736	19.994	2.799	0.200
7	CL1.....5445-5503...VDUB ->	83	104	349	2.769	20.794	3.599	0.200
8	CL1.....5445-5503...VDUB ->	84	101	349	2.803	20.194	2.999	0.200
1	CL1.....5445-5503...VDUB ->	85	107	349	2.836	21.394	4.199	0.200
2	CL1.....5445-5503...VDUB ->	86	107	349	2.870	21.394	4.199	0.200
3	CL1.....5445-5503...VDUB ->	87	104	349	2.903	20.794	3.599	0.200
4	CL1.....5445-5503...VDUB ->	88	104	349	2.936	20.794	3.599	0.200
5	CL1.....5445-5503...VDUB ->	89	105	349	2.970	20.994	3.799	0.200
6	CL1.....5445-5503...VDUB ->	90	104	349	3.003	20.794	3.599	0.200
7	CL1.....5445-5503...VDUB ->	91	104	349	3.036	20.794	3.599	0.200
8	CL1.....5445-5503...VDUB ->	92	104	349	3.070	20.794	3.599	0.200
9	CL1.....5445-5503...VDUB ->	93	104	349	3.103	20.794	3.599	0.200
10	CL1.....5445-5503...VDUB ->	94	104	349	3.136	20.794	3.599	0.200
11	CL1.....5445-5503...VDUB ->	95	102	349	3.170	20.394	3.199	0.200
12	CL1.....5445-5503...VDUB ->	96	100	349	3.203	19.994	2.799	0.200
13	CL1.....5445-5503...VDUB ->	97	98	349	3.237	19.594	2.399	0.200
14	CL1.....5445-5503...VDUB ->	98	96	349	3.270	19.195	1.999	0.200
15	CL1.....5445-5503...VDUB ->	99	95	349	3.303	18.995	1.799	0.200
16	CL1.....5445-5503...VDUB ->	100	93	349	3.337	18.595	1.400	0.200
17	CL1.....5445-5503...VDUB ->	101	90	349	3.370	17.995	0.800	0.200
18	CL1.....5445-5503...VDUB ->	102	90	349	3.403	17.995	0.800	0.200
19	CL1.....5445-5503...VDUB ->	103	88	349	3.437	17.595	0.400	0.200
20	CL1.....5445-5503...VDUB ->	104	85	349	3.470	16.995	-0.200	0.200
21	CL1.....5445-5503...VDUB ->	105	85	349	3.504	16.995	-0.200	0.200
22	CL1.....5445-5503...VDUB ->	106	83	349	3.537	16.595	-0.600	0.200
23	CL1.....5445-5503...VDUB ->	107	82	349	3.570	16.395	-0.800	0.200
24	CL1.....5445-5503...VDUB ->	108	80	349	3.604	15.996	-1.200	0.200
25	CL1.....5445-5503...VDUB ->	109	80	349	3.637	15.996	-1.200	0.200
26	CL1.....5445-5503...VDUB ->	110	79	349	3.670	15.796	-1.400	0.200
27	CL1.....5445-5503...VDUB ->	111	78	349	3.704	15.596	-1.600	0.200
28	CL1.....5445-5503...VDUB ->	112	76	349	3.737	15.196	-1.999	0.200
29	CL1.....5445-5503...VDUB ->	113	75	349	3.770	14.996	-2.199	0.200

CL1_Exp13_08-30-06_OB_DVCam_Ops_T123_ID27-29_JW_Ch2_5445_5503_P_VDUB.avi

Scale Factor - user units: 1.00000 image units: 1.00000

Aoi 1: WholeImage

Aoi 2: ThresholdTracking

Abs Frame	Filename	Rel Frame	x-px	y-px	Time (s)	x-Scaled (mm)	0'd x-Scaled (mm)	SF in/px
1	CL1....5445-5503...VDUB ->	71	342	316	2.369	68.133	-0.598	0.199
2	CL1....5445-5503...VDUB ->	72	346	316	2.402	68.930	0.199	0.199
3	CL1....5445-5503...VDUB ->	73	352	316	2.436	70.125	1.394	0.199
4	CL1....5445-5503...VDUB ->	74	358	316	2.469	71.320	2.589	0.199
5	CL1....5445-5503...VDUB ->	75	362	316	2.503	72.117	3.386	0.199
6	CL1....5445-5503...VDUB ->	76	367	316	2.536	73.113	4.382	0.199
7	CL1....5445-5503...VDUB ->	77	371	316	2.569	73.909	5.179	0.199
8	CL1....5445-5503...VDUB ->	78	375	316	2.603	74.706	5.976	0.199
9	CL1....5445-5503...VDUB ->	79	376	316	2.636	74.905	6.175	0.199
10	CL1....5445-5503...VDUB ->	80	377	316	2.669	75.104	6.374	0.199
11	CL1....5445-5503...VDUB ->	81	376	316	2.703	74.905	6.175	0.199
12	CL1....5445-5503...VDUB ->	82	376	316	2.736	74.905	6.175	0.199
13	CL1....5445-5503...VDUB ->	83	375	316	2.769	74.706	5.976	0.199
14	CL1....5445-5503...VDUB ->	84	375	316	2.803	74.706	5.976	0.199
15	CL1....5445-5503...VDUB ->	85	375	316	2.836	74.706	5.976	0.199
16	CL1....5445-5503...VDUB ->	86	374	316	2.870	74.507	5.776	0.199
17	CL1....5445-5503...VDUB ->	87	374	316	2.903	74.507	5.776	0.199
18	CL1....5445-5503...VDUB ->	88	373	316	2.936	74.308	5.577	0.199
19	CL1....5445-5503...VDUB ->	89	373	316	2.970	74.308	5.577	0.199
20	CL1....5445-5503...VDUB ->	90	370	316	3.003	73.710	4.980	0.199
21	CL1....5445-5503...VDUB ->	91	367	316	3.036	73.113	4.382	0.199
22	CL1....5445-5503...VDUB ->	92	364	316	3.070	72.515	3.785	0.199
23	CL1....5445-5503...VDUB ->	93	361	316	3.103	71.917	3.187	0.199
24	CL1....5445-5503...VDUB ->	94	360	316	3.136	71.718	2.988	0.199
25	CL1....5445-5503...VDUB ->	95	358	316	3.170	71.320	2.589	0.199
26	CL1....5445-5503...VDUB ->	96	357	316	3.203	71.121	2.390	0.199
27	CL1....5445-5503...VDUB ->	97	356	316	3.237	70.922	2.191	0.199
28	CL1....5445-5503...VDUB ->	98	353	316	3.270	70.324	1.594	0.199
29	CL1....5445-5503...VDUB ->	99	348	316	3.303	69.328	0.598	0.199
30	CL1....5445-5503...VDUB ->	100	344	316	3.337	68.531	-0.199	0.199
31	CL1....5445-5503...VDUB ->	101	343	316	3.370	68.332	-0.398	0.199
32	CL1....5445-5503...VDUB ->	102	341	316	3.403	67.934	-0.797	0.199
33	CL1....5445-5503...VDUB ->	103	339	316	3.437	67.535	-1.195	0.199
34	CL1....5445-5503...VDUB ->	104	337	316	3.470	67.137	-1.594	0.199
35	CL1....5445-5503...VDUB ->	105	336	316	3.504	66.938	-1.793	0.199
36	CL1....5445-5503...VDUB ->	106	336	316	3.537	66.938	-1.793	0.199
37	CL1....5445-5503...VDUB ->	107	336	316	3.570	66.938	-1.793	0.199
38	CL1....5445-5503...VDUB ->	108	336	316	3.604	66.938	-1.793	0.199
39	CL1....5445-5503...VDUB ->	109	336	316	3.637	66.938	-1.793	0.199
40	CL1....5445-5503...VDUB ->	110	336	316	3.670	66.938	-1.793	0.199
41	CL1....5445-5503...VDUB ->	111	337	316	3.704	67.137	-1.594	0.199
42	CL1....5445-5503...VDUB ->	112	338	316	3.737	67.336	-1.394	0.199
43	CL1....5445-5503...VDUB ->	113	340	316	3.770	67.734	-0.996	0.199

8.1.3 CL-2 Axial Mode Example Datasheet

General Notes/Physical Measurements

C

Notes

720x480 DV Converted to 640x480 square pixels.

"Left Cylinder" refers to the 'Smooth' boundary condition

"Right Cylinder" refers to the 'Pinning' boundary condition

The frame rate is (frames/s): **29.97**

Disturbance Type: **Axial**

The pinning lip is: **Dry**

Fluid Depth

(Measured from meniscus to bottom of cylinder)

Fluid depths measured at frame: **0**

	Rep. Point 1	Rep. Point 2	SF
<i>x</i>	180.5	456.5	0.189529744
<i>y</i>	320	306.5	0.191463312
	Depth (px)	Depth (mm)	
Smooth	158	29.9456996	
Pinning	165	31.5914465	
Difference	7	1.64574691	



Physical Dimensions:

Smooth Cylinder (Left)

	<i>x</i> -pixel	<i>y</i> -pixel	Actual	SF (in/pixel)	SF (mm/pixel)
Bottom of Cylinder <i>P1</i>	80	401			
Bottom of Cylinder <i>P2</i>	281	397		SF0	
Difference	201	4	1.5	0.00746121	0.189514716
Midpoint (<i>X0,Y0</i>)	180.5	399			

Pinning Cylinder (Right)

Bottom of Cylinder <i>P1</i>	357	390			
Bottom of Cylinder <i>P2</i>	556	388		SF1	
Difference	199	2	1.5	0.00753731	0.191447618
Midpoint (<i>X1,Y1</i>)	456.5	389			

Smooth Cylinder (Left)

Top of Cylinder <i>P1</i>	71	70			
Top of Cylinder <i>P2</i>	272	66		SF2	
Difference	201	4	1.5	0.00746121	0.189514716
Midpoint (<i>X2,Y2</i>)	171.5	68			

Average 0.00748658 0.190159016

1	2	3	4	5	6	7	8	9
---	---	---	---	---	---	---	---	---

Input SF Constants

	a	b	c
Scale Factor (SF) constants (in/px):	2.75448E-07	-7.4895E-09	0.00741448
Scale Factor (SF) constants (mm/px):	6.99638E-06	-1.9023E-07	0.18832777

The following information is taken after the response settles at frame:

269

Fluid Depth

(Measured from meniscus to bottom of cylinder)

Fluid depths measured at frame:

269

	Rep. Point 1	Rep. Point 2	SF
x	179.5	456	0.189534786
y	319	307	0.192435513
	Depth (px)	Depth (mm)	
Smooth	158	29.9464962	
Pinning	166	31.9442952	
Difference	8	1.99779898	



Physical Dimensions:

Smooth Cylinder (Left)

	x -pixel	y -pixel	Actual	SF (in/pixel)	SF (mm/pixel)
Bottom of Cylinder P1	79	400			
Bottom of Cylinder P2	280	396		SF0	
Difference	201	4	1.5	0.00746121	0.189514716
Midpoint (X0,Y0)	179.5	398			

Pinning Cylinder (Right)

Bottom of Cylinder P1	357	391			
Bottom of Cylinder P2	555	389		SF1	
Difference	198	2	1.5	0.00757537	0.192414427
Midpoint (X1,Y1)	456	390			

Smooth Cylinder (Left)

Top of Cylinder P1	71	70			
Top of Cylinder P2	272	66		SF2	
Difference	201	4	1.5	0.00746121	0.189514716
Midpoint (X2,Y2)	171.5	68			

Average				0.00749926	0.190481286
---------	--	--	--	------------	-------------

Response SF Constants

	a	b	c
Scale Factor (SF) constants (in/px):	4.12592E-07	-1.0002E-08	0.00739113
Scale Factor (SF) constants (mm/px):	1.04798E-05	-2.5406E-07	0.1877347

1	2	3	4	5	6	7	8	9
---	---	---	---	---	---	---	---	---

Approximate Results

Input Amplitude (mm)	6.06
Smooth Cylinder (Left)	
Period of Smooth Response (s):	1.03
Frequency of Smooth Response (1/s):	0.97
Settling Time of Smooth Response (s):	2.8
Pinning Cylinder (Right)	
	Dry
Period of Pinned Response (s):	0.95
Frequency of Pinned Response (1/s):	1.05
Settling Time of Pinned Response (s):	4.1

Additional Notes

1	2	3	4	5	6	7	8	9	
---	---	---	---	---	---	---	---	---	--

101
102
103
104
105
106
107
108
109
110
111
112
113
114
115
116
117
118
119
120
121
122
123
124
125
126
127
128
129
130
131
132
133
134
135
136
137
138
139
140
141
142
143
144
145
146
147
148
149
150

Input & Response Notes

Input Notes

Tracking is started at frame:

0

The input data was tracked:

at the bottom of the left cylinder.

Response Notes

Smooth Cylinder (Left)

The response with overlap starts at frame:

49

The center of the cylinder is at x-pixel location:

180

at frame

269

The meniscus was threshold tracked:

Downward

Pinning Cylinder (Right)

The response with overlap starts at frame:

49

The center of the cylinder is at x-pixel location:

456

at frame

269

The meniscus was threshold tracked:

Downward

Additional Notes

Labels

Axial Input
Smooth Response-Axial
Pinned Response-Axial
Response Comparison-Axial

1	2	3	4	5	6	7	8	9
---	---	---	---	---	---	---	---	---

1
2
3
4
5
6
7
8
9
10
11
12
13
14
15
16
17
18
19
20
21
22
23
24
25
26
27
28
29
30
31
32
33
34
35
36
37
38
39
40
41
42
43
44
45
46
47
48
49
50

CL2_Exp13_04-18-06_DL_Realtime_Ops_853-1340_JW_0039-0048_A_VDUB.avi

Scale Factor - user units: 1.00000 image units: 1.00000

Aoi 1: WholeImage

Aoi 2: ThresholdTracking

Abs Frame	Filename	Rel Frame	x-px	y-px	Time (s)	y-Scaled (mm)	O'd y-Scaled (mm)	SF in/px
1	CL2.....0039-0048...VDUB ->	1	181	385	0.033	72.966	0.000	0.190
2	CL2.....0039-0048...VDUB ->	2	181	385	0.067	72.966	0.000	0.190
3	CL2.....0039-0048...VDUB ->	3	181	385	0.100	72.966	0.000	0.190
4	CL2.....0039-0048...VDUB ->	4	181	385	0.133	72.966	0.000	0.190
5	CL2.....0039-0048...VDUB ->	5	181	385	0.167	72.966	0.000	0.190
6	CL2.....0039-0048...VDUB ->	6	181	385	0.200	72.966	0.000	0.190
7	CL2.....0039-0048...VDUB ->	7	181	385	0.234	72.966	0.000	0.190
8	CL2.....0039-0048...VDUB ->	8	181	385	0.267	72.966	0.000	0.190
9	CL2.....0039-0048...VDUB ->	9	181	385	0.300	72.966	0.000	0.190
10	CL2.....0039-0048...VDUB ->	10	181	385	0.334	72.966	0.000	0.190
11	CL2.....0039-0048...VDUB ->	11	181	385	0.367	72.966	0.000	0.190
12	CL2.....0039-0048...VDUB ->	12	181	385	0.400	72.966	0.000	0.190
13	CL2.....0039-0048...VDUB ->	13	181	385	0.434	72.966	0.000	0.190
14	CL2.....0039-0048...VDUB ->	14	181	385	0.467	72.966	0.000	0.190
15	CL2.....0039-0048...VDUB ->	15	181	385	0.501	72.966	0.000	0.190
16	CL2.....0039-0048...VDUB ->	16	181	385	0.534	72.966	0.000	0.190
17	CL2.....0039-0048...VDUB ->	17	181	385	0.567	72.966	0.000	0.190
18	CL2.....0039-0048...VDUB ->	18	181	385	0.601	72.966	0.000	0.190
19	CL2.....0039-0048...VDUB ->	19	181	385	0.634	72.966	0.000	0.190
20	CL2.....0039-0048...VDUB ->	20	181	385	0.667	72.966	0.000	0.190
21	CL2.....0039-0048...VDUB ->	21	181	385	0.701	72.966	0.000	0.190
22	CL2.....0039-0048...VDUB ->	22	181	385	0.734	72.966	0.000	0.190
23	CL2.....0039-0048...VDUB ->	23	181	385	0.767	72.966	0.000	0.190
24	CL2.....0039-0048...VDUB ->	24	181	385	0.801	72.966	0.000	0.190
25	CL2.....0039-0048...VDUB ->	25	181	385	0.834	72.966	0.000	0.190
26	CL2.....0039-0048...VDUB ->	26	181	385	0.868	72.966	0.000	0.190
27	CL2.....0039-0048...VDUB ->	27	181	385	0.901	72.966	0.000	0.190
28	CL2.....0039-0048...VDUB ->	28	181	385	0.934	72.966	0.000	0.190
29	CL2.....0039-0048...VDUB ->	29	181	385	0.968	72.966	0.000	0.190
30	CL2.....0039-0048...VDUB ->	30	181	385	1.001	72.966	0.000	0.190
31	CL2.....0039-0048...VDUB ->	31	181	385	1.034	72.966	0.000	0.190
32	CL2.....0039-0048...VDUB ->	32	181	385	1.068	72.966	0.000	0.190
33	CL2.....0039-0048...VDUB ->	33	181	385	1.101	72.966	0.000	0.190
34	CL2.....0039-0048...VDUB ->	34	181	387	1.134	73.344	0.379	0.190
35	CL2.....0039-0048...VDUB ->	35	181	389	1.168	73.723	0.758	0.190
36	CL2.....0039-0048...VDUB ->	36	181	391	1.201	74.102	1.137	0.190
37	CL2.....0039-0048...VDUB ->	37	181	395	1.235	74.860	1.894	0.190
38	CL2.....0039-0048...VDUB ->	38	181	401	1.268	75.997	3.031	0.190
39	CL2.....0039-0048...VDUB ->	39	181	407	1.301	77.133	4.168	0.190
40	CL2.....0039-0048...VDUB ->	40	181	409	1.335	77.512	4.547	0.190
41	CL2.....0039-0048...VDUB ->	41	181	409	1.368	77.512	4.547	0.190
42	CL2.....0039-0048...VDUB ->	42	181	407	1.401	77.133	4.168	0.190
43	CL2.....0039-0048...VDUB ->	43	181	397	1.435	75.239	2.273	0.190
44	CL2.....0039-0048...VDUB ->	44	181	391	1.468	74.102	1.137	0.190

CL2_Exp13_04-18-06_DL_Realtme_Ops_853-1340_JW_0039-0048_A_VDUB.avi

Scale Factor - user units: 1.00000 image units: 1.00000

Aoi 1: WholeImage

Aoi 2: ThresholdTracking

Abs Frame	Filename	Rel Frame	x -px	y -px	Time (s)	y -Scaled (mm)	O'd y -Scaled (mm)	SF in/px
1	CL2.....0039-0048...VDUB ->	49	180	218	1.635	41.325	-4.359	0.190
2	CL2.....0039-0048...VDUB ->	50	180	222	1.668	42.083	-3.601	0.190
3	CL2.....0039-0048...VDUB ->	51	180	241	1.702	45.684	0.000	0.190
4	CL2.....0039-0048...VDUB ->	52	180	251	1.735	47.579	1.895	0.190
5	CL2.....0039-0048...VDUB ->	53	180	254	1.768	48.147	2.463	0.190
6	CL2.....0039-0048...VDUB ->	54	180	257	1.802	48.716	3.032	0.190
7	CL2.....0039-0048...VDUB ->	55	180	258	1.835	48.905	3.221	0.190
8	CL2.....0039-0048...VDUB ->	56	180	259	1.869	49.095	3.411	0.190
9	CL2.....0039-0048...VDUB ->	57	180	259	1.902	49.095	3.411	0.190
10	CL2.....0039-0048...VDUB ->	58	180	259	1.935	49.095	3.411	0.190
11	CL2.....0039-0048...VDUB ->	59	180	258	1.969	48.905	3.221	0.190
12	CL2.....0039-0048...VDUB ->	60	180	257	2.002	48.716	3.032	0.190
13	CL2.....0039-0048...VDUB ->	61	180	256	2.035	48.526	2.842	0.190
14	CL2.....0039-0048...VDUB ->	62	180	255	2.069	48.337	2.653	0.190
15	CL2.....0039-0048...VDUB ->	63	180	253	2.102	47.958	2.274	0.190
16	CL2.....0039-0048...VDUB ->	64	180	252	2.135	47.768	2.084	0.190
17	CL2.....0039-0048...VDUB ->	65	180	251	2.169	47.579	1.895	0.190
18	CL2.....0039-0048...VDUB ->	66	180	250	2.202	47.389	1.705	0.190
19	CL2.....0039-0048...VDUB ->	67	180	248	2.236	47.010	1.326	0.190
20	CL2.....0039-0048...VDUB ->	68	180	247	2.269	46.821	1.137	0.190
21	CL2.....0039-0048...VDUB ->	69	180	246	2.302	46.631	0.947	0.190
22	CL2.....0039-0048...VDUB ->	70	180	244	2.336	46.252	0.568	0.190
23	CL2.....0039-0048...VDUB ->	71	180	243	2.369	46.063	0.379	0.190
24	CL2.....0039-0048...VDUB ->	72	180	242	2.402	45.873	0.189	0.190
25	CL2.....0039-0048...VDUB ->	73	180	241	2.436	45.684	0.000	0.190
26	CL2.....0039-0048...VDUB ->	74	180	240	2.469	45.494	-0.189	0.190
27	CL2.....0039-0048...VDUB ->	75	180	239	2.503	45.305	-0.379	0.190
28	CL2.....0039-0048...VDUB ->	76	180	238	2.536	45.115	-0.568	0.190
29	CL2.....0039-0048...VDUB ->	77	180	238	2.569	45.115	-0.568	0.190
30	CL2.....0039-0048...VDUB ->	78	180	238	2.603	45.115	-0.568	0.190
31	CL2.....0039-0048...VDUB ->	79	180	238	2.636	45.115	-0.568	0.190
32	CL2.....0039-0048...VDUB ->	80	180	238	2.669	45.115	-0.568	0.190
33	CL2.....0039-0048...VDUB ->	81	180	240	2.703	45.494	-0.189	0.190
34	CL2.....0039-0048...VDUB ->	82	180	241	2.736	45.684	0.000	0.190
35	CL2.....0039-0048...VDUB ->	83	180	241	2.769	45.684	0.000	0.190
36	CL2.....0039-0048...VDUB ->	84	180	242	2.803	45.873	0.189	0.190
37	CL2.....0039-0048...VDUB ->	85	180	244	2.836	46.252	0.568	0.190
38	CL2.....0039-0048...VDUB ->	86	180	244	2.870	46.252	0.568	0.190
39	CL2.....0039-0048...VDUB ->	87	180	244	2.903	46.252	0.568	0.190
40	CL2.....0039-0048...VDUB ->	88	180	245	2.936	46.442	0.758	0.190
41	CL2.....0039-0048...VDUB ->	89	180	245	2.970	46.442	0.758	0.190
42	CL2.....0039-0048...VDUB ->	90	180	245	3.003	46.442	0.758	0.190
43	CL2.....0039-0048...VDUB ->	91	180	245	3.036	46.442	0.758	0.190
44	CL2.....0039-0048...VDUB ->	92	180	245	3.070	46.442	0.758	0.190

CL2_Exp13_04-18-06_DL_Realtime_Ops_853-1340_JW_0039-0048_A_VDUB.avi

Scale Factor - user units: 1.00000 image units: 1.00000

Aoi 1: WholeImage

Aoi 2: ThresholdTracking

Abs Frame	Filename	Rel Frame	x -px	y -px	Time (s)	y -Scaled (mm)	O'd y -Scaled (mm)	SF in/px
1	CL2.....0039-0048...VDUB ->	49	456	201	1.635	38.685	-4.041	0.192
2	CL2.....0039-0048...VDUB ->	50	456	206	1.668	39.647	-3.078	0.192
3	CL2.....0039-0048...VDUB ->	51	456	221	1.702	42.533	-0.192	0.192
4	CL2.....0039-0048...VDUB ->	52	456	230	1.735	44.265	1.539	0.192
5	CL2.....0039-0048...VDUB ->	53	456	234	1.768	45.034	2.309	0.192
6	CL2.....0039-0048...VDUB ->	54	456	237	1.802	45.611	2.886	0.192
7	CL2.....0039-0048...VDUB ->	55	456	238	1.835	45.804	3.078	0.192
8	CL2.....0039-0048...VDUB ->	56	456	239	1.869	45.996	3.271	0.192
9	CL2.....0039-0048...VDUB ->	57	456	240	1.902	46.189	3.463	0.192
10	CL2.....0039-0048...VDUB ->	58	456	240	1.935	46.189	3.463	0.192
11	CL2.....0039-0048...VDUB ->	59	456	240	1.969	46.189	3.463	0.192
12	CL2.....0039-0048...VDUB ->	60	456	239	2.002	45.996	3.271	0.192
13	CL2.....0039-0048...VDUB ->	61	456	238	2.035	45.804	3.078	0.192
14	CL2.....0039-0048...VDUB ->	62	456	237	2.069	45.611	2.886	0.192
15	CL2.....0039-0048...VDUB ->	63	456	235	2.102	45.227	2.501	0.192
16	CL2.....0039-0048...VDUB ->	64	456	233	2.135	44.842	2.116	0.192
17	CL2.....0039-0048...VDUB ->	65	456	231	2.169	44.457	1.732	0.192
18	CL2.....0039-0048...VDUB ->	66	456	227	2.202	43.687	0.962	0.192
19	CL2.....0039-0048...VDUB ->	67	456	221	2.236	42.533	-0.192	0.192
20	CL2.....0039-0048...VDUB ->	68	456	219	2.269	42.148	-0.577	0.192
21	CL2.....0039-0048...VDUB ->	69	456	217	2.302	41.763	-0.962	0.192
22	CL2.....0039-0048...VDUB ->	70	456	215	2.336	41.379	-1.347	0.192
23	CL2.....0039-0048...VDUB ->	71	456	215	2.369	41.379	-1.347	0.192
24	CL2.....0039-0048...VDUB ->	72	456	214	2.402	41.186	-1.539	0.192
25	CL2.....0039-0048...VDUB ->	73	456	214	2.436	41.186	-1.539	0.192
26	CL2.....0039-0048...VDUB ->	74	456	214	2.469	41.186	-1.539	0.192
27	CL2.....0039-0048...VDUB ->	75	456	217	2.503	41.763	-0.962	0.192
28	CL2.....0039-0048...VDUB ->	76	456	219	2.536	42.148	-0.577	0.192
29	CL2.....0039-0048...VDUB ->	77	456	220	2.569	42.341	-0.385	0.192
30	CL2.....0039-0048...VDUB ->	78	456	222	2.603	42.725	0.000	0.192
31	CL2.....0039-0048...VDUB ->	79	456	225	2.636	43.303	0.577	0.192
32	CL2.....0039-0048...VDUB ->	80	456	225	2.669	43.303	0.577	0.192
33	CL2.....0039-0048...VDUB ->	81	456	229	2.703	44.072	1.347	0.192
34	CL2.....0039-0048...VDUB ->	82	456	230	2.736	44.265	1.539	0.192
35	CL2.....0039-0048...VDUB ->	83	456	230	2.769	44.265	1.539	0.192
36	CL2.....0039-0048...VDUB ->	84	456	231	2.803	44.457	1.732	0.192
37	CL2.....0039-0048...VDUB ->	85	456	231	2.836	44.457	1.732	0.192
38	CL2.....0039-0048...VDUB ->	86	456	231	2.870	44.457	1.732	0.192
39	CL2.....0039-0048...VDUB ->	87	456	231	2.903	44.457	1.732	0.192
40	CL2.....0039-0048...VDUB ->	88	456	229	2.936	44.072	1.347	0.192
41	CL2.....0039-0048...VDUB ->	89	456	229	2.970	44.072	1.347	0.192
42	CL2.....0039-0048...VDUB ->	90	456	227	3.003	43.687	0.962	0.192
43	CL2.....0039-0048...VDUB ->	91	456	225	3.036	43.303	0.577	0.192
44	CL2.....0039-0048...VDUB ->	92	456	223	3.070	42.918	0.192	0.192

8.1.4 CL-2 Push Mode Example Datasheet

General Notes/Physical Measurements

C

Notes

720x480 DV Converted to 640x480 square pixels.

"Left Cylinder" refers to the 'Smooth' boundary condition

"Right Cylinder" refers to the 'Pinning' boundary condition

The frame rate is (frames/s):

29.97

Disturbance Type:

Push

The pinning lip is:

Wet

Fluid Depth

(Measured from meniscus to bottom of cylinder)

Fluid depths measured at frame:

0

	Rep. Point 1	Rep. Point 2	SF
<i>x</i>	286	569	0.186374335
<i>y</i>	330.5	318	0.182265327
	Depth (px)	Depth (mm)	
Smooth	135	25.1605352	
Pinning	160	29.1624523	
Difference	25	4.00191701	



Physical Dimensions:

Smooth Cylinder (Left)

	<i>x</i> -pixel	<i>y</i> -pixel	Actual	SF (in/pixel)	SF (mm/pixel)
Bottom of Cylinder <i>P1</i>	184	398			
Bottom of Cylinder <i>P2</i>	388	398		SF0	
Difference	204	0	1.5	0.00735294	0.186764706
Midpoint (<i>X0,Y0</i>)	286	398			

Pinning Cylinder (Right)

Bottom of Cylinder <i>P1</i>	467	400			
Bottom of Pin <i>P2</i>	467	123		SF1	
Difference	0	277	2	0.00722022	0.183393502
Midpoint (<i>X1,Y1</i>)	467	261.5			

Smooth Cylinder (Left)

Top of Cylinder <i>P1</i>	182	82			
Top of Cylinder <i>P2</i>	388	82		SF2	
Difference	206	0	1.5	0.00728155	0.184951456
Midpoint (<i>X2,Y2</i>)	285	82			

Average 0.0072849 0.185036555

1	2	3	4	5	6	7	8	9
---	---	---	---	---	---	---	---	---

Input SF Constants

	a	b	c
Scale Factor (SF) constants (in/px):	-5.61576E-07	2.27688E-07	0.00742293
Scale Factor (SF) constants (mm/px):	-1.4264E-05	5.78327E-06	0.18854247

The following information is taken after the response settles at frame:

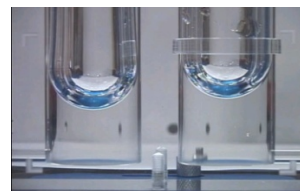
386

Fluid Depth

(Measured from meniscus to bottom of cylinder)

Fluid depths measured at frame: 386

	Rep. Point 1	Rep. Point 2	SF
x	176.5	459.5	0.185853646
y	333.5	319	0.185844799
	Depth (px)	Depth (mm)	
Smooth	133	24.7185349	
Pinning	162	30.1068574	
Difference	29	5.3883225	



Physical Dimensions:

Smooth Cylinder (Left)

	x -pixel	y -pixel	Actual	SF (in/pixel)	SF (mm/pixel)
Bottom of Cylinder P1	74	400			
Bottom of Cylinder P2	279	400		SF0	
Difference	205	0	1.5	0.00731707	0.185853659
Midpoint (X0,Y0)	176.5	400			

Pinning Cylinder (Right)

Bottom of Cylinder P1	357	399			
Bottom of Cylinder P2	562	401		SF1	
Difference	205	2	1.5	0.00731672	0.185844814
Midpoint (X1,Y1)	459.5	400			

Smooth Cylinder (Left)

Top of Cylinder P1	72	76			
Top of Cylinder P2	277	76		SF2	
Difference	205	0	1.5	0.00731707	0.185853659
Midpoint (X2,Y2)	174.5	76			

Average 0.00731696 0.18585071

Response SF Constants

	a	b	c
Scale Factor (SF) constants (in/px):	-1.23039E-09	7.59499E-12	0.00731729
Scale Factor (SF) constants (mm/px):	-3.12519E-08	1.92913E-10	0.1858591

1	2	3	4	5	6	7	8	9
---	---	---	---	---	---	---	---	---

Approximate Results

Input Amplitude (mm) 20.22956109

Smooth Cylinder (Left)

Period of Smooth Response (s): 2.29
Frequency of Smooth Response (1/s): 0.436681223
Settling Time of Smooth Response (s): 8.8

Pinning Cylinder (Right) **Wet**

Period of Pinned Response (s): 2.17
Frequency of Pinned Response (1/s): 0.460829493
Settling Time of Pinned Response (s): 9.3

Additional Notes

The right side of pinning cylinder is out of view prior to the input.
Dimensions are taken along the left side from the bottom of cylinder to the bottom of pin.

1	2	3	4	5	6	7	8	9	
---	---	---	---	---	---	---	---	---	--

101
102
103
104
105
106
107
108
109
110
111
112
113
114
115
116
117
118
119
120
121
122
123
124
125
126
127
128
129
130
131
132
133
134
135
136
137
138
139
140
141
142
143
144
145
146
147
148
149
150

Input & Response Notes

Input Notes

Tracking is started at frame:

0

The input data was tracked:

at the bottom of the left cylinder.

Response Notes

Smooth Cylinder (Left)

The response with overlap starts at frame:

66

The AOI is tracked at 1/4 the diameter from the:

Right

at frame

386

1/4 the diameter is at the point:

(227, 249)

Pinning Cylinder (Right)

The response with overlap starts at frame:

66

The AOI is tracked at 1/4 the diameter from the:

Right

at frame

386

1/4 the diameter is at the point:

(511, 221)

Additional Notes

Labels

Push Input

Smooth Response-Push

Pinned Response-Push

Response Comparison-Push

1	2	3	4	5	6	7	8	9
---	---	---	---	---	---	---	---	---

1
2
3
4
5
6
7
8
9
10
11
12
13
14
15
16
17
18
19
20
21
22
23
24
25
26
27
28
29
30
31
32
33
34
35
36
37
38
39
40
41
42
43
44
45
46
47
48
49
50

CL2_Exp12_12-20-05_OB_DVCam_Ops_ID01_BM_5900-5913_P_VDUB.avi

Scale Factor - user units: 1.00000 image units: 1.00000

Aoi 1: WholeImage

Aoi 2: ThresholdTracking

Abs Frame	Filename	Rel Frame	x-px	y-px	Time (s)	x-Scaled (mm)	0'd x-Scaled (mm)	SF in/px
1	CL2....5900-5913...VDUB ->	1	387	268	0.033	71.429	0.000	0.185
2	CL2....5900-5913...VDUB ->	2	387	268	0.067	71.429	0.000	0.185
3	CL2....5900-5913...VDUB ->	3	387	268	0.100	71.429	0.000	0.185
4	CL2....5900-5913...VDUB ->	4	387	268	0.133	71.429	0.000	0.185
5	CL2....5900-5913...VDUB ->	5	387	268	0.167	71.429	0.000	0.185
6	CL2....5900-5913...VDUB ->	6	387	268	0.200	71.429	0.000	0.185
7	CL2....5900-5913...VDUB ->	7	387	268	0.234	71.429	0.000	0.185
8	CL2....5900-5913...VDUB ->	8	387	268	0.267	71.429	0.000	0.185
9	CL2....5900-5913...VDUB ->	9	387	268	0.300	71.429	0.000	0.185
10	CL2....5900-5913...VDUB ->	10	387	268	0.334	71.429	0.000	0.185
11	CL2....5900-5913...VDUB ->	11	387	268	0.367	71.429	0.000	0.185
12	CL2....5900-5913...VDUB ->	12	387	268	0.400	71.429	0.000	0.185
13	CL2....5900-5913...VDUB ->	13	387	268	0.434	71.429	0.000	0.185
14	CL2....5900-5913...VDUB ->	14	387	268	0.467	71.429	0.000	0.185
15	CL2....5900-5913...VDUB ->	15	387	268	0.501	71.429	0.000	0.185
16	CL2....5900-5913...VDUB ->	16	387	268	0.534	71.429	0.000	0.185
17	CL2....5900-5913...VDUB ->	17	387	268	0.567	71.429	0.000	0.185
18	CL2....5900-5913...VDUB ->	18	387	268	0.601	71.429	0.000	0.185
19	CL2....5900-5913...VDUB ->	19	388	268	0.634	71.608	0.179	0.185
20	CL2....5900-5913...VDUB ->	20	388	268	0.667	71.608	0.179	0.185
21	CL2....5900-5913...VDUB ->	21	388	268	0.701	71.608	0.179	0.185
22	CL2....5900-5913...VDUB ->	22	388	268	0.734	71.608	0.179	0.185
23	CL2....5900-5913...VDUB ->	23	388	268	0.767	71.608	0.179	0.185
24	CL2....5900-5913...VDUB ->	24	387	268	0.801	71.429	0.000	0.185
25	CL2....5900-5913...VDUB ->	25	387	268	0.834	71.429	0.000	0.185
26	CL2....5900-5913...VDUB ->	26	386	268	0.868	71.250	-0.179	0.185
27	CL2....5900-5913...VDUB ->	27	386	268	0.901	71.250	-0.179	0.185
28	CL2....5900-5913...VDUB ->	28	386	268	0.934	71.250	-0.179	0.185
29	CL2....5900-5913...VDUB ->	29	386	268	0.968	71.250	-0.179	0.185
30	CL2....5900-5913...VDUB ->	30	386	268	1.001	71.250	-0.179	0.185
31	CL2....5900-5913...VDUB ->	31	386	268	1.034	71.250	-0.179	0.185
32	CL2....5900-5913...VDUB ->	32	386	268	1.068	71.250	-0.179	0.185
33	CL2....5900-5913...VDUB ->	33	387	268	1.101	71.429	0.000	0.185
34	CL2....5900-5913...VDUB ->	34	387	268	1.134	71.429	0.000	0.185
35	CL2....5900-5913...VDUB ->	35	387	268	1.168	71.429	0.000	0.185
36	CL2....5900-5913...VDUB ->	36	387	268	1.201	71.429	0.000	0.185
37	CL2....5900-5913...VDUB ->	37	386	268	1.235	71.250	-0.179	0.185
38	CL2....5900-5913...VDUB ->	38	386	268	1.268	71.250	-0.179	0.185
39	CL2....5900-5913...VDUB ->	39	386	268	1.301	71.250	-0.179	0.185
40	CL2....5900-5913...VDUB ->	40	386	268	1.335	71.250	-0.179	0.185
41	CL2....5900-5913...VDUB ->	41	386	268	1.368	71.250	-0.179	0.185
42	CL2....5900-5913...VDUB ->	42	386	268	1.401	71.250	-0.179	0.185
43	CL2....5900-5913...VDUB ->	43	386	268	1.435	71.250	-0.179	0.185
44	CL2....5900-5913...VDUB ->	44	385	268	1.468	71.071	-0.358	0.185

CL2_Exp12_12-20-05_OB_DVCam_Ops_ID01_BM_5900-5913_P_VDUB.avi

Scale Factor - user units: 1.00000 image units: 1.00000

Aoi 1: WholeImage

Aoi 2: ThresholdTracking

Abs Frame	Filename	Rel Frame	x-px	y-px	Time (s)	x-Scaled (mm)	0'd x-Scaled (mm)	SF in/px
1	CL2.....5900-5913...VDUB ->	66	213	249	2.202	39.587	-2.602	0.186
2	CL2.....5900-5913...VDUB ->	67	223	249	2.236	41.445	-0.743	0.186
3	CL2.....5900-5913...VDUB ->	68	231	249	2.269	42.932	0.743	0.186
4	CL2.....5900-5913...VDUB ->	69	237	249	2.302	44.047	1.858	0.186
5	CL2.....5900-5913...VDUB ->	70	239	249	2.336	44.419	2.230	0.186
6	CL2.....5900-5913...VDUB ->	71	243	249	2.369	45.162	2.974	0.186
7	CL2.....5900-5913...VDUB ->	72	246	249	2.402	45.719	3.531	0.186
8	CL2.....5900-5913...VDUB ->	73	247	249	2.436	45.905	3.717	0.186
9	CL2.....5900-5913...VDUB ->	74	250	249	2.469	46.463	4.274	0.186
10	CL2.....5900-5913...VDUB ->	75	252	249	2.503	46.835	4.646	0.186
11	CL2.....5900-5913...VDUB ->	76	255	249	2.536	47.392	5.204	0.186
12	CL2.....5900-5913...VDUB ->	77	256	249	2.569	47.578	5.389	0.186
13	CL2.....5900-5913...VDUB ->	78	259	249	2.603	48.135	5.947	0.186
14	CL2.....5900-5913...VDUB ->	79	262	249	2.636	48.693	6.505	0.186
15	CL2.....5900-5913...VDUB ->	80	263	249	2.669	48.879	6.690	0.186
16	CL2.....5900-5913...VDUB ->	81	263	249	2.703	48.879	6.690	0.186
17	CL2.....5900-5913...VDUB ->	82	263	249	2.736	48.879	6.690	0.186
18	CL2.....5900-5913...VDUB ->	83	263	249	2.769	48.879	6.690	0.186
19	CL2.....5900-5913...VDUB ->	84	263	249	2.803	48.879	6.690	0.186
20	CL2.....5900-5913...VDUB ->	85	263	249	2.836	48.879	6.690	0.186
21	CL2.....5900-5913...VDUB ->	86	262	249	2.870	48.693	6.505	0.186
22	CL2.....5900-5913...VDUB ->	87	260	249	2.903	48.321	6.133	0.186
23	CL2.....5900-5913...VDUB ->	88	259	249	2.936	48.135	5.947	0.186
24	CL2.....5900-5913...VDUB ->	89	258	249	2.970	47.950	5.761	0.186
25	CL2.....5900-5913...VDUB ->	90	257	249	3.003	47.764	5.575	0.186
26	CL2.....5900-5913...VDUB ->	91	255	249	3.036	47.392	5.204	0.186
27	CL2.....5900-5913...VDUB ->	92	255	249	3.070	47.392	5.204	0.186
28	CL2.....5900-5913...VDUB ->	93	254	249	3.103	47.206	5.018	0.186
29	CL2.....5900-5913...VDUB ->	94	252	249	3.136	46.835	4.646	0.186
30	CL2.....5900-5913...VDUB ->	95	250	249	3.170	46.463	4.274	0.186
31	CL2.....5900-5913...VDUB ->	96	248	249	3.203	46.091	3.903	0.186
32	CL2.....5900-5913...VDUB ->	97	247	249	3.237	45.905	3.717	0.186
33	CL2.....5900-5913...VDUB ->	98	246	249	3.270	45.719	3.531	0.186
34	CL2.....5900-5913...VDUB ->	99	244	249	3.303	45.348	3.159	0.186
35	CL2.....5900-5913...VDUB ->	100	241	249	3.337	44.790	2.602	0.186
36	CL2.....5900-5913...VDUB ->	101	239	249	3.370	44.419	2.230	0.186
37	CL2.....5900-5913...VDUB ->	102	238	249	3.403	44.233	2.044	0.186
38	CL2.....5900-5913...VDUB ->	103	236	249	3.437	43.861	1.673	0.186
39	CL2.....5900-5913...VDUB ->	104	234	249	3.470	43.489	1.301	0.186
40	CL2.....5900-5913...VDUB ->	105	232	249	3.504	43.118	0.929	0.186
41	CL2.....5900-5913...VDUB ->	106	231	249	3.537	42.932	0.743	0.186
42	CL2.....5900-5913...VDUB ->	107	230	249	3.570	42.746	0.558	0.186
43	CL2.....5900-5913...VDUB ->	108	229	249	3.604	42.560	0.372	0.186
44	CL2.....5900-5913...VDUB ->	109	227	249	3.637	42.188	0.000	0.186

CL2_Exp12_12-20-05_OB_DVCam_Ops_ID01_BM_5900-5913_P_VDUB.avi

Scale Factor - user units: 1.00000 image units: 1.00000

Aoi 1: WholeImage

Aoi 2: ThresholdTracking

Abs Frame	Filename	Rel Frame	x-px	y-px	Time (s)	x-Scaled (mm)	O'd x-Scaled (mm)	SF in/px
1	CL2....5900-5913...VDUB ->	66	501	221	2.202	93.108	-1.858	0.186
2	CL2....5900-5913...VDUB ->	67	508	221	2.236	94.408	-0.557	0.186
3	CL2....5900-5913...VDUB ->	68	509	221	2.269	94.594	-0.372	0.186
4	CL2....5900-5913...VDUB ->	69	510	221	2.302	94.780	-0.186	0.186
5	CL2....5900-5913...VDUB ->	70	512	221	2.336	95.152	0.186	0.186
6	CL2....5900-5913...VDUB ->	71	513	221	2.369	95.338	0.372	0.186
7	CL2....5900-5913...VDUB ->	72	517	221	2.402	96.081	1.115	0.186
8	CL2....5900-5913...VDUB ->	73	520	221	2.436	96.638	1.672	0.186
9	CL2....5900-5913...VDUB ->	74	522	221	2.469	97.010	2.044	0.186
10	CL2....5900-5913...VDUB ->	75	530	221	2.503	98.497	3.531	0.186
11	CL2....5900-5913...VDUB ->	76	535	221	2.536	99.426	4.460	0.186
12	CL2....5900-5913...VDUB ->	77	538	221	2.569	99.983	5.017	0.186
13	CL2....5900-5913...VDUB ->	78	541	221	2.603	100.541	5.575	0.186
14	CL2....5900-5913...VDUB ->	79	543	221	2.636	100.912	5.946	0.186
15	CL2....5900-5913...VDUB ->	80	545	221	2.669	101.284	6.318	0.186
16	CL2....5900-5913...VDUB ->	81	547	221	2.703	101.656	6.690	0.186
17	CL2....5900-5913...VDUB ->	82	547	221	2.736	101.656	6.690	0.186
18	CL2....5900-5913...VDUB ->	83	548	221	2.769	101.841	6.876	0.186
19	CL2....5900-5913...VDUB ->	84	549	221	2.803	102.027	7.061	0.186
20	CL2....5900-5913...VDUB ->	85	550	221	2.836	102.213	7.247	0.186
21	CL2....5900-5913...VDUB ->	86	550	221	2.870	102.213	7.247	0.186
22	CL2....5900-5913...VDUB ->	87	550	221	2.903	102.213	7.247	0.186
23	CL2....5900-5913...VDUB ->	88	550	221	2.936	102.213	7.247	0.186
24	CL2....5900-5913...VDUB ->	89	550	221	2.970	102.213	7.247	0.186
25	CL2....5900-5913...VDUB ->	90	549	221	3.003	102.027	7.061	0.186
26	CL2....5900-5913...VDUB ->	91	548	221	3.036	101.841	6.876	0.186
27	CL2....5900-5913...VDUB ->	92	547	221	3.070	101.656	6.690	0.186
28	CL2....5900-5913...VDUB ->	93	547	221	3.103	101.656	6.690	0.186
29	CL2....5900-5913...VDUB ->	94	545	221	3.136	101.284	6.318	0.186
30	CL2....5900-5913...VDUB ->	95	543	221	3.170	100.912	5.946	0.186
31	CL2....5900-5913...VDUB ->	96	541	221	3.203	100.541	5.575	0.186
32	CL2....5900-5913...VDUB ->	97	538	221	3.237	99.983	5.017	0.186
33	CL2....5900-5913...VDUB ->	98	535	221	3.270	99.426	4.460	0.186
34	CL2....5900-5913...VDUB ->	99	533	221	3.303	99.054	4.088	0.186
35	CL2....5900-5913...VDUB ->	100	531	221	3.337	98.682	3.717	0.186
36	CL2....5900-5913...VDUB ->	101	528	221	3.370	98.125	3.159	0.186
37	CL2....5900-5913...VDUB ->	102	525	221	3.403	97.567	2.602	0.186
38	CL2....5900-5913...VDUB ->	103	520	221	3.437	96.638	1.672	0.186
39	CL2....5900-5913...VDUB ->	104	517	221	3.470	96.081	1.115	0.186
40	CL2....5900-5913...VDUB ->	105	514	221	3.504	95.523	0.557	0.186
41	CL2....5900-5913...VDUB ->	106	510	221	3.537	94.780	-0.186	0.186
42	CL2....5900-5913...VDUB ->	107	508	221	3.570	94.408	-0.557	0.186
43	CL2....5900-5913...VDUB ->	108	505	221	3.604	93.851	-1.115	0.186
44	CL2....5900-5913...VDUB ->	109	503	221	3.637	93.479	-1.487	0.186

Chapter 9

Appendix: Additional Vane Gap Images

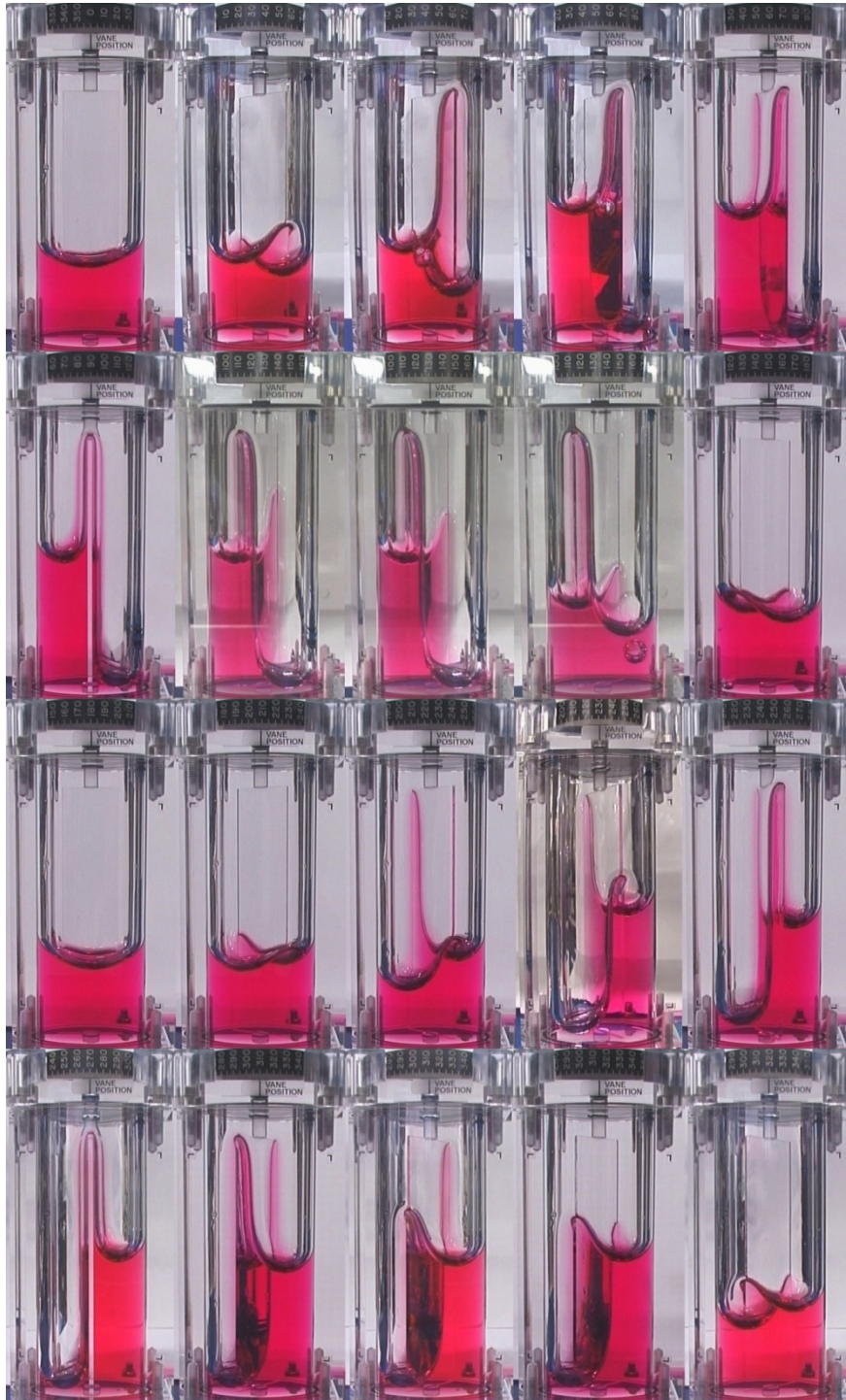


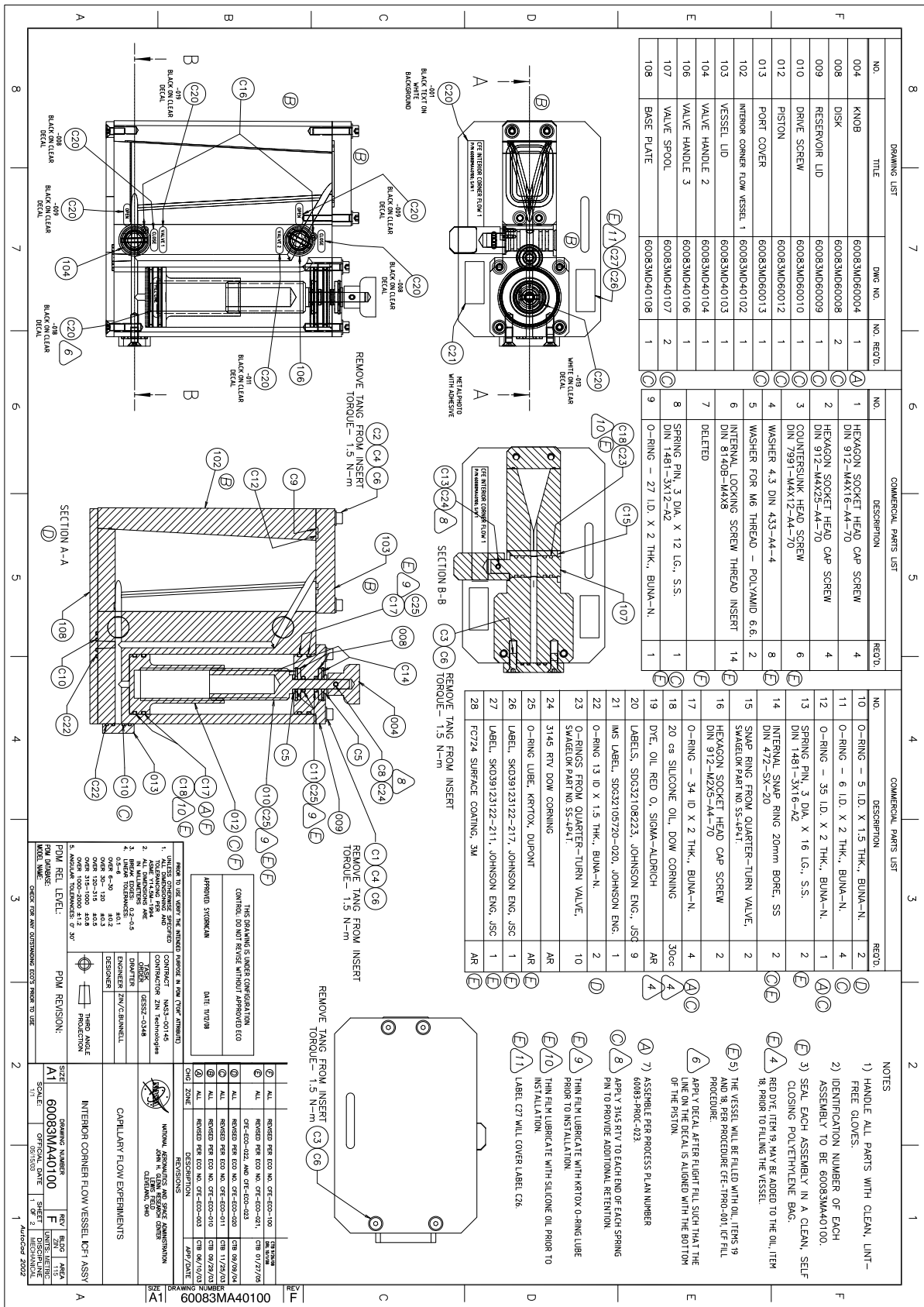
Figure 9.1: Receding and advancing bulk menisci for $\phi_{vd} = 90^\circ$.

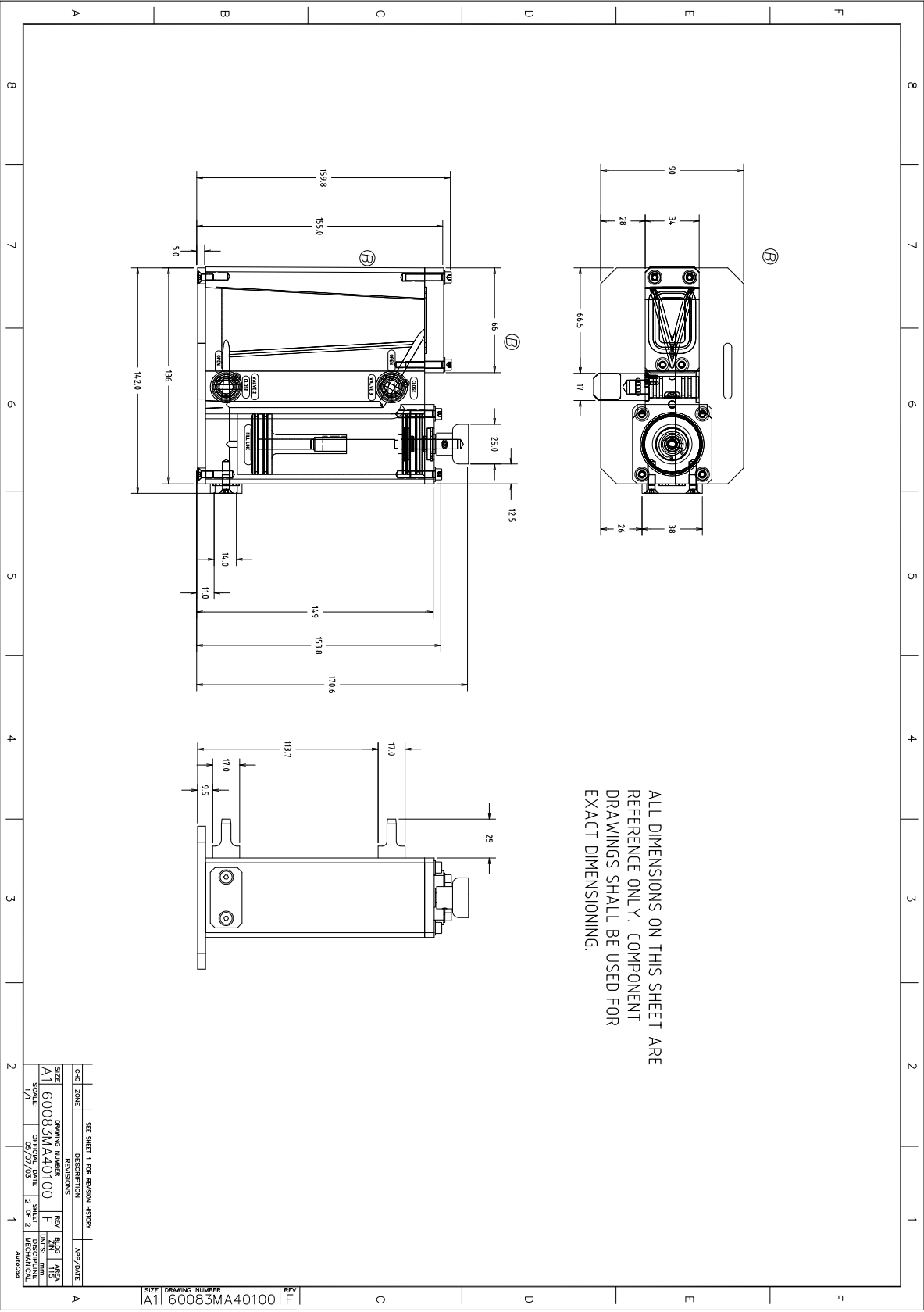


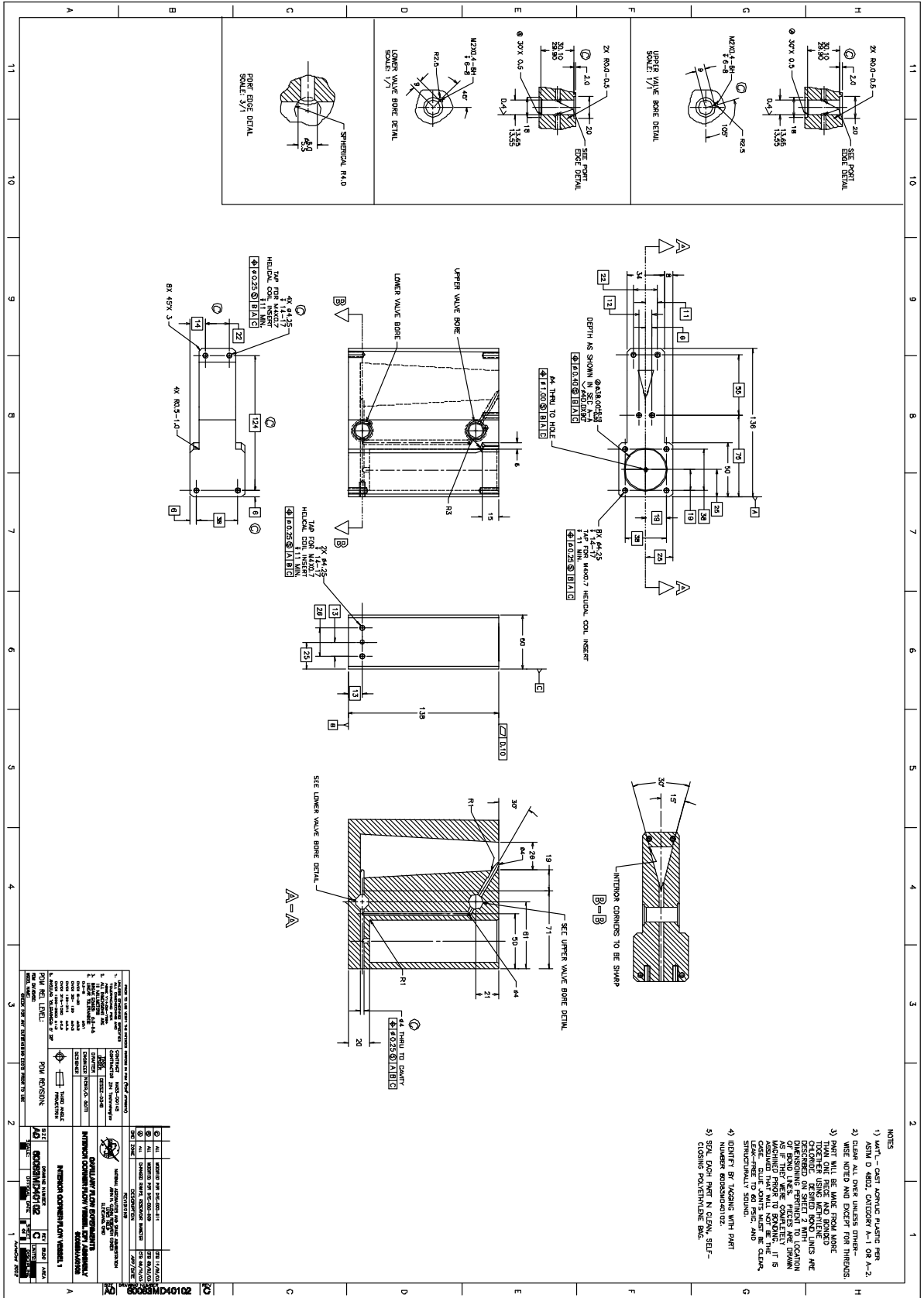
Figure 9.2: Receding and advancing bulk menisci for $\phi_{vd} = 90^\circ$.

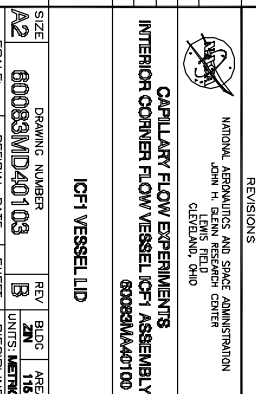
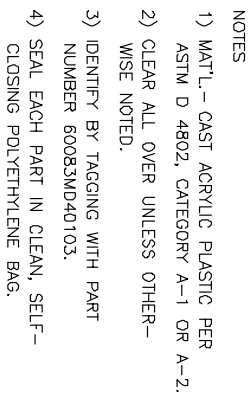
Chapter 10


Appendix: Complete CFE Design Drawings



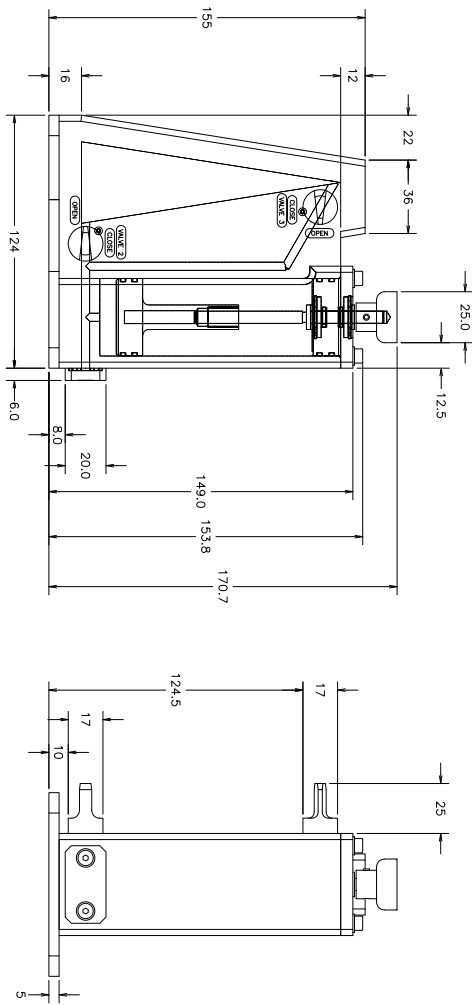
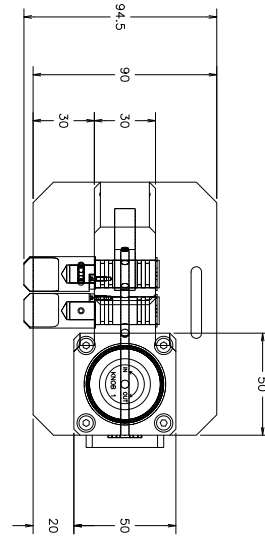




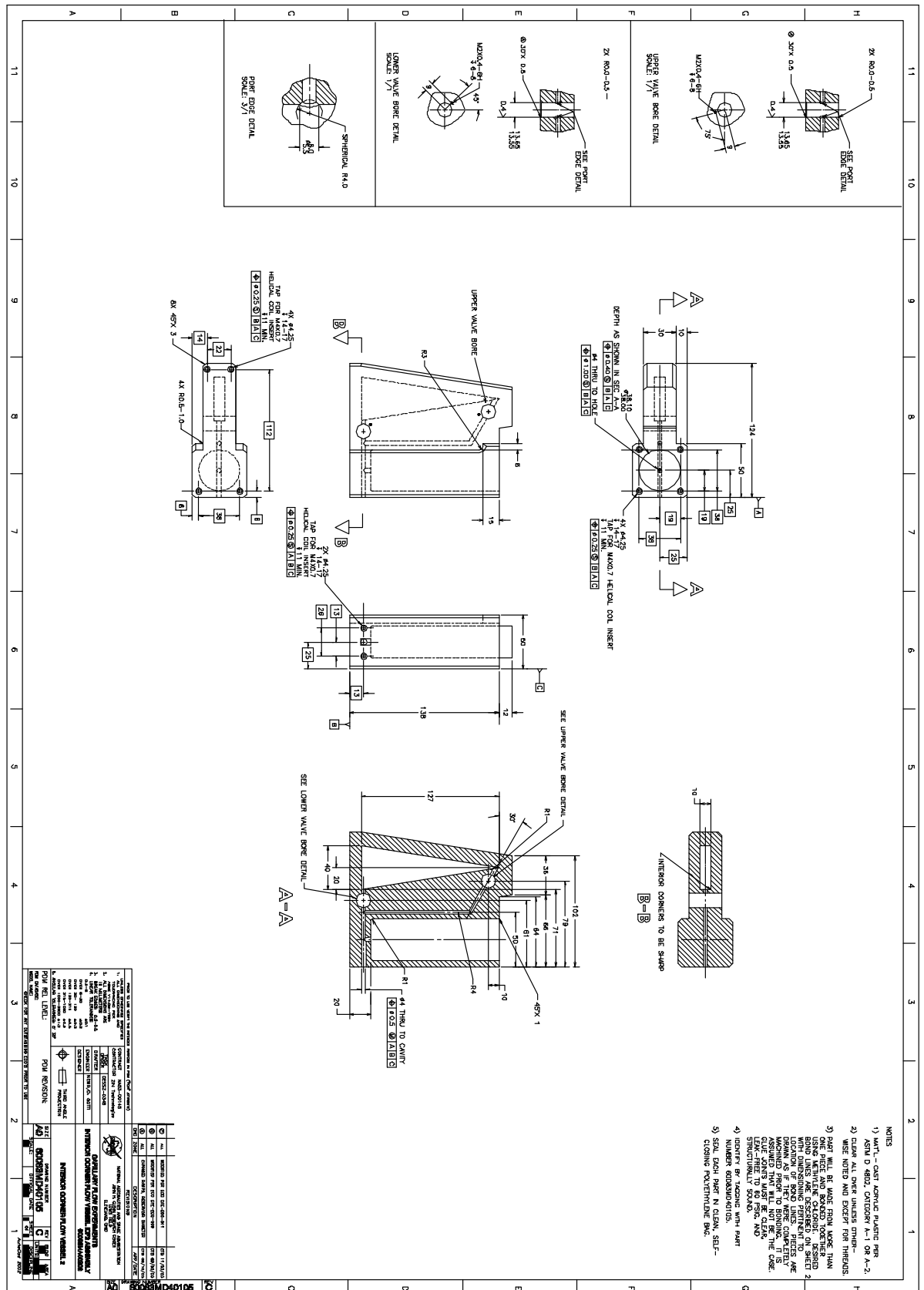


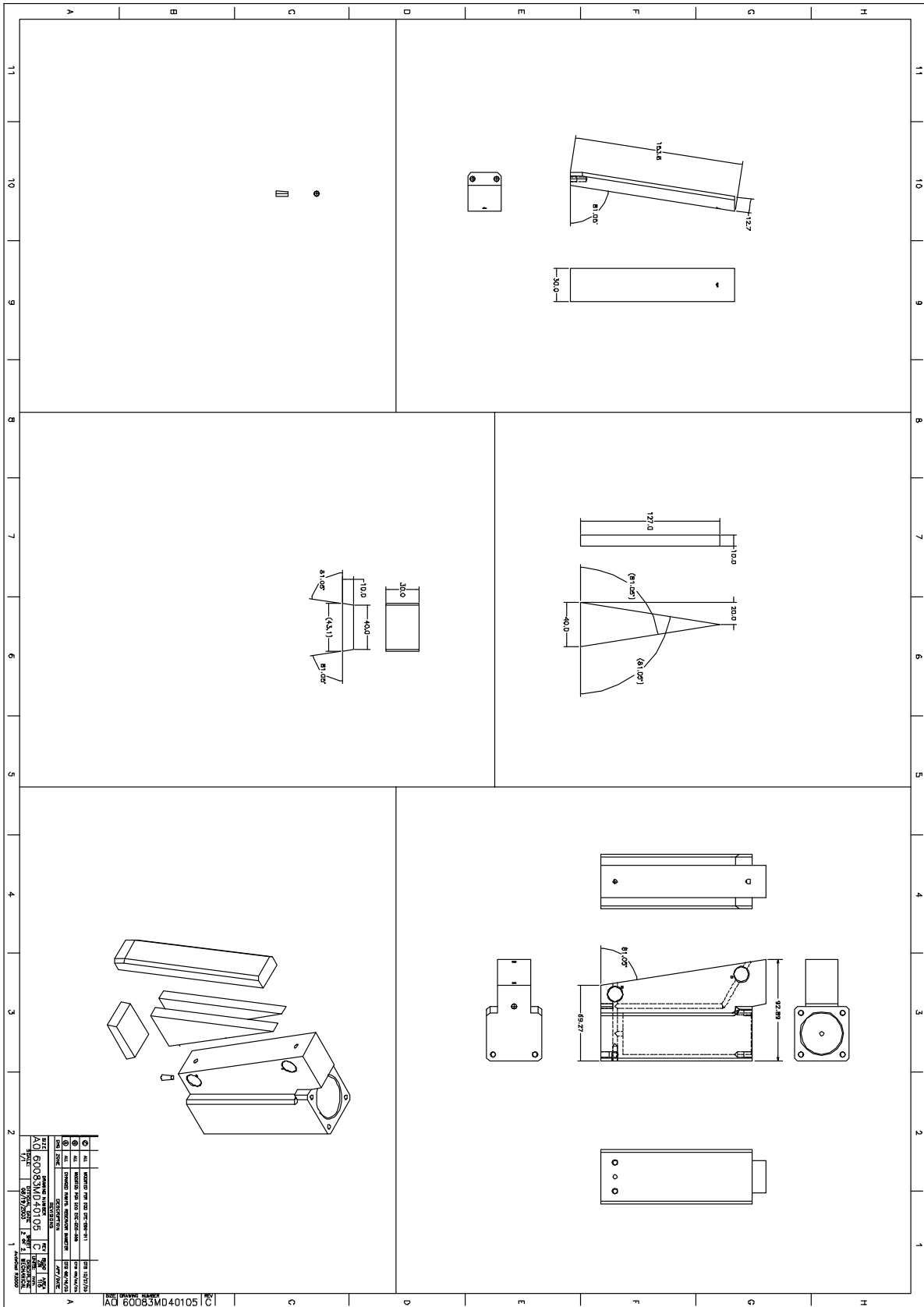
		NATIONAL AERONAUTICS AND SPACE ADMINISTRATION JOHN H. GLEN RESEARCH CENTER WASHINGTON, D.C. 20546-0001	
REVISIONS			
CAPILLARY FLOW EXPERIMENTS			
INTERIOR CORNER FLOW VESSEL ICFI ASSEMBLY			
82083MD401D			
ICFI VESSEL, LID			
SIZE	DRAWING NUMBER	REV	AREAS
A2	80083MD40103	B	2N 116
SCALE:	OFFICIAL DATE	SHEET	UNITS
1/1	8/8/80	1 of 1	DISCIPLINE
			MEDICAL

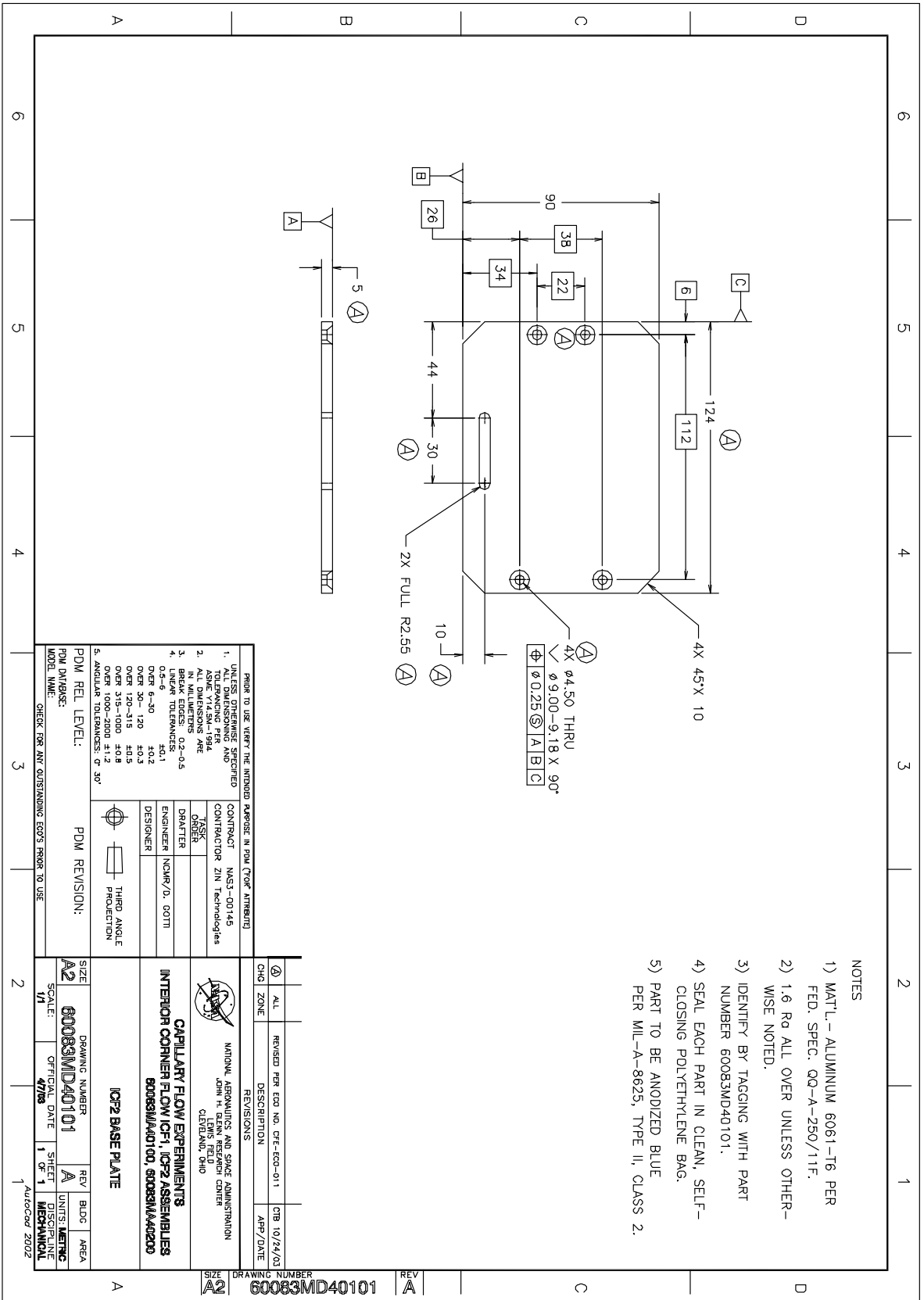
164

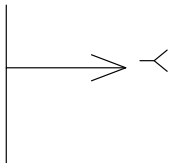
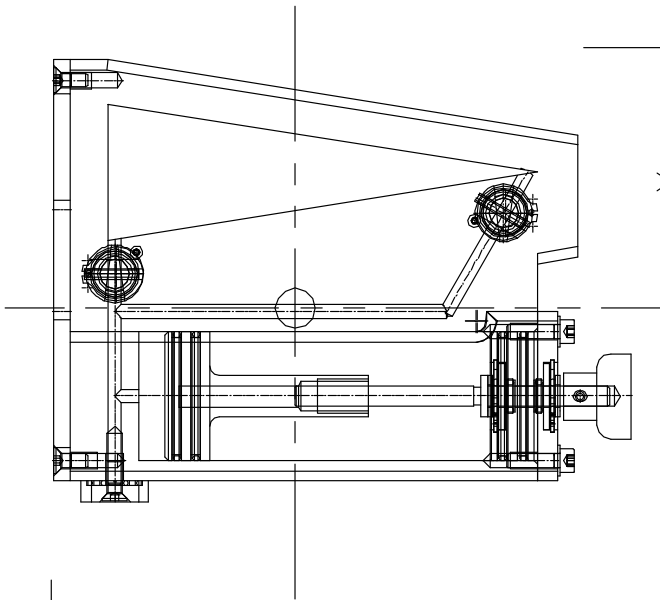
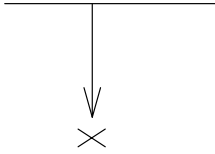
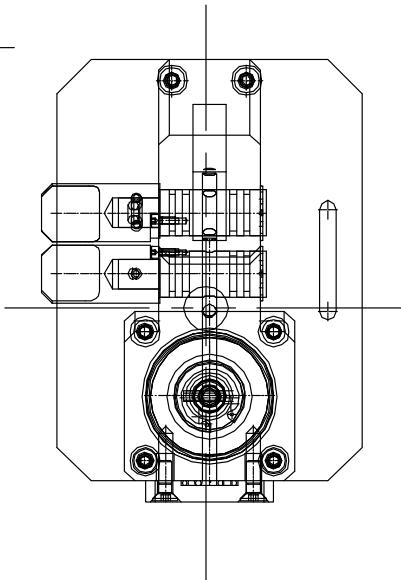


	SEE SHEET 1 FOR REVISION HISTORY	APP. DATE
CHG. ZONE	DESCRIPTION	
REVISIONS		
SIZE	DRAWING NUMBER	REV.
A1	60083M/A40200	D
SCALE:	OFFICIAL DATE	SHEET
1/1	05/07/03	2 OF 2
		DISCIPLINE
		MECHANICAL
		UNITS: mm
		PLD. AREA
		ZIN. 115









60083MA40200

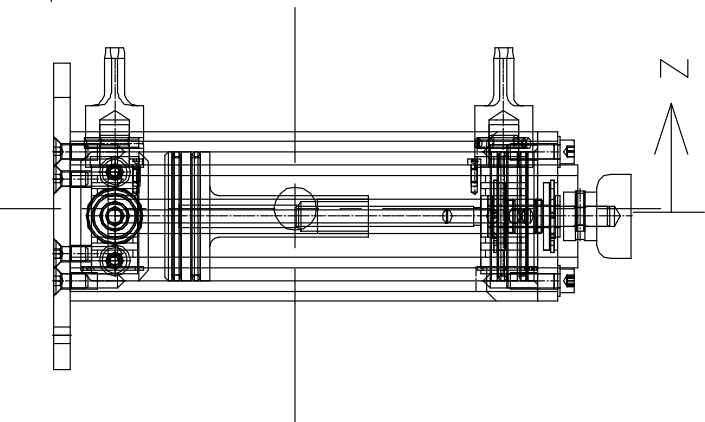
CENTER OF GRAVITY IS AT

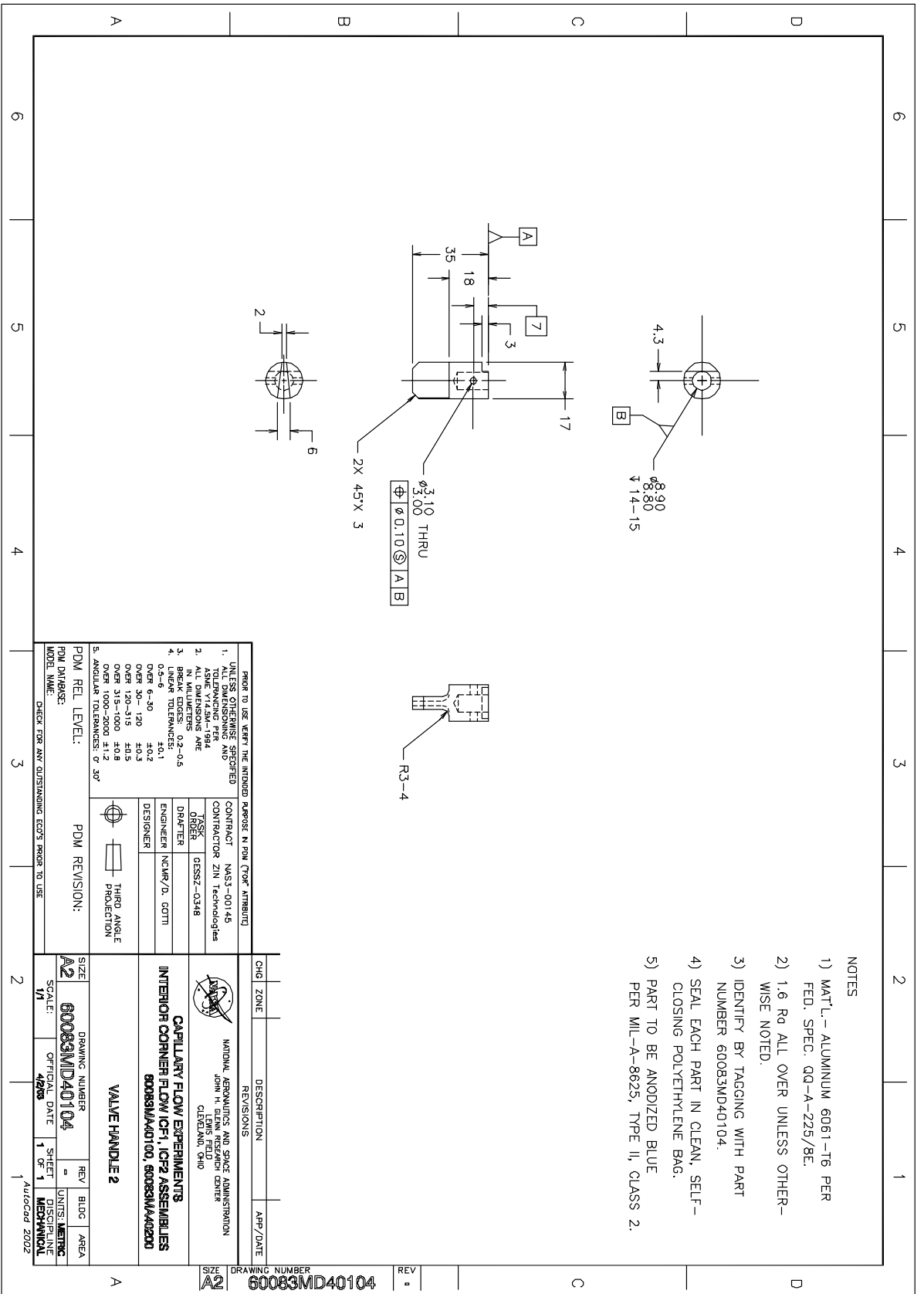
X = 72.67mm

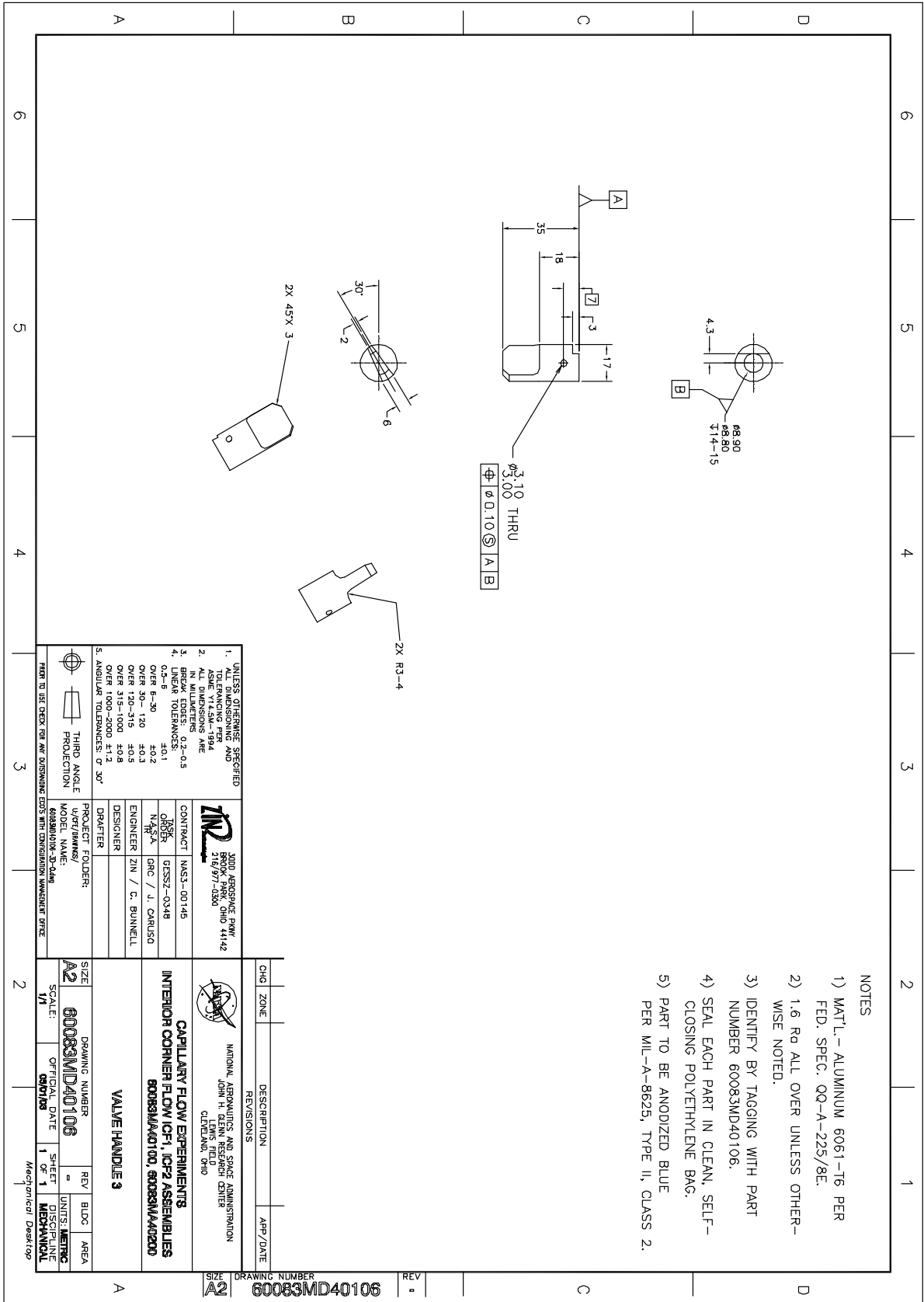
Y = 71.44mm

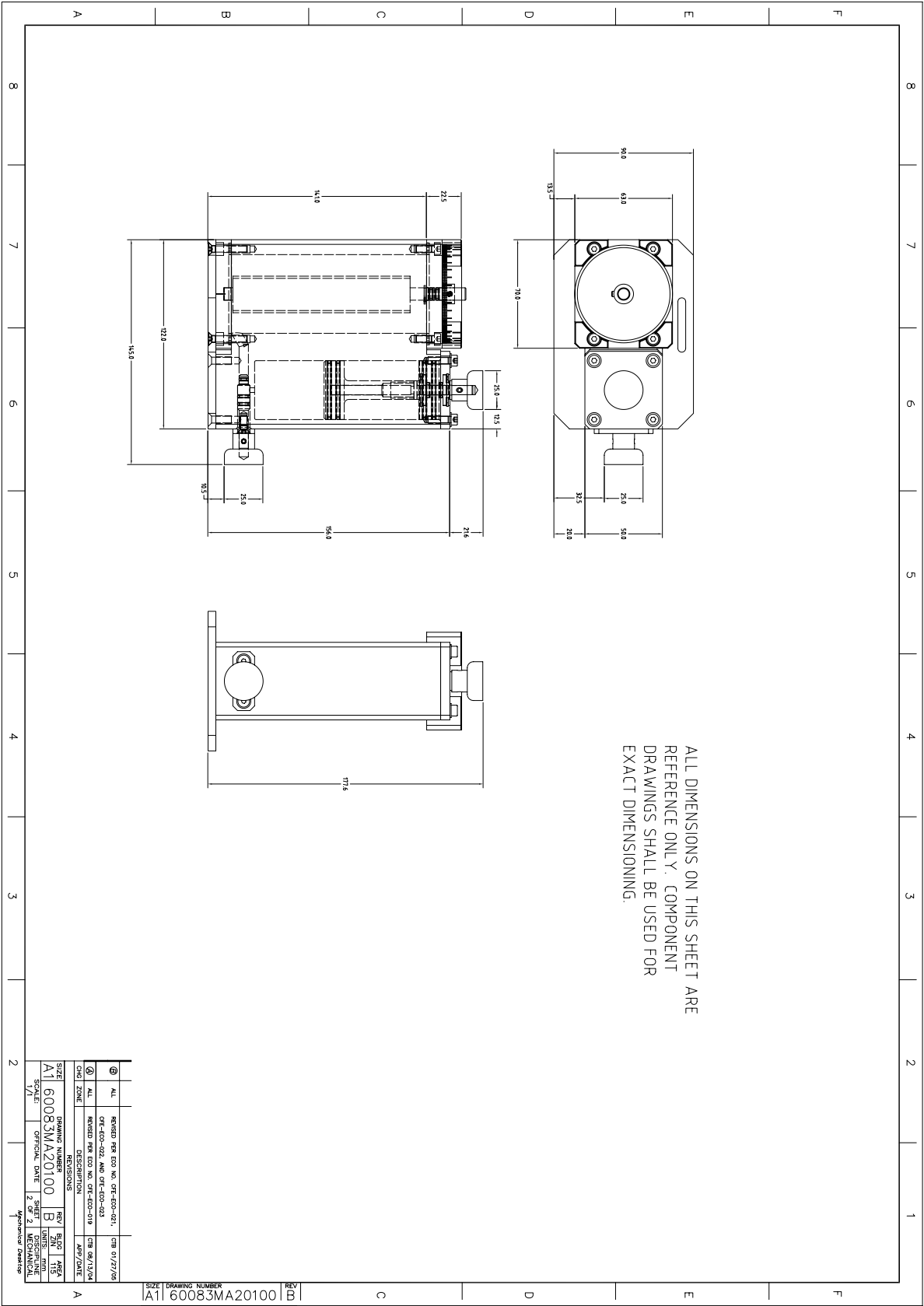
Z = 0.96mm

mass = 929 grams



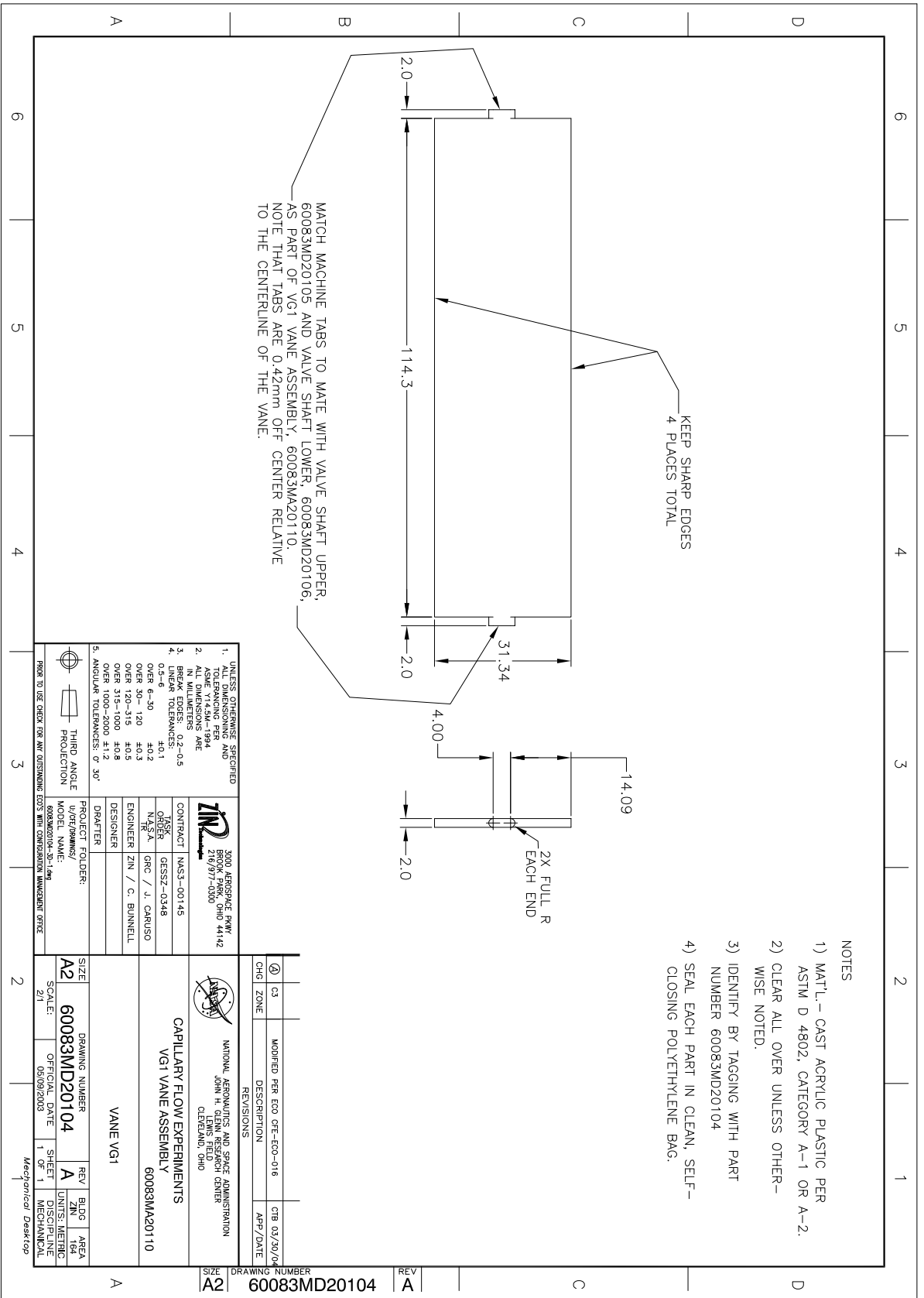




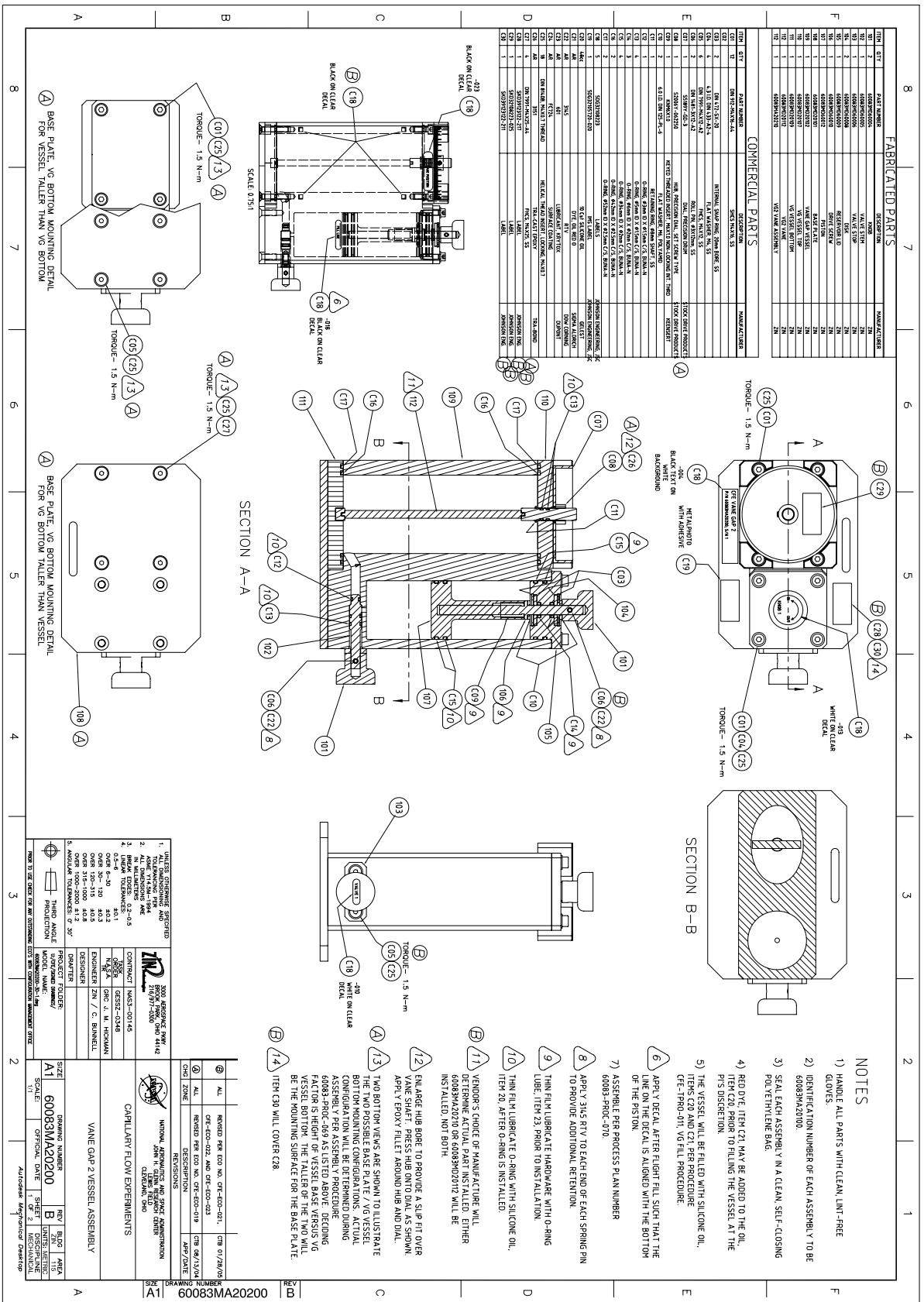


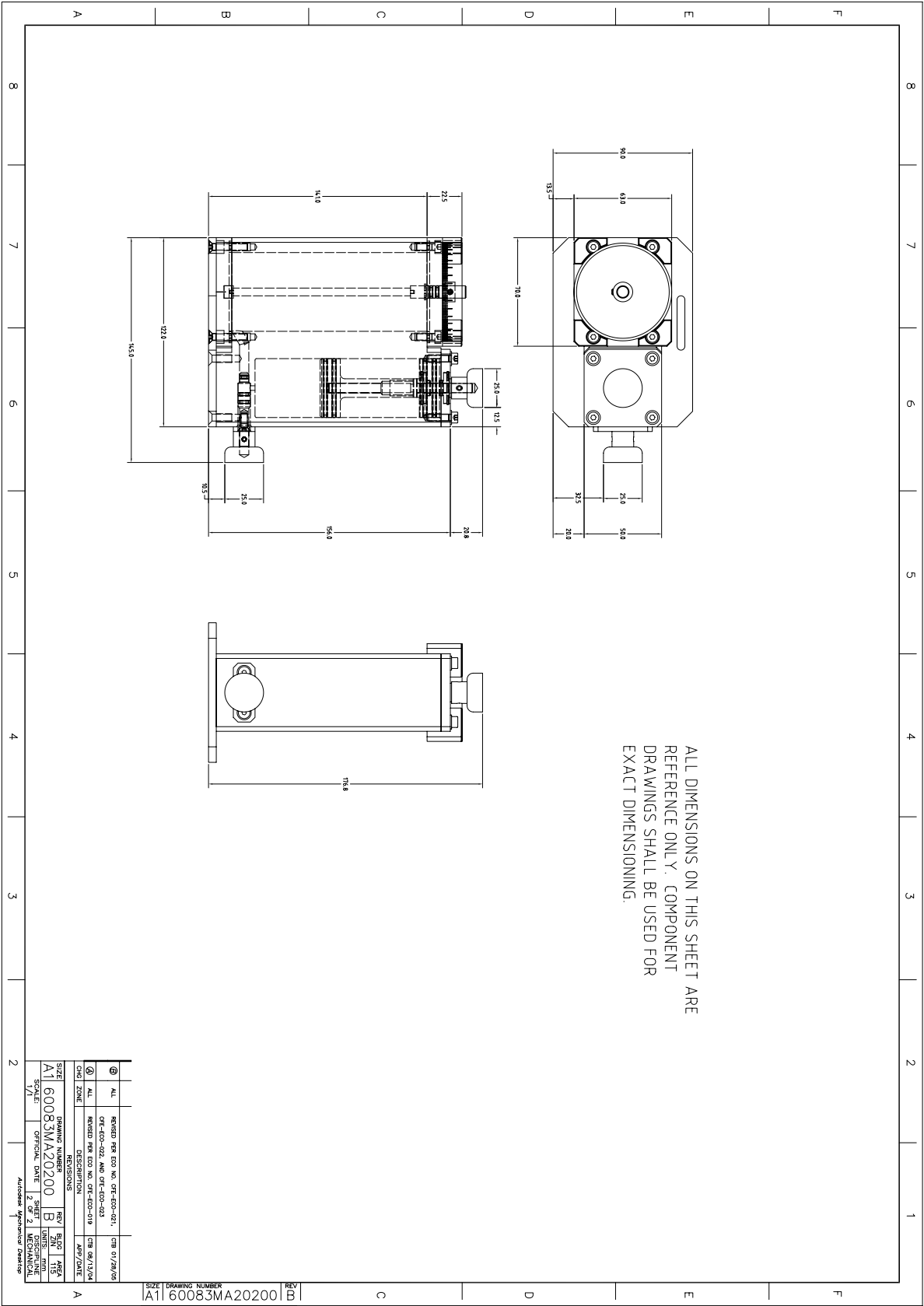
③	HL	WATER PUMP CO. NO. CR-400-001	CR 5/27/00
④	HL	CR-400-002 AND CR-400-003	
⑤	HL	WATER PUMP CO. NO. CR-400-019	CR 8/13/04
REVISIONS			
SIZE	DRAWING NUMBER	REV	DATE
A1	60083MA20100	B	1/25/01
SCALE	OFFICIAL DATE	UNITS	MM
1/1	2/2/01	2	MECHANICAL

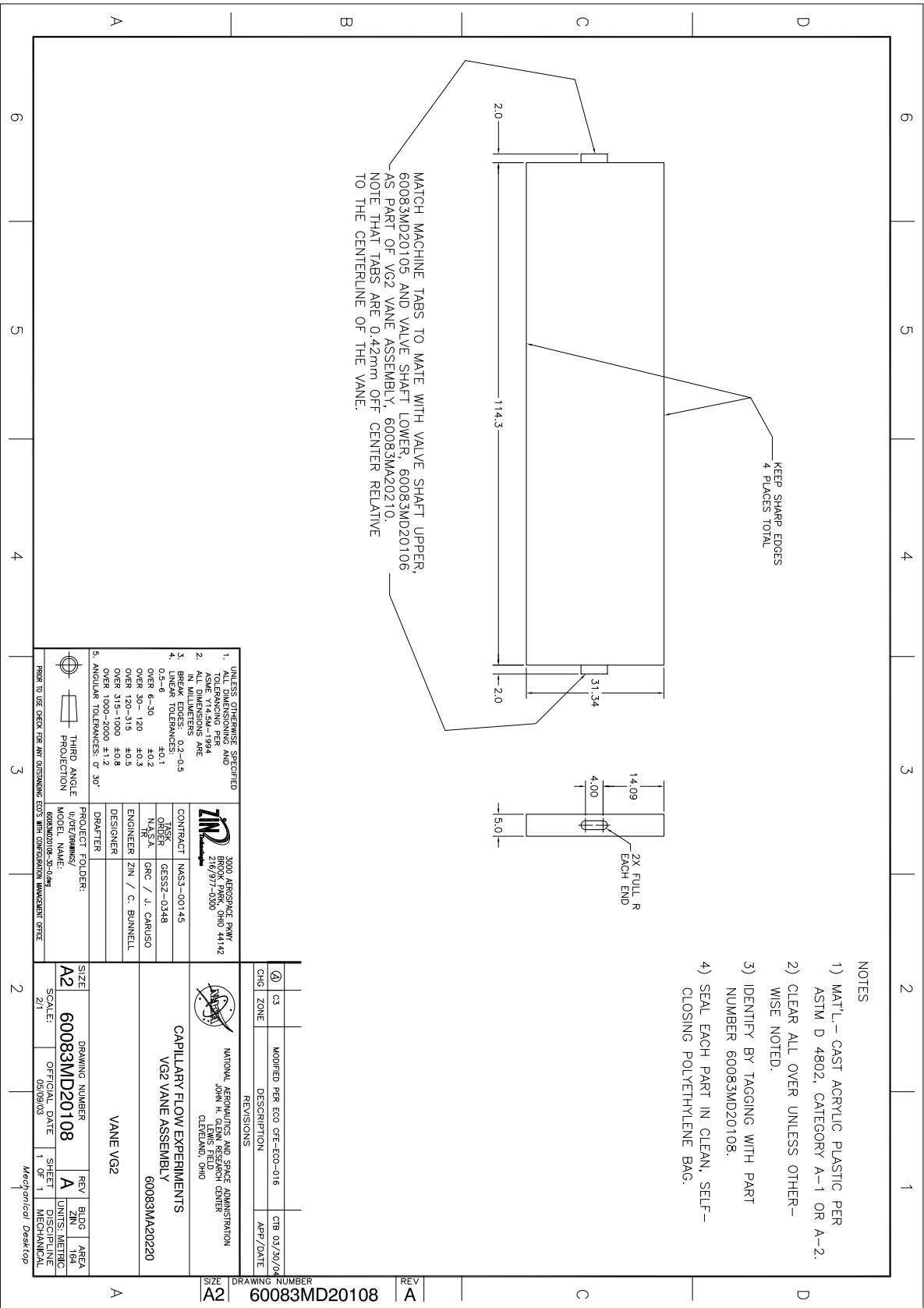
SIZE DRAWING NUMBER
A1 60083MA20100

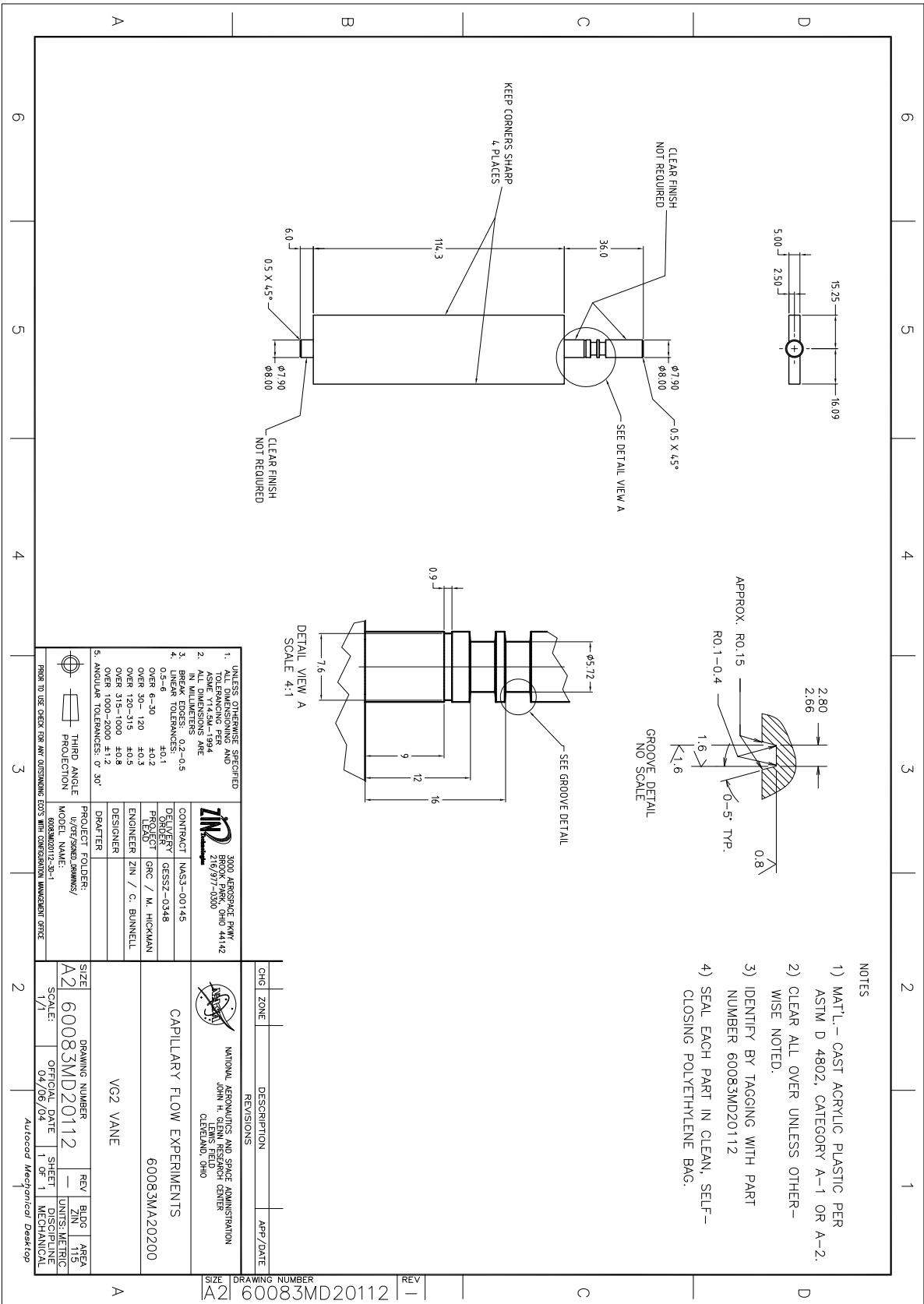


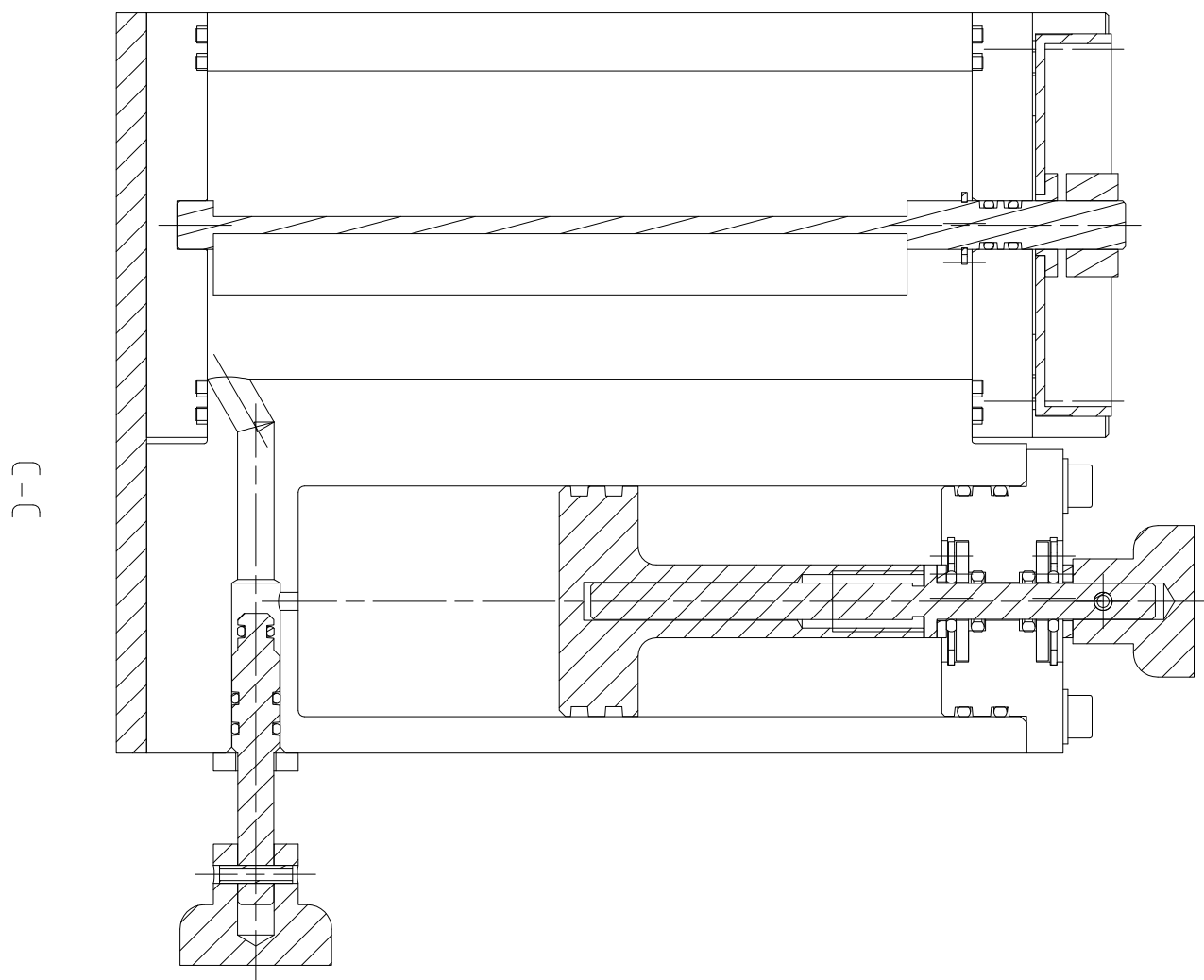
- 175



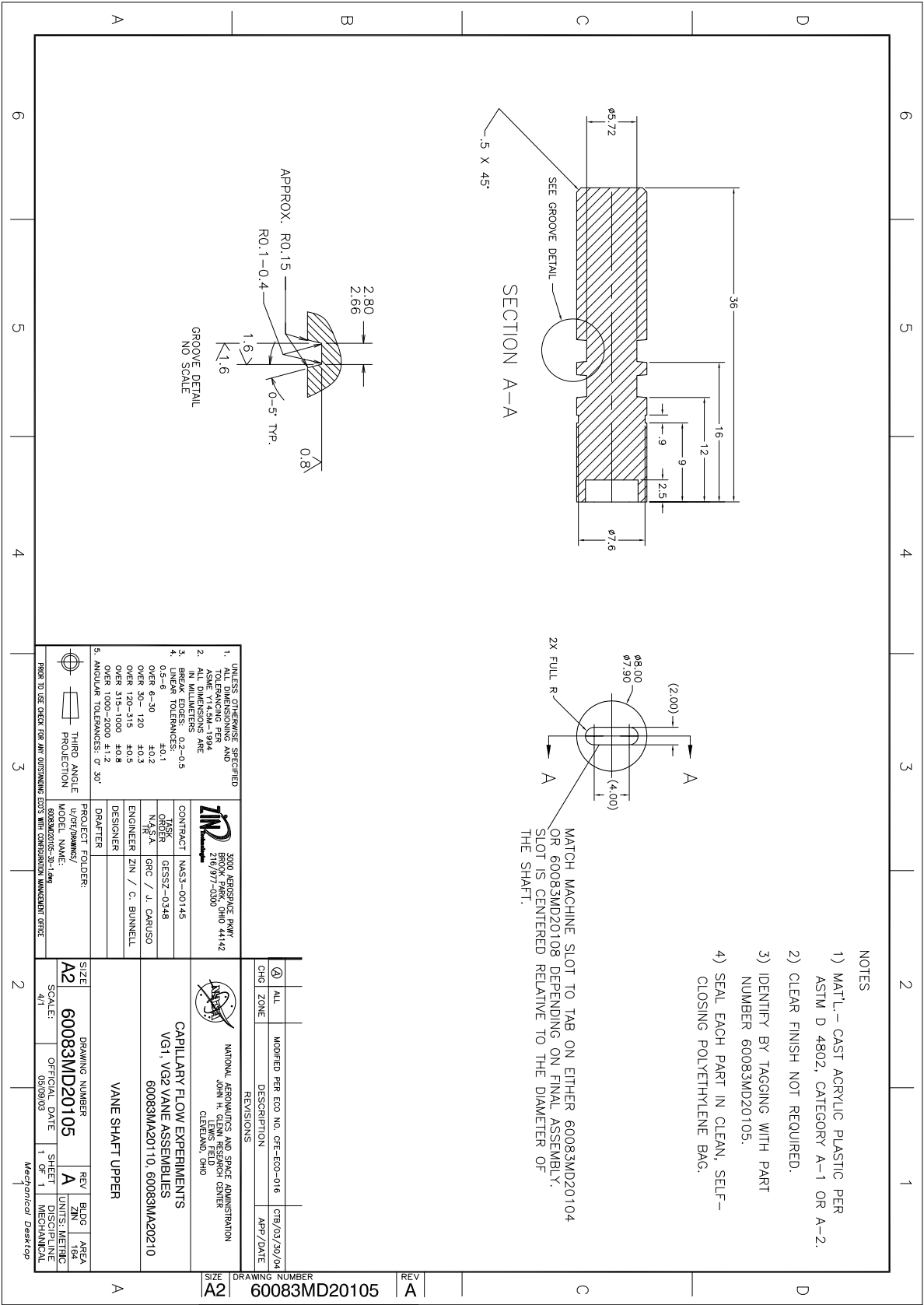


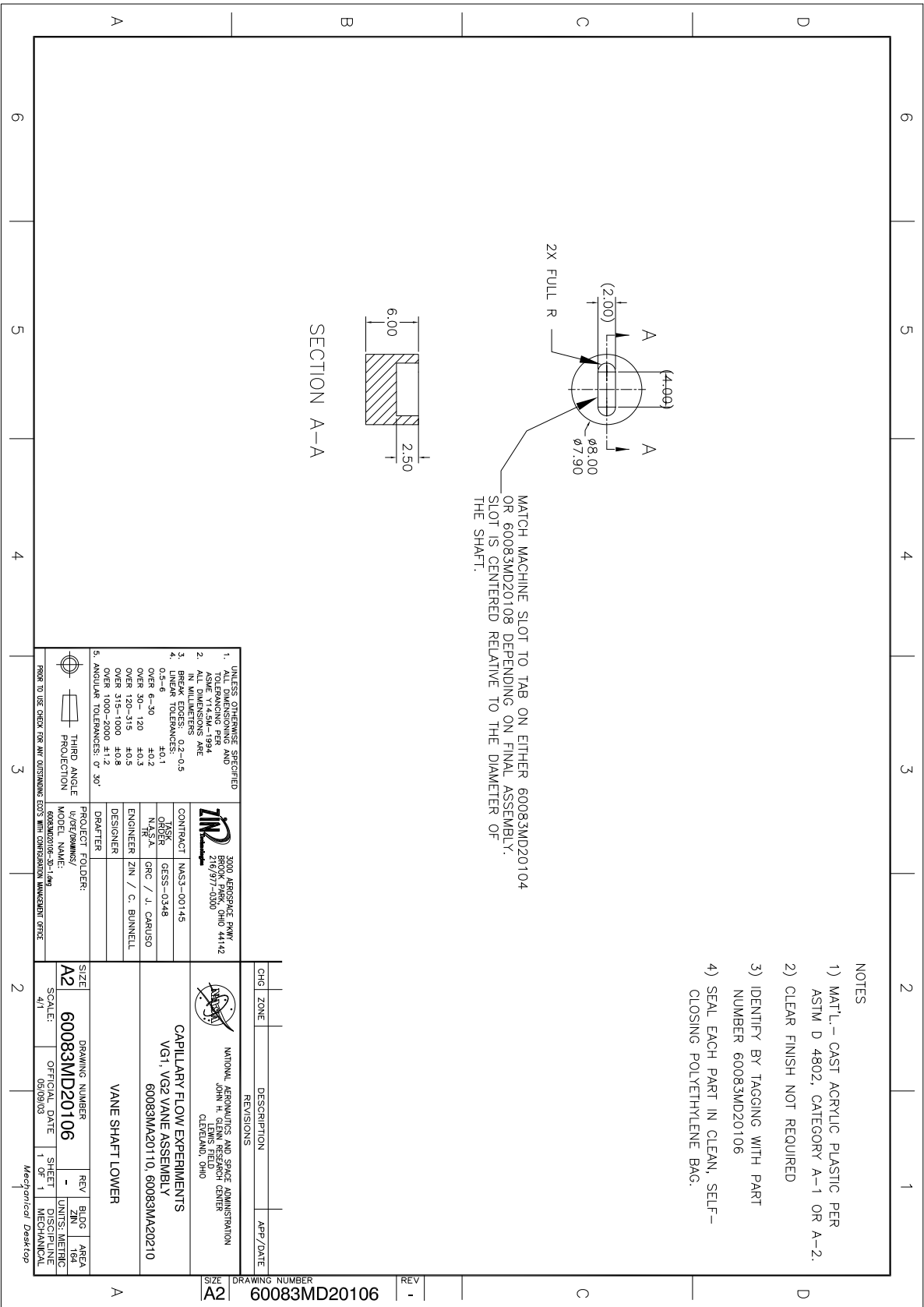


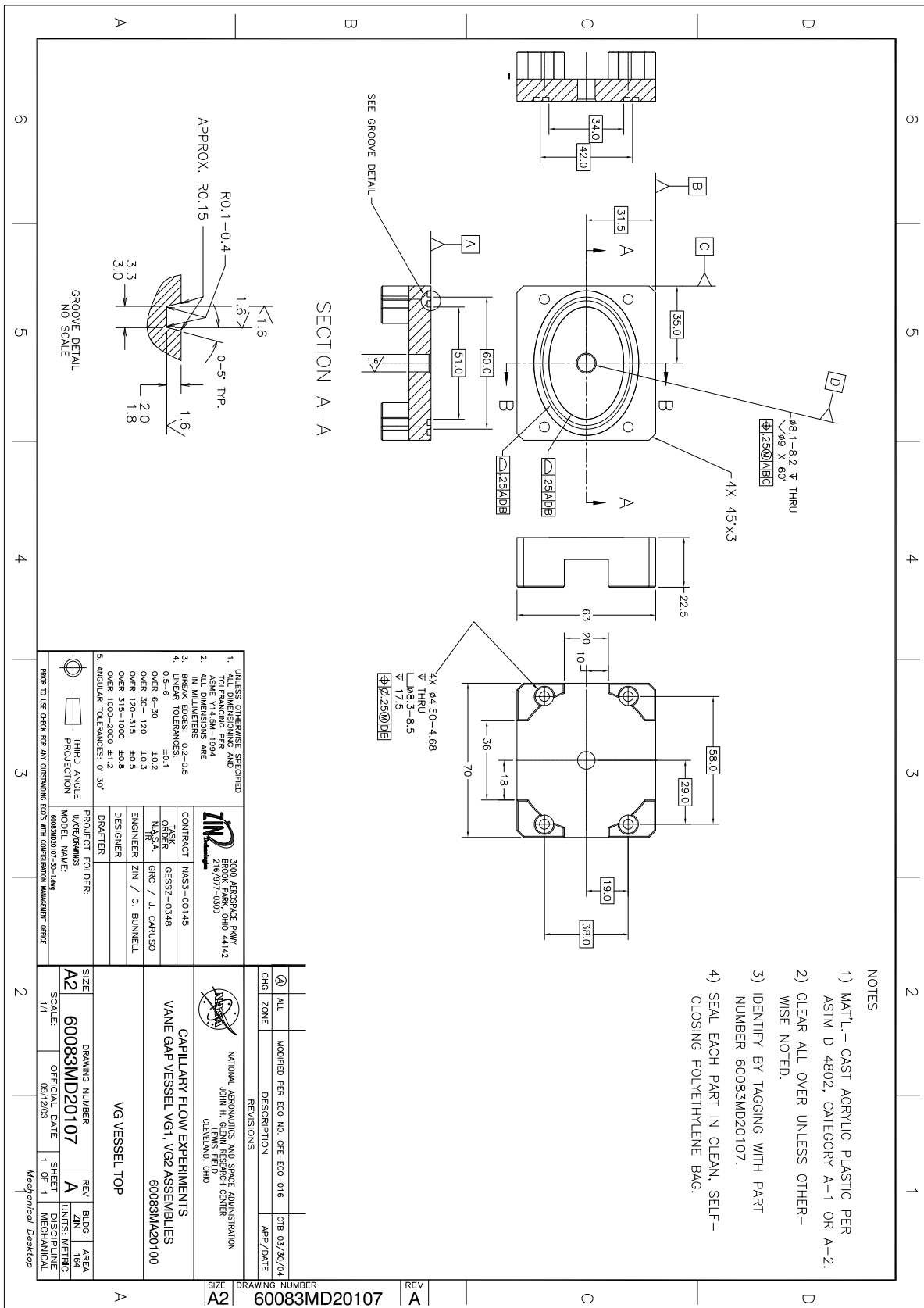


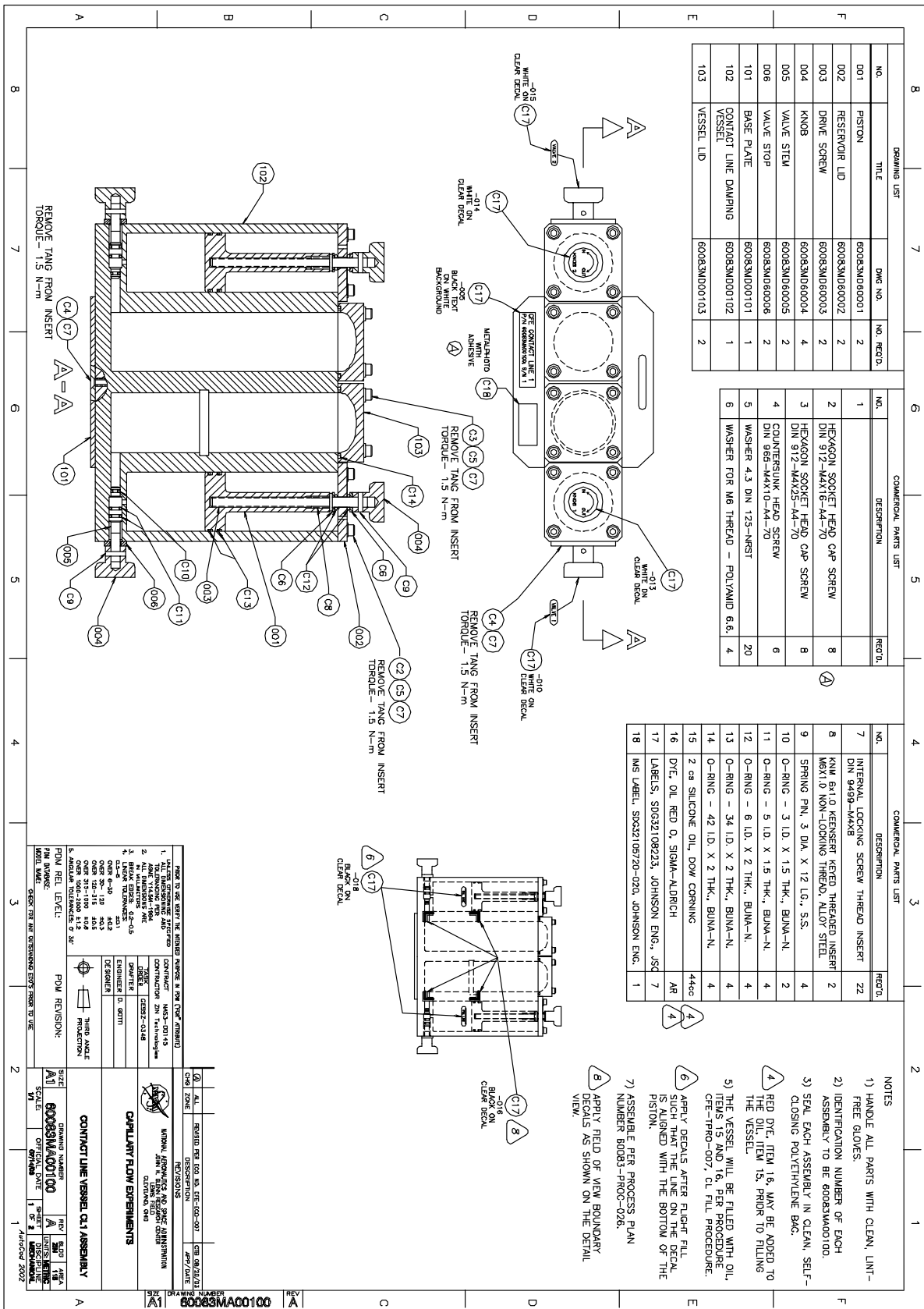


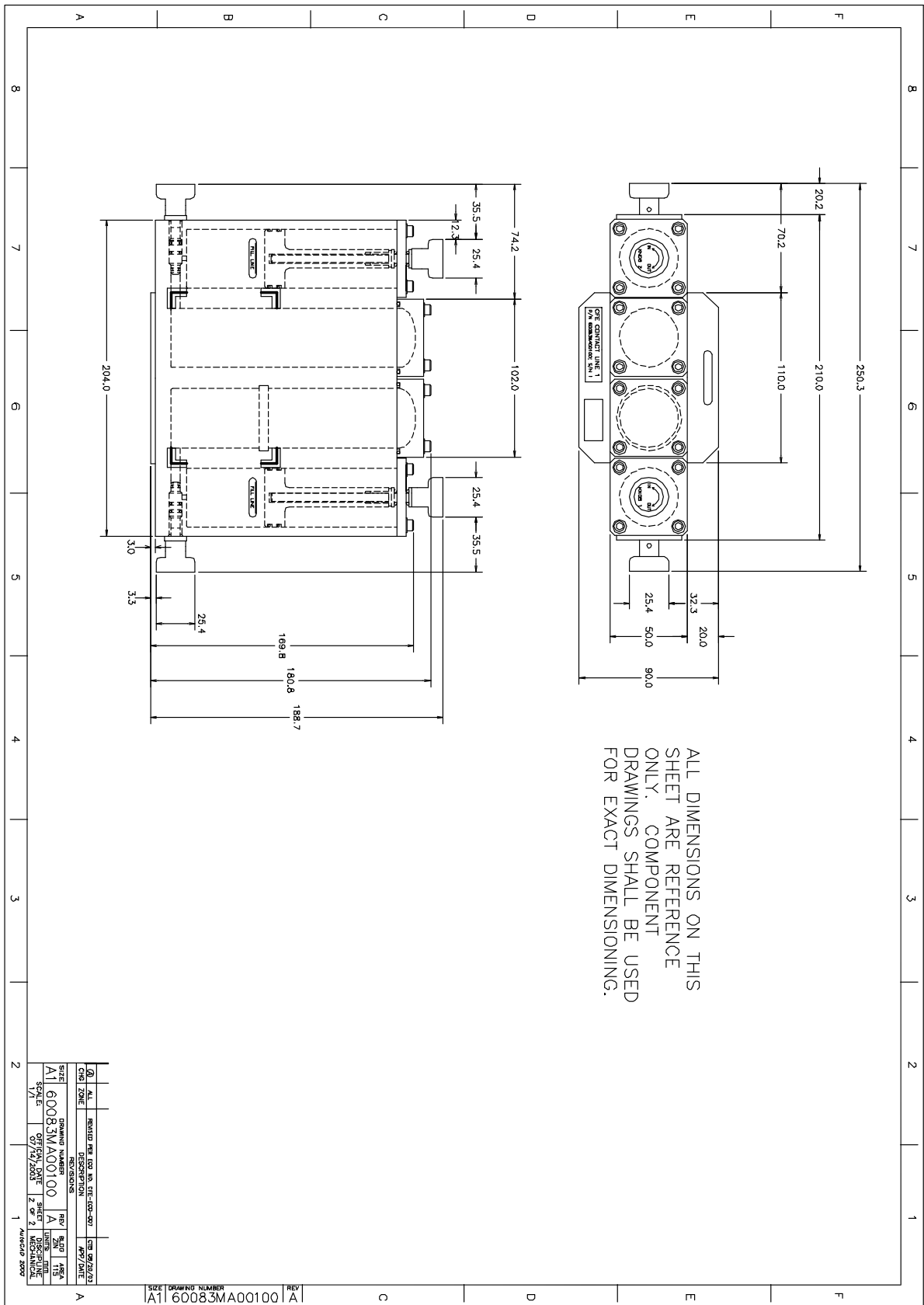


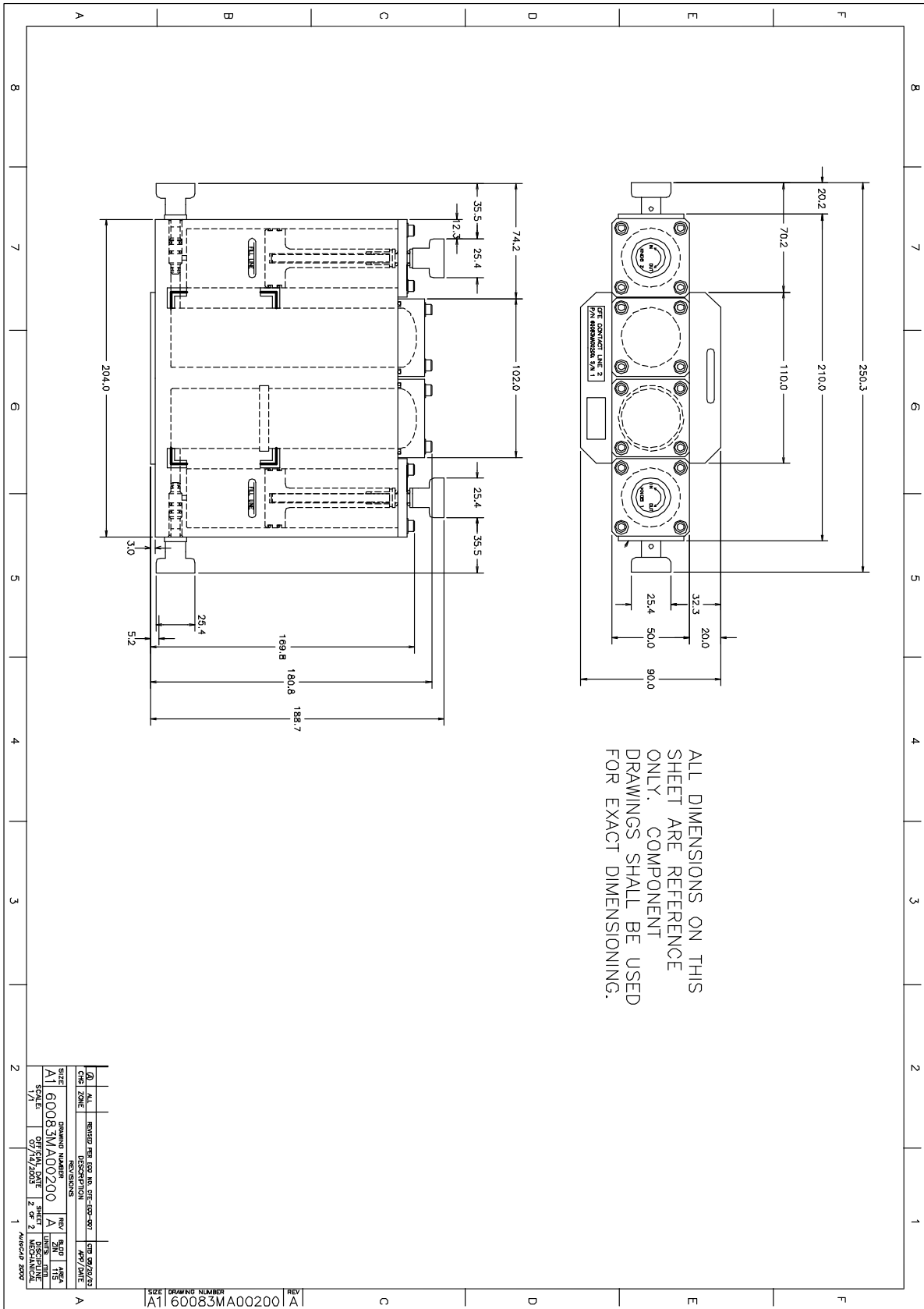




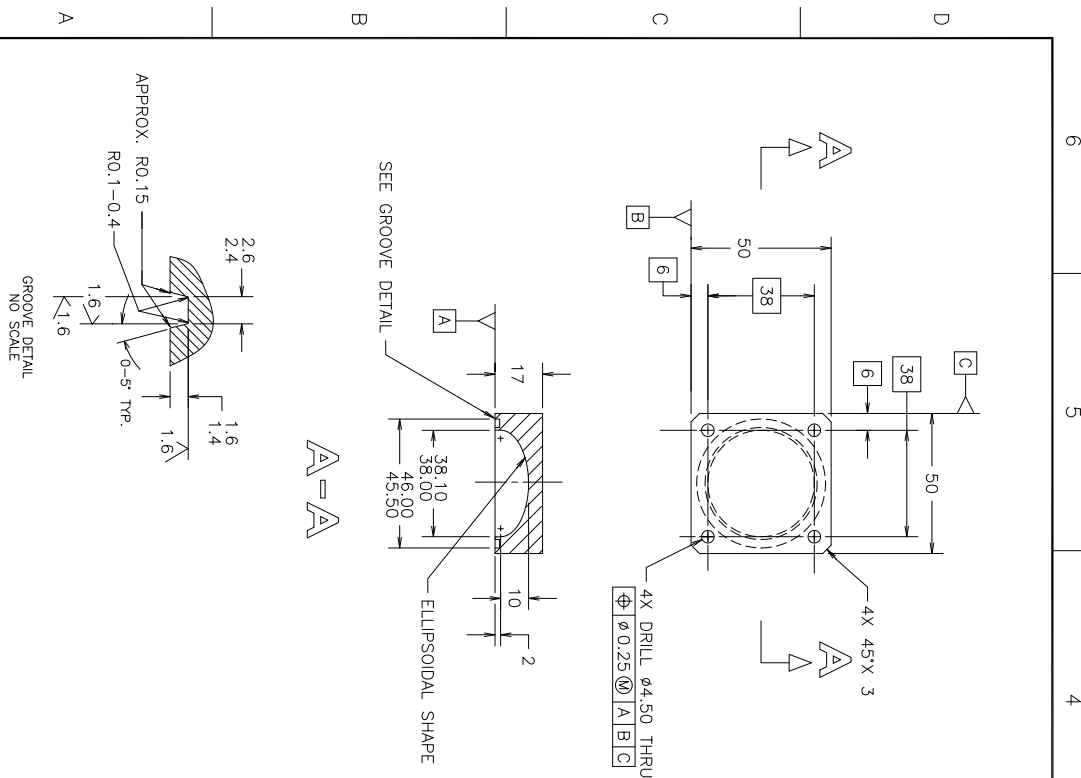










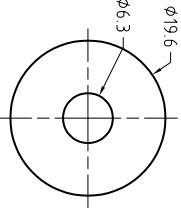
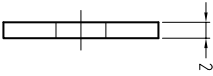



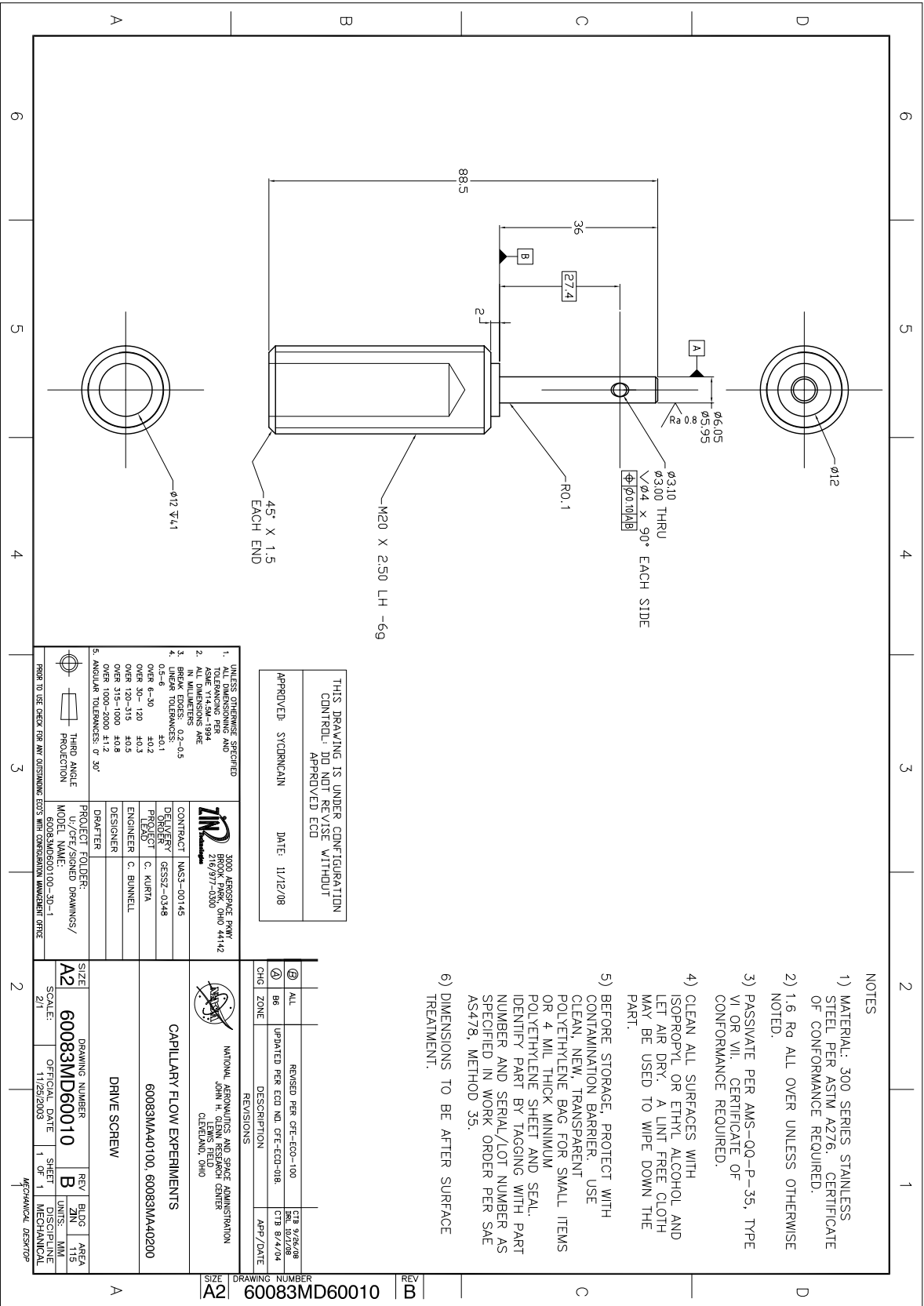


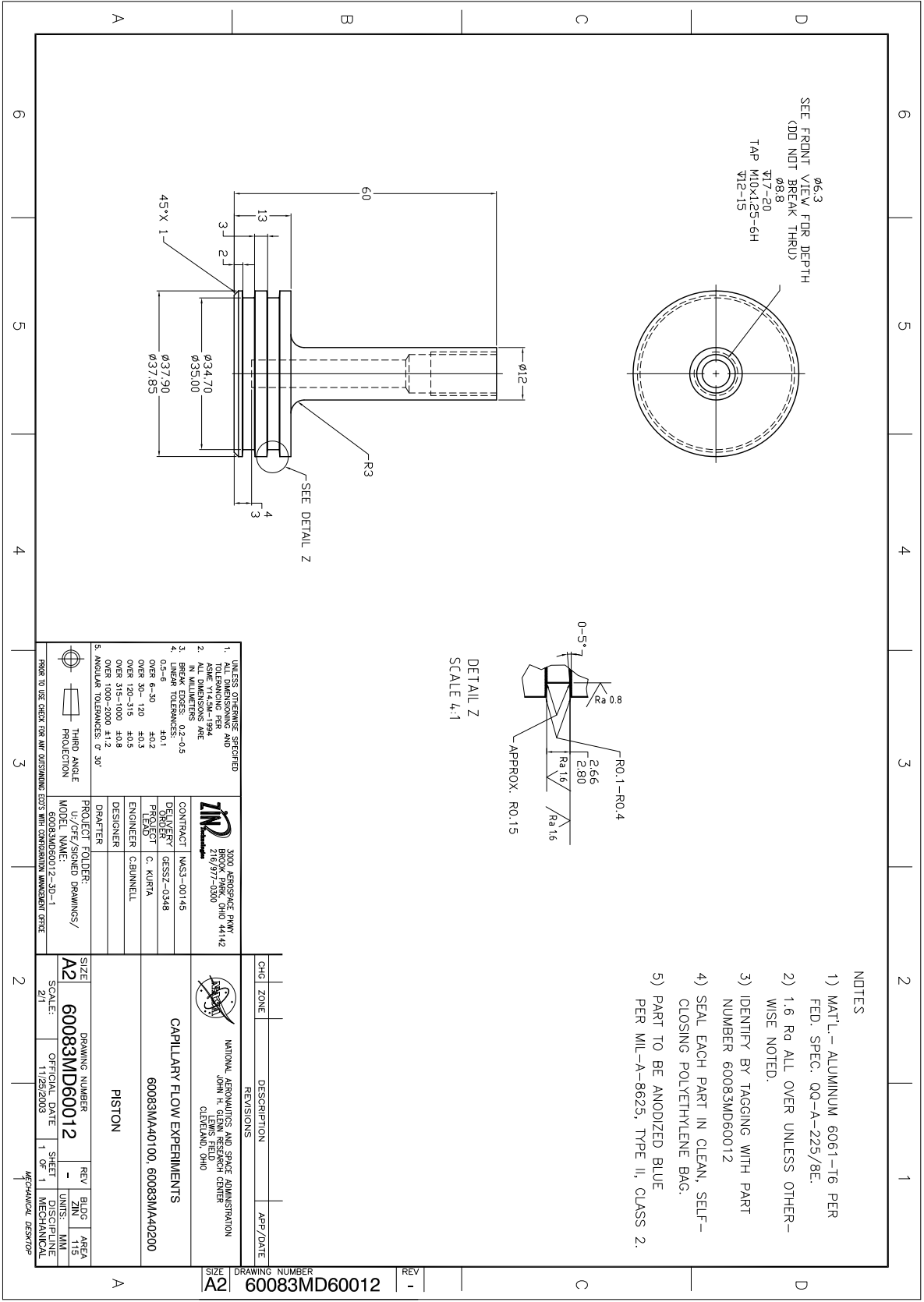
- NOTES
- 1) MATL- CAST ACRYLIC PLASTIC PER ASTM D 4802, CATEGORY A-1 OR A-2.
- 2) CLEAR ALL OVER UNLESS OTHERWISE NOTED.
- 3) IDENTIFY BY TAGGING WITH PART NUMBER 60083MD00103.
- 4) SEAL EACH PART IN CLEAN, SELF-CLOSING POLYETHYLENE BAG.

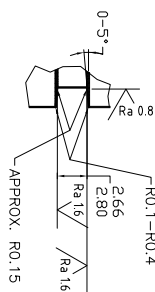
PRIOR TO USE, VERIFY THE INTENDED PURPOSE IN PDM (TYPIC ATTRIBUTE)									
UNLESS OTHERWISE SPECIFIED 1. ALL DIMENSIONS ARE IN INCHES ASME Y14.5M-1994 2. ALL DIMENSIONS ARE UNLESS OTHERWISE SPECIFIED 3. BREAK EDGES: 0.2-0.5 4. LINEAR TOLERANCES: 0.5-6 OVER 6-30: ±0.2 OVER 30-120: ±0.3 OVER 120-300: ±0.4 OVER 300-1000: ±0.8 OVER 1000-2000: ±1.2 5. ANGULAR TOLERANCES: 0°-30°									
PDM REL. LEVEL: MODEL NAME:		PDM REVISION:							
CHECK FOR ANY OUTSTANDING ECO'S PRIOR TO USE									

CHG. ZONE		DESCRIPTION REVISIONS		APP. DATE	
		NATIONAL INVENTORIES AND SPACE ADMINISTRATION JOHN H. GLENN RESEARCH CENTER CLEVELAND, OHIO		CAPILLARY FLOW EXPERIMENT CONTACT LINE VESSEL ASSEMBLY 60083MA00100 CL VESSEL, LID	
SIZE SCALE: 1/1		DRAWING NUMBER 60083MD00103		REV -	
OFFICIAL DATE 3/27/03		SHEET 1 OF 1		DISCIPLINE MECHANICAL	
		BLOC		AREA	

4		3		2		1													
C		B		A		A													
				<p>NOTES</p> <p>1) MAT'L.—ALUMINUM 6061-T6 PER FED. SPEC. QQ-A-250/11F.</p> <p>2) 1.6 Ra ALL OVER UNLESS OTHERWISE NOTED.</p> <p>3) IDENTIFY BY TAGGING WITH PART NUMBER 60083MD60008.</p> <p>4) SEAL EACH PART IN CLEAN, SELF-CLOSING POLYETHYLENE BAG.</p> <p>5) PART TO BE ANODIZED BLUE PER MIL-A-8625, TYPE II, CLASS 2.</p>															
<p>1. ALL DIMENSIONING AND TOLERANCING PER ASME Y14.5M-1994</p> <p>2. ALL DIMENSIONS ARE IN MILLIMETERS</p> <p>3. BREAK EDGES: 0.2-0.5</p> <p>4. LINEAR TOLERANCES:</p> <table border="1"> <tr> <td>0.5-6</td> <td>±0.1</td> </tr> <tr> <td>OVER 6-30</td> <td>±0.2</td> </tr> <tr> <td>OVER 30-120</td> <td>±0.3</td> </tr> <tr> <td>OVER 120-315</td> <td>±0.5</td> </tr> <tr> <td>OVER 315-1000</td> <td>±0.8</td> </tr> <tr> <td>OVER 1000-2000</td> <td>±1.2</td> </tr> </table> <p>5. ANGULAR TOLERANCES: σ 30°</p>				0.5-6	±0.1	OVER 6-30	±0.2	OVER 30-120	±0.3	OVER 120-315	±0.5	OVER 315-1000	±0.8	OVER 1000-2000	±1.2	<p>UNLESS OTHERWISE SPECIFIED</p> <p>3000 AEROSPACE PKWY BROOK PARK, OHIO 44142 216/977-0300</p> <p>ZIN <small>Manufacturing</small></p> <p>CONTRACT NAS3-00145 DELIVERY ORDER GESSZ-0348 PROJECT C. KURTA LEAD ENGINEER C. BUNNELL DESIGNER DRAFTER</p> <p>PROJECT FOLDER: U:/CFE/SIGNED DRAWINGS/ MODEL NAME: 60083MD60008-3D-1</p>			
0.5-6	±0.1																		
OVER 6-30	±0.2																		
OVER 30-120	±0.3																		
OVER 120-315	±0.5																		
OVER 315-1000	±0.8																		
OVER 1000-2000	±1.2																		
 <p>THIRD ANGLE PROJECTION</p>		<p>PRIOR TO USE CHECK FOR ANY OUTSTANDING ECO'S WITH CONFIGURATION MANAGEMENT OFFICE</p>																	
4		3		2		1													
C		B		A		A													
<p>SIZE A3</p> <p>DRAWING NUMBER 60083MD60008</p> <p>SCALE: 2/1</p> <p>OFFICIAL DATE 11/25/2003</p> <p>SHEET 1 OF 1</p> <p>DISCIPLINE MECHANICAL</p>		<p>CHG ZONE</p> <p>DESCRIPTION</p> <p>REVISIONS</p>		<p>APR/DAT</p>		<p>REV</p>													
<p>60083MD60008</p>		<p>DISK</p>		<p>60083MAA40100, 60083MAA40200</p>		<p>60083MD60008</p>													
<p>DISK</p>		<p>CAPILLARY FLOW EXPERIMENTS</p>		<p>NATIONAL AERONAUTICS AND SPACE ADMINISTRATION JOHN H. GLENN RESEARCH CENTER LEWIS FIELD CLEVELAND, OHIO</p>		<p>MECHANICAL DESKTOP</p>													

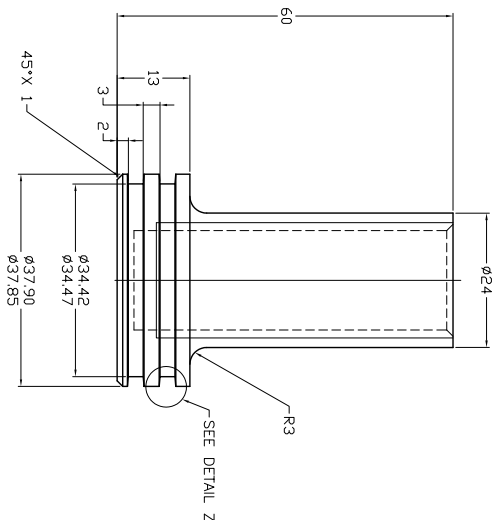






DETAIL Z
SCALE 4:1

- 4) CLEAN ALL SURFACES WITH ISOPROPYL OR ETHYL ALCOHOL AND LET AIR DRY. A LINT FREE CLOTH MAY BE USED TO WIPE DOWN THE PART.
- 5) BEFORE STORAGE, PROTECT WITH CONTAMINATION BARRIER. USE CLEAN, NEW, TRANSPARENT POLYETHYLENE BAG FOR SMALL ITEMS OR 4 MIL THICK MINIMUM POLYETHYLENE SHEET AND SEAL. IDENTIFY PART BY TAGGING WITH PART NUMBER AND SERIAL/LOT NUMBER AS SPECIFIED IN WORK ORDER PER SAE AS478, METHOD 35.
- 6) DIMENSIONS TO BE AFTER SURFACE TREATMENT.



-SEE DETAIL Z

THIS DRAWING IS UNDER CONFIGURATION
CONTROL: DO NOT REVISE WITHOUT
APPROVED ECD

APPROVED: SYCDRCNAIN DATE: 11/12/08

ALL	REVISED PER CFE-ECO-100	CTB 9/26/08 DRL 10/1/08
-----	-------------------------	----------------------------



NATIONAL AERONAUTICS AND SPACE ADMINISTRATION
JOHN H. GLENN RESEARCH CENTER
LEWIS FIELD
CLEVELAND, OHIO

CAPILLARY FLOW EXPERIMENTS

60083MA40100, 60083MA40200

PISTON

- | | |
|----------------------------|----------------------|
| UNLESS OTHERWISE SPECIFIED | 3000 KENSINGTON PARK |
| 1. TOLERANCING PER | BROOK PARK |
| ASME Y14.5M-1994 | 216/377-0300 |
| 2. UNLIT | |
| 3. BREAK EDGES: 0.2-0.5 | |
| 4. TOLERANCES: | |
| OVER 6-30 | ±0.2 |
| OVER 30-120 | ±0.3 |
| OVER 120-315 | ±0.5 |
| OVER 315-1000 | ±0.8 |
| OVER 1000-2000 | ±1.2 |
| 5. ANGULAR TOLERANCES: 0° | 30° |
| | DRAWER |
| | 1/25/05 |

THIRD ANGLE
PROJECTION

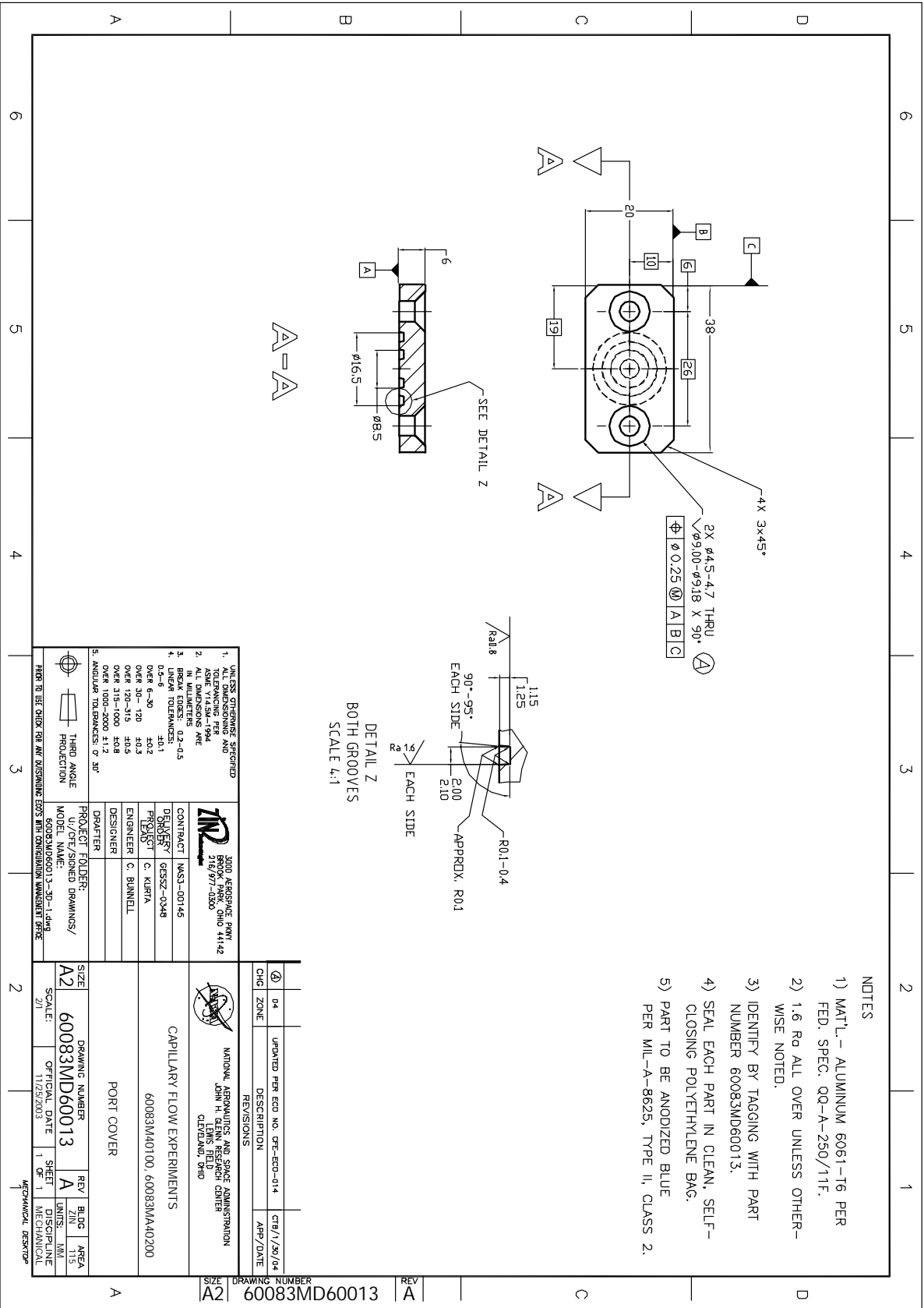
PRIOR TO USE CHECK FOR ANY OUTSTANDING EDO'S WITH CONFIGURATION MANAGEMENT OFFICE

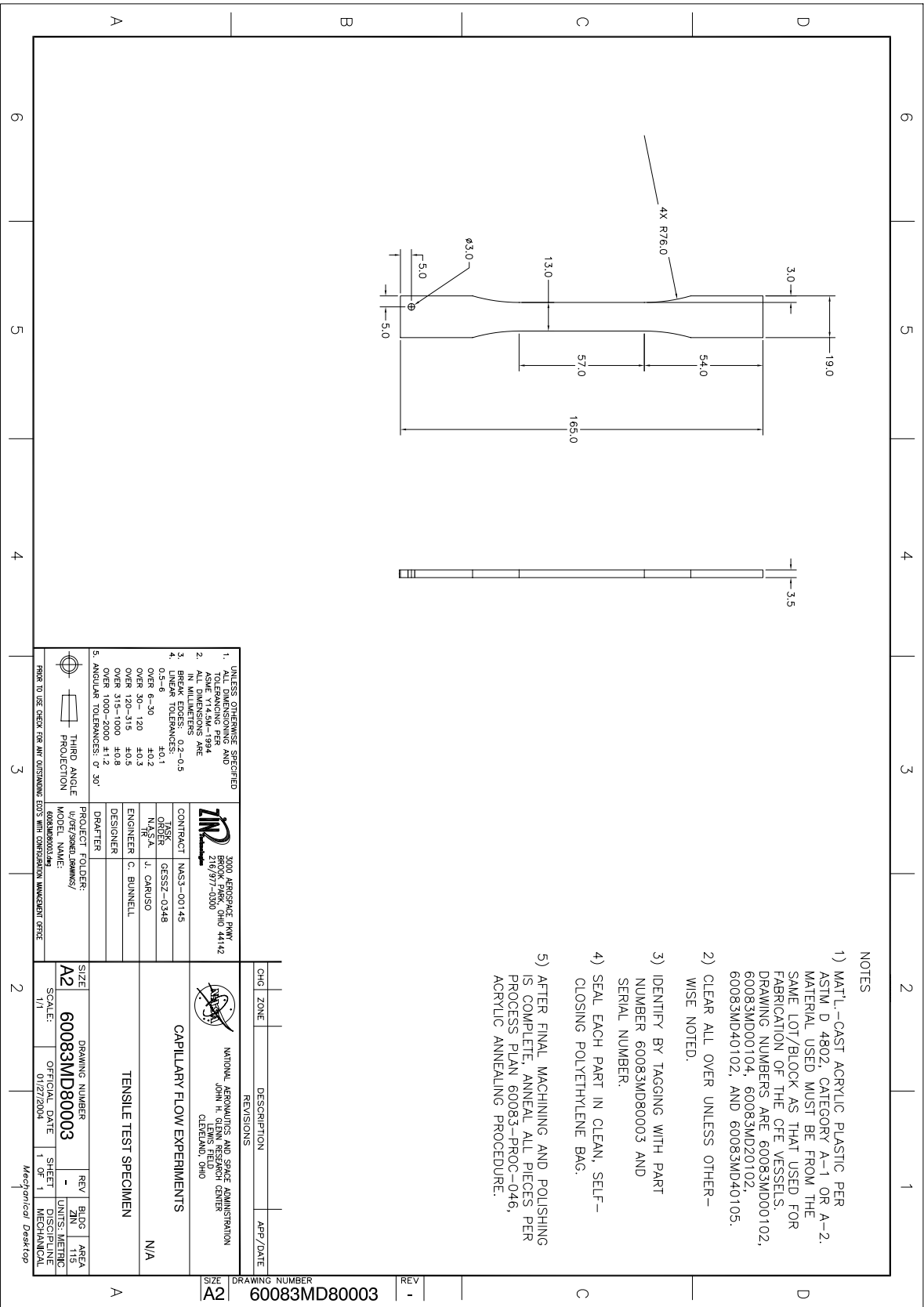
SIZE	DRAWING NUMBER	REV	BLDG ZIN	AREA
A2	60083MD60012	A		115
SCALE:	OFFICIAL DATE	SHEET	DISCIPLINE	
2/1	11/25/2003	1 OF 1	MECHANICAL	

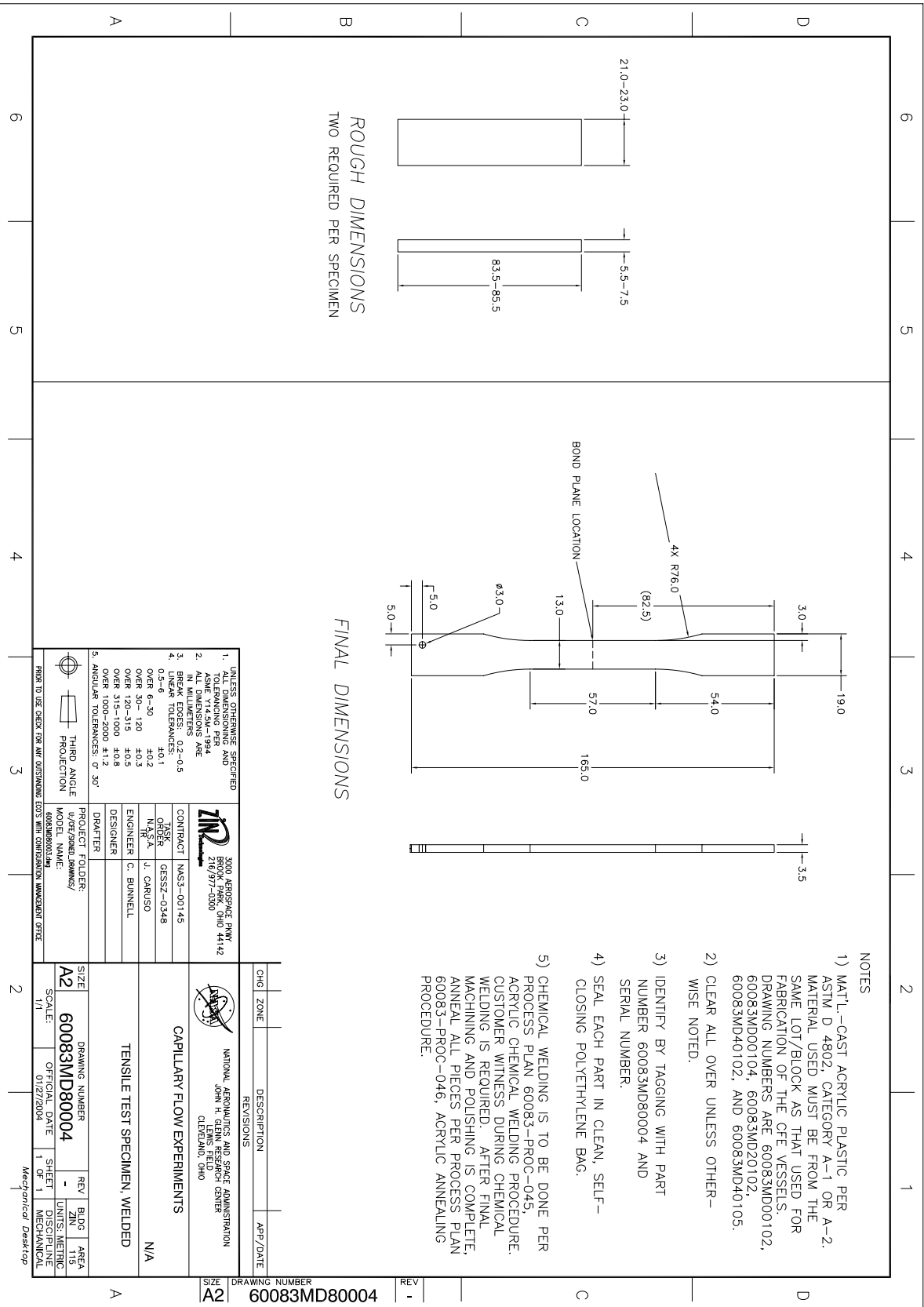
MECHANICAL DESKTOP¹

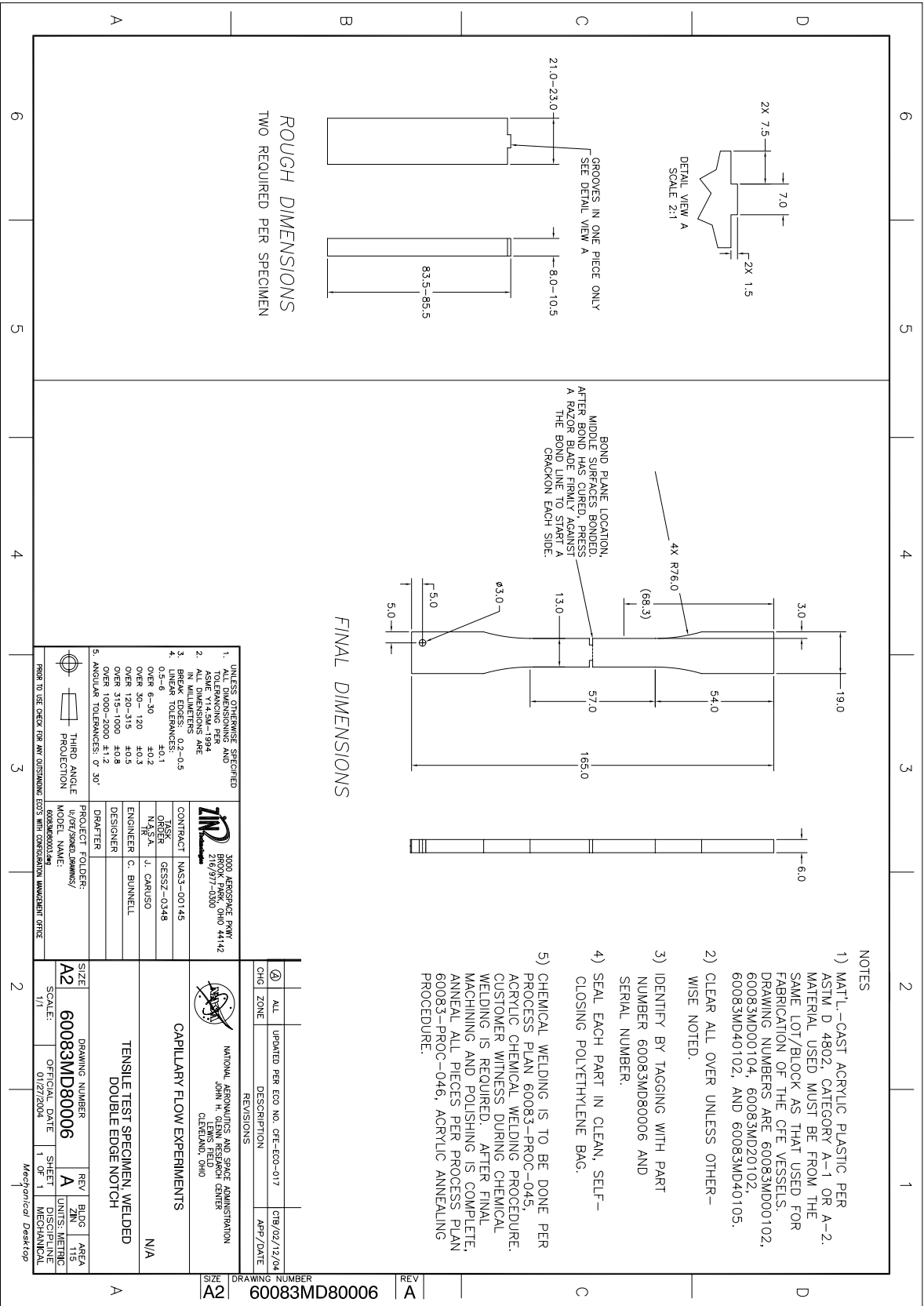
NOTES

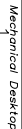
- 1) MATERIAL: 6061-T6 OR 6061T651 ALUMINUM PER AMS-QQ-A-250/11F. CERTIFICATE OF CONFORMANCE REQUIRED.

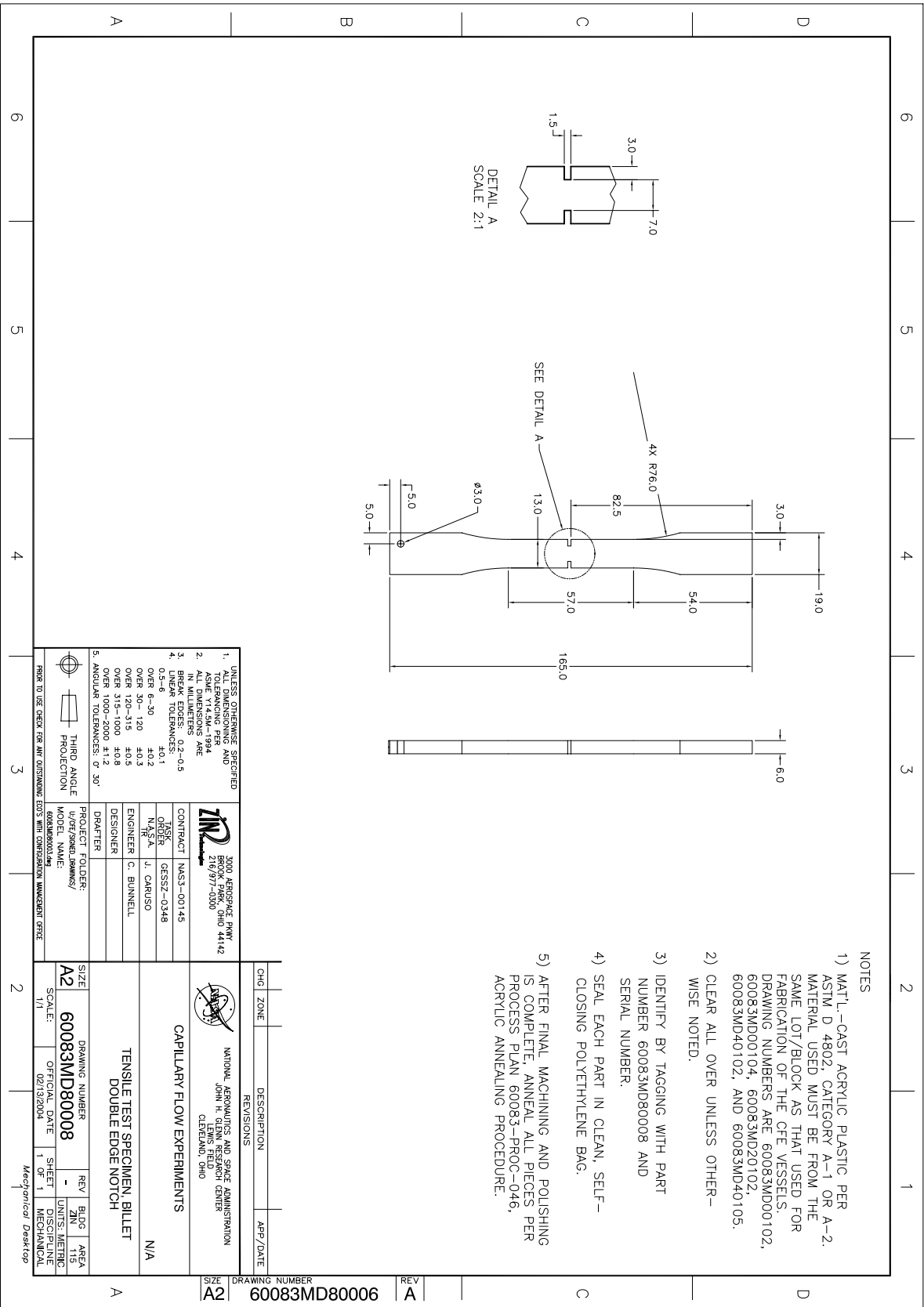


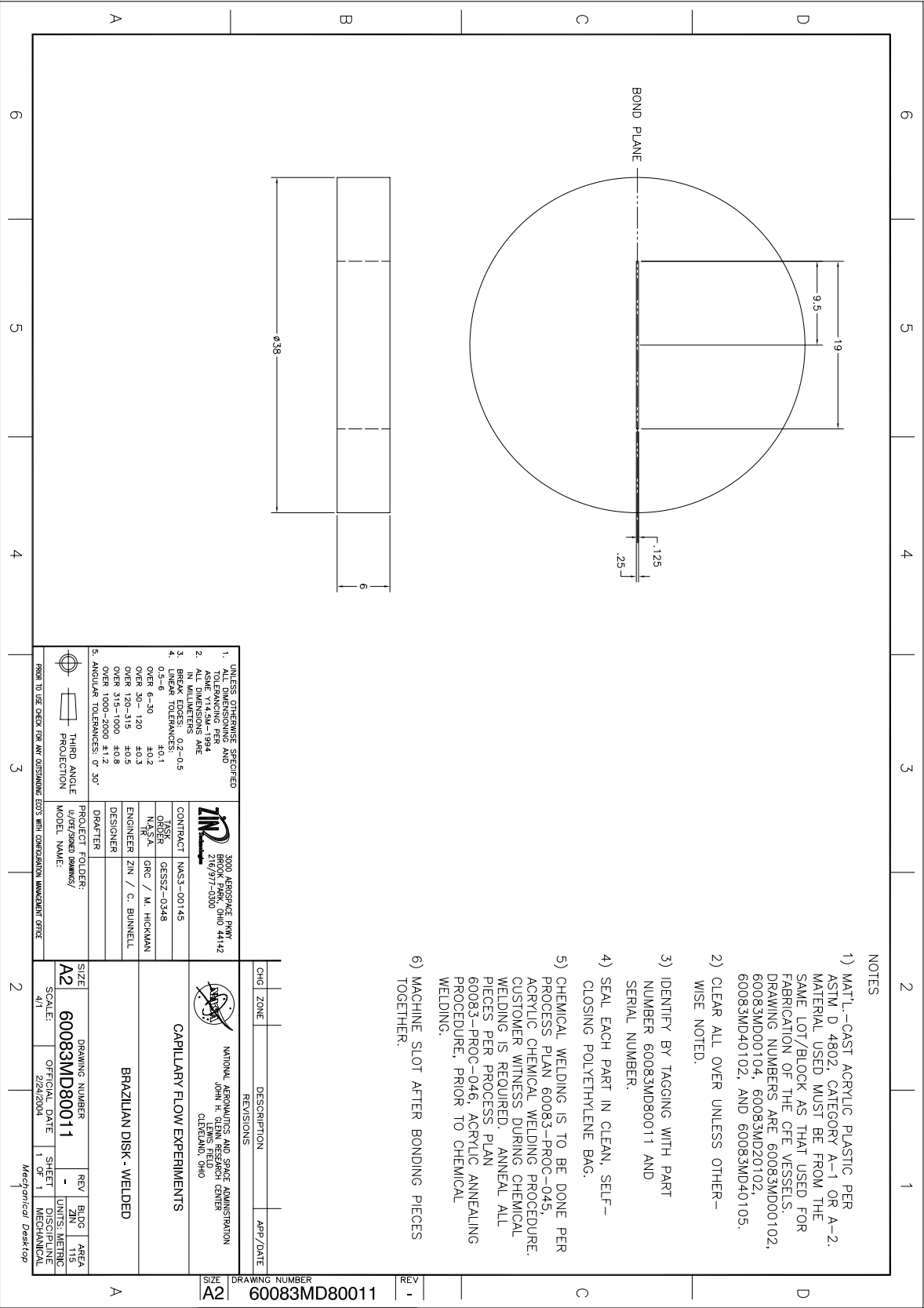


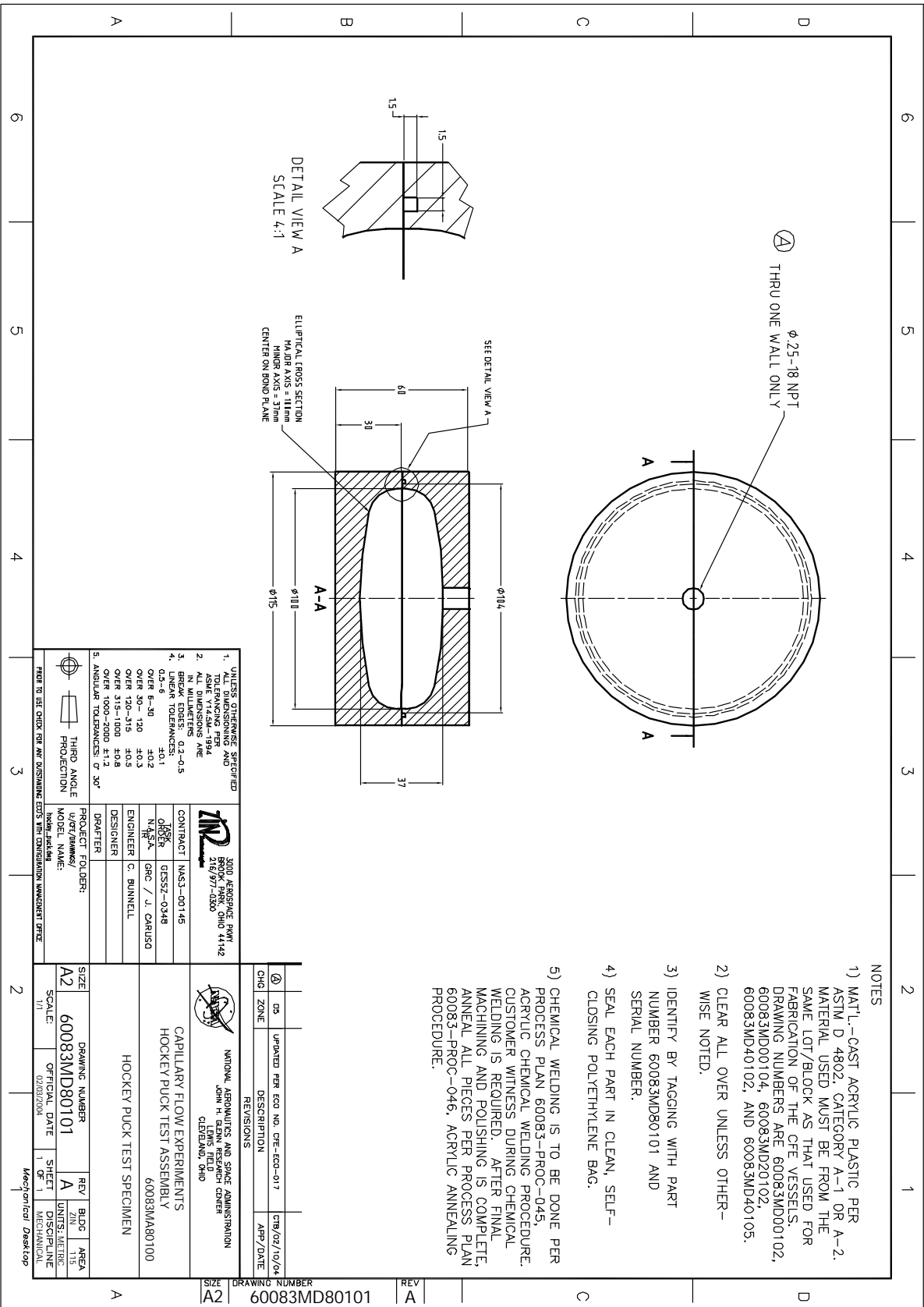


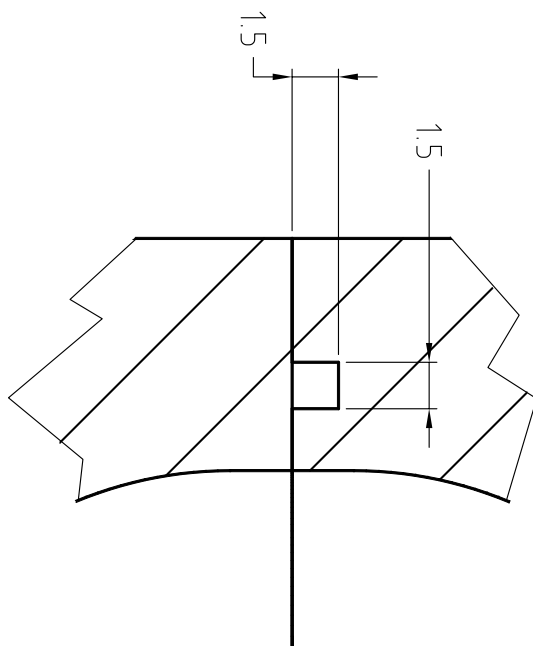












DETAIL VIEW A
SCALE 4:1

Chapter 11

Appendix: CFE Flight Crew Procedures

2.001 CFE SETUP

(podfall000364)

Page 1 of 6

OBJECTIVE:

Capillary Flow Experiment (CFE). In this procedure the crew will set up the CFE Unit and supporting equipment in order to test the flow of fluid in microgravity. During Progress /ATV/Shuttle flights different hardware will be sent up that will allow three types of Capillary Flow Experiments to be performed.

STATION PARTS:

CFE Contact Line 1 P/N 60083MA00100
CFE Contact Line 2 P/N 60083MA00200
CFE Interior Corner Flow 1 P/N 60083MA40100
CFE Interior Corner Flow 2 P/N 60083MA40200
CFE Vane Gap 1 P/N 60083MA20100
CFE Vane Gap 2 P/N 60083MA20200
Ziploc Bags (stowed in Foam)
Foam (stowed in CFE)

STATION TOOLS:

MWA Work Surface Area P/N SEG33110270-301
MWA Utility Kit P/N SJG33110310-301
Multi-use Bracket(s) P/N SEG33107631-301
PD100 Camcorder P/N SEZ16103293-301
Digital CC Video/Power IF Cable P/N SED33111490-303
Fine Point Sharpie P/N 528-40674-1
Scissors P/N 10104-20006-03
IP Clamp P/N SEG33111394-30X

STATION MATERIALS:

Dry Wipe P/N SEG33107170-306
Printer Paper (RIM) [2] P/N SEG33110070-301
General Purpose Tape 1" P/N 528-41798-5
Aluminum Tape P/N 3M425

1. Select a location for the Maintenance Work Area (MWA) based on the following criteria:

LIGHTING	SHADOWS	CAMCORDER MOUNTING	CREW ACCESSIBILITY

Good lighting is critical to getting good images of the fluid in the vessels. Equal lighting front and back is required for best results. Select a mounting location that has working lights above the rack and directly across from the rack, both at full intensity. Adjacent lights should be set to equal intensity.	Avoid any location that will cast shadows across the CFE vessel. Shadows adversely affect the video data. Shadows adjacent to the CFE vessel are acceptable including shadows across the white background pieces of paper.	Mount PD100 Camcorder either from the deck or from the overhead using Multi-use Bracket(s) and crew ingenuity. Exact instructions cannot be given due to the dynamic nature of equipment mounting and location within the ISS. Shorter camera mounting is easier and may make it desirable to move the MWA closer to either the deck or overhead.	CFE is a crew intensive experiment with continued interaction from the crew. Position MWA to provide comfortable access for all activities.
--	--	---	---

Refer to [5.004 CFE VESSEL AND CAMERA CONFIGURATION](#).

2. ✓MWA Work Surface Area is set up
[A.2.6 MAINTENANCE WORK AREA \(MWA\) INSTALLATION](#) step 1, (US SODF: IFM: Reference (Volume 6): Appendix A: ISS IVA Tools)
3. Unstow and Tmptry stow near MWA Work Surface Area:
MWA Utility Kit
Multi-Use Bracket(s)
IP Clamp
PD100 Camcorder
Digital CC Video/Power IF Cable
Printer Paper (RIM) (two sheets)
Scissors
Dry Wipe
General Purpose Tape 1"
Fine Point Sharpie
Aluminum Tape

CAUTION

Do not mount the PD100 camcorder to the MWA because the camcorder needs to provide an independent record of motion to avoid loss of science data.

4. Mount PD100 camcorder on Multi-Use Bracket(s) with the following constraints:

MULTI-USE BRACKET(S)	CAMCORDER LENS	CAMCORDER SETUP
Mount the Multi-use Bracket(s) to either an overhead or deck seat track or handrail. Mount the PD100 camcorder to the Multi-use Bracket(s). Mounting directly to the MWA is not acceptable. Refer to 5.004 CFE VESSEL AND CAMERA CONFIGURATION	The camera lens used should be the wide conversion lens. That will allow a short working distance as pictured in 5.004 CFE VESSEL AND CAMERA CONFIGURATION .	The camera setup needs to provide the desired fields of view for the CFE vessel undergoing operations. Final adjustments to the camera setup are completed once the field of view is verified after the CFE vessel is mounted to the MWA.

5. Perform [6.201 PD100 NOMINAL SETUP](#)

NOTE

1. Contact Line vessels have dedicated foam boxes. Interior Corner Flow and Vane Gap vessels do not and were packed using loose pieces of foam. Steps below referring to the foam are referring to the Contact Line foam boxes.
2. Minimize fingerprints upon test chamber surfaces.

6. Unstow:
Contact Line 1(Contact Line 2,Interior Corner Flow 1,Interior Corner Flow 2,Vane Gap 1,Vane Gap 2) per Execution Note
7. Remove **Contact Line 1(Contact Line 2,Interior Corner Flow 1,Interior Corner Flow 2,Vane Gap 1,Vane Gap 2)** from foam.
Tm pry stow foam.
8. Verify no visible oil leakage in outer Ziploc Bag.

If leakage visible in outer bag,

Replace **Contact Line 1(Contact Line 2,Interior Corner Flow 1,Interior Corner Flow 2,Vane Gap 1,Vane Gap 2)** in foam.
Stow: **Contact Line 1(Contact Line 2,Interior Corner Flow 1,Interior Corner Flow 2,Vane Gap 1,Vane Gap 2)**
Notify **POIC**

9. Using Scissors carefully cut heat seal from outer Ziploc Bag.
Tm pry stow Scissors.
Refer to [5.007 CFE VESSEL HEAT SEAL](#).
10. Remove **Contact Line 1(Contact Line 2,Interior Corner Flow 1,Interior Corner Flow 2,Vane Gap 1,Vane Gap 2)** from outer Ziploc Bag.
Tm pry stow outer Ziploc Bag.
11. Verify no visible oil leakage in inner Ziploc Bag.

If leakage visible in inner bag,
Replace **Contact Line 1(Contact Line 2,Interior Corner Flow 1,Interior Corner Flow 2,Vane Gap 1,Vane Gap 2)** in outer Ziploc Bag.

Replace **Contact Line 1(Contact Line 2,Interior Corner Flow 1,Interior Corner Flow 2,Vane Gap 1,Vane Gap 2)** in foam.

Stow: **Contact Line 1(Contact Line 2,Interior Corner Flow 1,Interior Corner Flow 2,Vane Gap 1,Vane Gap 2)**

*

Notify POIC

12. Using Scissors carefully cut heat seal from inner Ziploc Bag.
Tm pry stow Scissors.
13. Remove **Contact Line 1(Contact Line 2,Interior Corner Flow 1,Interior Corner Flow 2,Vane Gap 1,Vane Gap 2)** from inner Ziploc Bag.
Tm pry stow inner Ziploc Bag.
14. Remove Kapton Tape from **Contact Line 1(Contact Line 2,Interior Corner Flow 1,Interior Corner Flow 2,Vane Gap 1,Vane Gap 2)**.
Dispose of Kapton Tape.

MWA Utility Kit 15. Unstow:
#10 Fastener

- MWA Work Surface Area 16. Set up **Contact Line 1(Contact Line 2,Interior Corner Flow 1,Interior Corner Flow 2,Vane Gap 1,Vane Gap 2)** on Maintenance Work Area smooth surface between seat tracks avoiding contact with hinges and seat tracks.
There are two large center panels suitable for mounting CFE.
Mount the CFE vessel to the panel closest to the front edge of the MWA.
Align the **Contact Line 1(Contact Line 2,Interior Corner Flow 1,Interior Corner Flow 2,Vane Gap 1,Vane Gap 2)** to place #10 Fastener in the center of the mounting slot and install the #10 fastener.
√#10 fastener is securely tightened

Refer to [5.006 CFE SETUP DRAWING](#).

17. Using Dry wipe clean fingerprints from **Contact Line 1(Contact Line 2,Interior Corner Flow 1,Interior Corner Flow 2,Vane Gap 1,Vane Gap 2)**.

Dispose of Dry Wipe.

NOTE

1. The Printer Paper (RIM) serves as a backlit screen for the Contact Line 1(Contact Line 2,Interior Corner Flow 1,Interior Corner Flow 2,Vane Gap 1,Vane Gap 2)vessel and reflects light to illuminate the vessel from the back. This is the primary source of illumination. Proper lighting is necessary in order for data collection of the experiment.
2. Equal lighting in front and in back of test article should be ensured.

- MWA 18. Using Aluminum Tape, place one sheet of Printer Paper (RIM) behind the **Contact Line 1(Contact Line 2,Interior Corner Flow 1,Interior Corner Flow 2,Vane Gap 1,Vane Gap 2)** in a location that allows the reflected light to illuminate the back side of the **Contact Line 1(Contact Line 2,Interior Corner Flow 1,Interior Corner Flow 2,Vane Gap 1,Vane Gap 2)**. Place the second sheet of Printer Paper (RIM) on the MWA Work Surface Area surface behind the **Contact Line 1(Contact Line 2,Interior Corner Flow 1,Interior Corner Flow 2,Vane Gap 1,Vane Gap 2)**. Refer to [5.014 CFE SETUP ILLUSTRATION](#).

- PD 100 Camcorder 19. sel Menu

20. sel Etc, Others

21. sel REC Lamp

22. sel REC Lamp →OFF

23. √REC Lamp — OFF

24. Using Fine Point Sharpie, color small piece of paper to cover reflective Sony emblem on the front of the PD100 camcorder. Attach paper with General Purpose Tape 1" so that emblem is completely covered and no tape is visible.

25. Position the PD100 Camcorder so that the field of view shows the close up of the test chamber of the **Contact Line 1(Contact Line 2,Interior Corner Flow 1,Interior Corner Flow 2,Vane Gap 1,Vane Gap 2)**.

If CFE Contact Line,

 Refer to [5.002 CFE CONTACT LINE SMALL FIELD OF VIEW](#).

 Zoom out the PD100 Camcorder so that the Field of View shows the entire CFE Contact Line 1(2).

 Refer to [5.005 CFE CONTACT LINE CHAMBER FIELD OF VIEW](#).

If CFE Interior Corner Flow,

Set the Field of View per [5.008 CFE INTERIOR CORNER FLOW FIELD OF VIEW.](#)

If CFE Vane Gap,

Set the Field of View per [5.010 CFE VANE GAP CHAMBER FIELD OF VIEW.](#)

26. Stow:

Scissors

Aluminum Tape

General Purpose Tape 1"

27. Insert inner Ziploc Bag in outer Ziploc Bag.

Insert outer Ziploc Bag in foam.

Stow:

Foam (containing Ziploc Bags)

RESTOW TOOLS, PARTS, AND MATERIALS AS REQUIRED TO ORIGINAL LOCATIONS EXCEPT FOR:

MWA Utility Kit TO: proximity of MWA Work Surface Area

Multi-Use Bracket(s) TO: proximity of MWA Work Surface Area

PD100 Camcorder TO: proximity of MWA Work Surface Area

Digital CC Video/Power IF Cable TO: proximity of MWA Work Surface Area

Fine Point Sharpie TO: proximity of MWA Work Surface Area

IP Clamp TO: proximity of MWA Work Surface Area

MWA Work Surface Area TO: Per location chosen in step 1

Contact Line 1(Contact Line 2,Interior Corner Flow 1,Interior Corner Flow 2,Vane Gap 1,Vane Gap 2) TO: proximity of MWA Work Surface Area

2.002 CFE CONTACT LINE TEST OPERATIONS

(podfall000364)

Page 1 of 21 pages

OBJECTIVE:

Capillary Flow Experiment (CFE). During this procedure the data for the CFE Contact Line tests is recorded via Camcorder video and sound. The CFE tests are titled Background, Tap, Axial, Push, Slide, Multi-Slide, Swirl, Displacement, Bubbles, and Drainage.

STATION PARTS:

CFE Contact Line 1 P/N 60083MA00100

CFE Contact Line 2 P/N 60083MA00200

Mini DVCAM Tape [9] P/N SED33111489-305

STATION TOOLS:

MWA Work Surface Area P/N SEG33110270-301

MWA Utility Kit P/N SJG33110310-301

Fine Point Sharpie P/N 528-40674-1

PD100 Camcorder P/N SEZ16103293-301

STATION MATERIALS:

Dry Wipe P/N SEG33107170-306

NOTE

1. This procedure contains Near Real - Time video downlink or LAB VTR recording requirements.
2. AOS may be required for **POIC** to configure on board system for downlink of science or LAB VTR recording.

1. CFE BACKGROUND TEST

- 1.1 Visually inspect the vessel to determine if the pinning lip is dry. In general, a dry pinning lip diffracts light in such a manner that it is not possible to clearly see through the pinning lip in profile. Refer to [5.013 CFE PINNING LIP COMPARISON](#). If the pinning lip needs to be cleared of fluid at any time during this step,
Perform [step 11](#) and then resume this step where exited.
- 1.2 ✓ #10 fastener is securely tightened
- 1.3 Unstow: Mini DVCAM Tape (nine)
Tm pry stow close to PD100 Camcorder.
Insert Mini DVCAM Tape into PD100 Camcorder
- 1.4 ✓ PD100 Camcorder for CFE Contact Line 1(2) entire Field of View
✓ REC Lamp — OFF
✓ Sony emblem is covered
Refer to Figure [5.005 CFE CONTACT LINE CHAMBER FIELD OF VIEW](#)

CAUTION

1. Once fluid dispensing into the test chambers has begun, the process

CAUTION	
	for turning the knob needs to be consistent or a loss of science will occur.
2.	The smooth cylinder fluid will be dispensed before the pinning cylinder in order to reduce disturbances that could impact science associated with the pinning lip.
3.	Loss of science will occur if the CFE Contact Line 1(2) is disturbed and agitated during the Background run. The Background run is not repeatable.

NOTE	
1.	Valve 2 and Knob 2 are associated with the smooth cylinder. Refer to 5.001 CFE CONTACT LINE . Valve 2 remains open during all subsequent operations.
2.	Valve 1 and Knob 1 are associated with the pinning cylinder. Refer to 5.001 CFE CONTACT LINE . Valve 1 remains open during all subsequent operations.
3.	Bubbles in the fluid reservoirs are expected and a normal occurrence. No action is necessary other than fluid deployment as described below. Once deployed, the bubbles will find their way to the surface and pop during the background test.

Start Video Activity

1.5 PD100 Camcorder → ON

1.6 Voice into the PD100 Camcorder GMT, "Background Test", "CFE Contact Line 1(2)", and the module temperature from the PCS ECLSS page.

CFE Contact Line 1.7 With one hand supporting CFE Contact Line 1(2), gently pull Valve 2 to hard stop. High resistance may be encountered.

1.8 Slowly Turn Knob 2 CCW to stop at approximately 1/4 to 1/2 turn per second (approx. 40 revolutions, requires up to 2 to 3 minutes).

1.9 √CFE Contact Line 1(2) fluid has been fully dispensed into the smooth cylinder.

CAUTION	
	CFE Contact Line 1(2) fluid leakage may occur around the valves, and/or the piston.

1.10 √CFE Contact Line 1(2) for visible leakage

If leakage

Wipe with Dry Wipes.

2.002 CFE CONTACT LINE TEST OPERATIONS

(podfall000364)

Page 3 of 21 pages

If leakage continues,
* | | √ **POIC** to report leakage

CFE Contact Line 1.11 With one hand supporting CFE Contact Line 1(2), gently pull Valve 1 to hard stop. High resistance may be encountered.

1.12 Slowly Turn Knob 1 CCW to stop at approximately 1/4 to 1/2 turn per second (approx. 40 revolutions, requires up to 2 to 3 minutes).

1.13 √CFE Contact Line 1(2) fluid has been fully dispensed into the pinning cylinder.

CAUTION

CFE Contact Line 1(2) fluid leakage may occur around the valves, and/or the piston.

1.14 √CFE Contact Line 1(2) for visible leakage

If leakage
|
Wipe with Dry Wipes.

If leakage continues,
* | | √ **POIC** to report leakage

1.15 Zoom in the PD100 Camcorder so that the small Field of View is recorded. Refer to [5.002 CFE CONTACT LINE SMALL FIELD OF VIEW](#).

1.16 Voice observations (into recording PD100 Camcorder) concerning symmetry of interface on pinning lip of pinning cylinder and presence and approximate size of any bubbles.

1.17 √PD100 Camcorder recording CFE Contact Line 1(2) small Field of View
Refer to [5.002 CFE CONTACT LINE SMALL FIELD OF VIEW](#).

1.18 Allow video recording to continue for approximately 10 minutes or for the remainder of tape.
This first 10 minutes comprises the CFE Background test, and the experiment setup should remain undisturbed during this period.

End Video Activity

- 1.19 PD100 Camcorder → OFF
Eject Mini DVCAM Tape (used)
sw Mini DVCAM Tape → Save
- 1.20 Label Mini DVCAM Tape BACKGROUND and include approximate GMT.
- 1.21 Tmpy stow :
Mini DVCAM Tape (used)

2. CFE TAP TEST

- 2.1 Visually inspect the vessel to determine if the pinning lip is dry. In general, a dry pinning lip diffracts light in such a manner that it is not possible to clearly see through the pinning lip in profile. Refer to [5.013 CFE PINNING LIP COMPARISON](#)
If the pinning lip needs to be cleared of fluid at any time during this step,
Perform [step 11](#) and then resume this step where exited.
- 2.2 ✓#10 fastener is securely tightened.
- 2.3 Retrieve:
Mini DVCAM Tape (new)
Install Mini DVCAM Tape (new) in PD100 Camcorder.
- 2.4 ✓REC Lamp — Off
✓Sony emblem is covered
✓PD100 Camcorder viewing CFE Contact Line 1(2) small Field of View
Refer to [5.002 CFE CONTACT LINE SMALL FIELD OF VIEW](#)

CAUTION

1. The solitary Taps should begin very lightly and increase over time, but never to the point the pinning cylinder interface is destabilized or the fluid interfaces break up or bubbles form. Clearing the pinning edge takes considerable time and will reduce time for operations.
2. Time must be allowed after each Tap for the fluid motion to fully decay (damp out, settle, etc.) or science will be lost.
3. Each repeated Tap applied to the CFE Contact Line 1(2) must be in the same location, between the test cylinders, behind the CFE Contact Line 1(2), and within the Field of View without impairing the back lighting if this is possible. A tap location other than centered between the test chambers will not impart equal disturbances to each test chamber.

NOTE

NOTE

1. The solitary Taps increase in magnitude and may increase to the point of a medium knock. Never rap with knuckles. A Tap of a given magnitude is repeated once before increasing the magnitude of the Tap.
2. The small high frequency damped oscillations of the interface that result from solitary Tap will be recorded by video.
3. Valve 1 and Valve 2 remain open (extended) during the CFE test.

Start Video Activity

2.5 PD100 Camcorder → ON

2.6 Voice into the PD100 Camcorder GMT, "Tap Test", "CFE Contact Line 1(2)", and the module temperature from the PCS ECLSS page.

2.7 Using pad of index finger, very lightly apply one solitary Tap at the center of the backside of CFE Contact Line 1(2).

Using the PD100 Camcorder, voice observations of the fluid response.

Operator must wait at least 15 seconds after each tap.

Repeat Tap one time.

2.8 Repeat [step 2.7](#) with a medium tap.

2.9 Repeat [step 2.7](#) with a hard tap.

End Video Activity

2.10 PD100 Camcorder → OFF
Eject Mini DVCAM Tape(used)
sw Mini DVCAM Tape → Save

2.11 Label Mini DVCAM Tape TAP and include approximate GMT.

2.12 Tmpy stow:
Mini DVCAM Tape (used)

3. [CFE AXIAL TEST](#)

3.1 Visually inspect the vessel to determine if the pinning lip is dry. In general, a dry pinning lip diffracts light in such a manner that it is not possible to clearly see through the pinning lip in profile.

Refer to [5.013 CFE PINNING LIP COMPARISON](#).

If the pinning lip needs to be cleared of fluid at any time during this step,

Perform [step 11](#) and then resume this step where exited.

3.2 √#10 fastener is securely tightened

3.3 Retrieve:

Mini DVCAM Tape (new)

Install Mini DVCAM Tape (new) in PD100 Camcorder.

3.4 √PD100 Camcorder viewing CFE Contact Line 1(2) small Field of View

√Sony emblem is covered

√REC Lamp – Off

√Camera view in front face of CFE Contact Line vessel is orthogonal.

Refer to [5.002 CFE CONTACT LINE SMALL FIELD OF VIEW](#).

CAUTION

1. The Axial disturbances should be very small to start and increase gradually with each disturbance. The disturbance should never be large enough to destabilize the pinning cylinder interface, form bubbles, or break-up the fluid interfaces. Clearing the pinning edge takes considerable time and will reduce time for operations.
2. Time must be allowed after each Axial disturbance for the fluid motion to fully decay (damp out, settle, etc.) or science will be lost.

NOTE

1. An axial mode disturbance is created by deflecting and releasing the MWA much like a diver on a spring board. The disturbance will excite axial oscillation modes on the liquid surfaces in the cylinders.
2. Special care must be taken to impart the disturbance quickly. The action should be to depress the MWA with an immediate release to avoid seeing one disturbance from deflecting the MWA and another disturbance when releasing it.
3. Valve 1 and Valve 2 remain open (extended) during the CFE test.

Start Video Activity

3.5 PD100 Camcorder → ON

3.6 Voice into the PD100 Camcorder GMT, "Axial Test", "CFE Contact Line 1(2)", and the module temperature from the PCS ECLSS page.

3.7 Beginning with extremely weak deflections, using finger, depress and release the MWA (using MWA as cantilever) to impart an axial mode disturbance to the interfaces (much like a diver on a diving board)

Operator must wait at least 15 seconds after each axial disturbance.

□ Repeat disturbance with approximately same deflection.

3.8 Repeat [step 3.7](#) with increased disturbance amplitude until it is perceived that further increases in disturbance amplitude will de-pin interface or eject liquid droplets from surface.

End Video Activity

- 3.9 PD100 Camcorder → OFF
Eject Mini DVCAM Tape (used).
sw Mini DVCAM Tape → Save
- 3.10 Label Mini DVCAM Tape AXIAL TEST and include approximate GMT.
- 3.11 Tmpy stow:
Mini DVCAM Tape (used)

4. CFE PUSH TEST

- 4.1 Visually inspect the vessel to determine if the pinning lip is dry. In general, a dry pinning lip diffracts light in such a manner that it is not possible to clearly see through the pinning lip in profile. Isolated drops in the pinning lip may be tolerated if they do not touch surfaces of the cylinder below the pinning lip.
Refer to [5.013 CFE PINNING LIP COMPARISON](#).
If the pinning lip needs to be cleared of fluid at any time during this step,
Perform [step 11](#) and then resume this step where exited.
- 4.2 Loosen, but do not remove, the #10 Fastener that secures the CFE Contact Line 1(2) to the Maintenance Work Area through the slot in the base plate, such that the CFE Contact Line 1(2) may slide smoothly left to right in field of view without excess slop.
- 4.3 Retrieve:
Mini DVCAM Tape (new)
Install a Mini DVCAM Tape (new) in PD100 Camcorder.
- 4.4 ✓PD100 Camcorder viewing CFE Contact Line 1(2) small Field of View is zoomed out to show entire range of motion.
✓Sony emblem is covered
✓REC LAMP – Off
✓Camera view in front face of CFE Contact Line vessel is orthogonal
Refer to [5.002 CFE CONTACT LINE SMALL FIELD OF VIEW](#).

CAUTION

1. The Push should begin very light and increase gradually with each Push, but never to the point the pinning cylinder interface is de-pinned or the fluid interfaces break up or bubbles form. Clearing the pinning edge takes considerable time and will reduce time for operations.
2. Time must be allowed after each Push for the fluid motion to fully decay or science will be lost.

NOTE

1. The Push disturbance is a half period oscillation and is introduced when the Push stops abruptly and the fluid experiences a larger amplitude lateral impulse.
2. Valve 1 and Valve 2 remain open (extended) during the CFE test.
3. It is desirable to avoid abrupt impacts with the ends of the slot to reduce the risk of de-pinning the interface in the pinning cylinder.
4. Each push test and its repeat will be accomplished by pushing the CFE Contact Line 1(2) to the left, waiting the full 15 seconds, and then pushing it back to the right again waiting the full 15 seconds at the completion of motion.
5. Drift after a push can be minimized by readjusting the #10 fastener prior to each push as necessary.

Start Video Activity

4.5 PD100 Camcorder → ON

4.6 Voice into the PD100 Camcorder GMT, "Push Test", "CFE Contact Line 1(2)", and the module temperature from the PCS ECLSS page.

4.7 Very slowly slide the CFE Contact Line 1(2) right close to the end of the mounting slot. Avoid abrupt impact with slot end.
Do not disturb the interface.

Operator must wait at least 15 seconds before proceeding.

4.8 With a finger on the right hand side of the CFE Contact Line 1(2), lightly push the CFE Contact Line 1(2) left at an approximately constant rate a distance of 10mm. Avoid abrupt impact with slot end.

Using the PD100 Camcorder, voice the event.

Using the PD100 Camcorder, voice observations of the fluid response.

Drift and/or rotation may occur at the end of motion and is acceptable and should remain untouched for the prescribed time delay.

Operator must wait at least 15 seconds after each push disturbance.

With a finger on the left hand side of the CFE Contact Line 1(2), lightly push the CFE Contact Line 1(2) right at an approximately constant rate a distance of 10mm. Avoid abrupt impact with slot end

Using the PD100 Camcorder, voice the event.

Using the PD100 Camcorder, voice observations of the fluid response.

Drift and/or rotation may occur at the end of motion and is acceptable and should remain untouched for the prescribed time delay.

⌌ Operator must wait at least 15 seconds after each push disturbance.

If interesting or noticeably different behavior between cylinders results,
Repeat Push up to two times.

4.9 Repeat [step 4.8](#) moving 15 mm each time.

4.10 Repeat [step 4.8](#) moving 20 mm each time.

4.11 Repeat [step 4.8](#) moving 25 mm each time.

4.12 Repeat [step 4.8](#) moving 30 mm each time.

End Video Activity

4.13 PD100 Camcorder → OFF
Eject Mini DVCAM Tape (used).
sw Mini DVCAM Tape → Save

4.14 Label Mini DVCAM Tape PUSH and include approximate GMT.

4.15 Tmpy stow:
Mini DVCAM Tape (used)

5. [CFE SLIDE TEST](#)

5.1 Visually inspect the vessel to determine if the pinning lip is dry. In general, a dry pinning lip diffracts light in such a manner that it is not possible to clearly see through the pinning lip in profile. Isolated drops in the pinning lip may be tolerated if they do not touch surfaces of the cylinder below the pinning lip.

Refer to [5.013 CFE PINNING LIP COMPARISON](#).

If the pinning lip needs to be cleared of fluid at any time during this step,
Perform [step 11](#) and then resume this step where exited.

5.2 Loosen, but do not remove, the #10 Fastener that secures the CFE Contact Line 1(2) to the Maintenance Work Area through the slot in the base plate, such that the CFE Contact Line 1(2) may slide smoothly left to right in field of view without excess slop.

5.3 Retrieve:
Mini DVCAM Tape (new)
Install a Mini DVCAM Tape (new) in PD100 Camcorder.

- 5.4 ✓PD100 Camcorder viewing CFE Contact Line 1(2) small Field of View is zoomed out to show entire range of motion.
✓Sony emblem is covered
✓REC LAMP – Off

Refer to [5.002 CFE CONTACT LINE SMALL FIELD OF VIEW](#).

CAUTION

1. Begin with a weak Slide. The Slides should not increase to the point the pinning cylinder interface is de-pinned or the fluid interfaces break up or bubbles form. Clearing the pinning edge takes considerable time and will reduce time for operations.
2. Time must be allowed after each Slide test for the fluid motion to fully decay or science will be lost.

NOTE

1. A Slide is a one period lateral oscillation, (back and forth), completed within the Field of View at the approximate natural frequency of the interface (predicted to be approximately 1.5-2 Hz). Crew must identify the approximate natural frequency during operations.
2. Valve 1 and Valve 2 remain open (extended) during the CFE test.
3. It is desirable to avoid hitting the ends of the slot to reduce the risk of depinning the interface.
4. Drift after a slide can be minimized by readjusting the #10 fastener prior to each slide as necessary.
5. Each Slide applied to the CFE Contact Line 1(2) must be in same orientation (left to right) across the FIELD OF VIEW, with the same grip on the CFE Contact Line 1(2).

Start Video Activity

- 5.5 PD100 Camcorder → ON
- 5.6 Voice into the PD100 Camcorder GMT, "Slide Test", "CFE Contact Line 1(2)", and the module temperature from the PCS ECLSS page.
- 5.7 Very slowly slide the CFE Contact Line 1(2) right, close to the end of the mounting slot. Avoid abrupt impact with slot end.
Do not disturb the interface.
Operator must wait at least 15 seconds before proceeding.
- 5.8 Lightly Slide CFE Contact Line 1(2) in Field of View laterally (left to right) one period a distance of about 10mm (peak to peak amplitude). Avoid abrupt impact with slot ends.
Using the PD100 Camcorder, voice the event.
Using the PD100 Camcorder, voice observations of the fluid response.

Drift and/or rotation may occur at the end of motion and is acceptable and should remain untouched for the prescribed time delay.

Operator must wait at least 15 seconds after each slide disturbance.

LL Repeat one time.

If interesting or noticeably different behavior between cylinders results,

Repeat Slide up to two times.

5.9 Repeat [step 5.8](#) moving 15 mm each time.

5.10 Repeat [step 5.8](#) moving 20 mm each time.

5.11 Repeat [step 5.8](#) moving 25 mm each time.

5.12 Repeat [step 5.8](#) moving 30 mm each time.

6. [CFE MULTI-SLIDE TEST](#)

6.1 Visually inspect the vessel to determine if the pinning lip is dry. In general, a dry pinning lip diffracts light in such a manner that it is not possible to clearly see through the pinning lip in profile. Isolated drops in the pinning lip may be tolerated if they do not touch surfaces of the cylinder below the pinning lip.

Refer to [5.013 CFE PINNING LIP COMPARISON](#)

If the pinning lip needs to be cleared of fluid at any time during this step,

Perform [step 11](#) and then resume this step where exited.

6.2 Loosen, but do not remove, the #10 Fastener that secures the CFE Contact Line 1(2) to the Maintenance Work Area through the slot in the base plate, such that the CFE Contact Line 1(2) may slide smoothly left to right in field of view without excess slop.

CAUTION

1. Begin with a weak multiple, lateral oscillation, (back and forth). The Slides should not increase to the point the pinning cylinder interface is de-pinned or the fluid interfaces break up or bubbles form. Clearing the pinning edge takes considerable time and will reduce time for operations.
2. Time must be allowed after each Multi-Slide Test for the fluid motion to fully decay or science will be lost.

NOTE

1. A Slide is now defined as multiple (2, 3, 4) period lateral oscillations completed within the Field of View, at the approximate natural frequency of the interface (predicted to be approximately 1.5-2 Hz). Crew must identify the approximate natural frequency during operations.

NOTE

2. Valve 1 and Valve 2 remain open (extended) during the CFE test.
3. It is desirable to avoid hitting the ends of the mounting slot to avoid the risk of de-pinning the interface.
4. Drift after a multi-slide can be minimized by readjusting the #10 fastener prior to each multi-slide as necessary.
5. Each multiple oscillation Slide applied to the CFE Contact Line 1(2) must be in same orientation (left to right) across the FIELD OF VIEW, with the same grip on the CFE Contact Line 1(2).

6.3 Voice into the PD100 Camcorder GMT, "Multi-Slide Test", "CFE Contact Line 1(2)", and the module temperature from the PCS ECLSS page.

6.4 Slide CFE Contact Line 1(2) two full cycles with a peak to peak distance of about 10mm in the Field of View. Avoid abrupt impact with slot ends.

Using the PD100 Camcorder, voice the event.

Using the PD100 Camcorder, voice observations of the fluid response.

Drift and/or rotation may occur at the end of motion and is acceptable and should remain untouched for the prescribed time delay.

Operator must wait at least 15 seconds after each slide disturbance.

Repeat Multi-Slide one time.

If interesting or noticeably different behavior between cylinders results,

Repeat multiple Slide up to two times.

6.5 Repeat [step 6.4](#) moving 15 mm each time.

6.6 Repeat [step 6.4](#) moving 20 mm each time.

6.7 Repeat [step 6.4](#) moving 25 mm each time.

6.8 Repeat [step 6.4](#) moving 30 mm each time.

6.9 As video tape allows, continue Slides of increasing number of oscillations (3, 4), being careful to avoid depinning the interface.

End Video Activity

6.10 PD100 Camcorder → OFF
Eject Mini DVCAM Tape (used).
sw Mini DVCAM Tape → Save

6.11 Label Mini DVCAM Tape SLIDE and include approximate GMT.

- 6.12 Tmpy stow:
Mini DVCAM Tape (used)

7. [CFE SWIRL TEST](#)

- 7.1 Visually inspect the vessel to determine if the pinning lip is dry. In general, a dry pinning lip diffracts light in such a manner that it is not possible to clearly see through the pinning lip in profile. Isolated drops in the pinning lip may be tolerated if they do not touch surfaces of the cylinder below the pinning lip.

Refer to [5.013 CFE PINNING LIP COMPARISON](#).

Perform the first swirl test with a dry pinning lip. The remaining swirl tests may be performed with a wet pinning lip.

If the pinning lip needs to be cleared of fluid for the first test, Perform [step 11](#) and then resume this step where exited.

- 7.2 Retrieve
Mini DVCAM Tape (new)

Install a Mini DVCAM Tape (new) in PD100 Camcorder.

- 7.3 ✓PD100 Camcorder viewing CFE Contact Line 1(2) small FIELD OF VIEW is zoomed out to show full range of motion

✓Sony emblem is covered

✓REC LAMP – Off

Refer to [5.002 CFE CONTACT LINE SMALL FIELD OF VIEW](#).

CAUTION

1. Begin with a single period Swirl at the approximate natural Swirl frequency, increasing the number of Swirl cycles for subsequent tests (1, 5, and 10 cycles). The decay of the Swirl perturbations to the fluid interfaces will be recorded on video. Try not to excite the surfaces to the point the pinning cylinder interface is depinned or fluid interfaces break up or bubbles form. Clearing the pinning edge takes considerable time and will reduce time for operations.
2. Time must be allowed after each Swirl for the fluid motion to fully decay or science will be lost.

NOTE

1. Swirl is a swirling slosh mode that may be induced into the fluid using an elliptical or circular sliding motion of the CFE Contact Line 1(2) in the plane of the Maintenance Work Area. A Swirl disturbance diameter is based on the natural frequency and will be determined by the crew during operations. It is expected to be no greater than 30 to 40 mm. When increasing the number of cycles in subsequent tests, try to keep at natural frequency of fluid. Note also that the Swirl frequency is likely to be lower than the previously tested Slide frequency.
2. Valve 1 and Valve 2 remain open (extended) during the CFE test.

NOTE

3. Each Swirl applied to the CFE Contact Line 1(2) must be in same orientation across the camera FIELD OF VIEW, with the same grip on the CFE Contact Line 1(2).

MWA

- 7.4 Remove and Tmpy stow #10 Fastener while holding with one hand the CFE Contact Line 1(2) to the MWA surface.

Start Video Activity

- 7.5 PD100 Camcorder → ON

- 7.6 Voice into the PD100 Camcorder GMT, "Swirl Test", "CFE Contact Line 1(2)", and the module temperature from the PCS ECLSS page.

- 7.7 Complete a one cycle Swirl using CFE Contact Line 1(2) in the Field of View with a Swirl diameter of about 30 to 40mm or less. Perform the swirl holding CFE Contact Line 1(2) against the MWA and release to free float when cycle(s) are complete.

Using the PD100 Camcorder, voice the event.

Using the PD100 Camcorder, voice observations of the fluid response.

Drift and/or rotation may occur at the end of motion and is acceptable and should remain untouched for the prescribed time delay.

Operator must wait at least 60 seconds after each swirl disturbance.

- Repeat Swirl one time.

If interesting or noticeably different behavior between cylinders results,

Repeat Swirl up to two times.

- 7.8 Repeat [step 7.7](#) with a five cycle Swirl.

- 7.9 Repeat [step 7.7](#) with a ten cycle Swirl.

- 7.10 Attach CFE Contact Line 1(2) to Maintenance Work Area using #10 Fastener.

End Video Activity

- 7.11 PD100 Camcorder → OFF
Eject Mini DVCAM Tape (used).
sw Mini DVCAM Tape → Save

- 7.12 Label Mini DVCAM Tape SWIRL and include approximate GMT.

- 7.13 Tmpy Stow:
Mini DVCAM Tape (used)

8. [CFE DISPLACEMENT TEST](#)

- 8.1 Visually inspect the vessel to determine if the pinning lip is dry. In general, a dry pinning lip diffracts light in such a manner that it is not possible to clearly see through the pinning lip in profile. Isolated drops in the pinning lip may be tolerated if they do not touch surfaces of the cylinder below the pinning lip.

Refer to [5.013 CFE PINNING LIP COMPARISON](#).

Perform the first displacement test with a dry pinning lip. The remaining displacement tests may be performed with a wet pinning lip.

If the pinning lip needs to be cleared of fluid for the first test, Perform [step 11](#) and then resume this step where exited.

- 8.2 Loosen, but do not remove, the #10 Fastener that secures the CFE Contact Line 1(2) to the Maintenance Work Area through the slot in the base plate, such that the CFE Contact Line 1(2) may slide smoothly left to right in field of view without excess slop.

- 8.3 Retrieve
Mini DVCAM Tape (new)

Install a Mini DVCAM Tape (new) in PD100 Camcorder.

- 8.4 ✓Sony emblem is covered
✓REC LAMP – Off

Position the PD100 Camcorder for CFE Contact Line 1(2) tall Field of View.

Refer to [5.003 CFE CONTACT LINE TALL FIELD OF VIEW](#).

CAUTION

Time must be allowed after each Displacement for the fluid motion to fully decay or science will be lost.

NOTE

1. Displacement (abrupt start-stop) is accomplished by fairly rapid translation of the CFE Contact Line 1(2) to the degree that the pinning interface is destabilized. This is the first test where the interfaces are intentionally destabilized. A few drops and bubbles may be produced.
2. The test begins with light displacements which increase in vigor during the test sequence.
3. Interface disturbances caused by Displacement may take longer to damp out, three minutes predicted.
4. Valve 1 and Valve 2 remain open (extended) during the CFE test.
5. Drift after a restrained displacement can be minimized by readjusting the #10 fastener prior to each restrained displacement as necessary.
6. Try not to displace so significantly that the liquid moves a cylinder diameter distance above the pinning lip.

NOTE

7. Each displacement applied to the CFE Contact Line 1(2) must be in same orientation across the camera FIELD OF VIEW, with the same grip on the CFE Contact Line 1(2).

Start Video Activity

8.5 PD100 Camcorder → ON

8.6 Voice into the PD100 Camcorder GMT, "Displacement Test", "CFE Contact Line 1(2)", and the module temperature from the PCS ECLSS page.

8.7 Displace in Field of View location (light abrupt start/stop) large enough to destabilize the pinned interface.
Using the PD100 Camcorder, voice the event.
Using the PD100 Camcorder, voice observations of the fluid response.
Drift and/or rotation may occur at the end of motion and is acceptable and should remain untouched for the prescribed time delay.
Operator must wait at least three minutes after each displacement disturbance.

— Repeat one time.

8.8 Repeat [step 8.7](#) with a medium abrupt start/stop.

MWA

8.9 Remove and Tmpy stow #10 Fastener while holding with one hand the CFE Contact Line 1(2) to the MWA surface.

8.10 Repeat [step 8.7](#) three times, increasing vigor of disturbance with each Displacement. Maintain motion within field of view while sliding across MWA. Perform Displacement and release CFE Contact Line 1(2) to free float.

8.11 As video tape allows, continue with displacement, being careful to avoid large bubble formation.
Alternate methods of displacement (suggest combination Slide and Swirl) at crew discretion.
If interesting observation noted,
Try to repeat it.

8.12 Attach CFE Contact Line 1(2) to Maintenance Work Area using #10 Fastener.

End Video Activity

8.13 PD100 Camcorder → OFF
Eject Mini DVCAM Tape (used).
sw Mini DVCAM Tape → Save

8.14 Label Mini DVCAM Tape DISPLACEMENT and include approximate GMT.

8.15 Tmpy Stow:
Mini DVCAM Tape (used)

9. CFE BUBBLES TEST

NOTE

The pinning lip does not need to be cleared for this test.

9.1 Retrieve:
Mini DVCAM Tape (new)

Insert Mini DVCAM Tape (new) into PD100 Camcorder.

9.2 ✓PD100 Camcorder viewing CFE Contact Line 1(2) tall Field of View
✓Sony emblem is covered
✓REC LAMP – Off

Refer to [5.003 CFE CONTACT LINE TALL FIELD OF VIEW](#).

NOTE

1. Each Bubble test applied to the CFE Contact Line 1(2) must be in same orientation across the camcorder Field of View, with the same grip on the CFE Contact Line 1(2). At first only a small number of large diameter Bubbles should be developed via light agitation.
2. Bubbles are created by shaking the CFE Contact Line 1(2). If you see something interesting, try to repeat it.
3. Valve 1 and Valve 2 remain open (extended) during the CFE test.

Start Video Activity

9.3 PD100 Camcorder → ON

9.4 Voice into the PD100 Camcorder GMT, "Bubbles Test", "CFE Contact Line 1(2)", and the module temperature from the PCS ECLSS page.

9.5 Remove #10 Fastener from Maintenance Work Area and Tmpy stow to allow the CFE Contact Line 1(2) to be held in hand(s).

Agitate (shake) the CFE Contact Line 1(2) within the field of view of PD100 Camcorder (number of bubbles is approximately 1 to 3). Reattach the CFE Contact Line 1(2) to Maintenance Work Area using #10 Fastener.

Using the PD100 Camcorder, voice observations of the fluid response.

Allow resulting Bubbles of both cylinders to coalesce up to 4 minutes continuing to voice observations. Not all bubbles will coalesce.

2.002 CFE CONTACT LINE TEST OPERATIONS

(podfall000364)

Page 18 of 21 pages

Using crew discretion, return rogue drops to fluid mass and force bubbles to coalesce using centrifugal force if necessary.

- └─ Repeat Bubble generation technique within the Field of View of Camcorder with similar number of Bubbles.
Repeat anything unusual.

9.6 Repeat [step 9.5](#) up to ten times, increasing number of bubbles each time until reaching as close to a foam like state as possible.
Repeat anything unusual.

9.7 Attach CFE Contact Line 1(2) to Maintenance Work Area using #10 Fastener.

End Video Activity

9.8 PD100 Camcorder → OFF
Eject Mini DVCAM Tape (used).
sw Mini DVCAM Tape → Save

9.9 Label Mini DVCAM Tape BUBBLES and include approximate GMT.

9.10 Tmpy stow:
Mini DVCAM Tape(used)

10. [CFE DRAINAGE](#)

10.1 Visually inspect the vessel to determine if the pinning lip is dry. In general, a dry pinning lip diffracts light in such a manner that it is not possible to clearly see through the pinning lip in profile.
Refer to [5.013 CFE PINNING LIP COMPARISON](#).
If the pinning lip needs to be cleared of fluid at any time during this step,
Perform [step 11](#) and then resume this step where exited.

10.2 ✓#10 fastener is securely tightened

10.3 Retrieve:
Mini DVCAM Tape (new).
Insert a Mini DVCAM Tape (new) in PD100 Camcorder.

10.4 ✓Sony emblem is covered
✓REC LAMP – Off
✓PD100 Camcorder viewing CFE Contact Line 1(2) small FIELD OF VIEW is zoomed out to show full range of motion
Refer to [5.005 CFE CONTACT LINE CHAMBER FIELD OF VIEW](#).

Start Video Activity

10.5 PD100 Camcorder → ON

2.002 CFE CONTACT LINE TEST OPERATIONS

(podfall000364)

Page 19 of 21 pages

- 10.6 Voice into the PD100 Camcorder GMT, "Drainage Test", "CFE Contact Line 1(2)", and the module temperature from the PCS ECLSS page.
- 10.7 ✓CFE Contact Line 1(2) Valve 2 is open, (valve pulled out to hard stop)
- 10.8 Remove the fluid as fast as possible by turning Knob 2 CW without ingesting air into the reservoir. Retraction of the fluid at the end of the process should be very slow, to avoid ingesting air into the fluid reservoir. Not all of the fluid will be removed.
- 10.9 With one hand supporting CFE Contact Line 1(2), gently push Valve 2 to overcome high resistance to hard stop (closed).
- 10.10 ✓CFE Contact Line 1(2) Valve 1 is open, valve pulled out to (valve pulled out to hard stop)
- 10.11 Remove the fluid as fast as possible by turning Knob 1 CW without ingesting air into the reservoir. Retraction of the fluid at the end of the process should be very slow, to avoid ingesting air into the fluid reservoir. Not all of the fluid will be removed.
- 10.12 With one hand supporting CFE Contact Line 1(2), Gently push Valve 1 to overcome high resistance to hard stop (closed).

End Video Activity

- 10.13 PD100 Camcorder → OFF
Eject Mini DVCAM Tape (used).

sw Mini DVCAM Tape → Save

- 10.14 Label Mini DVCAM Tape DRAINAGE and include approximate GMT.
- 10.15 Stow:
Mini DVCAM Tapes (nine)

11. CFE DRYING THE PINNING LIP

NOTE

1. This process could take up to 15 minutes per attempt and may take several tries to get right, but is critical to achieving the science goals.
2. The most challenging aspect of the centrifuge method is slowing down smoothly without disturbing the pinning lip.
3. Liquid remaining in the groove serving as the pinning lip of the

NOTE

pinning cylinder should be cleared as needed. It is preferred that this liquid be moved to the base of the cylinder, clearing it by any force deemed acceptable.

4. Drops of fluid on the test chamber wall above the pinning lip are not a problem and may be ignored.
5. Small isolated drops residing in the pinning lip are also not a problem if they are clearly not touching the pinning cylinder walls below the pinning lip.

- 11.1 Remove test vessel from MWA and use centrifuge method (see movie clip for Mike Fincke's method). A higher angular velocity will likely be required to clear the pinning lip.
- 11.2 If the previous effort does not clear the pinning lip perform the following:
- 11.3 Drain the pinning cylinder by turning Knob 1 CW, without ingesting air bubbles into the reservoir.
- 11.4 With one hand supporting CFE Contact Line 1(2), gently push Valve 1 to overcome high resistance to hard stop (closed).
- 11.5 Remove #10 Fastener from Maintenance Work Area and tmpy stow to allow the CFE Contact Line 1(2) to be held in hand(s).
- 11.6 Use impulse type disturbances to the vessel (jerks, 'bonks', whatever, etc.) to clear the fluid in the pinning lip and hopefully move it below the pinning lip.
- 11.7 A combination of centrifugal force with impulse disturbances may be required to clear the pinning lip.
- 11.8 Use something like the Fincke centrifuge method to return the fluid in the Smooth cylinder to the base of the cylinder.
- 11.9 Gently re-secure CFE vessel to the MWA using the #10 fastener.
- 11.10 Visually inspect the test chambers for any fingerprints. Use a dry wipe to remove any if found.
- 11.11 With one hand supporting CFE Contact Line 1(2), gently pull Valve 1 to hard stop. High resistance may be encountered.
- 11.12 Slowly Turn Knob 1 CCW to stop at approximately 1/4 to 1/2 turn per second (approx. 40 revolutions, requires up to 2 to 3 minutes).

2.002 CFE CONTACT LINE TEST OPERATIONS

(podfall000364)

Page 21 of 21 pages

11.13 √CFE Contact Line 1(2) fluid has been fully dispensed into the pinning cylinder.

11.14 Continue operations.

RESTOW TOOLS, PARTS, MATERIALS AS REQUIRED TO ORIGINAL LOCATIONS,
EXCEPT FOR:

Mini DVCAM Tape [9] P/N SED33111489-305 TO: CTB, for return to Houston

2.003 CFE TEARDOWN

(podfall000364)

Page 1 of 2 pages

OBJECTIVE:

Capillary Flow Experiment (CFE). This procedure stows the CFE experiment and its supporting equipment.

STATION PARTS:

CFE Contact Line 1 P/N 60083MA00100
CFE Contact Line 2 P/N 60083MA00200
CFE Interior Corner Flow 1 P/N 60083MA40100
CFE Interior Corner Flow 2 P/N 60083MA40200
CFE Vane Gap 1 P/N 60083MA20100
CFE Vane Gap 2 P/N 60083MA20200
Ziploc Bags (stowed in foam)
Foam (stowed in CFE)

STATION TOOLS:

MWA Work Surface Area P/N SEG33110270-301
MWA Utility Kit P/N SJG33110310-301
Multi-Use Bracket(s) P/N SEG33107631-301
IP Clamp P/N SEG33111394-30X
PD100 Camcorder P/N SEZ16103293-301
Digital CC Video/Power IF Cable P/N SED33111490-303
Fine Point Sharpie P/N 528-40674-1
IP Clamp P/N SEG33111394-30x

NOTE

Contact Line vessels have dedicated foam boxes. Interior Corner Flow and Vane Gap vessels do not and were packed using loose pieces of foam. Steps below referring to the foam are referring to the Contact Line foam boxes.

1. Unstow:
Ziploc Bags
Foam
2. Remove inner Ziploc Bag from Outer Ziploc bag.
Tmpry stow both bags.

- MWA Work Surface Area
3. Remove #10 Fastener from **Contact Line 1(Contact Line 2,Interior Corner Flow 1,Interior Corner Flow 2,Vane Gap 1,Vane Gap 2)** and Tmpry stow # 10 Fastener.
 4. Remove **Contact Line 1(Contact Line 2,Interior Corner Flow 1,Interior Corner Flow 2,Vane Gap 1,Vane Gap 2)** from Maintenance Work Surface Area.
 5. Insert **Contact Line 1(Contact Line 2,Interior Corner Flow 1,Interior Corner Flow 2,Vane Gap 1,Vane Gap 2)** into inner Ziploc Bag.
Seal inner Ziploc Bag.

6. Insert **Contact Line 1(Contact Line 2,Interior Corner Flow 1,Interior Corner Flow 2,Vane Gap 1,Vane Gap 2)** into outer Ziploc Bag such that Ziploc seal is at opposing ends of vessel.
Seal outer Ziploc Bag.
7. Insert **Contact Line 1(Contact Line 2,Interior Corner Flow 1,Interior Corner Flow 2,Vane Gap 1,Vane Gap 2)** into foam.
8. Stow:
Contact Line 1(Contact Line 2,Interior Corner Flow 1,Interior Corner Flow 2,Vane Gap 1,Vane Gap 2)

MWA Utility Kit 9. Stow:
#10 Fastener

10. √CFE tape has been removed from PD100 Camcorder and stowed.
11. Remove Sony emblem cover from PD100 Camcorder.
Dispose of Sony emblem cover.

PD100 Camcorder 12. sel Menu
sel Etc, Others
sel REC Lamp
REC Lamp → ON
√REC Lamp – On

13. Remove Printer Paper (RIM) and Aluminum Tape.
Dispose of Printer Paper (RIM) and Aluminum Tape in ISS trash.
14. Stow:
MWA Utility Kit
Multi-Use Bracket(s)
IP Clamp
PD100 Camcorder
Digital CC Video/Power IF Cable
Fine Point Sharpie

RESTOW TOOLS, PARTS, AND MATERIALS AS REQUIRED TO ORIGINAL LOCATIONS EXCEPT FOR:

MWA Utility Kit TO: Stowage List
Multi-Use Bracket(s) TO: Stowage List
PD100 Camcorder TO: Stowage List
Digital CC Video/Power IF Cable TO: Stowage List
Fine Point Sharpie TO: Stowage List
IP Clamp TO: Stowage List
Contact Line 1(Contact Line 2,Interior Corner Flow 1,Interior Corner Flow 2,Vane Gap 1,Vane Gap 2) TO: Stowage List

2.004 CFE INTERIOR CORNER FLOW TEST OPERATIONS

(cfe1all000036)

Page 1 of 13 pages

OBJECTIVE:

Capillary Flow Experiments (CFE). The objectives of CFE Interior Corner Flow are to record the passive capillary driven redistribution of liquid in a container in low-g due to the specific fluid properties and 3-D geometry of the container. The digitized video will be compared with current theory. Tests will also be performed to note the spontaneous phase separation characteristics of such flows when bubbles are introduced into the liquid.

PARTS:

CFE Interior Corner Flow 1 P/N 60083MA40100

CFE Interior Corner Flow 2 P/N 60083MA40200

Mini DVCAM Tape (per execution note) P/N SED33111489-305

TOOLS:

MWA Work Surface Area P/N SEG33110270-301

MWA Utility Kit P/N SJG33110310-301

Fine Point Sharpie P/N 528-40674-1

PD100 Camcorder P/N SEZ16103293-301

MATERIALS:

Dry Wipe

Gray Tape - crew choice

1. INTERIOR CORNER FLOW CAMERA SETUP

- 1.1 Unstow: Mini DVCAM Tape (per execution note)
Tm pry stow close to PD100 Camcorder.
Insert Mini DVCAM Tape into PD100 Camcorder.

- 1.2 ✓#10 fastener is securely tightened.

NOTE

The camera view and the front face of the Interior Corner Flow vessel should be orthogonal.

- PD100 Camcorder 1.3 ✓PD100 Camcorder for CFE Interior Corner Flow 1(2)
entire Field of View

Refer to [5.008 CFE INTERIOR CORNER FLOW FIELD OF VIEW](#)

✓REC Lamp — Off

✓Sony emblem is covered

✓PD100 Camcorder view is orthogonal to the front face of the
Interior Corner Flow vessel.

Gauge by eye.

Start Video Activity

- 1.4 PD100 Camcorder → On

- CFE Interior Corner Flow 1.5 Open VALVE 2 (1/4 turn CCW to hard stop)

- 1.6 Turn KNOB 1 CCW to prime the tube between VALVE 2 and vertex
of the test chamber. Add fluid to the point the liquid interface

2.004 CFE INTERIOR CORNER FLOW TEST OPERATIONS

(cfe1all000036)

Page 2 of 13 pages

reaches the end of the tube without injecting fluid into the test chamber.

Refer to [5.009 CFE INTERIOR CORNER FLOW CHAMBER PRIMING LOCATION](#)

1.7 Close VALVE 2 (1/4 turn CW to hard stop).

2. [DRY SURFACE TEST](#)

CAUTION

Dry Surface Test is not repeatable.

2.1 Voice into the PD100 Camcorder GPS time, " Dry Surface Test", "CFE Interior Corner Flow 1(2)", and the module temperature from the PCS ECLSS page.

2.2 Open VALVE 1 (1/4 turn CCW to hard stop).

CAUTION

As the fluid is dispensed into the test chamber, the process for turning the knob needs to remain rapid and as nearly steady and continuous as possible or a loss of science may occur.

NOTE

Several small bubbles may form in the transport line and reservoir during the initial fill. These initial bubbles are unavoidable and are acceptable.

2.3 In a fairly rapid but continuous manner, turn KNOB 1 CCW to hard stop at approximately 1-2 revolutions per second (approximately 10 revolutions, requires up to 5 to 10 seconds).

2.4 √CFE Interior Corner Flow 1(2) fluid has been fully dispensed into the test chamber.

CAUTION

CFE Interior Corner Flow 1(2) fluid leakage may occur around the valves, and/or the piston.

2.5 √CFE Interior Corner Flow 1(2) for visible leakage (without moving the unit or obscuring the camera field of view)

If leakage, wipe with Dry Wipes.

* If leakage continues,

√**POIC** to report leakage

NOTE

The fluid movement is expected to take about 2 minutes, but 3 minutes of recording is requested to ensure no loss of science. The desired science is in the movement of the fluid to the equilibrium position—a slow migration of fluid from the base to the 'top' (vertex) of the container.

- 2.6 With hands off the vessel, observe the flow of the fluid from the base of the test chamber to the vertex (top), and voice observations of general fluid behavior, (bubbles if any, etc.) into the PD100 Camcorder.

Refer to [5.011 CFE INTERIOR CORNER FLOW EQUILIBRIUM PATTERNS](#) for expected final fluid configuration.

- 2.7 Wait 3 minutes to allow the fluid to reach its equilibrium condition.

End Video Activity

PD100 Camcorder 2.8

PD100 Camcorder → Off

3. [WET SURFACE TESTS](#)

- 3.1 √PD100 Camcorder for CFE Interior Corner Flow 1(2) entire Field of View

Refer to [5.008 CFE INTERIOR CORNER FLOW FIELD OF VIEW](#)

√REC Lamp — Off

√Sony emblem is covered

√PD100 Camcorder view is orthogonal to the front face of the Interior Corner Flow vessel.

Gauge by eye.

- 3.2 Use tape or paper to mark the footprint of the Interior Corner Flow vessel on the MWA surface so that it can easily be returned to approximately the same position.

Provide two pieces of tape at diagonally opposite corners of the base plate to provide temporary restraint during repeated removal/install cycles in this step and the next.

- 3.3 Remove #10 Fastener and temp stow. Use tape to secure the vessel to the MWA

Start Video Activity

- 3.4 PD100 Camcorder → On

- 3.5 Voice into the PD100 Camcorder: GPS time, "Wet Surface Tests 1(2)", "CFE Interior Corner Flow 1(2)" and the module temperature from the PCS ECLSS page.

2.004 CFE INTERIOR CORNER FLOW TEST OPERATIONS

(cfe1all000036)

Page 4 of 13 pages

- 3.6 Remove the vessel from the MWA and use Jeff Williams' CFE centrifuge method to relocate the fluid to the base of the vessel. As gently as possible, return the vessel to the MWA within five seconds and reattach using the tape. Minor bumps on contact are acceptable. Try to place the vessel back to its original position when reattaching to the MWA. Do not adjust the vessel position after placement back onto the MWA.
- 3.7 Without obstructing the camera view, observe the flow of the fluid from the base of the test chamber to the vertex (top), and voice observations of general fluid behavior, (bubbles if any, etc.) into the PD100 Camcorder.

Refer to [5.011 CFE INTERIOR CORNER FLOW EQUILIBRIUM PATTERNS](#) for expected final fluid configuration.

- 3.8 Wait 3 minutes for fluid to reach its equilibrium condition.

- 3.9 Repeat [step 3.6](#) to [step 3.8](#).

End Video Activity

PD100 Camcorder

3.10 PD100 Camcorder → Off

4. [LOOP TESTS](#)

- 4.1 Open VALVE 2 (1/4 turn CCW to hard stop)
√VALVE 1 – Open

Start Video Activity

- 4.2 PD100 Camcorder → On
- 4.3 Voice into the PD100 Camcorder, GPS time, "Interior Corner Flow Loop Tests", "CFE Interior Corner Flow 1(2)" and the module temperature from the PCS ECLSS page.
- 4.4 Remove the vessel from the MWA and use Jeff Williams' CFE centrifuge method to relocate the fluid to the base of the vessel. As gently as possible, return the vessel to the MWA within five seconds and reattach using the tape. Minor bumps on contact are acceptable. Try to place the vessel back to its original position when reattaching to the MWA. Do not adjust the vessel position after placement back onto the MWA.
- 4.5 Without obstructing the camera view, observe the flow of the fluid from the base of the test chamber to the vertex (top), and voice observations of general fluid behavior, (bubbles if any, etc.) into the PD100 Camcorder.

Refer to [5.011 CFE INTERIOR CORNER FLOW EQUILIBRIUM PATTERNS](#) for expected final fluid configuration.

4.6 Wait 3 minutes for fluid to reach its equilibrium condition.

4.7 Repeat [step 4.4](#) to [step 4.6](#).

End Video Activity

4.8 PD100 Camcorder → Off

4.9 Retrieve the #10 fastener and re-secure the CFE Interior Corner Flow vessel to the MWA.

5. [SLOSH TESTS](#)

5.1 ✓PD100 Camcorder for CFE Interior Corner Flow 1(2) entire Field of View

Refer to [5.008 CFE INTERIOR CORNER FLOW FIELD OF VIEW](#)

✓REC Lamp – Off

✓Sony emblem is covered

5.2 Close VALVE 2 (1/4 turn CW to hard stop).

5.3 ✓All fluid from reservoir dispensed into test chamber
Close VALVE 1 (1/4 turn CW to hard stop).

Start Video Activity

5.4 PD100 Camcorder → On

5.5 Voice into PD100 Camcorder: GPS time, "Interior Corner Flow Slosh Tests", "CFE Interior Corner Flow 1(2)", and module temperature from the PCS ECLSS page.

5.6 Loosen #10 fastener securing Interior Corner Flow to MWA Work Surface Area allowing vessel to slide laterally in the field of view while remaining flush with the MWA Work Surface Area.

5.7 Using a variety of lateral slides (left to right in field of view) on the MWA Work Surface Area, laterally oscillate the Interior Corner Flow vessel (i.e. approximately 10 complete cycles), at the approximate natural frequency of the fluid surface (crew determined on orbit), to reorient the fluid in the test chamber to the point of forming large bubbles.

An observable redistribution of the fluid from the vertex to the base of the container is expected.

5.8 Before removing hands from vessel,

✓Vessel is orthogonal to the camera

Lightly tighten the #10 fastener to keep the vessel snug to the MWA.

2.004 CFE INTERIOR CORNER FLOW TEST OPERATIONS

(cfe1all000036)

Page 6 of 13 pages

- 5.9 Remove hands from the vessel and observe the return of the fluid to equilibrium.

Voice observations into PD100 Camcorder.

Refer to [5.011 CFE INTERIOR CORNER FLOW EQUILIBRIUM PATTERNS](#) for expected final fluid configuration.

- 5.10 Wait 3 minutes for the fluid to reach its equilibrium condition.

- 5.11 Repeat [step 5.6](#) to [step 5.10](#), increasing the lateral slide frequency to approximately double the natural frequency which was determined during the first set of lateral slides.

Repeat once increasing the lateral slide frequency to approximately triple the natural frequency or as high as possible by hand.

End Video Activity

- 5.12 PD100 Camcorder → Off
Eject Mini DVCAM Tape (used)
sw Mini DVCAM Tape → Save

- 5.13 Label Mini DVCAM Tape: CFE ICF Test and include GPS time.

- 5.14 Tmpy stow : Mini DVCAM Tape (used)

6. [BUBBLE SHAKE TEST](#)

- 6.1 Retrieve: Mini DVCAM Tape (new)
Install Mini DVCAM Tape (new) in PD100 Camcorder

- 6.2 ✓PD100 Camcorder for CFE Interior Corner Flow 1(2) entire Field of View

Refer to [5.008 CFE INTERIOR CORNER FLOW FIELD OF VIEW](#)

✓REC Lamp — Off

✓Sony emblem is covered

✓PD100 Camcorder view is orthogonal to the front face of the Interior Corner Flow vessel.

Gauge by eye.

- 6.3 ✓All fluid is in the test chamber
✓VALVE 1, VALVE 2 — closed

- 6.4 Use tape or paper to mark the footprint of the Interior Corner Flow vessel on the MWA surface so that it can easily be returned to approximately the same position.

Provide two pieces of tape at diagonally opposite corners of the base plate to provide temporary restraint during repeated removal/install cycles in this step and the next.

2.004 CFE INTERIOR CORNER FLOW TEST OPERATIONS

(cfe1all000036)

Page 7 of 13 pages

- 6.5 Remove #10 fastener and temp stow. Use tape to secure the vessel to the MWA.

Start Video Activity

- 6.6 PD100 Camcorder → On

- 6.7 Voice into the PD100 Camcorder: GPS time, Interior Corner Flow Bubble Shake Tests", "CFE Interior Corner Flow 1(2) and the module temperature from the PCS ECLSS page.

- 6.8 Remove the vessel from the MWA and shake vessel vigorously in a manner that produces bubbles (in field of view if possible).

As gently as possible, return the vessel to the MWA within five seconds and reattach using the tape. Minor bumps on contact are acceptable. Try to place the vessel back to its original position when reattaching to the MWA. Do not adjust the vessel position after placement back onto the MWA.

- 6.9 Without obstructing the camera view, observe the return of the fluid to equilibrium, including phase separation and coalescence (If any) Voice observations into PD100 Camcorder.

Refer to [5.011 CFE INTERIOR CORNER FLOW EQUILIBRIUM PATTERNS](#) for expected final fluid configuration.

- 6.10 Wait 5 to 15 minutes for the fluid to reach its equilibrium condition.

- 6.11 Repeat [step 6.8](#) to [step 6.10](#), as many times as Mini DVCAM Tape allows.

End Video Activity

- 6.12 PD100 Camcorder → Off
Eject Mini DVCAM Tape (used)
sw Mini DVCAM Tape → Save

- 6.13 Label Mini DVCAM Tape: CFE- Bubble Shake Test and include GPS time.

- 6.14 Tmpy stow: Mini DVCAM Tape (used)

7. [BUBBLE RESERVOIR TEST](#)

- 7.1 Retrieve: Mini DVCAM Tape (new)
Install Mini DVCAM Tape (new) in PD100 Camcorder

- 7.2 ✓PD100 Camcorder for CFE Interior Corner Flow 1(2) entire Field of View

Refer to [5.008 CFE INTERIOR CORNER FLOW FIELD OF VIEW](#)

✓REC Lamp — Off

2.004 CFE INTERIOR CORNER FLOW TEST OPERATIONS

(cfe1all000036)

Page 8 of 13 pages

- √Sony emblem is covered
- √PD100 Camcorder view is orthogonal to the front face of the Interior Corner Flow vessel.
- Gauge by eye.

- 7.3 Use tape or paper to mark the footprint of the Interior Corner Flow vessel on the MWA surface so that it can easily be returned to approximately the same position.

Provide two pieces of tape at diagonally opposite corners of the base plate to provide temporary restraint during repeated removal/install cycles in this step.

Start Video Activity

- 7.4 PD100 Camcorder → On

- 7.5 Open VALVE 2 (1/4 turn CCW to hard stop)

√VALVE 1 — closed

- 7.6 Turn KNOB 1 CW at a rate of approximately 1-2 revolutions per second. This withdrawal rate should ingest air into the transport tubes and reservoir. Turn KNOB 1 CW until the bottom of the piston reaches the Fill Line noted on the reservoir. The intent is to get both air and liquid into the reservoir.

- 7.7 Close VALVE 2 (1/4 turn CW to hard stop)
Open VALVE 1 (1/4 turn CCW to hard stop)

- 7.8 Remove #10 fastener and temp stow. Use tape to secure the vessel to the MWA.

- 7.9 Voice into the PD100 Camcorder: "GPS time, Interior Corner Flow Bubble Reservoir Tests", "CFE Interior Corner Flow 1(2) and the module temperature from the PCS ECLSS page.

- 7.10 Remove the Interior Corner Flow vessel from the MWA and shake vessel vigorously in a manner that produces bubbles (in field of view if possible).

- 7.11 As gently as possible, return the vessel to the MWA within five seconds and reattach using the tape. Minor bumps on contact are acceptable. Try to place the vessel back to its original position when reattaching to the MWA. Do not adjust the vessel position after placement back onto the MWA.

In a fairly rapid but continuous manner, turn KNOB 1 CCW to hard stop at approximately 1-2 revolutions per second (approximately 10 revolutions, requires up to 5 to 10 seconds).

2.004 CFE INTERIOR CORNER FLOW TEST OPERATIONS

(cfe1all000036)

Page 9 of 13 pages

- 7.12 Remove hands from vessel and observe the return of the fluid to equilibrium, including phase separation and coalescence (If any) Voice observations into PD100 Camcorder.

Refer to [5.011 CFE INTERIOR CORNER FLOW EQUILIBRIUM PATTERNS](#) for expected final fluid configuration.

- 7.13 Wait 10 to 15 minutes for the fluid to reach its equilibrium condition.

- 7.14 Close VALVE 1 (1/4 turn CW to hard stop).

- 7.15 Repeat [step 7.5](#) to [step 7.14](#), as many times as Mini DVCAM Tape allows.

End Video Activity

- 7.16 PD100 Camcorder → Off
Eject Mini DVCAM Tape (used)
sw Mini DVCAM Tape → Save

- 7.17 Label Mini DVCAM Tape: CFE- Bubble Res Test and include GPS time.

- 7.18 Tmpary stow : Mini DVCAM Tape (used)

8. [FOAM SHAKE TEST](#)

- 8.1 Retrieve: Mini DVCAM Tape (new)
Install Mini DVCAM Tape (new) in PD100 Camcorder

- 8.2 √PD100 Camcorder for CFE Interior Corner Flow 1(2) entire Field of View

Refer to [5.008 CFE INTERIOR CORNER FLOW FIELD OF VIEW](#)

√REC Lamp — Off

√Sony emblem is covered

√PD100 Camcorder view is orthogonal to the front face of the Interior Corner Flow vessel.

Gauge by eye.

- 8.3 √All fluid is in the test chamber
Close VALVE 1 (1/4 turn CW to hard stop)
Close VALVE 2 (1/4 turn CW to hard stop)

- 8.4 Use tape or paper to mark the footprint of the Interior Corner Flow vessel on the MWA surface so that it can easily be returned to approximately the same position.

Provide two pieces of tape at diagonally opposite corners of the base plate to provide temporary restraint during repeated removal/install cycles in this step.

2.004 CFE INTERIOR CORNER FLOW TEST OPERATIONS

(cfe1all000036)

Page 10 of 13 pages

- 8.5 Remove #10 fastener and temp stow. Use tape to secure the vessel to the MWA.

Start Video Activity

- 8.6 PD100 Camcorder → On
- 8.7 Voice into the PD100 Camcorder: "GPS time, Interior Corner Flow Foam Shake Tests, "CFE Interior Corner Flow 1(2) and the module temperature from the PCS ECLSS page.
- 8.8 Remove the vessel from the MWA and shake vessel vigorously in a manner that produces foam (many small bubbles) in field of view if possible. Select the shake direction which produces the best foam.
- As gently as possible, return the vessel to the MWA within five seconds and reattach using the tape. Minor bumps on contact are acceptable. Try to place the vessel back to its original position when reattaching to the MWA. Do not adjust the vessel position after placement back onto the MWA.
- 8.9 Without obstructing the camera view, observe the return of the fluid to equilibrium, including phase separation and coalescence (If any)
- Voice observations into PD100 Camcorder
- Refer to [5.011 CFE INTERIOR CORNER FLOW EQUILIBRIUM PATTERNS](#) for expected final fluid configuration.
- 8.10 Wait 5 to 15 minutes for the fluid to reach its equilibrium condition.
- 8.11 Repeat [step 8.8](#) to [step 8.10](#) as many times as Mini DVCAM Tape allows. The operator should try different shake directions to find the best foam and should also investigate the use of centrifugal force to locate the foam in the base of the test chamber.

End Video Activity

- 8.12 PD100 Camcorder → Off
Eject Mini DVCAM Tape (used)
sw Mini DVCAM Tape → Save
- 8.13 Label Mini DVCAM Tape: CFE Foam Shake Test and include GPS time.
- 8.14 Tmpy stow : Mini DVCAM Tape (used)
- 8.15 Retrieve the #10 fastener and re-secure the CFE Interior Corner Flow vessel to the MWA.

9. [FOAM RESERVOIR TEST](#)

2.004 CFE INTERIOR CORNER FLOW TEST OPERATIONS

(cfe1all000036)

Page 11 of 13 pages

- 9.1 Retrieve: Mini DVCAM Tape (new)
Install Mini DVCAM Tape (new) in PD100 Camcorder
- 9.2 ✓PD100 Camcorder for CFE Interior Corner Flow 1(2) entire Field of View
Refer to [5.008 CFE INTERIOR CORNER FLOW FIELD OF VIEW](#)
✓REC Lamp – Off
✓Sony emblem is covered
✓PD100 Camcorder view is orthogonal to the front face of the Interior Corner Flow vessel.
Gauge by eye.
- 9.3 Use tape or paper to mark the footprint of the Interior Corner Flow vessel on the MWA surface so that it can easily be returned to approximately the same position.

Provide two pieces of tape at diagonally opposite corners of the base plate to provide temporary restraint during repeated removal/install cycles in this step.

Start Video Activity

- 9.4 PD100 Camcorder → On
- 9.5 Open VALVE 2 (1/4 turn CCW to hard stop).
✓VALVE 1 – Closed
- 9.6 Turn KNOB 1 CW at a rate of approximately 1-2 revolutions per second. This withdrawal rate should ingest air and most of the fluid into the transport tubes and reservoir. Turn KNOB 1 CW until the bottom of the piston reaches the Fill Line noted on the reservoir. Continue turning KNOB 1 CW until the bottom of the piston is about twice as high as the Fill Line. The intent is to get equal parts air and liquid into the reservoir.
- 9.7 Close VALVE 2 (1/4 turn CW to hard stop)
Open VALVE 1 (1/4 turn CCW to hard stop)
- 9.8 Remove #10 Fastener and temp stow. Use tape to secure the vessel to the MWA.
- 9.9 Voice into the PD100 Camcorder: GPS time, Interior Corner Flow Foam Reservoir Tests", "CFE Interior Corner Flow 1(2) and the module temperature from the PCS ECLSS page.
- 9.10 Remove the Interior Corner Flow vessel from the MWA and shake vessel vigorously in a manner that produces foam (in field of view if possible).
- 9.11 As gently as possible, return the vessel to the MWA within five seconds and reattach using the tape. Minor bumps on contact are

2.004 CFE INTERIOR CORNER FLOW TEST OPERATIONS

(cfe1all000036)

Page 12 of 13 pages

acceptable. Try to place the vessel back to its original position when reattaching to the MWA. Do not adjust the vessel position after placement back onto the MWA.

In a fairly rapid but continuous manner, turn KNOB 1 CCW to hard stop at approximately 1-2 revolutions per second (approximately 20 revolutions, requires up to 10 to 15 seconds).

- 9.12 Remove hands from vessel and observe the return of the fluid to equilibrium, including phase separation and coalescence (If any) Voice observations into PD100 Camcorder

Refer to [5.011 CFE INTERIOR CORNER FLOW EQUILIBRIUM PATTERNS](#) for expected final fluid configuration.

- 9.13 Wait 10 to 15 minutes for the fluid to reach its equilibrium condition.

- 9.14 Close VALVE 1 (1/4 turn CW to hard stop)

- 9.15 Repeat [step 9.5](#) to [step 9.14](#) as many times as Mini DVCAM Tape allows. The operator should try different shake directions to find the best foam and may also investigate varying the amount of air in the test chamber.

End Video Activity

- 9.16 PD100 Camcorder → Off
Eject Mini DVCAM Tape (used)
sw Mini DVCAM Tape → Save

- 9.17 Label Mini DVCAM Tape: CFE- Foam Res Test and include GPS time.

- 9.18 Tmpy stow : Mini DVCAM Tape (used)

- 9.19 Retrieve the #10 fastener and re-secure the CFE Interior Corner Flow vessel to the MWA.

10. [DRAINAGE](#)

- 10.1 Open VALVE 2 (1/4 turn CCW to hard stop)

√VALVE 1 — closed

NOTE

Additional ingestion of bubbles into the transport line is not desirable at this point and may be minimized by reducing the rate of liquid withdrawal. Small flow reversals might help recover from bubble ingestion events. Bubbles already in the transport lines should be ignored.

2.004 CFE INTERIOR CORNER FLOW TEST OPERATIONS

(cfe1all000036)

Page 13 of 13 pages

- 10.2 Slowly turn KNOB 1 CW, withdrawing the fluid contents back into the reservoir to the approximate condition of the initial pre-primed state.

Refer to [5.008 CFE INTERIOR CORNER FLOW FIELD OF VIEW](#)

- 10.3 Close VALVE 2 (1/4 turn CW to hard stop).

- 10.4 VALVE 1, VALVE 2 — closed

- 10.5 Notify **POIC** of tape serial number and/or sequence number for each used tape.

- 10.6 Stow:

Mini DVCAM Tape (per execution note, used)
CFE Interior Corner Flow

RESTOW TOOLS, PARTS, MATERIALS AS REQUIRED TO ORIGINAL LOCATIONS
EXCEPT FOR:

Mini DVCAM Tape (per execution note) P/N SED33111489-305 TO: For return to
Houston

2.005 CFE VANE GAP 1 TEST OPERATIONS

(cfe1all000037)

Page 1 of 29 pages

OBJECTIVE:

Capillary Flow Experiments (CFE). The objective of this experiment is to observe fluid interface and critical wetting behavior in a cylindrical chamber with elliptic cross-section and an adjustable central vane. The critical vane-gap wetting phenomenon occurs at a critical vane angle where the fluid rises all the way up the vane gap. Vane Gap 1 provides a collection of data points for a perfectly wetting surface. Vane Gap 2 provides a collection of data points for a partially wetting surface. These two cases provide a reasonable approximation of the most common fluids stored in tanks for spaceflight applications.

STATION PARTS:

CFE Vane Gap 1 P/N 60083MA20100

Mini DVCAM Tape (per execution note) P/N SED33111489-305

STATION TOOLS:

MWA Work Surface Area P/N SEG33110270-301

MWA Utility Kit P/N SJG33110310-301

Fine Point Sharpie P/N 528-40674-1

PD100 Camcorder P/N SEZ16103293-301

1/8" L-Wrench (2 1/4" length) P/N AW4

STATION MATERIALS:

Dry Wipe

Gray Tape (crew preference)

NOTE

1. This procedure contains Near Real - Time video downlink or LAB VTR recording requirements.
2. AOS may be required for **POIC** to configure on board system for downlink of science or LAB VTR recording.
3. Minimize fingerprints within chamber field of view.
4. Bubbles in the fluid reservoirs are expected and a normal occurrence. No action is necessary other than fluid deployment as described below. Once deployed, the bubbles will find their way to the surface and pop during subsequent testing.

1. VANE GAP 1 BACKGROUND TEST

- 1.1 Unstow: Mini DVCAM Tape (per execution note)
Tm pry stow close to PD100 Camcorder.
Insert Mini DVCAM Tape into PD100 Camcorder.

- 1.2 √#10 Fastener is securely tightened

CAUTION

The camera view and the front face of the Vane Gap 1 vessel should be orthogonal or loss of science may occur.

- 1.3 √PD100 Camcorder for CFE Vane Gap 1 entire Field of View

2.005 CFE VANE GAP 1 TEST OPERATIONS

(cfe1all000037)

Page 2 of 29 pages

Refer to [5.010 CFE VANE GAP CHAMBER FIELD OF VIEW](#)

√REC Lamp — Off

√Sony emblem is covered

√Vane Position - 180 degrees

√PD100 Camcorder view is orthogonal to the front face of the CFE Vane Gap 1 vessel

Gauge by eye checking both the top view and the side view

CAUTION

After the fluid is dispensed into the elliptic test chamber, care should be taken not to disturb (i.e. adjust) the CFE Vane Gap 1 Vessel. Loss of science will occur if the vessel is disturbed and agitated during the background run. The Background run is not repeatable.

Start Video Activity

1.4 PD100 Camcorder → ON

1.5 Voice into the PD100 Camcorder GPS time, "Background Test", "CFE Vane Gap 1", and the module temperature from the PCS ECLSS page.

CFE Vane Gap 1.6 With one hand supporting CFE Vane Gap 1, gently pull VALVE 1 to hard stop.

1.7 Slowly turn KNOB 1 CCW at approximately $\frac{1}{4}$ to $\frac{1}{2}$ turn per second to stop. (Approximately 46 revolutions, requires up to 3 minutes).

1.8 √CFE Vane Gap 1 fluid has been fully dispensed into the test chamber.

CAUTION

CFE Vane Gap 1 fluid leakage may occur around the valve and/or the piston.

1.9 √CFE Vane Gap 1 for visible leakage

If leakage,

 | Wipe with Dry Wipes.

 | If leakage continues,

* | | √ **POIC** to report leakage

- 1.10 Voice observations about the fluid into recording PD100 Camcorder. (Include comments about the symmetry of the fluid in front of the vane relative to the fluid behind the vane).

If the fluid is not symmetric,

Use the pad of index finger and lightly tap the backside of the vessel within the PD100 Camcorder field of view (if possible).

Voice approximate number, size and location of any bubbles present.

- 1.11 √PD100 Camcorder recording CFE Vane Gap 1 Field of View

Refer to [5.010 CFE VANE GAP CHAMBER FIELD OF VIEW](#)

End Video Activity

PD100 Camcorder 1.12 PD100 Camcorder → Off

2. [VANE GAP 1 CW DRY TEST](#)

CAUTION

Special care should be taken to avoid any disturbances larger than a tap since the CW Dry Test is not repeatable.

NOTE

1. All references to critical vane gap wetting are specific to the vane gap on the front face of the vessel nearest the camera. Critical wetting does occur for the vane gap on the back face of the vessel, but is not pertinent to the crew procedures. The vane angles are selected to investigate the approach to the critical wetting angle and not the departure.
2. Vane angle adjustments are made by smoothly turning the Vane Position Indicator. An approximate 2 degree backlash is present on the Vane Position Indicator and it may be necessary to overturn the Vane Position Indicator approximately 2 degrees to establish the desired angle once the Vane Position Indicator is released.
3. When rotating Vane Position Indicator, care should be taken to keep the Vane Position Indicator visible and unobstructed in the camera Field of View.
4. After each vane angle adjustment a series of taps are applied to the Vane Gap 1 vessel. The small high frequency damped oscillations of the interface that result from taps will be recorded by video. The taps should allow the interface to relax and achieve a more ideal equilibrium. Taps are defined as: a set of 4 finger taps on the back side of the Vane Gap vessel imparted at an approximate rate metered by each syllable of a one second count "one-one-thousand" (similar to finger taps on the side of a fish tank).
5. Approximately 10 seconds should be allowed after each set of taps for all interface disturbances to decay (damp out, settle, etc.). As the crew becomes accustomed to the sensitivity of the liquid surface to

NOTE

the finger taps, the taps may be applied as necessary to speed (or coax) the establishment of an equilibrium surface.

6. Each set of taps is applied to the back side of CFE Vane Gap 1 and must be in the same location within the Field of View if possible.
7. Nominal prescribed vane angles are provided with preset angle increment. Smaller angle increments (5deg) are used near the expected critical vane wetting angles (predicted to be approximately 60 and 225 degrees). However, true critical angles will be determined in flight and crew discretion is requested to determine vane angle increments as critical conditions are approached. Critical vane angle precision is not expected to be better than ± 5 deg, but may be improved as determined in flight by crew.
8. The critical vane gap wetting phenomena occurs at a critical vane angle where the fluid rises all the way up the vane gap. It is recommended that the crew note (i.e. by jotting down) the two experimentally determined critical vane angles (predicted to be approximately 60 and 225 degrees) during the first performance of the experiment to better anticipate vane angle increments during subsequent and repeat runs of the experiment.
9. The tap and wait process is repeated for each vane angle setpoint.
10. VALVE 1 remains open (extended) during all the CFE Vane Gap 1 tests.
11. If uncertain of PD100 Camcorder tape remaining time, replace tape as necessary.

- 2.1 Voice into the PD100 Camcorder GPS time, "CW Dry Test", "CFE Vane Gap 1" and the module temperature from the PCS ECLSS page.

- 2.2— Slowly rotate Vane Position Indicator CW to a Vane Position of 15 degrees.

Allow 30 sec for the fluid surface to stabilize.

Using pad of index finger, lightly apply taps at prescribed location on CFE Vane Gap 1.

Wait ten seconds while observing fluid surface response.

If the fluid surface changes shape or position after the set of taps,

Apply another set of taps and observe the fluid surface for any change in shape or position again waiting ten seconds.

If any change in shape occurs,

Repeat as necessary until fluid shape and position are stable.

2.005 CFE VANE GAP 1 TEST OPERATIONS

(cfe1all000037)

Page 5 of 29 pages

Using the PD100 Camcorder, voice observations of the fluid response.

Allow resulting interface oscillations (if any) to fully decay (settle, dampen, approximately 10 seconds) continuing to voice observations.

- └─ Repeat for the following vane positions: 30, 40, 45, 50, 55, 60, 65, 75, 90, 105, 120, 135, 150, 165, 180, 195, 210, 220, 225, 230, 235, 240, 245, 250, 265, 280, 295, 310, 325, 340, 0.

End Video Activity

PD100 Camcorder 2.3 PD100 Camcorder → Off
Eject Mini DVCAM Tape (used)
sw Mini DVCAM Tape → Save

2.4 Label Mini DVCAM Tape: CFE-Vane Gap 1 Background-CW Dry Test and include GPS time.

2.5 Tmpy stow : Mini DVCAM Tape (used)

3. VANE GAP 1 CW WET TESTS

3.1 Visually inspect the fluid in the vessel without moving it. There should not be any liquid in contact with the lid of the test chamber.. In general, the fluid should cover the base and rise partially up the walls of the test chamber forming a rather large meniscus.

If at any time during this step the fluid configuration departs from this state,

Perform [4.001 CFE VANE GAP FLUID RELOCATION](#) all, then:

3.2 ✓#10 fastener is securely tightened

3.3 Retrieve: Mini DVCAM Tape (new)
Install Mini DVCAM Tape (new) in PD100 Camcorder

CAUTION

The camera view and the front face of the Vane Gap 1 vessel should be orthogonal or loss of science may occur.

3.4 ✓PD100 Camcorder for CFE Vane Gap 1 entire Field of view
Refer to [5.010 CFE VANE GAP CHAMBER FIELD OF VIEW](#)
✓REC Lamp — Off
✓Sony emblem is covered
✓Vane position - 0 degrees
✓PD100 Camcorder view is orthogonal to the front face of the CFE Vane Gap 1 vessel
Gauge by eye checking both the top view and the side view

NOTE

2.005 CFE VANE GAP 1 TEST OPERATIONS

(cfe1all000037)

Page 6 of 29 pages

NOTE

All of the notes in step 2 apply to this step and should be reviewed if necessary.

Start Video Activity

3.5 PD100 Camcorder → ON

3.6 Voice into the PD100 Camcorder GPS time, "CW Wet Test 1", "CFE Vane Gap 1" and the module temperature from the PCS ECLSS page.

3.7 Repeat [step 2.2](#).

3.8 Voice into the PD100 Camcorder GPS time, "CW Wet Test 2", "CFE Vane Gap 1" and the module temperature from the PCS ECLSS page.

3.9 Repeat [step 2.2](#).

End Video Activity

PD100 Camcorder 3.10 PD100 Camcorder → Off
Eject Mini DVCAM Tape (used)
sw Mini DVCAM Tape → Save

3.11 Label Mini DVCAM Tape: CFE-Vane Gap 1 CW Wet Tests 1 and 2 and include GPS time.

3.12 Tmpy stow : Mini DVCAM Tape (used)

4. [VANE GAP 1 CCW WET TESTS](#)

4.1 Visually inspect the fluid in the vessel. There should not be any liquid in contact with the lid of the test chamber. In general, the fluid should cover the base and rise partially up the walls of the test chamber forming a rather large meniscus.

If at any time during this step the fluid configuration departs from this state,

Perform [4.001 CFE VANE GAP FLUID RELOCATION](#) all, then:

4.2 √#10 fastener is securely tightened

4.3 Retrieve: Mini DVCAM Tape (new)
Install Mini DVCAM Tape (new) in PD100 Camcorder

CAUTION

The camera view and the front face of the Vane Gap 1 vessel should be orthogonal or loss of science may occur.

- 4.4 ✓ PD100 Camcorder for CFE Vane Gap 1 entire Field of View
 Refer to [5.010 CFE VANE GAP CHAMBER FIELD OF VIEW](#)
 ✓ REC Lamp — Off
 ✓ Sony emblem is covered
 ✓ Vane position — 0 degrees
 ✓ PD100 Camcorder view is orthogonal to the front face of the CFE
 Vane Gap 1 vessel
 Gauge by eye checking both the top view and the side view

NOTE

All of the notes in step 2 apply to this step and should be reviewed if necessary.

Start Video Activity

- 4.5 PD100 Camcorder → On
- 4.6 Voice into the PD100 Camcorder GPS time, "CCW Wet Test 1(2)", "CFE Vane Gap 1", and the module temperature from the PCS ECLSS page.
- 4.7 Slowly rotate Vane Position Indicator CCW to a Vane Position of 340 degrees.
 Allow 30 sec for the fluid and surface to stabilize.
 Using pad of index finger, lightly apply taps at prescribed location on CFE Vane Gap 1.
 Wait ten seconds while observing fluid surface response.
 If the fluid surface changes shape or position after the set of finger taps,
 Apply another set of taps and observe the fluid surface for any change in shape or position again waiting ten seconds.
 If any change in shape occurs,
 Repeat as necessary until fluid shape and position is stable
- Using the PD100 Camcorder, voice observations of the fluid response.
 Allow resulting interface oscillations (if any) to fully decay (settle, dampen, approximately 10 seconds) continuing to voice observations.
- Repeat for the following vane positions: 325, 310, 295, 280, 265, 250, 245, 240, 235, 230, 225, 220, 210, 195, 180, 165, 150, 135, 120, 105, 90, 75, 65, 60, 55, 50, 45, 40, 30, 15, 0.)
- 4.8 Repeat [step 4.7](#)

End Video Activity

PD100 Camcorder 4.9 PD100 Camcorder → Off
Eject Mini DVCAM Tape (used)
sw Mini DVCAM Tape → Save

4.10 Label Mini DVCAM Tape: Vane Gap 1 CCW Wet Test and include GPS time.

4.11 Tmpy stow : Mini DVCAM Tape (used)

5. VANE GAP 1 CONTINUOUS ROTATION TESTS

5.1 Visually inspect the fluid in the vessel. There should not be any liquid in contact with the lid of the test chamber. In general, the fluid should cover the base and rise partially up the walls of the test chamber forming a rather large meniscus.

If at any time during this step the fluid configuration departs from this state

Perform [4.001 CFE VANE GAP FLUID RELOCATION](#) all, then:

5.2 ✓#10 fastener is securely tightened

5.3 Retrieve: Mini DVCAM Tape (new)
Install Mini DVCAM Tape (new) in PD100 Camcorder.

CAUTION

The camera view and the front face of the Vane Gap 1 vessel should be orthogonal or loss of science may occur.

5.4 ✓PD100 Camcorder for CFE Vane Gap 1 entire Field of view
Refer to [5.010 CFE VANE GAP CHAMBER FIELD OF VIEW](#).

✓REC Lamp – Off

✓Sony emblem is covered

✓PD100 Camcorder view is orthogonal to the front face of the CFE Vane Gap 1 vessel

Gauge by eye checking both the top view and the side view.

NOTE

1. For these tests a 1/8" L-wrench is taped to the Vane Position Indicator like a crank so that the vane can be rotated smoothly and nearly continuously by hand.
2. After taping 1/8" L-Wrench to Vane Position Indicator, the wrench should be able to clear KNOB 1 when revolved.
3. Care should be taken not to obstruct the camera field of view of the Vane Angle Indicator.
4. Crew should concentrate more on maintaining constant rate of

NOTE

revolution than on data observation for this test.

5. This test provides dynamic data for comparison to the static data collected in the previous tests.

5.5 Retrieve:

1/8" L-Wrench

Gray Tape

5.6 Tear off two pieces of Gray Tape approximately 2" by 1".

Lay the 1/8" L-Wrench flat across the top of Vane Position Indicator shaft, centering wrench on shaft with the short end of the wrench pointing out from the test chamber like a crank handle.

Refer to [5.012 CFE VANE GAP L-WRENCH SET-UP](#)

One at a time, place strips of gray tape over wrench and shaft, securing the wrench to the Vane Position Indicator. Add additional strips of tape as necessary to secure wrench.

5.7 Tmpy stow:

Gray Tape

5.8 √Vane Position - 0 degrees

Wait ten seconds for any fluid oscillations to dampen out.

Start Video Activity

5.9 PD100 Camcorder → On

5.10 Voice into the PD100 Camcorder GPS time, "CW Continuous Rotation Test", "CFE Vane Gap 1", and the module temperature from the PCS ECLSS page.

5.11 Using the 1/8" L-Wrench attached to the Vane Position Indicator, rotate the vane CW through 720 degrees, at a rate of 10 deg/sec (2 complete revolutions, approximately 36 seconds per revolution).

5.12 √Vane Position - 0 degrees

Wait ten seconds for any fluid oscillations to dampen out.

5.13 Voice into the PD100 Camcorder GPS time, "CCW Continuous Rotation Test", "CFE Vane Gap 1" and the module temperature from the PCS ECLSS page.

5.14 Using the 1/8" L-Wrench attached to the Vane Position Indicator, rotate the vane CCW through 720 degrees, at a rate of 10 deg/sec (2 complete revolutions, approximately 36 seconds per revolution).

End Video Activity

2.005 CFE VANE GAP 1 TEST OPERATIONS

(cfe1all000037)

Page 10 of 29 pages

PD100 Camcorder 5.15 PD100 Camcorder → Off
Eject Mini DVCAM Tape (used)
sw Mini DVCAM Tape → Save

5.16 Label Mini DVCAM Tape: Vane Gap 1 Continuous Rotation Tests and include GPS time.

5.17 Tmpy stow : Mini DVCAM Tape (used)

5.18 Carefully remove the 1/8" L-Wrench and gray tape from the Vane Position Indicator. Be gentle as the vane shaft is plastic. Remove the gray tape from the 1/8" L-Wrench and dispose of in ISS trash.

6. VANE GAP 1 STEADY STATE FIRST QUADRANT TEST

6.1 Visually inspect the fluid in the vessel. There should not be any liquid in contact with the lid of the test chamber. In general, the fluid should cover the base and rise partially up the walls of the test chamber forming a rather large meniscus.

If at any time during this step the fluid configuration departs from this state,

Perform [4.001 CFE VANE GAP FLUID RELOCATION](#) all, then:

6.2 ✓ #10 fastener is securely tightened.

6.3 Retrieve: Mini DVCAM Tape (new)
Install Mini DVCAM Tape (new) in PD100 Camcorder.

CAUTION

The camera view and the front face of the Vane Gap 1 vessel should be orthogonal or loss of science may occur.

6.4 ✓ PD100 Camcorder for CFE Vane Gap 1 entire Field of View
Refer to [5.010 CFE VANE GAP CHAMBER FIELD OF VIEW](#).

✓ REC Lamp — Off

✓ Sony emblem is covered

✓ Vane position — 0 degrees

✓ PD100 Camcorder view is orthogonal to the front face of the CFE Vane Gap 1 vessel. Gauge by eye checking both the top view and the side view.

NOTE

1. This test does not require any tapping to aid in fluid redistribution. The operator only needs to adjust the vane position and wait the prescribed time for each step without disturbing the vessel for each setpoint.

NOTE

2. Vane angle adjustments are made by smoothly turning the Vane Position Indicator. An approximate 2 degree backlash is present on the Vane Position Indicator and it may be necessary to overturn the Vane Position Indicator approximately 2 degrees to establish the desired angle once the Vane Position Indicator is released.
3. When rotating Vane Position Indicator, care should be taken to keep the Vane Position Indicator visible and unobstructed in the camera Field of View.
4. VALVE 1 remains open (extended) during all the CFE Vane Gap 1 tests.
5. If the PD100 Camcorder tape remaining time is less than the prescribed wait time for the next setpoint, replace the tape before changing to the next setpoint.

Start Video Activity

6.5 PD100 Camcorder → On

6.6 Voice into the PD100 Camcorder GPS time, "Steady State Test", "CFE Vane Gap 1", and the module temperature from the PCS ECLSS page.

6.7 Allow 1 minute for camcorder to record baseline condition.

6.8 Per the table below, slowly rotate Vane Position Indicator CW to the Vane Position listed and wait the prescribed time.

Using the PD100 Camcorder, voice observations of the fluid response.

Vane Position	Wait Time	Setpoint description
37	1 minute	Last symmetric surface
43	15 minutes	Small gap critical wetting
52	15 minutes	Last angle before large gap wetting
58	15 minutes	Large gap critical wetting
75	5 minutes	Enroute to 90

2.005 CFE VANE GAP 1 TEST OPERATIONS

(cfe1all000037)

Page 12 of 29 pages

Vane Position	Wait Time	Setpoint description
90	5 minutes	Full asymmetric equilibrium

Repeat for the remaining vane positions and wait times:

6.9 Per the table below, rotate Vane Position Indicator CCW to the Vane Position listed and wait the prescribed time.

Using the PD100 Camcorder, voice observations of the fluid response.

Vane Position	Wait Time	Setpoint Description
52	15 minutes	Large gap de-wetting
37	15 minutes	Small gap de-wetting
0	1 minute	Baseline

Repeat for the remaining vane positions and wait times:

End Video Activity

PD100 Camcorder → Off
Eject Mini DVCAM Tape (used)
sw Mini DVCAM Tape → Save

6.11 Label Mini DVCAM Tape: CFE Vane Gap 1 Steady State Test and include GPS time.

6.12 Tmpy stow : Mini DVCAM Tape (used)

7. VANE GAP 1 SYMMETRY TEST

7.1 Visually inspect the fluid in the vessel. There should not be any liquid in contact with the lid of the test chamber. In general, the fluid should cover the base and rise partially up the walls of the test chamber forming a rather large meniscus.

If at any time during this step the fluid configuration departs from this state,

Perform [4.001 CFE VANE GAP FLUID RELOCATION](#) all, then:

7.2 ✓ #10 fastener is securely tightened.

7.3 Retrieve: Mini DVCAM Tape (new)
Install Mini DVCAM Tape (new) in PD100 Camcorder.

CAUTION

The camera view and the front face of the Vane Gap 1 vessel should be orthogonal or loss of science may occur.

- 7.4 ✓PD100 Camcorder for CFE Vane Gap 1 entire Field of View
Refer to [5.010 CFE VANE GAP CHAMBER FIELD OF VIEW](#).

✓REC Lamp – Off

✓Sony emblem is covered

✓Vane position – 0 degrees

✓PD100 Camcorder view is orthogonal to the front face of the CFE Vane Gap 1 vessel. Gauge by eye checking both the top view and the side view.

NOTE

1. This test does not require any tapping to aid in fluid redistribution. The operator only needs to adjust the vane position and wait the prescribed time for each setpoint without disturbing the vessel.
2. Vane angle adjustments for this test are different than the other tests in this procedure. For this test only, a large change in position needs to occur in a short time. This will require gripping the Vane Position Indicator in a different manner to allow for a quick 90 degree rotation in one motion if possible. Multiple steps are acceptable, but the motion needs to be completed in two seconds.
3. An approximate 2 degree backlash is present on the Vane Position Indicator and it may be necessary to overturn the Vane Position Indicator approximately 2 degrees to establish the desired angle once the Vane Position Indicator is released.
4. When rotating Vane Position Indicator, care should be taken to keep the Vane Position Indicator visible and unobstructed in the camera Field of View when the motion is completed. Temporarily obstructing the view of the Vane Position Indicator while making this quick 90 degree rotation is acceptable.
5. VALVE 1 remains open (extended) during all the CFE Vane Gap 1 tests.
6. If the PD100 Camcorder tape remaining time is less than the prescribed wait time for the next setpoint, replace the tape before performing the next setpoint.

Start Video Activity

- 7.5 PD100 Camcorder → On

- 7.6 Voice into the PD100 Camcorder GPS time, "Symmetry Test ", "CFE Vane Gap 1", and the module temperature from the PCS ECLSS page.

7.7 Allow 1 minute for camcorder to record baseline condition.

7.8 Quickly rotate Vane Position Indicator CW to a Vane Position of 90 degrees. The motion must be completed in approximately two seconds or less including any fine adjustments. It is desirable to perform the position change in one continuous motion if possible.

Using the PD100 Camcorder, voice observations of the fluid response.

Wait 15 minutes. This will assure that the fluid achieves a steady state condition.

7.9 Quickly rotate Vane Position Indicator CCW to a Vane Position of 0 degrees. The motion must be completed in approximately two seconds or less including any fine adjustments. It is desirable to perform the position change in one continuous motion if possible.

Using the PD100 Camcorder, voice observations of the fluid response.

Wait 3 minutes. This will assure that the fluid achieves a steady state condition.

End Video Activity

PD100 Camcorder 7.10 PD100 Camcorder → Off
Eject Mini DVCAM Tape (used)
sw Mini DVCAM Tape → Save

7.11 Label Mini DVCAM Tape: CFE Vane Gap 1 Symmetry Test and include GPS time.

7.12 Tmpy stow : Mini DVCAM Tape (used)

8. VANE GAP 1 STEADY STATE FOURTH QUADRANT TEST

8.1 Visually inspect the fluid in the vessel. There should not be any liquid in contact with the lid of the test chamber. In general, the fluid should cover the base and rise partially up the walls of the test chamber forming a rather large meniscus.

If at any time during this step the fluid configuration departs from this state,

Perform [4.001 CFE VANE GAP FLUID RELOCATION](#) all, then:

8.2 ✓#10 fastener is securely tightened

8.3 Retrieve: Mini DVCAM Tape (new)
Install Mini DVCAM Tape (new) in PD100 Camcorder

CAUTION

The camera view and the front face of the Vane Gap 1 vessel should be orthogonal or loss of science may occur.

- 8.4 ✓PD100 Camcorder for CFE Vane Gap 1 entire Field of View
Refer to [5.010 CFE VANE GAP CHAMBER FIELD OF VIEW](#)
✓REC Lamp — Off
✓Sony emblem is covered
✓Vane position — 0 degrees
✓PD100 Camcorder view is orthogonal to the front face of the CFE Vane Gap 1 vessel. Gauge by eye checking both the top view and the side view.

NOTE

1. This test does not require any tapping to aid in fluid redistribution. The operator only needs to adjust the vane position and wait the prescribed time for each step without disturbing the vessel for each setpoint.
2. Vane angle adjustments are made by smoothly turning the Vane Position Indicator. An approximate 2 degree backlash is present on the Vane Position Indicator and it may be necessary to overturn the Vane Position Indicator approximately 2 degrees to establish the desired angle once the Vane Position Indicator is released.
3. When rotating Vane Position Indicator, care should be taken to keep the Vane Position Indicator visible and unobstructed in the camera Field of View.
4. VALVE 1 remains open (extended) during all the CFE Vane Gap 1 tests.
5. If the PD100 Camcorder tape remaining time is less than the prescribed wait time for the next setpoint, replace the tape before changing to the next setpoint.

- 8.5 PD100 Camcorder → On

Start Video Activity

- 8.6 Voice into the PD100 Camcorder GPS time, "Steady State Test 2 ", "CFE Vane Gap 1", and the module temperature from the PCS ECLSS page.

- 8.7 Allow 1 minute for camcorder to record baseline condition.

- 8.8 Per the table below, slowly rotate Vane Position Indicator CCW to the Vane Position listed and wait the prescribed time.

Using the PD100 Camcorder, voice observations of the fluid response.

2.005 CFE VANE GAP 1 TEST OPERATIONS

(cfe1all000037)

Page 16 of 29 pages

Vane Position	Wait Time	Setpoint description
335	1 minute	Intermediate symmetric
320	1 minute	Last symmetric surface
315	15 minutes	Global asymmetric shift
311	5 minutes	Small gap critical wetting
308	5 minutes	Large gap critical wetting
290	1 minute	Intermediate asymmetric
270	1 minute	Full asymmetric equilibrium

Repeat for the remaining vane positions and wait times:

8.9 Per the table below, slowly rotate Vane Position Indicator CW to the Vane Position listed and wait the prescribed time.

Using the PD100 Camcorder, voice observations of the fluid response.

Vane Position	Wait Time	Setpoint description
311	5 minutes	Large gap de-wetting
315	5 minutes	Small gap de-wetting
320	15 minutes	Global asymmetric shift
335	1 minute	Intermediate symmetric
0	3 minute	Baseline

Repeat for the remaining vane positions and wait times:

End Video Activity

2.005 CFE VANE GAP 1 TEST OPERATIONS

(cfe1all000037)

Page 17 of 29 pages

PD100 Camcorder 8.10 PD100 Camcorder → Off
Eject Mini DVCAM Tape (used)
sw Mini DVCAM Tape → Save

8.11 Label Mini DVCAM tape CFE Vane Gap 1 SS Q4 and include GPS time.

8.12 Tmpy stow : Mini DVCAM Tape (used)

9. VANE GAP 1 SYMMETRY TEST 2

9.1 Visually inspect the fluid in the vessel. There should not be any liquid in contact with the lid of the test chamber. In general, the fluid should cover the base and rise partially up the walls of the test chamber forming a rather large meniscus.

If at any time during this step the fluid configuration departs from this state,

Perform [4.001 CFE VANE GAP FLUID RELOCATION](#) all, then:

9.2 ✓ #10 fastener is securely tightened.

9.3 Retrieve: Mini DVCAM Tape (new)
Install Mini DVCAM Tape (new) in PD100 Camcorder.

CAUTION

The camera view and the front face of the Vane Gap 1 vessel should be orthogonal or loss of science may occur.

9.4 ✓ PD100 Camcorder for CFE Vane Gap 1 entire Field of View
Refer to [5.010 CFE VANE GAP CHAMBER FIELD OF VIEW](#).

✓ REC Lamp — Off

✓ Sony emblem is covered

✓ Vane position — 0 degrees

✓ PD100 Camcorder view is orthogonal to the front face of the CFE Vane Gap 1 vessel. Gauge by eye checking both the top view and the side view.

NOTE

1. This test does not require any tapping to aid in fluid redistribution. The operator only needs to adjust the vane position and wait the prescribed time for each setpoint without disturbing the vessel.
2. Vane angle adjustments for this test are different than the other tests in this procedure. For this test only, a large change in position needs to occur in a short time. This will require gripping the Vane Position Indicator in a different manner to allow for a quick 90 degree rotation in one motion if possible. Multiple steps are acceptable, but the motion needs to be completed in

NOTE

two seconds.

3. An approximate 2 degree backlash is present on the Vane Position Indicator and it may be necessary to overturn the Vane Position Indicator approximately 2 degrees to establish the desired angle once the Vane Position Indicator is released.
4. When rotating Vane Position Indicator, care should be taken to keep the Vane Position Indicator visible and unobstructed in the camera Field of View when the motion is completed. Temporarily obstructing the view of the Vane Position Indicator while making this quick 90 degree rotation is acceptable.
5. VALVE 1 remains open (extended) during all the CFE Vane Gap 1 tests.
6. If the PD100 Camcorder tape remaining time is less than the prescribed wait time for the next setpoint, replace the tape before performing the next setpoint.

Start Video Activity

9.5 PD100 Camcorder → On

9.6 Voice into the PD100 Camcorder GPS time, "Symmetry Test ", "CFE Vane Gap 1", and the module temperature from the PCS ECLSS page.

9.7 Allow 1 minute for camcorder to record baseline condition.

9.8 Quickly rotate Vane Position Indicator CCW to a Vane Position of 270 degrees. The motion must be completed in approximately two seconds or less including any fine adjustments. It is desirable to perform the position change in one continuous motion if possible.

Using the PD100 Camcorder, voice observations of the fluid response.

Wait 15 minutes. This will assure that the fluid achieves a steady state condition.

9.9 Quickly rotate Vane Position Indicator CW to a Vane Position of 0 degrees. The motion must be completed in approximately two seconds or less including any fine adjustments. It is desirable to perform the position change in one continuous motion if possible.

Using the PD100 Camcorder, voice observations of the fluid response.

Wait 3 minutes. This will assure that the fluid achieves a steady state condition.

End Video Activity

2.005 CFE VANE GAP 1 TEST OPERATIONS

(cfe1all000037)

Page 19 of 29 pages

PD100 Camcorder9.10 PD100 Camcorder → Off
Eject Mini DVCAM Tape (used)
sw Mini DVCAM Tape → Save

9.11 Label Mini DVCAM Tape: CFE Vane Gap 1 Symmetry Test and include GPS time.

9.12 Tmpy stow : Mini DVCAM Tape (used)

10. VANE GAP 1 STEADY STATE SECOND QUADRANT TEST

10.1 Visually inspect the fluid in the vessel. There should not be any liquid in contact with the lid of the test chamber. In general, the fluid should cover the base and rise partially up the walls of the test chamber forming a rather large meniscus.

If at any time during this step the fluid configuration departs from this state,

Perform [4.001 CFE VANE GAP FLUID RELOCATION](#) all, then:

10.2 ✓#10 fastener is securely tightened

CAUTION

The camera view and the front face of the Vane Gap 1 vessel should be orthogonal or loss of science may occur.

10.3 ✓PD100 Camcorder for CFE Vane Gap 1 entire Field of View
Refer to [5.010 CFE VANE GAP CHAMBER FIELD OF VIEW](#)
✓REC Lamp — Off
✓Sony emblem is covered
✓Vane position — 180 degrees
✓PD100 Camcorder view is orthogonal to the front face of the CFE Vane Gap 1 vessel. Gauge by eye checking both the top view and the side view.

NOTE

1. This test does not require any tapping to aid in fluid redistribution. The operator only needs to adjust the vane position and wait the prescribed time for each step without disturbing the vessel for each setpoint.
2. Vane angle adjustments are made by smoothly turning the Vane Position Indicator. An approximate 2 degree backlash is present on the Vane Position Indicator and it may be necessary to overturn the Vane Position Indicator approximately 2 degrees to establish the desired angle once the Vane Position Indicator is released.
3. When rotating Vane Position Indicator, care should be taken to keep the Vane Position Indicator visible and unobstructed in the camera Field of View.

2.005 CFE VANE GAP 1 TEST OPERATIONS

(cfe1all000037)

Page 20 of 29 pages

NOTE

4. VALVE 1 remains open (extended) during all the CFE Vane Gap 1 tests.
5. If the PD100 Camcorder tape remaining time is less than the prescribed wait time for the next setpoint, replace the tape before changing to the next setpoint.

Start Video Activity

10.4 PD100 Camcorder → On

10.5 Voice into the PD100 Camcorder GPS time, "Steady State Test 3 ", "CFE Vane Gap 1", and the module temperature from the PCS ECLSS page.

10.6 Allow 1 minute for camcorder to record baseline condition.

10.7 Per the table below, slowly rotate Vane Position Indicator CCW to the Vane Position listed and wait the prescribed time.

Using the PD100 Camcorder, voice observations of the fluid response.

Vane Position	Wait Time	Setpoint description
145	1 minute	Intermediate symmetric
139	1 minute	Last symmetric surface
137	15 minutes	Possible global asymmetric shift
135	15 minutes	Small gap critical wetting (certain global shift)
128	1 minute	Intermediate between wettings
125	5 minutes	Large gap critical wetting
120	1 minute	Enroute to 90
90	3 minutes	Full asymmetric equilibrium

Repeat for the remaining vane positions and wait times:

2.005 CFE VANE GAP 1 TEST OPERATIONS

(cfe1all000037)

Page 21 of 29 pages

- 10.8 Per the table below, slowly rotate Vane Position Indicator CW to the Vane Position listed and wait the prescribed time.

Using the PD100 Camcorder, voice observations of the fluid response.

Vane Position	Wait Time	Setpoint description
125	1 minute	Intermediate asymmetric equilibrium
127	5 minutes	Large gap de-wetting
133	1 minute	Intermediate between de-wettings
136	15 minutes	Possible global shift
139	5 minutes	Small gap de-wetting
160	1 minute	Intermediate symmetric
180	3 minutes	Baseline

- Repeat for the remaining vane positions and wait times:

End Video Activity

PD100 Camcorder → Off
Eject Mini DVCAM Tape (used)
sw Mini DVCAM Tape → Save

- 10.10 Label Mini DVCAM Tape: CFE Vane Gap 1 SS Q2 and include GPS time.

- 10.11 Tmpy stow : Mini DVCAM Tape (used)

11. VANE GAP 1 SYMMETRY TEST 3

- 11.1 Visually inspect the fluid in the vessel. There should not be any liquid in contact with the lid of the test chamber. In general, the fluid should cover the base and rise partially up the walls of the test chamber forming a rather large meniscus.

If at any time during this step the fluid configuration departs from this state,

Perform [4.001 CFE VANE GAP FLUID RELOCATION](#) all, then:

11.2 ✓#10 fastener is securely tightened.

11.3 Retrieve: Mini DVCAM Tape (new)
Install Mini DVCAM Tape (new) in PD100 Camcorder.

CAUTION

The camera view and the front face of the Vane Gap 1 vessel should be orthogonal or loss of science may occur.

11.4 ✓PD100 Camcorder for CFE Vane Gap 1 entire Field of View
Refer to [5.010 CFE VANE GAP CHAMBER FIELD OF VIEW](#).

✓REC Lamp – Off

✓Sony emblem is covered

✓Vane position – 180 degrees

✓PD100 Camcorder view is orthogonal to the front face of the CFE Vane Gap 1 vessel. Gauge by eye checking both the top view and the side view.

NOTE

1. This test does not require any tapping to aid in fluid redistribution. The operator only needs to adjust the vane position and wait the prescribed time for each setpoint without disturbing the vessel.
2. Vane angle adjustments for this test are different than the other tests in this procedure. For this test only, a large change in position needs to occur in a short time. This will require gripping the Vane Position Indicator in a different manner to allow for a quick 90 degree rotation in one motion if possible. Multiple steps are acceptable, but the motion needs to be completed in two seconds.
3. An approximate 2 degree backlash is present on the Vane Position Indicator and it may be necessary to overturn the Vane Position Indicator approximately 2 degrees to establish the desired angle once the Vane Position Indicator is released.
4. When rotating Vane Position Indicator, care should be taken to keep the Vane Position Indicator visible and unobstructed in the camera Field of View when the motion is completed. Temporarily obstructing the view of the Vane Position Indicator while making this quick 90 degree rotation is acceptable.
5. VALVE 1 remains open (extended) during all the CFE Vane Gap 1 tests.

NOTE

6. If the PD100 Camcorder tape remaining time is less than the prescribed wait time for the next setpoint, replace the tape before performing the next setpoint.

Start Video Activity

11.5 PD100 Camcorder → On

11.6 Voice into the PD100 Camcorder GPS time, "Symmetry Test 3 ", "CFE Vane Gap 1", and the module temperature from the PCS ECLSS page.

11.7 Allow 1 minute for camcorder to record baseline condition.

11.8 Quickly rotate Vane Position Indicator CCW to a Vane Position of 90 degrees. The motion must be completed in approximately two seconds or less including any fine adjustments. It is desirable to perform the position change in one continuous motion if possible.

Using the PD100 Camcorder, voice observations of the fluid response.

Wait 15 minutes. This will assure that the fluid achieves a steady state condition.

11.9 Quickly rotate Vane Position Indicator CW to a Vane Position of 139 degrees. The motion must be completed in approximately two seconds or less including any fine adjustments. It is desirable to perform the position change in one continuous motion if possible.

Using the PD100 Camcorder, voice observations of the fluid response.

Wait 5 minutes. This will assure that the fluid achieves a steady state condition.

11.10 Quickly rotate Vane Position Indicator CW to a Vane Position of 180 degrees. The motion must be completed in approximately two seconds or less including any fine adjustments. It is desirable to perform the position change in one continuous motion if possible.

Using the PD100 Camcorder, voice observations of the fluid response.

Wait 3 minutes. This will assure that the fluid achieves a steady state condition.

End Video Activity

PD100 Camcorder 11.11 PD100 Camcorder → Off
Eject Mini DVCAM Tape (used)

sw Mini DVCAM Tape → Save

11.12 Label Mini DVCAM Tape: CFE Vane Gap 1 Symmetry Test 3 and include GPS time.

11.13 Tmpiry stow : Mini DVCAM Tape (used)

12. VANE GAP 1 STEADY STATE THIRD QUADRANT TEST

12.1 Visually inspect the fluid in the vessel. There should not be any liquid in contact with the lid of the test chamber. In general, the fluid should cover the base and rise partially up the walls of the test chamber forming a rather large meniscus.

If at any time during this step the fluid configuration departs from this state,

Perform [4.001 CFE VANE GAP FLUID RELOCATION](#) all, then:

12.2 ✓#10 fastener is securely tightened

12.3 Retrieve: Mini DVCAM Tape (new)

Install Mini DVCAM Tape (new) in PD100 Camcorder

CAUTION

The camera view and the front face of the Vane Gap 1 vessel should be orthogonal or loss of science may occur.

12.4 ✓PD100 Camcorder for CFE Vane Gap 1 entire Field of View
Refer to [5.010 CFE VANE GAP CHAMBER FIELD OF VIEW](#)

✓REC Lamp — Off

✓Sony emblem is covered

✓Vane position — 180 degrees

✓PD100 Camcorder view is orthogonal to the front face of the CFE Vane Gap 1 vessel. Gauge by eye checking both the top view and the side view.

NOTE

1. This test does not require any tapping to aid in fluid redistribution. The operator only needs to adjust the vane position and wait the prescribed time for each step without disturbing the vessel for each setpoint.
2. Vane angle adjustments are made by smoothly turning the Vane Position Indicator. An approximate 2 degree backlash is present on the Vane Position Indicator and it may be necessary to overturn the Vane Position Indicator approximately 2 degrees to establish the desired angle once the Vane Position Indicator is released.

2.005 CFE VANE GAP 1 TEST OPERATIONS

(cfe1all000037)

Page 25 of 29 pages

NOTE

3. When rotating Vane Position Indicator, care should be taken to keep the Vane Position Indicator visible and unobstructed in the camera Field of View.
4. VALVE 1 remains open (extended) during all the CFE Vane Gap 1 tests.
5. If the PD100 Camcorder tape remaining time is less than the prescribed wait time for the next setpoint, replace the tape before changing to the next setpoint.

Start Video Activity

12.5 PD100 Camcorder → On

12.6 Voice into the PD100 Camcorder GPS time, "Steady State Test 4 ", "CFE Vane Gap 1", and the module temperature from the PCS ECLSS page.

12.7 Allow 1 minute for camcorder to record baseline condition.

12.8 Per the table below, slowly rotate Vane Position Indicator CW to the Vane Position listed and wait the prescribed time.

Using the PD100 Camcorder, voice observations of the fluid response.

Vane Position	Wait Time	Setpoint description
220	1 minute	Last symmetric surface
224	15 minutes	Small gap critical wetting (possibly no global shift)
230	15 minutes	Global asymmetric shift
232	5 minutes	Large gap critical wetting
250	1 minute	Intermediate asymmetric
270	3 minutes	Full asymmetric equilibrium

Repeat for the remaining vane positions and wait times:

2.005 CFE VANE GAP 1 TEST OPERATIONS

(cfe1all000037)

Page 26 of 29 pages

- 12.9 Per the table below, slowly rotate Vane Position Indicator CCW to the Vane Position listed and wait the prescribed time.

Using the PD100 Camcorder, voice observations of the fluid response.

Vane Position	Wait Time	Setpoint description
235	1 minute	Intermediate asymmetric
230	5 minutes	Large gap de-wetting
225	15 minutes	Global symmetric shift
220	5 minutes	Small gap de-wetting
200	1 minute	Intermediate symmetric
180	3 minutes	Baseline

- 12.10 Repeat for the remaining vane positions and wait times:

End Video Activity

PD100 Camcorder → Off
Eject Mini DVCAM Tape (used)

sw Mini DVCAM Tape → Save

- 12.11 Label Mini DVCAM Tape: CFE Vane Gap 1 SS Q3 and include GPS time.

- 12.12 Tmpy stow : Mini DVCAM Tape (used)

13. VANE GAP 1 SYMMETRY TEST 4

- 13.1 Visually inspect the fluid in the vessel. There should not be any liquid in contact with the lid of the test chamber. In general, the fluid should cover the base and rise partially up the walls of the test chamber forming a rather large meniscus.

If at any time during this step the fluid configuration departs from this state,

Perform [4.001 CFE VANE GAP FLUID RELOCATION](#) all, then:

2.005 CFE VANE GAP 1 TEST OPERATIONS

(cfe1all000037)

Page 27 of 29 pages

13.2 ✓#10 fastener is securely tightened.

13.3 Retrieve: Mini DVCAM Tape (new)
Install Mini DVCAM Tape (new) in PD100 Camcorder.

CAUTION

The camera view and the front face of the Vane Gap 1 vessel should be orthogonal or loss of science may occur.

13.4 ✓PD100 Camcorder for CFE Vane Gap 1 entire Field of View
Refer to [5.010 CFE VANE GAP CHAMBER FIELD OF VIEW](#).

✓REC Lamp – Off



✓Sony emblem is covered

✓Vane position – 180 degrees

✓PD100 Camcorder view is orthogonal to the front face of the CFE Vane Gap 1 vessel. Gauge by eye checking both the top view and the side view.

NOTE

1. This test does not require any tapping to aid in fluid redistribution. The operator only needs to adjust the vane position and wait the prescribed time for each setpoint without disturbing the vessel.
2. Vane angle adjustments for this test are different than the other tests in this procedure. For this test only, a large change in position needs to occur in a short time. This will require gripping the Vane Position Indicator in a different manner to allow for a quick 90 degree rotation in one motion if possible. Multiple steps are acceptable, but the motion needs to be completed in two seconds.
3. An approximate 2 degree backlash is present on the Vane Position Indicator and it may be necessary to overturn the Vane Position Indicator approximately 2 degrees to establish the desired angle once the Vane Position Indicator is released.
4. When rotating Vane Position Indicator, care should be taken to keep the Vane Position Indicator visible and unobstructed in the camera Field of View when the motion is completed. Temporarily obstructing the view of the Vane Position Indicator while making this quick 90 degree rotation is acceptable.
5. VALVE 1 remains open (extended) during all the CFE Vane Gap 1 tests.
6. If the PD100 Camcorder tape remaining time is less than the prescribed wait time for the next setpoint, replace the tape before performing the next setpoint.

 Start Video Activity 

13.5 PD100 Camcorder → On

13.6 Voice into the PD100 Camcorder GPS time, "Symmetry Test 4 ", "CFE Vane Gap 1", and the module temperature from the PCS ECLSS page.

13.7 Allow 1 minute for camcorder to record baseline condition.

13.8 Quickly rotate Vane Position Indicator CW to a Vane Position of 270 degrees. The motion must be completed in approximately two seconds or less including any fine adjustments. It is desirable to perform the position change in one continuous motion if possible.

Using the PD100 Camcorder, voice observations of the fluid response.

Wait 15 minutes. This will assure that the fluid achieves a steady state condition.

13.9 Quickly rotate Vane Position Indicator CW to a Vane Position of 320 degrees. The motion must be completed in approximately two seconds or less including any fine adjustments. It is desirable to perform the position change in one continuous motion if possible.


Using the PD100 Camcorder, voice observations of the fluid response.

Wait 5 minutes. This will assure that the fluid achieves a steady state condition.

13.10 Quickly rotate Vane Position Indicator CW to a Vane Position of 0 degrees. The motion must be completed in approximately two seconds or less including any fine adjustments. It is desirable to perform the position change in one continuous motion if possible.

Using the PD100 Camcorder, voice observations of the fluid response.

Wait 3 minutes. This will assure that the fluid achieves a steady state condition.

 End Video Activity 

PD100 Camcorder → Off
Eject Mini DVCAM Tape (used)

sw Mini DVCAM Tape → Save

2.005 CFE VANE GAP 1 TEST OPERATIONS

(cfe1all000037)

Page 29 of 29 pages

13.12 Label Mini DVCAM Tape: CFE Vane Gap 1 Symmetry Test 4 and include GPS time.

13.13 Tmpy stow : Mini DVCAM Tape (used)

14. VANE GAP 1 POST TEST FLUID WITHDRAWAL

14.1 Visually inspect the fluid in the vessel. There should not be any obvious amount of liquid in contact with the lid of the test chamber. In general, the fluid should cover the base and rise partially up the walls of the test chamber forming a rather large meniscus.

If at any time during this step the fluid configuration departs from this state,

Perform [4.001 CFE VANE GAP FLUID RELOCATION](#) all, then:

14.2 ✓#10 fastener is securely tightened

CFE Vane Gap 14.3 Position vane angle to 0 degrees.

14.4 Slowly turn KNOB 1 CW initially at approximately ½ turn per second to stop (approx. 46 revolutions), retracting as much fluid into reservoir without ingesting bubbles. Withdrawal rate must be reduced significantly to avoid ingestion of air bubbles during the final stages of the drain procedure (complete drain could take up to 5 minutes). Not all fluid will be removed from container. Remove only as much as is possible without ingesting bubbles beyond VALVE 1.

14.5 With one hand supporting CFE Vane Gap 1, gently push VALVE 1 to hard stop.

14.6 Stow:
Mini DVCAM Tapes (per execution note, used)
Gray Tape
CFE Vane Gap
1/8" L-Wrench (2 1/4" length)

RESTOW TOOLS, PARTS, MATERIALS AS REQUIRED TO ORIGINAL LOCATIONS EXCEPT FOR:

Mini DVCAM Tape (per execution note) P/N SED33111489-305 TO: For return to Houston

2.006 CFE VANE GAP 2 TEST OPERATIONS

(cfe1all000038)

Page 1 of 24 pages

OBJECTIVE:

Capillary Flow Experiments (CFE). The objective of this experiment is to observe fluid interface and critical wetting behavior in a cylindrical chamber with elliptic cross-section and an adjustable central vane. The critical vane-gap wetting phenomenon occurs at a critical vane angle where the fluid rises all the way up the vane gap. Vane Gap 2 provides a collection of data points for a partially wetting surface. Vane Gap 1 provides a collection of data points for a perfectly wetting surface. These two cases provide a reasonable approximation of the most common fluids stored in tanks for spaceflight applications.

STATION PARTS:

CFE Vane Gap 2 P/N 60083MA20200

Mini DVCAM Tape [per execution note] P/N SED33111489-305

STATION TOOLS:

MWA Work Surface Area P/N SEG33110270-301

MWA Utility Kit P/N SJG33110310-301

Fine Point Sharpie P/N 528-40674-1

PD100 Camcorder P/N SEZ16103293-301

1/8" L-Wrench (2 1/4" length) P/N AW4

STATION MATERIALS:

Dry Wipe

Gray Tape (crew preference)

NOTE

1. This procedure contains Near Real - Time video downlink or LAB VTR recording requirements.
2. AOS may be required for **POIC** to configure on board system for downlink of science or LAB VTR recording.
3. Minimize fingerprints within chamber field of view.
4. Bubbles in the fluid reservoirs are expected and a normal occurrence. No action is necessary other than fluid deployment as described below. Once deployed, the bubbles will find their way to the surface and pop during subsequent testing.

1. VANE GAP 2 BACKGROUND TEST

- 1.1 Unstow: Mini DVCAM Tape (per execution note)
Tm pry stow close to PD100 Camcorder.
Insert Mini DVCAM Tape into PD100 Camcorder.
- 1.2 √#10 Fastener is securely tightened.

CAUTION

The camera view and the front face of the Vane Gap 2 vessel should be orthogonal or loss of science may occur.

- 1.3 √PD100 Camcorder for CFE Vane Gap 2 entire Field

2.006 CFE VANE GAP 2 TEST OPERATIONS

(cfe1all000038)

Page 2 of 24 pages

Refer to [5.010 CFE VANE GAP CHAMBER FIELD OF VIEW](#)

√REC Lamp — Off

√Sony emblem is covered

√Vane Position - 0 degrees

√PD100 Camcorder view is orthogonal to the front face of the CFE Vane Gap 2 vessel

Gauge by eye checking both the top view and the side view

CAUTION

After the fluid is dispensed into the elliptic test chamber, care should be taken not to disturb (i.e. adjust) the CFE Vane Gap 2 Vessel. Loss of science will occur if the vessel is disturbed and agitated during the background run. The Background run is not repeatable.

Start Video Activity

1.4 PD100 Camcorder → ON

1.5 Voice into the PD100 Camcorder GPS time, "Background Test", "CFE Vane Gap 2", and the module temperature from the PCS ECLSS page.

CFE Vane Gap 21.6 With one hand supporting CFE Vane Gap 2, gently pull VALVE 1 to hard stop.

1.7 Slowly turn KNOB 1 CCW at approximately 1/4 to 1/2 turn per second to stop. (Approximately 46 revolutions, requires up to 3 minutes).

1.8 √CFE Vane Gap 2 fluid has been fully dispensed into the test chamber.

CAUTION

CFE Vane Gap 2 fluid leakage may occur around the valve, and/or the piston.

1.9 √CFE Vane Gap 2 for visible leakage

If leakage,

| Wipe with Dry Wipes.

| If leakage continues,

| | √ **POIC** to report leakage

- 1.10 Voice observations about the fluid into recording PD100 Camcorder. (Include comments about the symmetry of the fluid in front of the vane relative to the fluid behind the vane.).

If the fluid is not symmetric,

- | Use the pad of index finger and lightly tap the backside of the vessel within the PD100 Camcorder field of view (if possible).
- | Voice approximate number, size and location of any bubbles present.

- 1.11 PD100 Camcorder recording CFE Vane Gap 2 Field of View

Refer to [5.010 CFE VANE GAP CHAMBER FIELD OF VIEW](#)

2. [VANE GAP 2 CW DRY TEST](#)

CAUTION

Special care should be taken to avoid any disturbances larger than a tap since the CW Dry Test is not repeatable.

NOTE

1. All references to critical vane gap wetting are specific to the vane gap on the front face of the vessel nearest the camera. Critical wetting does occur for the vane gap on the back face of the vessel, but is not pertinent to the crew procedures. The vane angles are selected to investigate the approach to the critical wetting angle and not the departure.
2. Vane angle adjustments are made by smoothly turning the Vane Position Indicator. An approximate 2 degree backlash is present on the Vane Position Indicator and it may be necessary to overturn the Vane Position Indicator approximately 2 degrees to establish the desired angle once the Vane Position Indicator is released.
3. When rotating Vane Position Indicator, care should be taken to keep the Vane Position Indicator visible and unobstructed in the camera Field of View.
4. After each vane angle adjustment a series of taps are applied to the Vane Gap 2 vessel. The small high frequency damped oscillations of the interface that result from taps will be recorded by video. The taps should allow the interface to relax and achieve a more ideal equilibrium. Taps are defined as: a set of 4 finger taps on the back side of the Vane Gap vessel imparted at an approximate rate metered by each syllable of a one second count "one-one-thousand" (similar to finger taps on the side of a fish tank).
5. Approximately 10 seconds should be allowed after each set of taps for all interface disturbances to decay (damp out, settle, etc.). As the crew becomes accustomed to the sensitivity of the liquid surface to the finger taps, the taps may be applied as necessary to speed (or

NOTE

coax) the establishment of an equilibrium surface.

6. Each set of taps is applied to the back side of CFE Vane Gap 2 and must be in the same location within the Field of View if possible.
7. Nominal prescribed vane angles are provided with preset angle increment. Smaller angle increments (5deg) are used near the expected critical vane wetting angles (predicted to be approximately 60 and 225 degrees). However, true critical angles will be determined in flight and crew discretion is requested to determine vane angle increments as critical conditions are approached. Critical vane angle precision is not expected to be better than ± 5 degrees, but may be improved as determined in flight by crew.
8. The critical vane gap wetting phenomena occurs at a critical vane angle where the fluid rises all the way up the vane gap. It is recommended that the crew note (i.e. by jotting down) the two experimentally determined critical vane angles (predicted to be approximately 60 and 225 degrees) during the first performance of the experiment to better anticipate vane angle increments during subsequent and repeat runs of the experiment.
9. The tap and wait process is repeated for each vane angle setpoint.
10. VALVE 1 remains open (extended) during all the CFE Vane Gap 2 tests.
11. If uncertain of PD100 Camcorder tape remaining time, replace tape as necessary.

2.1 Voice into the PD100 Camcorder GPS time, "CW Dry Test", "CFE Vane Gap 2" and the module temperature from the PCS ECLSS page.

2.2— Slowly rotate Vane Position Indicator CW to a Vane Position of 15 degrees.

Allow 30 sec for the fluid and surface to stabilize.

Using pad of index finger, apply taps at prescribed location on CFE Vane Gap 2.

Wait ten seconds while observing fluid surface response.

If the fluid surface changes shape or position after the set of taps,

Apply another set of taps and observe the fluid surface for any change in shape or position again waiting ten seconds.

If any change in shape occurs,

Repeat as necessary until fluid shape and position are stable.

Using the PD100 Camcorder, voice observations of the fluid response.

2.006 CFE VANE GAP 2 TEST OPERATIONS

(cfe1all000038)

Page 5 of 24 pages

Allow resulting interface oscillations (if any) to fully decay (settle, dampen, approximately 10 seconds) continuing to voice observations.

- └─ Repeat for the following vane positions: 30, 45, 60, 65, 70, 75, 80, 90, 105, 120, 135, 150, 165, 180, 195, 210, 230, 235, 240, 245, 250, 255, 265, 280, 295, 310, 325, 340, 0.

End Video Activity

PD100 Camcorder 2.3 PD100 Camcorder → OFF
Eject Mini DVCAM Tape (used)
sw Mini DVCAM Tape → Save

2.4 Label Mini DVCAM Tape: CFE-Vane Gap 2 Background - CW Dry Test and include GPS time time.

2.5 Tmpy stow : Mini DVCAM Tape (used)

3. VANE GAP 2 CW WET TESTS

- 3.1 Visually inspect the fluid in the vessel without moving it. There should not be any liquid in contact with the lid of the test chamber. In general, the fluid should cover the base and rise partially up the walls of the test chamber forming a rather large meniscus.

If at any time during this step the fluid configuration departs from this state,

Perform [4.001 CFE VANE GAP FLUID RELOCATION](#) all, then:

- 3.2 ✓#10 fastener is securely tightened

- 3.3 Retrieve: Mini DVCAM Tape (new)
Install Mini DVCAM Tape (new) in PD100 Camcorder.

CAUTION

The camera view and the front face of the Vane Gap 2 vessel should be orthogonal or loss of science may occur.

- 3.4 ✓PD100 Camcorder for CFE Vane Gap 2 entire Field of view
Refer to [5.010 CFE VANE GAP CHAMBER FIELD OF VIEW](#)
✓REC Lamp – Off
✓Sony emblem is covered
✓Vane position - 0 degrees
✓PD100 Camcorder view is orthogonal to the front face of the CFE Vane Gap 2 vessel

Gauge by eye checking both the top view and the side view

NOTE

All of the notes in step 2 apply to this step and should be reviewed

2.006 CFE VANE GAP 2 TEST OPERATIONS

(cfe1all000038)

Page 6 of 24 pages

NOTE

if necessary.

Start Video Activity

3.5 PD100 Camcorder → ON

3.6 Voice into the PD100 Camcorder GPS time, "CW Wet Test 1(2)", "CFE Vane Gap 2" and the module temperature from the PCS ECLSS page.

3.7 Repeat [step 2.2](#), twice.

End Video Activity

PD100 Camcorder 3.8 PD100 Camcorder → Off
Eject Mini DVCAM Tape (used)
sw Mini DVCAM Tape → Save

3.9 Label Mini DVCAM Tape: CFE-Vane Gap 2 CW Wet Tests 1 and 2 and include GPS time time.

3.10 Tmpary stow : Mini DVCAM Tape (used)

4. [VANE GAP 2 CCW WET TESTS](#)

4.1 Visually inspect the fluid in the vessel. There should not be any liquid in contact with the lid of the test chamber. In general, the fluid should cover the base and rise partially up the walls of the test chamber forming a rather large meniscus.

If at any time during this step the fluid configuration departs from this state,

Perform [4.001 CFE VANE GAP FLUID RELOCATION](#) all, then:

4.2 ✓#10 fastener is securely tightened.

4.3 Retrieve: Mini DVCAM Tape (new)
Install Mini DVCAM Tape (new) in PD100 Camcorder

CAUTION

The camera view and the front face of the Vane Gap 2 vessel should be orthogonal or loss of science may occur.

4.4 ✓PD100 Camcorder for CFE Vane Gap 2 entire Field of View
Refer to [5.010 CFE VANE GAP CHAMBER FIELD OF VIEW](#)
✓REC Lamp — Off
✓Sony emblem is covered
✓Vane position - 0 degrees

2.006 CFE VANE GAP 2 TEST OPERATIONS

(cfe1all000038)

Page 7 of 24 pages

√PD100 Camcorder view is orthogonal to the front face of the CFE Vane Gap 2 vessel
Gauge by eye checking both the top view and the side view

NOTE

All of the notes in step 2 apply to this step and should be reviewed if necessary

Start Video Activity

4.5 PD100 Camcorder → On

4.6 Voice into the PD100 Camcorder GPS time, "CCW Wet Test 1(2)", "CFE Vane Gap 2", and the module temperature from the PCS ECLSS page.

4.7 Slowly rotate Vane Position Indicator CCW to a Vane Position of 340 degrees.

Allow 30 sec for the fluid and surface to stabilize.

Using pad of index finger, lightly apply taps at prescribed location on CFE Vane Gap 2.

Wait ten seconds while observing fluid surface response.

If the fluid surface changes shape or position after the set of taps,

Apply another set of taps and observe the fluid surface for any change in shape or position again waiting ten seconds.

If any change in shape occurs,

Repeat as necessary until fluid shape and position is stable

Using the PD100 Camcorder, voice observations of the fluid response.

Allow resulting interface oscillations (if any) to fully decay (settle, dampen, approximately 10 seconds) continuing to voice observations.

Repeat for the following vane positions: 325, 310, 295, 280, 265, 255, 250, 245, 240, 235, 230, 210, 195, 180, 165, 150, 135, 120, 105, 90, 80, 75, 70, 65, 60, 45, 30, 15, 0.

4.8 Repeat [step 4.7](#)

End Video Activity

PD100 Camcorder 4.9 PD100 Camcorder → Off
Eject Mini DVCAM Tape (used)
sw Mini DVCAM Tape → Save

4.10 Label Mini DVCAM Tape: Vane Gap 2 CCW Wet Test and include GPS time time.

4.11 Tmpy stow : Mini DVCAM Tape (used)

5. VANE GAP 2 CONTINUOUS ROTATION TESTS

5.1 Visually inspect the fluid in the vessel. There should not be any liquid in contact with the lid of the test chamber. In general, the fluid should cover the base and rise partially up the walls of the test chamber forming a rather large meniscus.

If at any time during this step the fluid configuration departs from this state,

Perform [4.001 CFE VANE GAP FLUID RELOCATION](#) all, then:

5.2 ✓#10 fastener is securely tightened

5.3 Retrieve: Mini DVCAM Tape (new)
Install Mini DVCAM Tape (new) in PD100 Camcorder

CAUTION

The camera view and the front face of the Vane Gap 2 vessel should be orthogonal or loss of science may occur.

5.4 ✓PD100 Camcorder for CFE Vane Gap 2 entire Field of view
Refer to [5.010 CFE VANE GAP CHAMBER FIELD OF VIEW](#)
✓REC Lamp – Off
✓Sony emblem is covered
✓PD100 Camcorder view is orthogonal to the front face of the CFE Vane Gap 2 vessel
Gauge by eye checking both the top view and the side view

NOTE

1. For these tests a 1/8" L-wrench is taped to the Vane Position Indicator like a crank so that the vane can be rotated smoothly and nearly continuously by hand
2. After taping 1/8" L-Wrench to Vane Position Indicator, the wrench should be able to clear KNOB 1 when revolved.
3. Care should be taken not to obstruct the camera field of view of the Vane Angle Indicator.
4. Crew should concentrate more on maintaining constant rate of revolution than on data observation for this test.
5. This test provides dynamic data for comparison to the static data collected in the previous tests.

5.5 Retrieve:
1/8" L-Wrench

Gray Tape

- 5.6 Tear off two pieces of Gray Tape approximately 2" by 1".

Lay the 1/8" L-Wrench flat across the top of Vane Position Indicator shaft, centering wrench on shaft with the short end of the wrench pointing out from the test chamber like a crank handle. Refer to [5.012 CFE VANE GAP L-WRENCH SET-UP](#)

One at a time, place strips of gray tape over wrench and shaft, securing the wrench to the Vane Position Indicator. Add additional strips of tape as necessary to secure wrench.

- 5.7 Tmpy stow:
Gray Tape

- 5.8 √Vane Position - 0 degrees
Wait ten seconds for any fluid oscillations to dampen out.

Start Video Activity

- 5.9 PD100 Camcorder → On

- 5.10 Voice into the PD100 Camcorder GPS time, "CW Continuous Rotation Test", "CFE Vane Gap 2", and the module temperature from the PCS ECLSS page.

- 5.11 Using the 1/8" L-Wrench attached to the Vane Position Indicator, rotate the vane CW through 720 degrees, at a rate of 10 deg/sec (2 complete revolutions, approximately 36 seconds per revolution).

- 5.12 √Vane Position - 0 degrees
Wait ten seconds for any fluid oscillations to dampen out.

- 5.13 Voice into the PD100 Camcorder GPS time, "CCW Continuous Rotation Test", "CFE Vane Gap 2" and the module temperature from the PCS ECLSS page.

- 5.14 Using the 1/8" L-Wrench attached to the Vane Position Indicator, rotate the vane CCW through 720 degrees, at a rate of 10 deg/sec (2 complete revolutions, approximately 36 seconds per revolution).

End Video Activity

PD100 Camcorder 5.15 PD100 Camcorder → Off
Eject Mini DVCAM Tape (used)
sw Mini DVCAM Tape → Save

- 5.16 Label Mini DVCAM Tape: Vane Gap 2 Continuous Rotation Tests and include GPS time time.

- 5.17 Tmpy stow : Mini DVCAM Tape (used)

- 5.18 Carefully remove the 1/8" L-Wrench and gray tape from the Vane Position Indicator. Be gentle as the vane shaft is plastic. Remove the gray tape from the 1/8" L-Wrench and dispose of in ISS trash.

6. VANE GAP 2 CW WET TEST PART TWO

- 6.1 Visually inspect the fluid in the vessel. There should not be any liquid in contact with the lid of the test chamber. In general, the fluid should cover the base and rise partially up the walls of the test chamber forming a rather large meniscus.

If at any time during this step the fluid configuration departs from this state,

Perform [4.001 CFE VANE GAP FLUID RELOCATION](#) all, then:

- 6.2 ✓ #10 fastener is securely tightened
- 6.3 Retrieve: Mini DVCAM Tape (new)
Install Mini DVCAM Tape (new) in PD100 Camcorder

CAUTION

The camera view and the front face of the Vane Gap 2 vessel should be orthogonal or loss of science may occur.

- 6.4 ✓ PD100 Camcorder for CFE Vane Gap 2 entire Field of View
Refer to [5.010 CFE VANE GAP CHAMBER FIELD OF VIEW](#)
✓ REC Lamp – Off
✓ Sony emblem is covered
✓ Vane position – 0 degrees
✓ PD100 Camcorder view is orthogonal to the front face of the CFE Vane Gap 2 vessel. Gauge by eye checking both the top view and the side view.

NOTE

1. This test does not require any tapping to aid in fluid redistribution. The operator only needs to adjust the vane position and wait the prescribed time for each step without disturbing the vessel for each setpoint.
2. Vane angle adjustments are made by smoothly turning the Vane Position Indicator. An approximate 2 degree backlash is present on the Vane Position Indicator and it may be necessary to overturn the Vane Position Indicator approximately 2 degrees to establish the desired angle once the Vane Position Indicator is released.
3. When rotating Vane Position Indicator, care should be taken to keep the Vane Position Indicator visible and unobstructed in the camera Field of View.

NOTE

4. VALVE 1 remains open (extended) during all the CFE Vane Gap 2 tests.

Start Video Activity

6.5 PD100 Camcorder→On

6.6 Voice into the PD100 Camcorder GPS time, "CW Wet Test Part Two", "CFE Vane Gap 2", and the module temperature from the PCS ECLSS page.

6.7 Allow 1 minute for camcorder to record baseline condition.

6.8 Slowly rotate Vane Position Indicator CW to a Vane Position of 53 degrees.

Allow 30 seconds for the fluid surface to stabilize. If slight fluid motion persists, wait an additional 2 minutes.

Using the PD100 Camcorder, voice observations of the fluid response.

Repeat for the following vane positions: 57, 62, 68, 73, 77, 82, 118, 125, 130, 135, 142, 233, 237, 242, 243, 247, 253, 257, 270, 293, 297, 302, 308, 313, 318, 323, 0.

End Video Activity

PD100 Camcorder 6.9 PD100 Camcorder→Off
Eject Mini DVCAM Tape (used)
sw Mini DVCAM Tape → Save

6.10 Label Mini DVCAM Tape: CFE-Vane Gap 2 CW Wet Test Two and include GPS time.

6.11 Tmpary stow: Mini DVCAM Tape (used)

7. VANE GAP 2 CCW WET TEST PART TWO

7.1 Visually inspect the fluid in the vessel. There should not be any liquid in contact with the lid of the test chamber. In general, the fluid should cover the base and rise partially up the walls of the test chamber forming a rather large meniscus.

If at any time during this step the fluid configuration departs from this state,

Perform [4.001 CFE VANE GAP FLUID RELOCATION](#) all, then:

7.2 √#10 fastener is securely tightened.

7.3 Retrieve: Mini DVCAM Tape (new)

Install Mini DVCAM Tape (new) in PD100 Camcorder

CAUTION

The camera view and the front face of the Vane Gap 2 vessel should be orthogonal or loss of science may occur.

7.4 ✓PD100 Camcorder for CFE Vane Gap 2 entire Field of View

Refer to [5.010 CFE VANE GAP CHAMBER FIELD OF VIEW](#)

✓REC Lamp – Off

✓Sony emblem is covered

✓Vane position – 0 degrees

✓PD100 Camcorder view is orthogonal to the front face of the CFE Vane Gap 2 vessel. Gauge by eye checking both the top view and the side view.

NOTE

1. This test does not require any tapping to aid in fluid redistribution. The operator only needs to adjust the vane position and wait the prescribed time for each step without disturbing the vessel for each setpoint.
2. Vane angle adjustments are made by smoothly turning the Vane Position Indicator. An approximate 2 degree backlash is present on the Vane Position Indicator and it may be necessary to overturn the Vane Position Indicator approximately 2 degrees to establish the desired angle once the Vane Position Indicator is released.
3. When rotating Vane Position Indicator, care should be taken to keep the Vane Position Indicator visible and unobstructed in the camera Field of View.
4. VALVE 1 remains open (extended) during all the CFE Vane Gap 2 tests.

Start Video Activity

7.5 PD100 Camcorder→On

7.6 Voice into the PD100 Camcorder GPS time, "CCW Wet Test Part Two", "CFE Vane Gap 2", and the module temperature from the PCS ECLSS page.

7.7 Allow 1 minute for camcorder to record baseline condition.

7.8 Slowly rotate Vane Position Indicator CCW to a Vane Position of 323 degrees.

Allow 30 seconds for the fluid surface to stabilize. If slight fluid motion persists, wait an additional 2 minutes

2.006 CFE VANE GAP 2 TEST OPERATIONS

(cfe1all000038)

Page 13 of 24 pages

Using the PD100 Camcorder, voice observations of the fluid response.

- └─ Repeat for the following vane positions: 318, 313, 308, 302, 297, 293, 270, 257, 253, 247, 243, 242, 237, 233, 142, 135, 130, 125, 118, 82, 77, 73, 68, 62, 57, 53, 0.

End Video Activity

PD100 Camcorder 7.9 PD100 Camcorder→Off
Eject Mini DVCAM Tape (used)
sw Mini DVCAM Tape → Save

7.10 Label Mini DVCAM Tape: CFE-Vane Gap 2 CCW Wet Test Two and include GPS time.

7.11 Tmpy stow : Mini DVCAM Tape (used)

8. VANE GAP 2 CW WET TEST PART THREE

8.1 Visually inspect the fluid in the vessel. There should not be any liquid in contact with the lid of the test chamber. In general, the fluid should cover the base and rise partially up the walls of the test chamber forming a rather large meniscus.

If at any time during this step the fluid configuration departs from this state,

Perform [4.001 CFE VANE GAP FLUID RELOCATION](#) all, then:

8.2 ✓#10 fastener is securely tightened.

8.3 Retrieve: Mini DVCAM Tape (new)
Install Mini DVCAM Tape (new) in PD100 Camcorder

CAUTION

The camera view and the front face of the Vane Gap 2 vessel should be orthogonal or loss of science may occur.

8.4 ✓PD100 Camcorder for CFE Vane Gap 2 entire Field of View

Refer to [5.010 CFE VANE GAP CHAMBER FIELD OF VIEW](#)

✓REC Lamp – Off

✓Sony emblem is covered

✓Vane position – 0 degrees

✓PD100 Camcorder view is orthogonal to the front face of the CFE Vane Gap 2 vessel. Gauge by eye checking both the top view and the side view.

NOTE

1. This test does not require any tapping to aid in fluid redistribution. The operator only needs to adjust the vane position and wait the prescribed time for each step without

NOTE

disturbing the vessel for each setpoint.

2. Vane angle adjustments are made by smoothly turning the Vane Position Indicator. An approximate 2 degree backlash is present on the Vane Position Indicator and it may be necessary to overturn the Vane Position Indicator approximately 2 degrees to establish the desired angle once the Vane Position Indicator is released.
3. When rotating Vane Position Indicator, care should be taken to keep the Vane Position Indicator visible and unobstructed in the camera Field of View.
4. VALVE 1 remains open (extended) during all the CFE Vane Gap 2 tests.

Start Video Activity

8.5 PD100 Camcorder→On

8.6 Voice into the PD100 Camcorder GPS time, "CW Wet Test Part Three", "CFE Vane Gap 2", and the module temperature from the PCS ECLSS page.

8.7 Allow 1 minute for camcorder to record baseline condition.

8.8 Slowly rotate Vane Position Indicator CW to a Vane Position of 50 degrees.

Allow 30 seconds for the fluid surface to stabilize. If slight fluid motion persists, wait an additional 2 minutes

Using the PD100 Camcorder, voice observations of the fluid response.

Repeat for the following vane positions: 52, 54, 56, 58, 60, 62, 64, 66, 68, 70, 72, 74, 76, 78, 80, 90, 118, 120, 122, 124, 126, 128, 130, 132, 134, 136, 138, 140, 142, 144, 146, 148, 180

End Video Activity

PD100 Camcorder 8.9 PD100 Camcorder→Off
Eject Mini DVCAM Tape (used)
sw Mini DVCAM Tape → Save

8.10 Label Mini DVCAM Tape: CFE-Vane Gap 2 CW Wet Test Three and include GPS time.

8.11 Tmpary stow : Mini DVCAM Tape (used)

9. VANE GAP 2 CCW WET TEST PART THREE

- 9.1 Visually inspect the fluid in the vessel. There should not be any liquid in contact with the lid of the test chamber. In general, the fluid should cover the base and rise partially up the walls of the test chamber forming a rather large meniscus.

If at any time during this step the fluid configuration departs from this state,

Perform [4.001 CFE VANE GAP FLUID RELOCATION](#) all, then:

- 9.2 ✓#10 fastener is securely tightened.

- 9.3 Retrieve: Mini DVCAM Tape (new)
Install Mini DVCAM Tape (new) in PD100 Camcorder

CAUTION

The camera view and the front face of the Vane Gap 2 vessel should be orthogonal or loss of science may occur.

- 9.4 ✓PD100 Camcorder for CFE Vane Gap 2 entire Field of View

Refer to [5.010 CFE VANE GAP CHAMBER FIELD OF VIEW](#)

✓REC Lamp — Off

✓Sony emblem is covered

✓Vane position — 180 degrees

✓PD100 Camcorder view is orthogonal to the front face of the CFE Vane Gap 2 vessel. Gauge by eye checking both the top view and the side view.

NOTE

1. This test does not require any tapping to aid in fluid redistribution. The operator only needs to adjust the vane position and wait the prescribed time for each step without disturbing the vessel for each setpoint.
2. Vane angle adjustments are made by smoothly turning the Vane Position Indicator. An approximate 2 degree backlash is present on the Vane Position Indicator and it may be necessary to overturn the Vane Position Indicator approximately 2 degrees to establish the desired angle once the Vane Position Indicator is released.
3. When rotating Vane Position Indicator, care should be taken to keep the Vane Position Indicator visible and unobstructed in the camera Field of View.
4. VALVE 1 remains open (extended) during all the CFE Vane Gap 2 tests.

Start Video Activity

- 9.5 PD100 Camcorder→On

2.006 CFE VANE GAP 2 TEST OPERATIONS

(cfe1all000038)

Page 16 of 24 pages

9.6 Voice into the PD100 Camcorder GPS time, "CCW Wet Test Part Three", "CFE Vane Gap 2", and the module temperature from the PCS ECLSS page.

9.7 Allow 1 minute for camcorder to record baseline condition.

9.8 Slowly rotate Vane Position Indicator CCW to a Vane Position of 148 degrees.

Allow 30 seconds for the fluid surface to stabilize. If slight fluid motion persists, wait an additional 2 minutes

Using the PD100 Camcorder, voice observations of the fluid response.

Repeat for the following vane positions: 146, 144, 142, 140, 138, 136, 134, 132, 130, 128, 126, 124, 122, 120, 118, 90, 80, 78, 76, 74, 72, 70, 68, 66, 64, 62, 60, 58, 56, 54, 52, 50, 0

End Video Activity

PD100 Camcorder 9.9 PD100 Camcorder→Off
Eject Mini DVCAM Tape (used)
sw Mini DVCAM Tape → Save

9.10 Label Mini DVCAM Tape: CFE-Vane Gap 2 CCW Wet Test Three and include GPS time.

9.11 Tmpy stow : Mini DVCAM Tape (used)

10. VANE GAP 2 GAP STABILITY TEST

10.1 ✓#10 fastener is securely tightened

10.2 Retrieve: Mini DVCAM Tape (new)
Install Mini DVCAM Tape (new) in PD100 Camcorder

CAUTION

The camera view and the front face of the Vane Gap 2 vessel should be orthogonal or loss of science may occur.

10.3 ✓PD100 Camcorder for CFE Vane Gap 2 entire Field of View

Refer to [5.010 CFE VANE GAP CHAMBER FIELD OF VIEW](#)

✓REC Lamp – Off

✓Sony emblem is covered

✓Vane position – 0 degrees

✓PD100 Camcorder view is orthogonal to the front face of the CFE Vane Gap 2 vessel. Gauge by eye checking both the top view and the side view.

- 10.4 Use tape or paper to mark the location of the Vane Gap 2 vessel on the MWA surface so that it can easily be returned to approximately the same position.

NOTE

1. This test does not require any tapping to aid in fluid redistribution. The operator only needs to adjust the vane position and wait the prescribed time for each step without disturbing the vessel for each setpoint.
2. Vane angle adjustments are made by smoothly turning the Vane Position Indicator. An approximate 2 degree backlash is present on the Vane Position Indicator and it may be necessary to overturn the Vane Position Indicator approximately 2 degrees to establish the desired angle once the Vane Position Indicator is released.
3. When rotating Vane Position Indicator, care should be taken to keep the Vane Position Indicator visible and unobstructed in the camera Field of View.
4. VALVE 1 remains open (extended) during all the CFE Vane Gap 2 tests.

Start Video Activity

- 10.5 PD100 Camcorder → On
- 10.6 Voice into the PD100 Camcorder GPS time, "Gap Stability Test", "CFE Vane Gap 2", and the module temperature from the PCS ECLSS page.
- 10.7 Allow 1 minute for camcorder to record baseline condition.
- 10.8 Slowly rotate the vane CW to 90 degrees at approximately 3 degrees per second for a total movement duration of approximately 30 seconds.
- 10.9 Remove #10 Fastener and Tmpy stow.
- 10.10 Remove the vessel from the MWA and use a "soft" centrifuge method to relocate most of the fluid from the base to the lid. The goal is approximately two thirds of the fluid at the lid. This will provide enough fluid to bridge the gaps between the base and the vane, and between the lid and the vane.

As gently as possible, return the vessel to the MWA within five seconds and reattach using the #10 fastener. Minor bumps on contact are acceptable. Try to place the vessel back to its original position when reattaching to the MWA. Do not adjust the vessel position after placement back onto the MWA.

2.006 CFE VANE GAP 2 TEST OPERATIONS

(cfe1all000038)

Page 18 of 24 pages

10.11 Inspect test chamber interior surface for fluid film.

If present

POIC and wait for fluid film breakage

10.12 Wait 10 minutes to allow the fluid to reach its equilibrium condition.

10.13 Per the table below, slowly rotate Vane Position Indicator CCW to the Vane Position listed and wait the prescribed time. The gaps mentioned in this step are between the vane and the test chamber walls.

Using the PD100 Camcorder, voice observations of the fluid response.

Vane Position	Wait Time	Setpoint Description
65	3 minutes	Slow turn desired ~20 second movement duration
50	10 minutes	Possible large gap de-wetting
45	10 minutes	
35	10 minutes	Possible small gap de-wetting
20	10 minutes	
10	10 minutes	
0	10 minutes	

Repeat for the remaining vane positions and wait times until both gaps have de-wetted (it is possible that they won't de-wet).

If both gaps have de-wetted,

Proceed to the next step

10.14 Rotate vane CCW to 0 degrees if not already there.

End Video Activity

PD100 Camcorder 10.15 PD100 Camcorder → Off
Eject Mini DVCAM Tape (used)

sw Mini DVCAM Tape → Save

10.16 Label Mini DVCAM Tape: CFE Vane Gap 2 Gap Stability Test
and include GPS time.

10.17 Tmpy stow : Mini DVCAM Tape (used)

11. VANE GAP 2 ASYMMETRIC INTERFACE TEST 90

11.1 ✓ #10 fastener is securely tightened

11.2 Retrieve: Mini DVCAM Tape (new)
Install Mini DVCAM Tape (new) in PD100 Camcorder

CAUTION

The camera view and the front face of the Vane Gap 2 vessel
should be orthogonal or loss of science may occur.

11.3 ✓ PD100 Camcorder for CFE Vane Gap 2 entire Field of View

Refer to [5.010 CFE VANE GAP CHAMBER FIELD OF VIEW](#)

✓ REC Lamp – Off

✓ Sony emblem is covered

✓ Vane position – 0 degrees

✓ PD100 Camcorder view is orthogonal to the front face of the CFE
Vane Gap 2 vessel. Gauge by eye checking both the top view and
the side view.

11.4 Use tape or paper to mark the location of the Vane Gap 2 vessel
on the MWA surface so that it can easily be returned to
approximately the same position.

NOTE

1. This test does not require any tapping to aid in fluid redistribution. The operator only needs to adjust the vane position and wait the prescribed time for each step without disturbing the vessel for each setpoint.
2. Vane angle adjustments are made by smoothly turning the Vane Position Indicator. An approximate 2 degree backlash is present on the Vane Position Indicator and it may be necessary to overturn the Vane Position Indicator approximately 2 degrees to establish the desired angle once the Vane Position Indicator is released.

NOTE

3. When rotating Vane Position Indicator, care should be taken to keep the Vane Position Indicator visible and unobstructed in the camera Field of View.
4. VALVE 1 remains open (extended) during all the CFE Vane Gap 2 tests.

Start Video Activity

11.5 PD100 Camcorder → On

11.6 Voice into the PD100 Camcorder GPS time, "Asymmetric Interface Test 90", "CFE Vane Gap 2", and the module temperature from the PCS ECLSS page.

11.7 Allow 1 minute for camcorder to record baseline condition.

11.8 Slowly rotate the vane CW to 90 degrees at approximately 3 degrees per second for a total movement duration of approximately 30 seconds.

11.9 Remove #10 Fastener and Tmpy stow.

11.10 Remove the vessel from the MWA and use a centrifuge method to move most of the fluid from the base to the left side of the test chamber. Fluid will likely bridge the gaps between the vane and the test chamber walls.

As gently as possible, return the vessel to the MWA within five seconds and reattach using the #10 fastener. Minor bumps on contact are acceptable. Try to place the vessel back to its original position when reattaching to the MWA. Do not adjust the vessel position after placement back onto the MWA.

11.11 Inspect test chamber interior surface for fluid film.

If present

✓ **POIC** and wait for fluid film breakage

11.12 Allow 2 minutes to allow the fluid to reach its equilibrium condition.

11.13 Per the table below, slowly rotate Vane Position Indicator CCW to the Vane Position listed and wait the prescribed time. The gaps mentioned in this step are between the vane and the test chamber walls

2.006 CFE VANE GAP 2 TEST OPERATIONS

(cfe1all000038)

Page 21 of 24 pages

Using the PD100 Camcorder, voice observations of the fluid response.

Vane Position	Wait Time	Setpoint Description
80	2 minutes	
70	2 minutes	
60	2 minutes	
50	2 minutes	
40	2 minutes	
30	2 minutes	
20	2 minutes	
10	2 minutes	
0	2 minutes	

- └ Repeat for the remaining vane positions and wait times until a familiar (i.e. more symmetric) interface configuration is established.

When a familiar interface configuration is established

Proceed to the next step

11.14 Rotate vane to 0 degrees if not already there.

End Video Activity

PD100 Camcorder 11.15 PD100 Camcorder → Off
Eject Mini DVCAM Tape (used)

sw Mini DVCAM Tape → Save

11.16 Label Mini DVCAM Tape: CFE Vane Gap 2 Asymmetric Test 90
and include GPS time.

11.17 Tmpy stow : Mini DVCAM Tape (used)

12. VANE GAP 2 ASYMMETRIC INTERFACE TEST 0

12.1 ✓ #10 fastener is securely tightened

12.2 Retrieve: Mini DVCAM Tape (new)
Install Mini DVCAM Tape (new) in PD100 Camcorder

CAUTION

The camera view and the front face of the Vane Gap 2 vessel
should be orthogonal or loss of science may occur.

12.3 ✓ PD100 Camcorder for CFE Vane Gap 2 entire Field of View

Refer to [5.010 CFE VANE GAP CHAMBER FIELD OF VIEW](#)

√REC Lamp – Off

√Sony emblem is covered

√Vane position – 0 degrees

√PD100 Camcorder view is orthogonal to the front face of the CFE Vane Gap 2 vessel. Gauge by eye checking both the top view and the side view.

- 12.4 Use tape or paper to mark the location of the Vane Gap 2 vessel on the MWA surface so that it can easily be returned to approximately the same position.

NOTE

1. This test does not require any tapping to aid in fluid redistribution. The operator only needs to adjust the vane position and wait the prescribed time for each step without disturbing the vessel for each setpoint.
2. Vane angle adjustments are made by smoothly turning the Vane Position Indicator. An approximate 2 degree backlash is present on the Vane Position Indicator and it may be necessary to overturn the Vane Position Indicator approximately 2 degrees to establish the desired angle once the Vane Position Indicator is released.
3. When rotating Vane Position Indicator, care should be taken to keep the Vane Position Indicator visible and unobstructed in the camera Field of View.
4. VALVE 1 remains open (extended) during all the CFE Vane Gap 2 tests.

Start Video Activity

- 12.5 PD100 Camcorder → On

- 12.6 Voice into the PD100 Camcorder GPS time, "Asymmetric Interface Test 0", "CFE Vane Gap 2", and the module temperature from the PCS ECLSS page.

- 12.7 Allow 1 minute for camcorder to record baseline condition.

- 12.8 Remove #10 Fastener and Tmpy stow.

- 12.9 Remove the vessel from the MWA and use a centrifuge method to move most of the fluid from the base to the left side of the test chamber. Fluid should bridge the base and lid along the left side of the test chamber, but may not cover the lid and/or base.

As gently as possible, return the vessel to the MWA within five seconds and reattach using the #10 fastener. Minor bumps on

2.006 CFE VANE GAP 2 TEST OPERATIONS

(cfe1all000038)

Page 23 of 24 pages

contact are acceptable. Try to place the vessel back to its original position when reattaching to the MWA. Do not adjust the vessel position after placement back onto the MWA.

12.10 Inspect test chamber interior surface for fluid film.

If present

✓ **POIC** and wait for fluid film breakage

12.11 Allow 2 minutes to allow the fluid to reach its equilibrium condition.

12.12 Per the table below, slowly rotate Vane Position Indicator CW to the Vane Position listed and wait the prescribed time. The gaps mentioned in this step are between the vane and the test chamber walls.

Using the PD100 Camcorder, voice observations of the fluid response.

Vane Position	Wait Time	Setpoint Description
10	2 minutes	
20	2 minutes	
30	2 minutes	
40	2 minutes	
50	2 minutes	
60	2 minutes	
70	2 minutes	
80	2 minutes	
90	2 minutes	
0	1 minute	Slow CCW turn ~30 second movement duration

└ Repeat for the remaining vane positions and wait times until a familiar (i.e. more symmetric) interface configuration is established.

When a familiar interface configuration is established

Proceed to the next step

12.13 Move vane to 0 degrees if not already there.

End Video Activity

PD100 Camcorder 12.14

PD100 Camcorder → Off
Eject Mini DVCAM Tape (used)
sw Mini DVCAM Tape → Save

12.15 Label Mini DVCAM Tape: CFE Vane Gap 2 Asymmetric Test 0 and include GPS time.

12.16 Tmpy stow : Mini DVCAM Tape (used)

13. VANE GAP 2 POST TEST FLUID WITHDRAWAL

13.1 Visually inspect the fluid in the vessel. There should not be any liquid in contact with the lid of the test chamber. In general, the fluid should cover the base and rise partially up the walls of the test chamber forming a rather large meniscus.

If at any time during this step the fluid configuration departs from this state,

Perform [4.001 CFE VANE GAP FLUID RELOCATION](#) all, then:

13.2 ✓#10 fastener is securely tightened

CFE Vane Gap13.3 Position vane angle to 0 degrees.

13.4 Slowly turn KNOB 1 CW initially at approximately 1/4 to 1/2 turn per second to stop (approx. 46 revolutions), retracting as much fluid into reservoir without ingesting bubbles. Withdrawal rate must be reduced significantly to avoid ingestion of air bubbles during the final stages of the drain procedure (complete drain could take up to 5 minutes). Not all fluid will be removed from container. Remove only as much as is possible without ingesting bubbles beyond VALVE 1.

13.5 With one hand supporting CFE Vane Gap 2, gently push VALVE 1 to hard stop.

13.6 Notify **POIC** of tape serial number and/or sequence number for each used tape.

13.7 Stow:
Mini DVCAM Tapes (per execution note, used)
Gray Tape
CFE Vane Gap
1/8" L-Wrench (2 1/4" length)

RESTOW TOOLS, PARTS, MATERIALS AS REQUIRED TO ORIGINAL LOCATIONS EXCEPT FOR:

Mini DVCAM Tape [per execution note] P/N SED33111489-305 TO: For return to Houston

2.007 CFE CONTACT LINE TEST OPERATIONS - INCREMENT 13

(cfe1all000018)

Page 1 of 10 pages

OBJECTIVE:

Capillary Flow Experiment (CFE). During this procedure the data for the CFE Contact Line tests is recorded via Camcorder video and sound. The CFE tests are titled Axial, Slide, Multi-Slide and Drainage.

STATION PARTS:

CFE Contact Line 2 P/N 60083MA00200
Mini DVCAM Tape [3] P/N SED33111489-305

STATION TOOLS:

MWA Work Surface Area P/N SEG33110270-301
MWA Utility Kit P/N SJG33110310-301
Fine Point Sharpie P/N 528-40674-1
PD100 Camcorder P/N SEZ16103293-301

STATION MATERIALS:

Dry Wipe P/N SEG33107170-306

NOTE

1. This procedure contains Near Real - Time video downlink or LAB VTR recording requirements.
2. AOS may be required for **POIC** to configure on board system for downlink of science or LAB VTR recording.

1. CFE TEST CHAMBER FILL

- 1.1 Visually inspect the vessel to determine if the pinning lip is dry. In general, a dry pinning lip diffracts light in such a manner that it is not possible to clearly see through the pinning lip in profile.
Refer to [5.013 CFE PINNING LIP COMPARISON](#)
If the pinning lip needs to be cleared of fluid at any time during this step,
Perform [step 6](#) and then resume this step where exited.
- 1.2 ✓ #10 fastener is securely tightened
- 1.3 Unstow: Mini DVCAM Tapes (3)
Temporarily stow close to PD100 Camcorder
Insert Mini DVCAM Tape into PD100 Camcorder.
- 1.4 ✓ PD100 Camcorder for CFE Contact Line 2 entire Field of View
✓ REC Lamp – OFF
✓ Sony emblem is covered
Refer to Figure [5.005 CFE CONTACT LINE CHAMBER FIELD OF VIEW](#)

CAUTION

1. Once fluid dispensing into the test chambers has begun, the process for turning the knob needs to be consistent or a loss of science will occur.

CAUTION

2. The smooth cylinder fluid will be dispensed before the pinning cylinder in order to reduce disturbances that could impact science associated with the pinning lip.

NOTE

1. Valve 2 and Knob 2 are associated with the smooth cylinder. Refer to [5.001 CFE CONTACT LINE](#). Valve 2 remains open during all subsequent operations.
2. Valve 1 and Knob 1 are associated with the pinning cylinder. Refer to [5.001 CFE CONTACT LINE](#). Valve 1 remains open during all subsequent operations.
3. Bubbles in the fluid reservoirs are expected and a normal occurrence. No action is necessary other than fluid deployment as described below. Once deployed, the bubbles will find their way to the surface and pop.

Start Video Activity

1.5 PD100 Camcorder → ON

CFE Contact Line1.6 With one hand supporting CFE Contact Line 2, gently pull Valve 2 to hard stop. High resistance may be encountered.

1.7 Slowly Turn Knob 2 CCW to stop at approximately 1/4 to 1/2 turn per second (approx. 40 revolutions, requires up to 2 to 3 minutes).

1.8 ✓CFE Contact Line 2 fluid has been fully dispensed into the smooth cylinder.

CAUTION

CFE Contact Line 2 fluid leakage may occur around the valves, and/or the piston.

1.9 ✓CFE Contact Line 2 for visible leakage

If leakage

| Wipe with Dry Wipes.

If leakage continues,

* | ✓ **POIC** to report leakage

CFE Contact Line1.10 With one hand supporting CFE Contact Line 2, gently pull Valve 1 to hard stop. High resistance may be encountered.

- 1.11 Slowly Turn Knob 1 CCW to stop at approximately 1/4 to 1/2 turn per second (approx. 40 revolutions, requires up to 2 to 3 minutes).
- 1.12 ✓CFE Contact Line 2 fluid has been fully dispensed into the pinning cylinder.

CAUTION

CFE Contact Line 2 fluid leakage may occur around the valves, and/or the piston.

- 1.13 ✓CFE Contact Line 2 for visible leakage

If leakage

| Wipe with Dry Wipes.

If leakage continues,

* | ✓ **POIC** to report leakage

- 1.14 Zoom in the PD100 Camcorder so that the small Field of View is recorded. Refer to [5.002 CFE CONTACT LINE SMALL FIELD OF VIEW](#)
- 1.15 Voice observations (into recording PD100 Camcorder) concerning symmetry of interface on pinning lip of pinning cylinder and presence and approximate size of any bubbles.
- 1.16 PD100 Camcorder → OFF

End Video Activity

2. [CFE AXIAL TEST](#)

- 2.1 Visually inspect the vessel to determine if the pinning lip is dry. In general, a dry pinning lip diffracts light in such a manner that it is not possible to clearly see through the pinning lip in profile. Refer to [5.013 CFE PINNING LIP COMPARISON](#)
If the pinning lip needs to be cleared of fluid at any time during this step,
| Perform [step 6](#) and then resume this step where exited.
- 2.2 ✓#10 fastener is securely tightened.
- 2.3 ✓PD100 Camcorder viewing CFE Contact Line 2 small Field of View
✓Sony emblem is covered

√REC Lamp — Off

√Camera view in front face of CFE Contact Line vessel is orthogonal

Refer to [5.002 CFE CONTACT LINE SMALL FIELD OF VIEW](#)

CAUTION

1. The Axial disturbances should be very small to start and increase gradually with each disturbance. The disturbance should never be large enough to destabilize the pinning cylinder interface, form bubbles, or break-up the fluid interfaces. Clearing the pinning edge takes considerable time and will reduce time for operations
2. Time must be allowed after each Axial disturbance for the fluid motion to fully decay (damp out, settle, etc.) or science will be lost.

NOTE

1. An axial mode disturbance is created by deflecting and releasing the MWA much like a diver on a spring board. The disturbance will excite axial oscillation modes on the liquid surfaces in the cylinders.
2. Special care must be taken to impart the disturbance quickly. The action should be to depress the MWA with an immediate release to avoid seeing one disturbance from deflecting the MWA and another disturbance when releasing it.
3. Valve 1 and Valve 2 remain open (extended) during the CFE test.

Start Video Activity

2.4 PD100 Camcorder → ON

2.5 Voice into the PD100 Camcorder GMT, "Axial Test", "CFE Contact Line 2", and the module temperature from the PCS ECLSS page.

2.6 Beginning with extremely weak deflections, using finger, depress and release the MWA (using MWA as cantilever) to impart an axial mode disturbance to the interfaces (much like a diver on a diving board). Operator must wait at least 15 seconds after each axial disturbance.

Repeat disturbance with approximately same deflection.

2.7 Repeat [step 2.6](#) with increased disturbance amplitude until it is perceived that further increases in disturbance amplitude will de-pin interface or eject liquid droplets from surface.

End Video Activity

2.8 PD100 Camcorder → OFF
Eject Mini DVCAM Tape (used)
sw Mini DVCAM Tape → Save

2.9 Label Mini DVCAM Tape FILL and AXIAL TEST and include approximate GMT.

- 2.10 Tmpy stow:
Mini DVCAM Tape (used)

3. CFE SLIDE TEST

- 3.1 Visually inspect the vessel to determine if the pinning lip is dry. In general, a dry pinning lip diffracts light in such a manner that it is not possible to clearly see through the pinning lip in profile. Isolated drops in the pinning lip may be tolerated if they do not touch surfaces of the cylinder below the pinning lip.
Refer to [5.013 CFE PINNING LIP COMPARISON](#)
If the pinning lip needs to be cleared of fluid at any time during this step,
Perform [step 6](#) and then resume this step where exited.
- 3.2 Loosen, but do not remove, the #10 Fastener that secures the CFE Contact Line 2 to the Maintenance Work Area through the slot in the base plate, such that the CFE Contact Line 2 may slide smoothly left to right in field of view without excess slop.
- 3.3 Retrieve:
Mini DVCAM Tape (new)
Install a Mini DVCAM Tape (new) in PD100 Camcorder
- 3.4 ✓PD100 Camcorder viewing CFE Contact Line 2 small Field of View has been zoomed out slightly to show the entire range of motion.
✓Sony emblem is covered
✓REC Lamp — Off
✓Camera view in front face of CFE Contact Line vessel is orthogonal
Refer to [5.002 CFE CONTACT LINE SMALL FIELD OF VIEW](#)

CAUTION

1. Begin with a weak Slide. The Slides should not increase to the point the pinning cylinder interface is de-pinned or the fluid interfaces break up or bubbles form. Clearing the pinning edge takes considerable time and will reduce time for operations.
2. Time must be allowed after each Slide test for the fluid motion to fully decay or science will be lost.

NOTE

1. A Slide is a one period lateral oscillation, (back and forth), completed within the Field of View at the approximate natural frequency of the interface (predicted to be approximately 1.5-2 Hz). Crew must identify the approximate natural frequency during operations.
2. Valve 1 and Valve 2 remain open (extended) during the CFE test.
3. It is desirable to avoid hitting the ends of the slot to reduce the risk of depinning the interface.
4. Drift after a slide can be minimized by readjusting the #10 fastener prior to each slide as necessary.

NOTE

5. Each Slide applied to the CFE Contact Line 2 must be in same orientation (left to right) across the FIELD OF VIEW, with the same grip on the CFE Contact Line 2.

Start Video Activity

3.5 PD100 Camcorder → ON

3.6 Voice into the PD100 Camcorder GMT, "Slide Test", "CFE Contact Line 2", and the module temperature from the PCS ECLSS page.

3.7 Very slowly slide the CFE Contact Line 2 right, close to the end of the mounting slot. Avoid abrupt impact with slot end.
Do not disturb the interface.
Operator must wait at least 15 seconds before proceeding.

3.8 Lightly Slide CFE Contact Line 2 in Field of View laterally (left to right) one period a distance of about 10mm (peak to peak amplitude). Avoid abrupt impact with slot ends.
Using the PD100 Camcorder, voice the event.
Using the PD100 Camcorder, voice observations of the fluid response.
Drift and/or rotation may occur at the end of motion and is acceptable and should remain untouched for the prescribed time delay.
Operator must wait at least 15 seconds after each slide disturbance.

□ Repeat one time.
If interesting or noticeably different behavior between cylinders results,
Repeat Slide up to two times.

3.9 Repeat [step 3.8](#) moving 15 mm each time

3.10 Repeat [step 3.8](#) moving 20 mm each time

3.11 Repeat [step 3.8](#) moving 25 mm each time

3.12 Repeat [step 3.8](#) moving 30 mm each time

4. CFE MULTI-SLIDE TEST

4.1 Visually inspect the vessel to determine if the pinning lip is dry. In general, a dry pinning lip diffracts light in such a manner that it is not possible to clearly see through the pinning lip in profile. Isolated drops in the pinning lip may be tolerated if they do not touch surfaces of the cylinder below the pinning lip.

Refer to [5.013 CFE PINNING LIP COMPARISON](#)

If the pinning lip needs to be cleared of fluid at any time during this step,

Perform [step 6](#) and then resume this step where exited.

- 4.2 Loosen, but do not remove, the #10 Fastener that secures the CFE Contact Line 2 to the Maintenance Work Area through the slot in the base plate, such that the CFE Contact Line 2 may slide smoothly left to right in field of view without excess slop.

CAUTION

1. Begin with a weak multiple, lateral oscillation, (back and forth). The Slides should not increase to the point the pinning cylinder interface is de-pinned or the fluid interfaces break up or bubbles form. Clearing the pinning edge takes considerable time and will reduce time for operations.
2. Time must be allowed after each Multi-Slide Test for the fluid motion to fully decay or science will be lost.

NOTE

1. A Slide is now defined as multiple (2, 3, 4) period lateral oscillations completed within the Field of View, at the approximate natural frequency of the interface (predicted to be approximately 1.5-2 Hz). Crew must identify the approximate natural frequency during operations.
2. Valve 1 and Valve 2 remain open (extended) during the CFE test.
3. It is desirable to avoid hitting the ends of the mounting slot to avoid the risk of de-pinning the interface.
4. Drift after a multi-slide can be minimized by readjusting the #10 fastener prior to each multi-slide as necessary.
5. Each multiple oscillation Slide applied to the CFE Contact Line 2 must be in same orientation (left to right) across the FIELD OF VIEW, with the same grip on the CFE Contact Line 2.

- 4.3 Voice into the PD100 Camcorder GMT, "Multi-Slide Test", "CFE Contact Line 2", and the module temperature from the PCS ECLSS page.

- 4.4 Slide CFE Contact Line 2 two full cycles with a peak to peak distance of about 10mm in the Field of View. Avoid abrupt impact with slot ends.

Using the PD100 Camcorder, voice the event.

Using the PD100 Camcorder, voice observations of the fluid response.

Drift and/or rotation may occur at the end of motion and is acceptable and should remain untouched for the prescribed time delay.

2.007 CFE CONTACT LINE TEST OPERATIONS - INCREMENT 13

(cfe1all000018)

Page 8 of 10 pages

Operator must wait at least 15 seconds after each slide disturbance.

└─ Repeat Multi-Slide one time.

If interesting or noticeably different behavior between cylinders results,

Repeat multiple Slide up to two times.

4.5 Repeat [step 4.4](#) moving 15 mm each time.

4.6 Repeat [step 4.4](#) moving 20 mm each time.

4.7 Repeat [step 4.4](#) moving 25 mm each time.

4.8 Repeat [step 4.4](#) moving 30 mm each time.

4.9 As video tape allows, continue Slides of increasing number of oscillations (3, 4), being careful to avoid depinning the interface.

End Video Activity

4.10 PD100 Camcorder → OFF
Eject Mini DVCAM Tape (used)
sw Mini DVCAM Tape → Save

4.11 Label Mini DVCAM Tape SLIDE and include approximate GMT.

4.12 Tmpary stow:
Mini DVCAM Tape (used)

5. [CFE DRAINAGE](#)

5.1 Visually inspect the vessel to determine if the pinning lip is dry. In general, a dry pinning lip diffracts light in such a manner that it is not possible to clearly see through the pinning lip in profile.

Refer to [5.013 CFE PINNING LIP COMPARISON](#)

If the pinning lip needs to be cleared of fluid at any time during this step,

Perform [step 6](#) and then resume this step where exited.

5.2 √#10 fastener is securely tightened

5.3 √CFE Contact Line 2 Valve 2 is open, (valve pulled out to hard stop)

5.4 Remove the fluid as fast as possible by turning Knob 2 CW without ingesting air into the reservoir. Retraction of the fluid at the end of the process should be very slow, to avoid ingesting air into the fluid reservoir. Not all of the fluid will be removed.

5.5 With one hand supporting CFE Contact Line 2, gently push Valve 2 to overcome high resistance to hard stop (closed).

- 5.6 ✓CFE Contact Line 2 Valve 1 is open, valve pulled out to (valve pulled out to hard stop)
- 5.7 Remove the fluid as fast as possible by turning Knob 1 CW without ingesting air into the reservoir. Retraction of the fluid at the end of the process should be very slow, to avoid ingesting air into the fluid reservoir. Not all of the fluid will be removed.
- 5.8 With one hand supporting CFE Contact Line 2, Gently push Valve 1 to overcome high resistance to hard stop (closed).

6. CFE DRYING THE PINNING LIP

NOTE

1. This process could take up to 15 minutes per attempt and may take several tries to get right, but is critical to achieving the science goals.
2. The most challenging aspect of the centrifuge method is slowing down smoothly without disturbing the pinning lip.
3. Liquid remaining in the groove serving as the pinning lip of the pinning cylinder should be cleared as needed. It is preferred that this liquid be moved to the base of the cylinder, clearing it by any force deemed acceptable.
4. Drops of fluid on the test chamber wall above the pinning lip are not a problem and may be ignored.
5. Small isolated drops residing in the pinning lip are also not a problem if they are clearly not touching the pinning cylinder walls below the pinning lip.

- 6.1 Remove test vessel from MWA and use centrifuge method (see movie clip for Mike Fincke's method). A higher angular velocity will likely be required to clear the pinning lip.
- 6.2 If the previous effort does not clear the pinning lip perform the following:
- 6.3 Drain the pinning cylinder by turning Knob 1 CW, without ingesting air bubbles into the reservoir.
- 6.4 With one hand supporting CFE Contact Line 2, gently push Valve 1 to overcome high resistance to hard stop (closed).
- 6.5 Remove #10 Fastener from Maintenance Work Area and tmpry stow to allow the CFE Contact Line 2 to be held in hand(s).
- 6.6 Use impulse type disturbances to the vessel (jerks, 'bonks', whatever, etc.) to clear the fluid in the pinning lip and hopefully move it below the pinning lip.

2.007 CFE CONTACT LINE TEST OPERATIONS - INCREMENT 13

(cfe1all000018)

Page 10 of 10 pages

- 6.7 A combination of centrifugal force with impulse disturbances may be required to clear the pinning lip.
- 6.8 Use something like the Fincke centrifuge method to return the fluid in the Smooth cylinder to the base of the cylinder.
- 6.9 Gently re-secure CFE vessel to the MWA using the #10 fastener.
- 6.10 Visually inspect the test chambers for any fingerprints. Use a dry wipe to remove any if found.
- 6.11 With one hand supporting CFE Contact Line 2, gently pull Valve 1 to hard stop. High resistance may be encountered.
- 6.12 Slowly Turn Knob 1 CCW to stop at approximately 1/4 to 1/2 turn per second (approx. 40 revolutions, requires up to 2 to 3 minutes).
- 6.13 ✓CFE Contact Line 2 fluid has been fully dispensed into the pinning cylinder.
- 6.14 Continue operations.

RESTOW TOOLS, PARTS, MATERIALS AS REQUIRED TO ORIGINAL LOCATIONS.
EXCEPT FOR:

Mini DVCAM Tape [3] P/N SED33111489-305 TO: CTB, for return to Houston

REPORT DOCUMENTATION PAGE				Form Approved OMB No. 0704-0188	
<p>The public reporting burden for this collection of information is estimated to average 1 hour per response, including the time for reviewing instructions, searching existing data sources, gathering and maintaining the data needed, and completing and reviewing the collection of information. Send comments regarding this burden estimate or any other aspect of this collection of information, including suggestions for reducing this burden, to Department of Defense, Washington Headquarters Services, Directorate for Information Operations and Reports (0704-0188), 1215 Jefferson Davis Highway, Suite 1204, Arlington, VA 22202-4302. Respondents should be aware that notwithstanding any other provision of law, no person shall be subject to any penalty for failing to comply with a collection of information if it does not display a currently valid OMB control number.</p> <p>PLEASE DO NOT RETURN YOUR FORM TO THE ABOVE ADDRESS.</p>					
1. REPORT DATE (DD-MM-YYYY) 01-09-2009		2. REPORT TYPE Final Contractor Report		3. DATES COVERED (From - To) August 2004 - December 2007	
4. TITLE AND SUBTITLE The Capillary Flow Experiments Aboard the International Space Station: Increments 9–15 August 2004 to December 2007				5a. CONTRACT NUMBER	
				5b. GRANT NUMBER	
				5c. PROGRAM ELEMENT NUMBER	
6. AUTHOR(S) Jenson, Ryan, M.; Weislogel, Mark, M.; Tavan, Noel, T.; Chen, Yongkang; Semerjian, Ben; Bunnell, Charles, T.; Collicott, Steven, H.; Klatte, Jorg; Dreyer, Michael, E.				5d. PROJECT NUMBER NCC05-AA29A	
				5e. TASK NUMBER	
				5f. WORK UNIT NUMBER WBS 825080.04.02.20.08	
7. PERFORMING ORGANIZATION NAME(S) AND ADDRESS(ES) National Aeronautics and Space Administration John H. Glenn Research Center at Lewis Field Cleveland, Ohio 44135-3191				8. PERFORMING ORGANIZATION REPORT NUMBER E-16827	
9. SPONSORING/MONITORING AGENCY NAME(S) AND ADDRESS(ES) National Aeronautics and Space Administration Washington, DC 20546-0001				10. SPONSORING/MONITOR'S ACRONYM(S) NASA	
				11. SPONSORING/MONITORING REPORT NUMBER NASA/CR-2009-215586	
12. DISTRIBUTION/AVAILABILITY STATEMENT Unclassified-Unlimited Subject Categories: 28 and 34 Available electronically at http://gltrs.grc.nasa.gov This publication is available from the NASA Center for AeroSpace Information, 443-757-5802					
13. SUPPLEMENTARY NOTES					
14. ABSTRACT This report provides a summary of the experimental, analytical, and numerical results of the Capillary Flow Experiment (CFE) performed aboard the International Space Station (ISS). The experiments were conducted in space beginning with Increment 9 through Increment 16, beginning August 2004 and ending December 2007. Both 'primary' and 'extra science' experiments were conducted during 19 operations performed by 7 astronauts including: M. Fincke, W. McArthur, J. Williams, S. Williams, M. Lopez-Alegria, C. Anderson, and P. Whitson. CFE consists of 6 approximately 1 to 2 kg handheld experiment units designed to investigate a selection of capillary phenomena of fundamental and applied importance, such as large length scale contact line dynamics (CFE-Contact Line), critical wetting in discontinuous structures (CFE-Vane Gap), and capillary flows and passive phase separations in complex containers (CFE-Interior Corner Flow). Highly quantitative video from the simply performed flight experiments provide data helpful in benchmarking numerical methods, confirming theoretical models, and guiding new model development. In an extensive executive summary, a brief history of the experiment is reviewed before introducing the science investigated. A selection of experimental results and comparisons with both analytic and numerical predictions is given. The subsequent chapters provide additional details of the experimental and analytical methods developed and employed. These include current presentations of the state of the data reduction which we anticipate will continue throughout the year and culminate in several more publications. An extensive appendix is used to provide support material such as an experiment history, dissemination items to date (CFE publication, etc.), detailed design drawings, and crew procedures. Despite the simple nature of the experiments and procedures, many of the experimental results may be practically employed to enhance the design of spacecraft engineering systems involving capillary interface dynamics.					
15. SUBJECT TERMS Fluid flow; Capillary Flow					
16. SECURITY CLASSIFICATION OF:			17. LIMITATION OF ABSTRACT UU	18. NUMBER OF PAGES 326	19a. NAME OF RESPONSIBLE PERSON STI Help Desk (email: help@sti.nasa.gov)
a. REPORT U	b. ABSTRACT U	c. THIS PAGE U			19b. TELEPHONE NUMBER (include area code) 443-757-5802

